Trace Organic Chemicals in the Water Cycle: Occurrence in Wastewater Treatment Plants and Removal by Biological and Chemical Treatment

by

Nina Hermes

born in Meppen (Germany)

Accepted dissertation thesis for the partial fulfilment of the requirements for a Doctor of Natural Sciences

Fachbereich 3: Mathematik/Naturwissenschaften

Universität Koblenz-Landau

Reviewers:

Prof. Dr. Wolfgang Imhof

Prof. Dr. Thomas A. Ternes

Examiners:

Prof. Dr. Wolfgang Imhof

Prof. Dr. Thomas A. Ternes

PA Dr. Carola Winkelmann

Date of the oral examination: 3rd February 2021

"O glücklich, wer noch hoffen kann,
aus diesem Meer des Irrtums aufzutauchen.
Was man nicht weiß, das eben brauchte man,
und was man weiß, kann man nicht brauchen."

Johann Wolfgang von Goethe, Faust

Danksagung

und Alex Weizel waren nicht nur ein willkommener Zeitvertreib, sondern brachten auch immer wieder neue Erkenntnisse zu der eigenen Arbeit.

Nicht nur innerhalb der BfG habe ich viel Unterstützung bekommen, auch von außerhalb kam die ein oder andere wertvolle Hilfestellung. So danke ich Holger Lutze von der Universität Duisburg-Essen für die verschiedenen Denkanstöße in den Ozonungs-Arbeiten, sowie Per Falås von der Universität Lund für die Probenahme an der dortigen Pilotanlage. Zudem konnte ich auf vielen Tagungen und Konferenzen mit verschiedenen Experten die Themen meiner Arbeit diskutieren und so ein Stück weiter voran bringen.

Zuletzt danke ich auch noch meiner Familie und meinen Freunden. Bei ihnen fand ich jedesmal Halt, wenn es in der Doktorarbeit doch einfach zu viel und zu stressig wurde. Und auch in den schwierigsten Phasen waren sie immer für mich da. Auch an meine alte Hochschule, der Hochschule Bonn-Rhein-Sieg geht ein intensiver Dank. Die Erstellung der Publikationen und der Dissertation hätte noch wesentlich mehr Zeit in Anspruch genommen, wenn ich nicht in meiner gewohnten Abschlussarbeits-Umgebung daran hätte schreiben können. "Meinen" Schreibbüros habe ich es zu verdanken, dass diese Arbeit schließlich fertig werden konnte.

Zu guter Letzt: danke, Prinzessin Karo, für deine Durchhaltevermögen. Und danke, liebe Toffifee, dass du anschliessend übernommen hast.

Summary

Water scarcity is already an omnipresent problem in many parts of the world, especially in sub-Saharan Africa. The dry years 2018 and 2019 showed that also in Germany water resources are finite. Projections and predictions for the next decades indicate that renewal rates of existing water resources will decline due the growing influence of climate change, but that water extraction rates will increase due to population growth. It is therefore important to find alternative and sustainable methods to make optimal use of the water resources currently available. For this reason, the reuse of treated wastewater for irrigation and recharge purposes has become one focus of scientific research in this field. However, it must be taken into account that wastewater contains so-called micro-pollutants, i.e., substances of anthropogenic origin. These are, e.g., pharmaceuticals, pesticides and industrial chemicals which enter the wastewater, but also metabolites that are formed in the human body from pharmaceuticals or personal care products. Through the treatment in wastewater treatment plants (WWTPs) as well as through chemical, biological and physical processes in the soil passage during the reuse of water, these micropollutants are transformed to new substances, known as transformation products (TPs), which further broaden the number of contaminants that can be detected within the whole water cycle.

Despite the fact that the presence of human metabolites and environmental TPs in untreated and treated wastewater has been known for a many years, they are rarely included in common routine analysis methods. Therefore, a first goal of this thesis was the development of an analysis method based on liquid chromatography - tandem mass spectrometry (LC-MS/MS) that contains a broad spectrum of frequently detected micropollutants including their known metabolites and TPs. The developed multi-residue analysis method contained a total of 80 precursor micropollutants and 74 metabolites and TPs of different substance classes. The method was validated for the analysis of different water matrices (WWTP influent and effluent, surface water and groundwater from a bank filtration site). The influence of the MS parameters on the quality of the analysis data was studied. Despite the high number of analytes, a sufficient number of datapoints per peak was maintained, ensuring a high sensitivity and precision as well as a good recovery for all matrices. The selection of the analytes proved to be relevant as 95% of the selected micropollutants were detected in at least one sample. Several micropollutants were quantified that were not in the focus of other current multi-residue analysis methods (e.g. oxypurinol). The relevance of including metabolites and TPs was demonstrated by the frequent detection of, e.g., clopidogrel acid and valsartan acid at higher concentrations than their precursors, the latter even being detected in samples of bank filtrate water.

By the integration of metabolites, which are produced in the body by biological processes, and biological and chemical TPs, the multi-residue analysis method is also suitable for elucidating

degradation mechanisms in treatment systems for water reuse that, e.g., use a soil passage for further treatment. In the second part of the thesis, samples from two treatment systems based on natural processes were analysed: a pilot-scale above-ground sequential biofiltration system (SBF) and a full-scale soil aquifer treatment (SAT) site. In the SBF system mainly biological degradation was observed, which was clearly demonstrated by the detection of biological TPs after the treatment. The efficiency of the degradation was improved by an intermediate aeration, which created oxic conditions in the upper layer of the following soil passage. In the SAT system a combination of biodegradation and sorption processes occurred. By the different behaviour of some biodegradable micropollutants compared to the SBF system, the influence of redox conditions and microbial community was observed. An advantage of the SAT system over the SBF system was found in the sorption capacity of the natural soil. Especially positively charged micropollutants showed attenuation due to ionic interactions with negatively charged soil particles. Based on the physico-chemical properties at ambient pH, the degree of removal in the investigated systems and the occurrence in the source water, a selection of process-based indicator substances was proposed.

Within the first two parts of this thesis a micropollutant was frequently detected at elevated concentrations in WWTPs effluents, which was not previously in the focus of environmental research: the antidiabetic drug sitagliptin (STG). STG showed low degradability in biological systems and thus it was investigated to what extend chemical treatment by ozonation can ensure attenuation of it. STG contains an aliphatic primary amine as the principal point of attack for the ozone molecule. There is only limited information about the behaviour of this functional group during ozonation and thus, STG served as an example for other micropollutants containing aliphatic primary amines. A pH-dependent degradation kinetic was observed due to the protonation of the primary amine at lower pH values. At pH values in the range 6 - 8, which is typical for the environment and in WWTPs, STG showed degradation kinetics in the range of 10^3 $M^{-1}s^{-1}$ and thus belongs to the group of readily degradable substances. However, complete degradation can only be expected at significantly higher pH values (> 9). The transformation of the primary amine moiety into a nitro group was observed as the major degradation mechanism for STG during ozonation. Other mechanisms involved the formation of a diketone, bond breakages and the formation of trifluoroacetic acid (TFA). Investigations at a pilot-scale ozonation plant using the effluent of a biological degradation of a municipal WWTP as source water confirmed the results of the laboratory studies: STG could not be removed completely even at high ozone doses and the nitro compound was formed as the main TP and remained stable during further ozonation and subsequent biological treatment. It can therefore be assumed that under realistic conditions both a residual concentration of STG and the formed main TP as well as other stable TPs such as TFA can be detected in the effluents of a WWTP consisting of conventional biological treatment followed by ozonation and subsequent biological polishing steps.

Kurzfassung

In vielen Teilen der Welt, vor allem in Subsahara-Afrika, ist Wasserknappheit bereits ein allgegenwärtiges Problem. Doch die Trockenjahre 2018 und 2019 zeigten, dass auch in Deutschland die Wasserressourcen endlich sind. Projektionen und Vorhersagen für die nächsten Jahrzehnte weisen zudem darauf hin, dass durch den steigenden Einfluss des Klimawandels die Erneuerungsraten der bestehenden Wasserressourcen zurückgehen, die Entnahmemengen aber aufgrund von Populationswachstum steigen werden. Es ist demnach an der Zeit, alternative und nachhaltige Methoden zu finden, die derzeit vorhandenen Wasserressourcen optimal zu nutzen. Daher rückte in den ver-gangenen Jahren die Wiederverwendung von geklärtem Abwasser zur Bewässerung landwirtschaftlicher Flächen und/oder der Grundwasseranreicherung in den Fokus der Wissenschaft. Dabei ist aber zu berücksichtigen, dass in geklärtem Abwasser sogenannte Spurenstoffe zu finden sind, d.h. Substanzen, die durch anthropogenen Einfluss in den Wasserkreislauf gelangen. Dabei handelt es sich z.B. um Pharmazeutika, Pestizide und Industriechemikalien, aber auch um Metabolite, die im menschlichen Körper gebildet werden und in das Abwasser gelangen. Durch die Wasseraufbereitungsschritte in den Kläranlagen als auch durch biologische, chemische und physikalische Prozesse in der Bodenpassage bei der Wiederverwendung des geklärten Abwassers werden diese Spurenstoffe zu anderen Substanzen, den Transformationsprodukten (TPs), umgewandelt, die das Spektrum der Spurenstoffe zusätzlich erweitern.

Trotz der Tatsache, dass das Vorhandensein von Human-Metaboliten und TPs in ungeklärtem und geklärten Abwasser seit langem bekannt ist, werden sie in gängigen Routine-Messmethoden nur selten berücksichtigt. Daher war es ein erstes Ziel dieser Dissertation eine Analyse-Methode zu erstellen, basierend auf Flüssigchromatographie-Tandem Massenspektrometrie (LC-MS/MS), die ein möglichst breites Spektrum an Spurenstoffen inklusive bekannter Metabolite und TPs enthält. Die entwickelte Multi-Analyt-Methode umfasst insgesamt 80 Ausgangssubstanzen und 74 Metabolite und TPs verschiedener Substanzklassen und ist für die Anwendung in verschiedenen Wassermatrices (Zu- und Ablauf von Kläranlagen, Oberflächenwasser und Grundwasser aus einer Uferfiltrationsanlage) validiert. Dabei wurde auch der Einfluss der MS-Parameter auf die Qualität der Analysedaten untersucht. Trotz der hohen Anzahl an Substanzen konnte eine ausreichende Anzahl an Datenpunkten je Peak generiert werden, wodurch eine hohe Empfindlichkeit und Präzision sowie eine gute Wiederfindung für alle Matrices erreicht wurden. Die Auswahl der Analyten erwies sich als relevant für die Untersuchung von Umweltmatrices, da 95% der Substanzliste in mindestens einer Probe nachgewiesen wurden. Mehrere Spurenstoffe, die bisher nicht im Fokus der gegenwärtigen Multi-Analyt-Methoden standen, wurden bei erhöhten Konzentrationen im Wasserkreislauf quantifiziert (z.B. Oxypurinol). Die Relevanz der Untersuchung von Metaboliten und TPs zeigte sich durch den Nachweis von z.B. Clopidogrel-Säure und Valsartansäure mit deutlich höheren Konzen-

trationen als ihre Ausgangssubstanzen. Valsartansäure konnte zudem sogar im Uferfiltrat detektiert werden.

Durch die Einbindung der Metabolite, die durch biologische Prozesse im Körper entstehen, und den biologischen und chemischen TPs, eignet sich die Multi-Analyt-Methode auch zur Aufklärung von Abbaumechanismen in natürlichen Behandlungssystemen zur Wasserwiederverwendung, wozu es in der Literatur bisher nur wenige Angaben gibt. Im Rahmen der Dissertation wurden Proben aus zwei Systemen analysiert, einem im Pilotmaßstab entwickelten oberirdischen sequenziellen Biofiltrationssystem (SBF) und einem großmaßstäblichen Bodenpassagen-System (SAT). Im SBF-System konnten hauptsächlich biologische Abbaumechanismen beobachtet werden, was durch die Entstehung biologischer TPs deutlich gezeigt wurde. Die Effizienz des Abbaus wurde dabei durch eine Zwischenbelüftung erhöht, die oxische Bedingungen hervorrief. Im SAT-System kam es zu einer Kombination von Bioabbau- und Sorptionsprozessen. Es wurde beobachtet, dass bei einigen biologisch abbaubaren Spurenstoffen ein geringerer Abbau erreicht wurde als im SBF-System, was auf unterschiedliche Redox-Bedingungen und eine andere mikrobielle Gemeinschaft zurückzuführen war. Als Vorteil des SAT-Systems gegenüber des SBF erwies sich die Sorptionsfähigkeit des natürlichen Bodens. Vor allem positiv geladene Spurenstoffe zeigten eine Entfernung aufgrund von ionischen Wechselwirkungen mit negativ geladenen Bodenpartikeln. Auf der Grundlage ihrer physikalisch-chemischen Eigenschaften bei Umgebungs-pH, ihres Entfernungsgrades in den untersuchten Systemen und ihres Vorkommens im einfließenden Wasser konnte eine Auswahl von prozessbasierten Indikatorsubstanzen vorgeschlagen werden.

In den vorherigen Arbeiten wurde in Kläranlagenabläufen häufig ein Spurenstoff in erhöhten Konzentrationen nachgewiesen, der bisher wenig im Fokus der Umweltforschung stand: das Antidiabetikum Sitagliptin (STG). STG zeigt nur eine geringe Abbaubarkeit in biologischen Systemen. Daher wurde untersucht, inwieweit eine chemische Aufbereitung mittels Ozonung einen Abbau gewährleisten kann. STG weist in seiner Struktur ein aliphatisches primäres Amin als entscheidende Angriffsstelle für das Ozonmolekül auf. In der Literatur finden sich kaum Informationen zum Verhalten dieser funktionellen Gruppe während der Ozonung. Die in dieser Dissertation erzielten Ergebnisse können daher exemplarisch für andere Spurenstoffe mit Amingruppen herangezogen werden. Es zeigte sich eine pH-abhängige Abbaukinetik aufgrund der Protonierung des primären Amins bei niedrigen pH-Werten. Bei für die Umwelt und Kläranlagen typischen pH-Werten im Bereich 6 - 8 wies STG Abbaukinetiken mittels Ozon im Bereich 10^3 $M^{-1}s^{-1}$ auf, mit einem vollständigen Abbau kann allerdings erst bei deutlich höheren pH-Werten > 9 gerechnet werden. Die Transformation des primären Amins zu einer Nitro-Gruppe wurde als Hauptabbaumechanismus in der Ozonung identifiziert. Ebenfalls wurde die Entstehung weiterer TPs wie z.B. eines Diketons und Trifluoressigsäure (TFA) beobachtet. Untersuchungen an einer Pilotanlage, bei der die Ozonung unter realen Bedingungen mit dem Ablauf einer konventionellen Kläranlage durchgeführt wurde, bestätigte die Ergebnisse der Laboruntersuchungen: STG wurde auch bei einer hohen Ozondosis nicht vollständig entfernt und die Nitro-Verbindung erwies sich als Haupt-TP, das weder bei weiterer Ozonung noch in einer nachgeschalteten biologischen Behandlung abgebaut wurde. Es ist daher davon auszugehen, dass unter realen Bedingungen sowohl eine Restkonzentration an STG als auch das Haupt-TP sowie weitere TPs wie TFA im Ablauf einer Kläranlage bestehend aus konventioneller biologischer Aufreinigung, Ozonung und nachgeschalteter biologischer Aufreinigung auffindbar sind.

Contents

Chapter 1

General Introduction

1.1 Water scarcity and pollution by micropollutants

"Leaving no one behind" is the title and slogan of the most recent World Water Development Report by the United Nations [1]. Still more than 2 billion people in the world live under high water stress and more than 4 billion people experience water scarcity for at least one month a year. Sub-Saharan Africa is heavily impacted by water stress, where the availability of water as well as accessibility to it are critically limited in many regions. But water scarcity is of growing concern worldwide and is mainly driven by two factors: (i) reduction of renewal rates of freshwater resources due to climate change and (ii) growing demand of freshwater due to population growth [1–7].

The earth's freshwater resources are limited. Only about 3% of the total water is available as freshwater which can be used for drinking water production. Most of it, about 69%, is stored as glaciers, 30% as groundwater and only about 1% as surface water reservoirs (rivers, streams, lakes) [4]. The latter can be renewed by precipitation (e.g. rainfall) while most of the groundwater resources count as non-renewable [4]. However, some aquifers are recharged by natural infiltration of rainwater or surface water. Both sources are affected by climate change. Rising temperatures increase evaporation rates of surface waters and deficits in rainfall, which are expected for the next years, lead to decreased renewal rates [4]. Furthermore, with less precipitation, surface waters impaired by treated wastewater (see later this chapter) will experience a concentration of micropollutants due to less dilution by renewed and unaffected water. This might cause problems for freshwater production, when impaired water is used as a source [8, 9]. Although projections about the influence
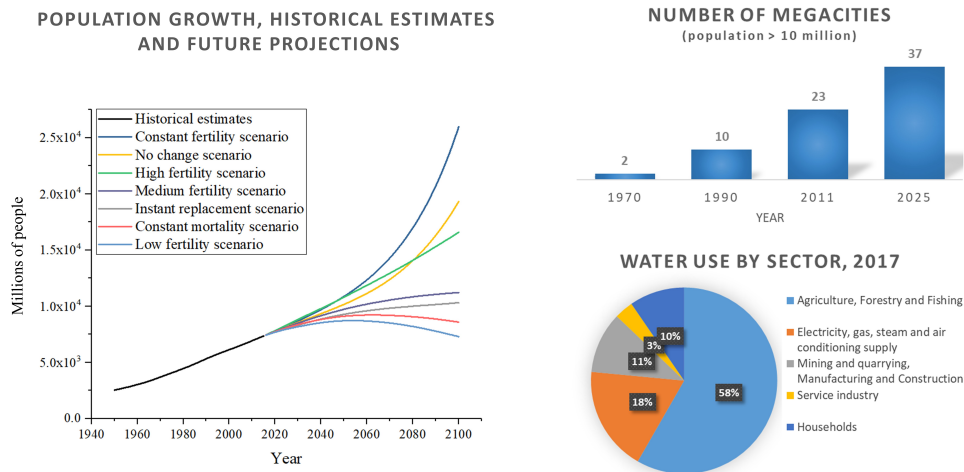
Figure 1.1: Population growth [13], number of megacities [12] and water use by sector in 2017 [5]

of climate change on water scarcity show great uncertainties, on average they reveal a higher likelihood for increasing water scarcity in most parts of the world within the next decades [10].

The influence of climate change on water scarcity is quite low when comparing it to the influence of the second parameter: water demand due to population growth [11]. Within the next few years the world population is projected to increase by several million people (Figure 1.1) [12, 13]. An exponential growth can already and still be observed for several countries in Africa. With population urbanization, cities will grow and by 2050 more than half of the world population will be urban [12]. There are already more than 20 megacities (population > 10 million) in the world and it is projected that more megacities and more big cities (population > 1 million) will grow due to urbanization (Figure 1.1) [12]. This puts high pressure on water treatment and on water supply. Drinking water consumption, however, only makes up a small fraction of freshwater demand (Figure 1.1) [5, 12]. Most freshwater is abstracted for agriculture and industry and these sectors will grow due to increased population. Thus, more freshwater will be needed in the future and abstraction rates will rise [1, 12].

In many parts of the world, particularly in the arid and semi-arid regions, water scarcity

already is an acute problem [1]. But also south and mid-European countries experience this phenomenon. In 2006, Bixio et al. (2006) [14] stated that, according to the water stress index, half of European countries were affected by water stress to some degree. This not only included southern European countries such as Cyprus and Spain but also Belgium and Germany.

Projections for the future see increasing mean temperatures, particularly in summer, decreasing mean precipitation [15], increasing population growth in developing countries and expanding industry. All these factors will lead to an increased water demand while resources for freshwater will decline. Therefore, ways and methods have to be found to artificially recharge these freshwater resources. It already is quite common to have effluents of wastewater treatment plants (WWTPs) released into surface waters such as streams and lakes. Thus, these resources contain a certain amount of reclaimed water. By natural or forced infiltration (e.g. bank filtration) the surface water percolates through the soil and by reaching the groundwater the aquifer is recharged. However, it is already known that anthropogenic substances can be found in all aqueous environmental matrices [16].

There are several terms to name these substances, for example micropollutants, trace organic chemicals (TOrCs or TrOCs) or chemicals of emerging concern (CECs). The first two terms comprise any anthropogenic substances, being regulated or not. Thus, pesticides, pharmaceuticals, personal care products, industrial chemicals and life style products fall under the terms micropollutants and TOrCs. CECs is used mainly for non-regulated substances, i.e. all of the aforementioned ones except for pesticides which have fixed threshold values in several regulations, for example the Water Framework Directive. In this thesis, the term micropollutants will be used.

Micropollutants reach the water cycle by several routes. WWTPs have been identified as a main source for contamination (Figure 1.2, blue circle) [9, 17–21]. WWTPs, either municipal or industrial, receive water from households, hospitals and industry and, therefore, the wastewater contains micropollutants of various substance classes. Furthermore, not only precursor compounds such as unchanged pharmaceuticals or sweeteners (named "P" in Figure 1.2) reach the WWTP. When consumed by people the substances may be metabolized and thus metabolites (named "M" in Figure 1.2) may also reach WWTPs. Both precursors and metabolites then undergo the treatment processes of the WWTP, causing new substances to emerge from transformation reactions, e.g., during biological or chemical treatment. Thus, the effluent of the WWTP not only contains precursors and metabolites, but also transformation products (named "TP" in Figure 1.2) [9, 17, 22]. The
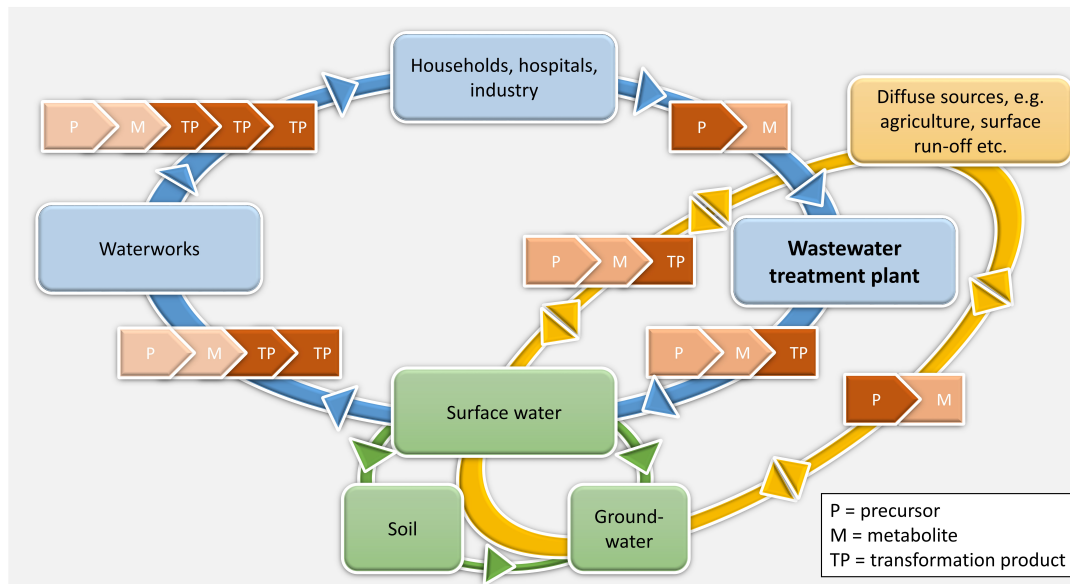
Figure 1.2: Origin and routes of micropollutants in the water cycle. Blue circle: WWTP route; Green circle: environmental route; Yellow circle: diffuse source route. Alignment of "TP" shows the different generations of TPs formed at the sequenced treatment and degradation steps

range of concentration for the micropollutants in WWTP effluents is usually quite high with micropollutants being detected in the upper µg/L range (e.g. metoprolol [8] and oxi-purinol [23]) to those in the low ng/L range (e.g. naproxen [8]). The WWTP effluent is discharged into a receiving water, mainly surface water. From there it reaches the soil as well as groundwater (Figure 1.2, green circle) [16, 22] and in all three compartments further biotic and abiotic processes lead to transformations of the micropollutants. Since for the production of drinking water surface- or groundwater is mainly used which, in some cases, is impacted by WWTP effluents [24], the cocktail of precursors, metabolites and TPs of different transformation stages can reach the waterworks. Here, further treatment removes some of these micropollutants but also causes further transformations so that TPs might reach the consumers. However, concentrations found in rivers, lakes and groundwater are usually very low (mid to low ng/L range, depending on the amount of wastewater and the dilution factor) and only those micropollutants can be detected in the drinking water which are present at elevated concentrations or that are recalcitrant to all treatment techniques applied in the chain. Nevertheless, some micropollutants already are detected in finished drinking water [9, 22]. WWTPs are not the only entry path of micropollutants: also by

diffuse sources such as agriculture, micropollutants can reach the water cycle (Figure 1.2, yellow circle). Run-off from agricultural land is of huge concern particularly after heavy rain events since substances such as pesticides then reach the water cycle without any pre-treatment and may directly enter source waters for drinking water production. Furthermore, when impaired or contaminated water is unintentionally used, for example for irrigation, this might result in crop uptake of micropollutants [20].

The occurrence patterns of micropollutants usually differ between countries [25] and even between regions within one country [8] and depend on the consumption of pharmaceuticals, usage numbers for pesticides and regulations concerning the allowance to use specific substances [22]. Taking pesticides as an example, there are substances which are not allowed for usage in Europe but may be applied in the USA or other countries. Other pesticides such as atrazine can still be detected in Europe although they are not allowed to be used due to their recalcitrant characteristics. However, although the occurrence pattern may differ, some micropollutants can be found worldwide. In a comparison of the occurrence of 71 micropollutants in Africa and Europe, Fekadu et al. (2019) [25] found regional differences in the occurrence of micropollutants which was explainable by different consumption patterns. For micropollutants detectable on both continents (e.g. carbamazepine, diazepam and venlafaxine), concentrations in Africa were much higher. In several regions of Africa there is no or only minimal wastewater treatment and the difference in concentration of micropollutants showed the immense importance of water treatment for the protection of freshwater resources.

Although there are several studies on the occurrence of micropollutants in the aquatic environment, information in the literature about the occurrence and fate of metabolites and TPs during wastewater treatment and in natural waters is scarce [22]. There is research focussing on the identification of TPs but mainly in lab-scale or pilot-scale experiments. Metabolites and TPs are usually not included in monitoring strategies in the field to assess the efficiency of a treatment technique. However, they are a crucial factor in risk analysis. In many transformation processes the structure of the precursor substance is only slightly altered and the TP might preserve the basic function of the precursor substance [9, 22]. Thus, even if the precursor were removed during water treatment, the (eco)toxicological effects might still be present. Moreover, the TP might show completely different characteristics compared to the precursor in terms of toxicity, mobility and persistence [9]. Furthermore, in some cases metabolites are present at higher concentrations than their precursor. The antibiotic erythromycin for example is not stable in water and is already

metabolized in the human body to a dehydrated metabolite. Thus, the occurrence of erythromycin must be monitored via the detection of its metabolite [22]. In an extensive review, Evgenidou et al. (2015) [22] summarized the recent literature about TP formation and detection. The vast number of TPs covered in this review emphasizes the necessity of their implementation into monitoring studies.

1.2 Wastewater management

Wastewater management has a long history which is closely linked to sanitation [26]. In the European context, while in ancient Rome sewer and drainage systems were used to carry away wastewater and use it as, e.g., fertilizer for agriculture, this infrastructure was not maintained in the medieval period. It took until the age of industrialisation and urbanisation that disposal of waste and wastewater became an important topic again. New sewer systems were built in the mid nineteenth century all over the world to collect wastewater in the cities in cesspits or cesspools and carry it away for discharge into streams or apply it in agriculture [26–28]. With growing cities and higher quantities of wastewater, treatment of the wastewater became an important task now. At the beginning of the 20th century, the concept of biochemical oxygen demand (BOD) was introduced and first attempts were made to reduce the BOD leading to the developments in primary and secondary water treatment [26, 30]. Later on, with better understanding of the impact of wastewater, more sophisticated analytical techniques and the continuous detection of new anthropogenic micropollutants in environmental water matrices, developments went towards more advanced treatment [26]. And finally, when the problem of water scarcity became more prominent due to increased water demand, the natural practices applied in sewage farms prior to the construction of WWTPs returned to mind [27] leading to the concepts of managed aquifer recharge (MAR).

1.2.1 Engineered wastewater management - Wastewater treatment plant

Initially, WWTPs were not designed for the removal of micropollutants [29]. Their main purpose was the elimination of solid matter and the reduction of BOD. Later, WWTPs were upgraded for nitrogen and phosphor removal [26, 30]. The degradation of micropollutants was a side effect of the techniques established. The fate of the micropollutants in WWTPs is influenced by several factors, such as characteristics of the specific micropollutant, the
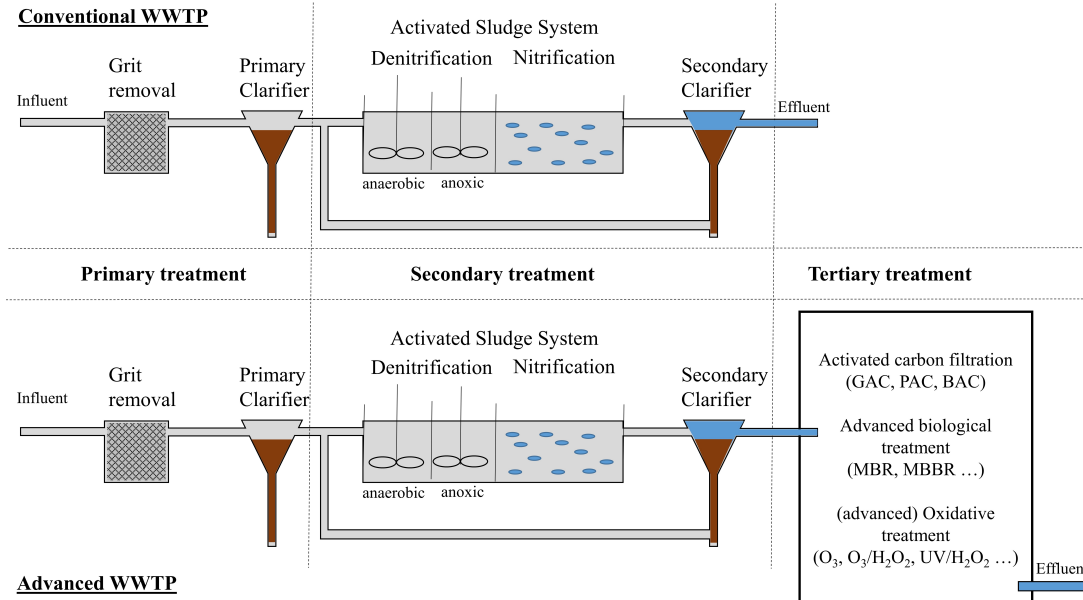
Figure 1.3: Scheme of WWTPs with conventional and advanced treatment. GAC, PAC, BAC: granulated, powdered, biologically activated carbon; MBR: membrane bioreactor; MBBR: moving bed biofilm reactor; O_3: ozone; H_2O_2: hydrogen peroxide; UV: ultraviolet

plant configuration and operating parameters [20].

1.2.1.1 Conventional wastewater treatment

Most WWTPs use conventional secondary treatment [17]. The conventional WWTP consists of a pre-treatement for the removal of solid matter and of a secondary, biological treatment [31]. The WWTP is separated into three parts (Figure 1.3): the primary clarifier, the biological treatment and the secondary clarifier. For the biological treatment there are mainly two established techniques: (i) attached growth techniques, for example trickling filters and (ii) suspended growth such as the activated sludge process [17, 31]. The main removal processes are biodegradation and sorption [20].

Biological trickling filters have been in use for water treatment for several decades. They consist of a three-part system with a distribution part where the wastewater flows in, the biofilm surface where the water trickles down and an aeration part [32]. Trickling filters were found not to be very efficient for the removal of micropollutants and further optimization of the technique led to the development of the moving bed biofilm reactor (MBBR), which is described in the next chapter. The more common system, particularly

in Europe, is activated sludge treatment [32]. In large aeration tanks the growth of a bacterial community takes place in the presence of dissolved oxygen, i.e. under aerobic conditions [32].

The extent of the attenuation by biodegradation depends on several parameters such as the solid retention time (SRT), hydraulic retention time (HRT), biomass concentration, pH, temperature, redox conditions and the chemical structure of the micropollutant [19, 31]. It was found that, in general, longer SRTs enhance the biological degradation due to longer contact times between the micropollutants and the microbial community. Additionally, the biomass concentration is increased, which makes the process more stable and resistant towards shock events [19, 20]. Furthermore, in some studies an influence of the temperature on the efficiency of biodegradation was observed with better removal at higher temperatures due to the enhanced microbial activity while temperatures above 45 °C had a negative effect [20, 31]. The pH value not only defines the ionization state of the micropollutants (which influences their solubility) but also affects the physiology of the bacteria [31]. Redox conditions are classified as anaerobic, anoxic and aerobic and play a crucial role in biodegradation [31]. Some micropollutants show biodegradability independent of the redox conditions but several studies indicated that aerobic conditions are more favourable for most micropollutants [31]. However, there are also micropollutants for which higher attenuation values were observed under anaerobic conditions [31]. Hybrid systems, consisting of zones with different redox-conditions therefore are nowadays under study to enhance the biodegradation [31].

The biodegradability of micropollutants is strongly influenced by their chemical structure and physico-chemical properties [33]. It is, for example, known that electron-withdrawing functional groups such as nitro-groups and halogens decrease the biodegradability while electron-donating substituents such as amines on aromatic rings can have a positive influence [33, 34]. A parameter for assessing the biodegradability of a micropollutant is its specific biodegradation kinetic constant k_{biol} which can be determined in lab-scale batch experiments and pseudo-first order kinetics are calculated by Formula 1.1 [19, 31, 35].

$$-ln\frac{c}{c_0} = k_{biol} * c_{ss} * t \tag{1.1}$$

Here, c_0 refers to the initial concentration of the micropollutant, c_{ss} is the concentration of suspended solids (given in grams, g_{ss}), and t is the incubation time (given in days, d). High k_{biol} values ($> 10 \, L/(g_{ss} \cdot d)$) were frequently observed for ibuprofen, caffeine

and estriol which are readily biodegradable [31]. Micropollutants such as carbamazepine and iopamidol show low values (< 0.1 L/(g$_{ss}$ · d)) [31] and are therefore recalcitrant in biodegradation.

Several studies reveal the inefficient removal for micropollutants in conventional activated sludge (CAS) treatment [36, 37]. Carbamazepine for example is a frequently detected pharmaceutical all over the world and was shown to be recalcitrant towards CAS treatment [20]. For some other substances, such as diclofenac, differing removal efficiencies were found in the range of no removal at all to moderate removal, depending on the WWTP itself [20]. Thus, efforts were made to upgrade existing wastewater treatment processes by advanced techniques.

1.2.1.2 Advanced wastewater treatment

As already mentioned, WWTPs have been identified as the main sources for water contamination with micropollutants. This is due to the fact that many substances are persistent towards biological degradation or they can only be degraded to a minor extent. Therefore, research is moving towards more advanced treatment techniques (Figure 1.3) [38], for example activated carbon filtration, advanced biological treatment and ozonation.

Activated carbon: In activated carbon (AC) filtration a wide range of micropollutants are removed from wastewater by adsorption onto the surface of the filter [36]. Adsorption techniques are viewed as simple and cost efficient techniques in wastewater treatment which can easily be integrated. However, during adsorption processes competition reactions may hinder the attenuation of micropollutants [36]; either different molecules compete for the same adsorption site or bigger molecules hinder the adsorption by blocking the pores. Thus, several characteristics of the filter (surface area, particle size, pore size distribution) influence its efficiency towards the attenuation of micropollutants. Mainly two forms of AC are used in wastewater treatment: i) powdered activated carbon (PAC) which can be dosed directly into the biological treatment unit and ii) granular activated carbon (GAC) which usually is applied as a separate unit in the form of a packed column [36]. Both forms mainly differ in particle size and, as indicated, in the way of application. But also the nature of the micropollutants affects the efficiency of the adsorption process; characteristics such as polarity, molecular weight, chemical structure and charge of the micropollutants have a significant effect on the process [36]. A further development of GAC is the so called biologically activated carbon (BAC) filter. Here, microorganisms accumulate on the

surface of the activated carbon which makes the filter biologically active [32]. Thus, in BAC micropollutants are attenuated by adsorption as well as metabolic reactions.

Optimized biological treatment: Next to the development of new techniques for water treatment, also optimization of the currently available methods is a topic of ongoing research. Since WWTPs are already equipped with a biological treatment step and since it is known that many substances are biodegradable, this step of water treatment could be optimized. The optimization of the biological treatment aims towards an increase of SRTs at comparable HRTs, i.e. the time of treatment is the same but the contact time between treated water and the microbial community is increased.

Membrane bioreactors (MBRs) combine the activated sludge treatment with a solid-liquid separation by a membrane [20]. The main removal processes for MBRs are biodegradation and sorption. The molecular mass of most micropollutants typically is less than 1000 Da and only low retention is provided by the membranes which typically are used in microfiltration and ultrafiltration (retention size > 10,000 DA) [20]. But a further barrier is generated by sludge deposits on the membrane, elongating the SRT compared to CAS systems [20, 32]. However, there is only little information about the exact underlying removal mechanisms for micropollutants and the formation of TPs although it is a widely accepted alternative to CAS and already in use in full-scale. It is assumed that for MBR the same parameters influence the efficiency as for CAS [20].

Biological trickling filters are common techniques for the conventional biological treatment [32]. However, they have several drawbacks such as an ineffective working volume [39]. Optimizing of this technique led to the invention of the moving bed biofilm reactor (MBBR) [39]. MBBRs mainly work on biodegradation. Here, a biofilm grows on a support medium and these MBBR disks can be loaded into the same system as used for CAS [20]. The design of the MBBR leads to higher SRTs compared to CAS. Although MBBR showed to be a promising tool for removal of micropollutants, most studies were performed in lab-scale or pilot-scale or focused on a small number of micropollutants. A drawback of MBBRs may be high energy costs since aeration is needed for mixing [39]. Mixing, however, is challenging: in the early stage of biofilm development the carriers are light, have a low density and float. As soon as they become attached with biomass they get heavier and mixing capabilities have to be improved. To assess the full potential of the treatment, stagnancy has to be avoided also in regions with low air-flow patterns [39].

Ozonation: Chemical oxidation with, for example, chlorine and ozone has long been used in water treatment for disinfection purposes [40] but soon it was noticed that these

practices lead to the formation of disinfection byproducts (DBPs) with high potential to cause severe health issues such as cancer. Thus, the processes were changed and oxidants such as chloramine or chlorine dioxide were used instead. However, with the ongoing detection of new micropollutants in WWTPs, techniques such as ozonation again were of interest due to their ability to react with a wide range of substances causing their degradation during water treatment.

The first reported application of ozonation in a drinking water treatment plant dates back to 1893 [36]. Later on the potential for attenuation of micropollutants was observed also for application in WWTPs. In ozonation there are two reaction pathways:

1. Direct reaction with the ozone molecule. This reaction type is highly selective to electron-rich moieties such as olefins, deprotonated amines or activated aromatics. Typically, reaction rate constants range over multiple orders up to 10^5 $M^{-1}s^{-1}$ [18, 29, 36, 41].

2. Indirect reactions with hydroxyl radicals (OH). The OH-radicals are generated from ozone decay as well as during reactions of ozone with effluent organic matter (EfOM). This reaction type shows low selectivity and much higher rate constant are observed than during direct reactions [18, 29, 36, 41].

The efficiency of the ozonation depends on properties of the micropollutants such as their chemical structure (e.g. the presence of electron-withdrawing or electron-donating substituents) and the acid dissociation constant pK_a (leading to pH dependent reaction rate constants) as well as on temperature and pH of the matrix [36]. The reaction rate constant of a specific micropollutant is a crucial factor for the efficiency of ozonation on that substance. Thus, many studies deal with the elucidation of reaction rate constants for specific substances in lab-scale experiments. Simultaneously, transformation products are identified and transformation pathways are proposed.

The most well-studied functional group in ozonation is the C-C-double bond, i.e. the reaction of ozone with olefins. It was first described by Criegee in 1975 [46] and thus was called the Criegee-mechanism. It involves the attack of the ozone molecule at the double bond, forming an ozonide, and the following cleavage of the double bond, leading to carbonyl compounds as reaction products (Figure 1.4). Olefins react readily with ozone and show high reaction constants, which could be observed with several micropollutants such as carbamazepine [42, 43]. However, the substituents to the olefinic moiety have a
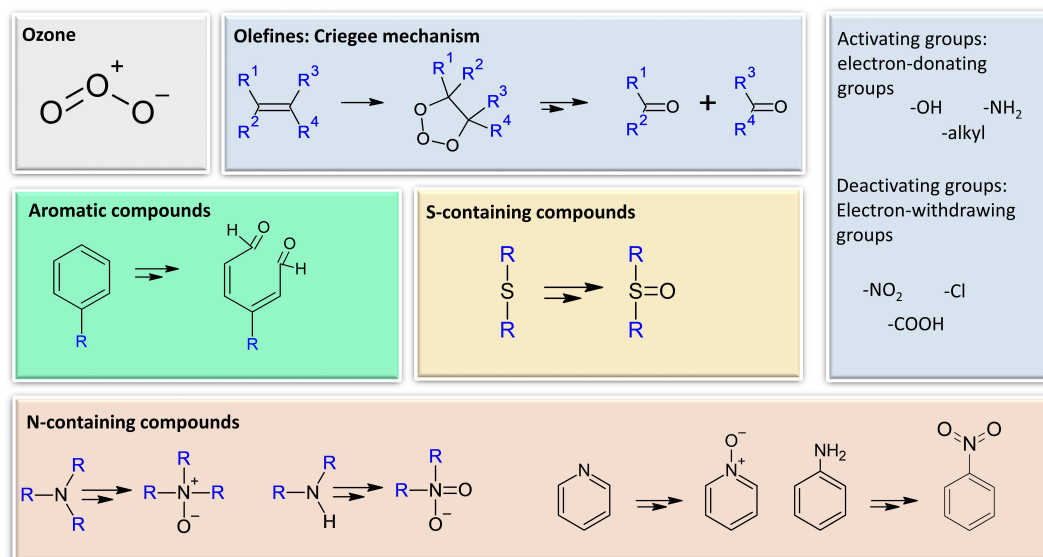
Figure 1.4: Proposed reaction mechanisms of the direct reaction of ozone with different functional groups [41–45]

huge influence on the reactivity. Electron-donating substituents such as -OH and -NH$_2$ increase reactivity while electron-withdrawing groups such as -NO$_2$, -COOH and halogens decrease reactivity [41] (Figure 1.4).

The reactivity of aromatic compounds also highly depends on the substituents to the aromatic ring since these have activating and deactivating characteristics (Figure 1.4). Activating groups, i.e. electron-donating groups, direct the reaction to the carbon at the ortho- and para-positions [41] and cause higher reaction rates. Deactivating groups, i.e. electron-withdrawing groups, direct reactions, if happening at all, to the deactivated meta-position and reaction rates are usually very low. For benzene derivates the order of reaction would be: nitrobenzene < chlorobenzene < benzene < toluene < phenol [41, 42]. Wibaut et al. [47] published a review in 1950 on the mechanistic aspects of ozone reaction with simple aromatics, studying the effects of various substituents on the reaction velocity. Since many micropollutants contain aromatic moieties, studies on the mechanism of degradation are still performed. An extensive collection of reaction rates and mechanisms is described in von Sonntag and von Gunten (2012) [42].

The reactions of olefins and aromatic compounds during ozonation have been studied well. But there are also functional groups for which there is only little information about

reaction mechanisms and reactivity. One of these understudied groups are the sulphur containing micropollutants. The few available studies on product formation in the reaction of sulphides with ozone yielded sulfoxides (Figure 1.4) leading to the assumption that oxygen atom transfer was the main mechanism in the reaction [42, 43].

Another understudied group are the nitrogen containing micropollutants [43, 44]. There was research on tertiary amines, e.g. tramadol, venlafaxine and clarithromycine, finding N-oxides as major TPs from the ozonation [43, 48, 49], as well as on N-heterocyclic aromatic compounds yielding N-oxides and degradation products based on the Criegee-mechanism [50]. It was proposed that the lone electron pair at the nitrogen is the point of attack in direct reactions of the ozone molecule with N-containing structures [42, 43]. However, until a recent study [44] the reaction mechanisms of aliphatic amines were mostly unknown except for the already mentioned tertiary amines and some secondary amines forming N-oxides as products [43]. Lim et al. (2019) [44] ozonated simple aliphatic amines (primary, secondary and tertiary). For primary and secondary amines the main TPs were nitro-compounds while for the tertiary amine the N-oxides dominated. Formation of a nitro moiety is also known in the ozonation of aromatic amines such as for anilines [45] but reaction might preferentially occur at the aromatic ring and not at the nitrogen.

At typically applied ozone dosages of 0.6 to 1.0 mg O_3/mg dissolved organic carbon (DOC) [51] no mineralization can be achieved for the micropollutants but they are transformed [18, 43]. TPs (formed from micropollutants) and disinfection byproducts (DBPs, formed from EfOM) play a crucial role in the ozonation process since some of them, for example bromate or *N*-nitrosodimethylamine (NDMA), exhibit higher toxicity than the precursor substances [29, 36]. Although it always is referred to as ozonation, pilot- and full-scale applications should be considered so-called advanced oxidation processes (AOPs). In ozone-based AOPs, the generation of hydroxyl radicals is promoted, for example by addition of hydrogen peroxide (H_2O_2) or other catalysts [52]. But also when ozonation is performed at elevated pH values, degradation of ozone forming hydroxyl radicals is promoted [52]. Since ozonation in wastewater treatment is applied at pH values in the range of 6 - 8, decay of ozone is enhanced and thus there will be a certain proportion of radical reactions. Other forms of AOPs are UV-based (UV/ H_2O_2, UV/O_3, UV/Cl_2), electrochemical, catalytic (Fenton process, photocatalytic) or physical (electrohydraulic discharge, ultrasound, microwave, electron beam). A comprehensive review on the different techniques including the formation of byproducts and data on energy efficiency was published by Miklos et al. (2018) [52].

1.2.2 Natural processes for wastewater management - Managed aquifer recharge

Reuse of wastewater gained popularity nowadays due to the increased demand for water and a lot of research is performed to implement water reuse schemes particularly in areas with increased water scarcity. Engineered but also natural solutions are considered and the basic principle of sewage farms finds growing interest. The different techniques of this intended recharge of water to aquifers fall under the term Managed Aquifer Recharge (MAR) and are summarized in Table 1.1 [53, 54].

Table 1.1: Types of MAR [2, 53, 54]

MAR technique	Description	Purpose
Aquifer storage and recovery (ASR)	Injection of water into a well for storage and recovery from the same well	storage
Aquifer storage transfer and recovery (ASTR)	Injection of water into a well for storage and recovery from a different well, generally to provide additional water treatment	Treatment and storage
Bank filtration	Extraction of infiltrated riverwater from a well or caisson near or under a river or lake to induce infiltration from the surface water body thereby improving and making more consistent the quality of water recovered	Treatment and storage
Dune filtration	Infiltration of water from ponds constructed in dunes and extraction from wells or ponds at lower elevation for water quality improvement and to balance supply and demand	Treatment and storage
Infiltration ponds	Ponds constructed usually off-stream where surface water is diverted and allowed to infiltrate (generally through an unsaturated zone) to the underlying unconfined aquifer	Storage
Percolation tanks	A term used in India to describe harvesting of water in reservoirs built in ephemeral waddies where water is retained and infiltrates through the base to enhance storage in unconfined aquifers and is extracted down-valley for town water supply or irrigation	Storage
Rainwater harvesting	Roof runoff is diverted into a well or a caisson filled with sand or gravel and allowed to percolate to the water-table where it is collected by pumping from a well	Storage
Soil aquifer treatment (SAT)	Treated sewage effluent, known as reclaimed water, is intermittently infiltrated through infiltration ponds to facilitate nutrient and pathogen removal in passage through the unsaturated zone for recovery by wells after residence in the aquifer	Treatment and storage
Sand damns	Built in waddies in arid areas on low permeability lithology, these trap sediment when flow occurs, and following successive floods the sand dam is raised to create an "aquifer"which can be tapped by wells in dry seasons	Storage
Underground dams	In ephemeral streams where basement highs constrict flows, a trench is constructed across the streambed keyed to the basement and backfilled with low permeability materials to help retain flood flows in saturated alluvium for stock and domestic use	Storage
Recharge release	Dams on ephemeral streams are used to detain flood water and uses may include slow release of water into underlying aquifers, thereby significantly enhancing recharge	Storage

While most of the techniques are intended for storage purpose only, ASTR, bank fil-
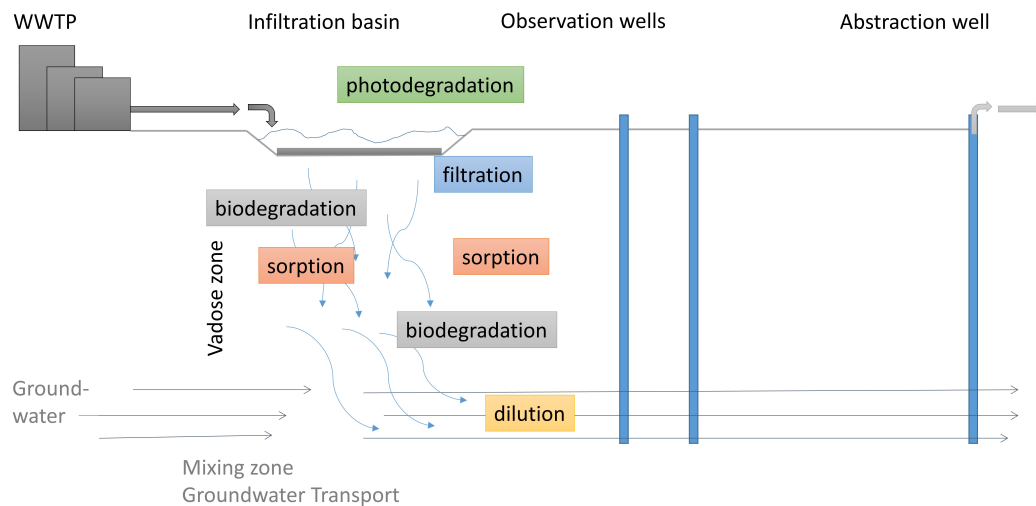
Figure 1.5: Scheme of the SAT process and associated attenuation mechanisms. Adapted from [56]

tration, dune filtration and SAT are so-called water treatment-type MAR techniques [2]. These make use of natural attenuation processes during percolation of the water through the soil to improve the water quality. In SAT techniques (as well as in constructed wetlands), reclaimed water is used as feed water [2, 7, 53–55]. Effluent of a WWTP is transferred to a spreading basin, the water infiltrates through a thin layer of biologically active soil (about 1 m), then percolates through the vadose zone (depending on the site and groundwater level, 3 - 30 m) and remains in the aquifer for several months up to years before it is extracted for its intended use (Figure 1.5) [55, 56].

Physical, chemical and biological processes occur during soil passage through the vadose (unsaturated) zone of the soil. The most important removal mechanisms are biodegradation and sorption [7, 28, 33, 57, 58]. The biological degradation in soil is similar to the mechanism in WWTPs. However, it is highly dependent of the metabolic capability of the site-specific microbial community and of parameters such as redox conditions, temperatures and HRT [58]. The pore size of the soil defines the ability of transport and water storage [3], which in turn affects the microbial community in terms of nutrient and oxygen supply and thus influences the bacterial activity. Fichtner et al. (2019) [3] found that optimal growth of the bacterial community is achieved if 60% of the pore space is

filled with water. This was the case for soils with a mean pore diameter of about 230 µm (medium-sized pores).

For the ability of a micropollutant to sorb to sludge or soil, the physico-chemical properties are of huge importance [31]. There are mainly two forms of sorption: i) hydrophobic partitioning, i.e. hydrophobic affinity of non-polar micropollutants to soil organic matter and ii) physical sorption, i.e. sorption by electrostatic forces [33, 58]. The organic carbon partition coefficient K_{OC} and the octanol-water partition coefficient K_{OW} can be used as indicative parameters for hydrophobic interactions: non-polar micropollutants with a log $K_{OW} > 4$ are most likely to sorb to soil [31, 33]. This assumption is not applicable for physical sorption of ionic compounds. Here, the pK_a of the micropollutant as well as the pH of the soil and water have to be considered since mainly ionic interactions are responsible for sorption [33, 58]. Micropollutants being positively charged at environmental pH values, such as atenolol and clarithromycin, easily sorb onto sludge and soil [31] due to the negative charges at their surfaces. These physico-chemical processes, i.e. cation exchange and sorption, have a limited capacity and breakthrough of micropollutants can occur after longer operation time when the sorption capacity is exhausted and the micropollutants are not retarded anymore [28].

Martinez-Hernandez et al. (2016) [59] studied the role of sorption and biodegradation for five different micropollutants (acetaminophen, carbamazepine, caffeine, naproxen and sulfamethoxazole) during soil passage in batch-experiments. They found that sorption played a key role for the removal of certain micropollutants that are able to sorb (e.g. caffeine and sulfamethoxazole) and that biodegradation was also associated with this sorption. However, micropollutants such as naproxen and carbamazepine showed no ability to sorb and only minor biodegradation was observed at the formation of TPs. He et al. (2016) [60] studied the effect of different operating conditions (packing material, HRT) on the removal of micropollutants. They selected a set of substances (42 in total) with different physico-chemical properties (K_{OC}, pK_a, presence of COOH) to also evaluate the relationship between removal and operating conditions by means of substance properties. The tested soils had different characteristics concerning total organic carbon (TOC) and cation exchange capacity. They observed that for readily biodegradable substances the packing material had no influence on the removal efficiency, while for antibiotics soils with high TOC and cation exchange capacity enhanced sorption. Removal of most micropollutants was increased with longer HRT and vadose conditions. Kodesova et al. (2015) [61] and Chefetz et al. (2008) [62] studied the sorption of seven micropollutants in thirteen dif-

ferent soils. For substances such as sulfamethoxazole they found positive correlations to soil acidity, while sorption of other substances such as trimethoprim and carbamazepine correlated to soil organic matter and cation exchange capacity.

Further attenuation processes in SAT are photodegradation, filtration and dilution [7, 58]. Photodegradation can occur directly to the micropollutants (e.g. for diclofenac) or indirectly by reactive species formed by solar radiation (e.g. for carbamazepine and sulfamethoxazole) [63]. However, photodegradation only happens in open water ponds and is particularly relevant in summer or areas with high solar radiation. Filtration, mainly occurring in the top layer of the soil, removes suspended matter such as algae [3, 28]. This necessitates the periodical clearing of the recharge basin. Often, in constructed basins, a filter layer such as technical sand is used which can be renewed during drying periods. Dilution occurs by the transfer into the groundwater stream.

In SAT systems, as well as in all MAR systems containing a soil passage, several parameters influence the efficiency of water purification, for example site characteristics (feed water quality, hydrogeological conditions, residence time), microbial community as well as wetting and drying cycles. But also the physico-chemical properties of the micropollutants and environmental conditions (temperature, moisture content, organic carbon, dissolved oxygen (DO) content) are of importance [7, 33, 55, 57, 58, 60, 64]. In general, oxic conditions in the upper soil layer followed by anoxic conditions with varying redox conditions were found to enhance removal efficiency for a variety of micropollutants [33, 58, 64]. With a set of compounds with low molecular weight, Rauch-Williams et al. (2010) [64] studied the effect of abiotic vs. biotic conditions and the influence of biodegradable dissolved organic carbon (BDOC) on the attenuation of micropollutants in column experiments. They found substance specific behaviour under most conditions but in general removal efficiencies were higher under oxic conditions at the top layer of the soil passage. Furthermore, they found a strong positive influence of increased BDOC that enhanced biomass growth and therefore biological degradation. Only two micropollutants, carbamazepine and primidone, remained persistent under the studied conditions.

SAT and other soil-passage-based MAR techniques showed to be a suitable and cost-efficient treatment step for reclaimed water with the advantages of improved water quality and seasonal and long-term water storage. SAT serves as an additional barrier for micropollutants and has the potential of being easily integrated with conventional and advanced WWTPs [7] but it has some limitations and drawbacks. It has high land use requirements, which has to be suitable, in terms of hydrogeological conditions, and well characterised, in

terms of residence and travel time [7, 58]. However, where the hydrogeological conditions are given and the feed water is of sufficient quality, SAT might be combined with agricultural use by spreading the reclaimed water onto agricultural fields from where it then recharges the aquifer. But as stated, the feed water quality must be sufficient for the use on crops and other agricultural products.

A further drawback is the long time-span from spreading to usage as drinking water: usually the water resides several months in the aquifer before it is withdrawn for treatment in waterworks for the drinking water production [65]. Thus, there are attempts towards a reduction in residence time of the reclaimed water in the aquifer. At a well-studied SAT-site in Israel, the Shafdan project, a short SAT (sSAT) of about 22 days retention time was tested and evaluated [65, 66]. Biologically active dual-media filtration and ozonation were used as pre-treatment steps to improve the quality of the feed water so that the shortage of the HRT in SAT had no negative effect on the elimination of micropollutants. Furthermore, by pre-treatment, another major disadvantage of SAT, the clogging of the infiltration field was reduced enabling longer operation times.

1.2.3   The multi-barrier approach

Experience from decades of research on treatment techniques, for wastewater as well as for drinking water, showed that there is no single technique which provides the performance needed to accomplish a sufficient water quality which is in accordance with regulations. Thus, a combination of techniques is needed, i.e. multiple barriers have to be implemented between the source of micropollutants to the, e.g., finished drinking water. In general, the alignment of wastewater treatment, discharge into surface waters and abstraction of water for drinking water treatment already is a multi-barrier approach. However, experience showed that the single steps in this cycle also have to be upgraded. An example for such a multi-barrier approach including wastewater reuse and groundwater recharge is shown in Figure 1.6. The WWTP consists of several treatment steps from pre-treatment to the final effluent, either in the conventional or in the advanced set-up (Figure 1.6). From the chapters above it is clear that the conventional set-up is not sufficient for the removal of micropollutants, thus, more barriers have to be implemented, for example ozonation followed by subsequent treatment. The most widely used hybrid, multi-barrier system here is a combination of conventional biological treatment and ozonation followed by subsequent biological treatment (e.g. sand filtration, SAT, MBR, MBBR) or adsorption tech-
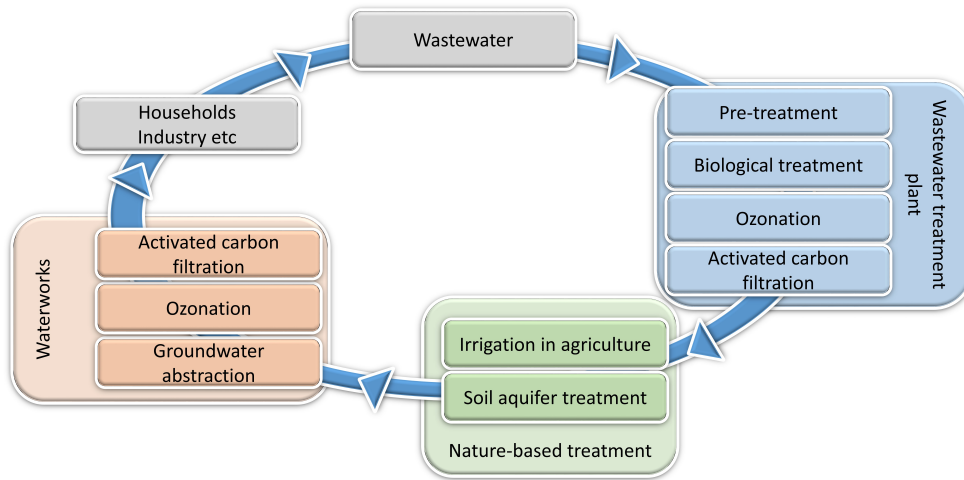
Figure 1.6: Example for a multi-barrier approach from the source of micropollutants via wastewater treatment to drinking water treatment

niques [18, 29, 67–69]. These systems aim towards attenuation of precursor substances as well as further transformation or removal of the formed TPs and DBPs to reduce the load of micropollutants and the (eco)toxicological risks to the receiving waters. If the treated water is intended to be used for reuse purposes, i.e. irrigation in agriculture or for groundwater recharge, an additional barrier is added by introducing the soil passage. Also at this stage the implementation of multiple barriers can be achieved. Regnery et al. (2016) [70] introduced the SMART concept which combines a short riverbank filtration step with a re-aeration followed by artificial recharge and recovery. This configuration improved the attenuation of micropollutants compared to conventional MAR systems and might be an upgrade option for conventional SAT or CW systems. Finally, ground- or surface water is abstracted and treated in another multi-barrier approach to achieve the finished drinking water.

The implementation of new treatment options into an existing treatment scheme is connected with increasing implementation and maintenance costs. Thus it has to be decided on a site-specific basis, if and how an upgrade to an advanced multi-barrier system is feasible. The suitability of the treated water for reuse and recharge purposes has to be evaluated [7, 71] and there is a substantial demand of space. Furthermore, there is still a

huge gap of knowledge concerning the fate of micropollutants and their TPs in advanced treatment and reuse schemes.

1.3 Water analysis - from target to non-target analysis

1.3.1 Developments in water analysis

Liquid chromatography-mass spectrometry (LC-MS) is becoming the most widely applied analysis technique in water analysis for the detection of micropollutants. This was possible due to the invention of electrospray ionization (ESI) and atmospheric pressure chemical ionization (APCI) which enabled the coupling of LC with MS [72]. Before, gas chromatography (GC) -MS was routinely used. From the early 1970s, GC-MS was applied in drinking water analysis for the detection and identification of contaminants. A huge amount of knowledge could be collected with these early instruments, for example the identification of the first DBP chloroform in 1974 [73] and the detection and identification of pesticides [74]. During this period the beginnings of what we now know as "non-target" analysis were developed since knowledge about occurring micropollutants was scarce and the identification of these "unknowns" had just begun [72]. Over time this task became easier since development of spectral databases such as NIST and Wiley went forward in the late 1990s. It soon became clear that GC-MS suffered a huge disadvantage when it came to water analysis: it was limited to volatile and nonpolar compounds. But it soon became evident that polar micropollutants such as pharmaceuticals, pesticides and industrial chemicals were of high importance in water analysis [75] and only could be analysed after time-consuming sample preparation including derivatisation to enable the analysis by GC [74]. Different technological developments, which occurred in parallel since the end of the 20$^{\text{th}}$ century, aided the progress in this field [72]:

- The aforementioned introduction of ESI and APCI

- The development of robust and sensitive high resolution mass spectrometry (HRMS) instruments such as the Oritrap and time-of-flight (TOF) mass spectrometry

- The development of openly accessible chemical compound databases (e.g. PubChem and Chemspider) as well as online mass spectral libraries (e.g. MassBank and mzCloud)

With the growing knowledge of micropollutants being present in the environment, there was the need for their quantification and what can be called target analysis methods emerged. Target analysis requires MS instruments with high sensitivity and selectivity to detect and quantify low concentrations of pre-defined micropollutants in a complex matrix background. For these purposes triple quadrupole (QqQ) instruments are widely used and LC-MS/MS methods with the monitoring of at least two transitions of each target micropollutant were developed [75]. In the example of the analysis methods of pesticides the developments in environmental analysis can be followed very well: first they were detected and identified by GC-HRMS methods, then quantified by GC-MS techniques, often after derivatisation due to their polarity and thermal instability. With the development of LC-MS techniques derivatisation was not necessary and due to more strict threshold values in water regulations, instruments and methods enabling a high sensitivity were needed for the quantification. Thus, LC-MS/MS methods were developed [74, 76]. With the findings of an increasing number of micropollutants in environmental waters, the trend went towards multi-residue analytical methods [17]. Tens to hundreds of compounds are analysed simultaneously within one chromatographic method. However, these methods have limitations in the amount of targets that can be analysed without the loss of accuracy or sensitivity due to too short analysis time [75]. Thus, researchers went a step back and aimed to reduce the target lists by the selection of indicator and surrogate substances that represent the majority of micropollutants in the environment [58, 77]. The selection of indicators must be site-specific and representative for the purpose. For example, for the qualitative determination of domestic wastewater in rivers, micropollutants can be analysed that are persistent during conventional wastewater treatment such as carbamazepine or primidone as intrinsic tracers [77]. Other micropollutants such as antihistamines or UV blocker might be used as indicators for seasonal variability [77]. However, there is only little agreement between research groups concerning the number of necessary indicators and the substances to be selected. Either way, target analysis requires knowledge about the relevant micropollutants to be monitored, based on available consumption, partitioning and degradation data.

Progress in the development of TOF-MS instruments as well as the Orbitrap and hybrid technologies such as quadrupole-TOF (QTOF) increased the detection and identification capabilities of these instruments and made them an important tool in modern water analysis [75]. By the use of these HRMS techniques some limitations of the target analysis methods are overcome and the analytical window in water analysis is widened [72, 75].

Non-target analysis is not based on detection of single transitions of pre-selected micro-pollutants but performs full-scan analysis on the sample with acquisition of fragmentation patterns based on data or information (in)dependant analysis. The obtained data can be searched for post-selected targets (suspect screening) and real unknowns [75]. Compared to target analysis methods, non-target analysis requires a higher degree of data processing [72, 78, 79]. After the data acquisition, automated peak detection and exact mass filtering is performed (peak picking) for each sample leading to lists of so-called features, i.e. the unique combination of exact mass and retention time [80]. Based on the chromatographic data such as retention time and peak shape, a componentisation is performed to group associated features such as isotopes and adducts [79]. By an alignment step the feature lists of several samples are combined to gain a full list over all analysed samples. These steps usually produce a huge number of features, and thus, certain data reduction steps are necessary which include the application of a blank correction (subtraction of detected features in blank samples) and rule based filters such as deletion of isotopes and adducts. The features can be annotated by in-house databases and by a suspect screening to mark already known micropollutants. The remaining features represent the real unknowns and the list usually still contains hundreds to thousands of features. For subsequent identification of these, further data reduction steps have to applied, e.g. priorisation steps such as data-driven (e.g. temporal or spatial profiles) or experiment-driven (e.g. persistence, elimination/formation over a process) priorisation [72] since structure identification requires a high amount of work which could last several weeks to months.

1.3.2 Identification of unknowns

Non-target screening provides information about the exact mass, the retention time, the MS^1 and the MS^2 spectra. These can be used for the identification of the substance but it is still a difficult task to tackle. It is time-consuming, not fully automatable and there is no guarantee of success. However, the increasing work in this field, the development of spectral libraries and the discovery of basic rules on fragmentation ease the procedure of structure elucidation compared to the beginnings in water analysis. Two types of unknowns are distinguished [81]:

- The real unknowns, e.g. masses that are detected for the first time and there is no background information about the source or nature of that mass that might aid the identification

- Targeted unknowns, e.g. transformation products of known micropollutants which are identified in laboratory studies

Although there is background information for the second type of unknowns, since they are derivatives of a known substance with a known structure and a known fragmentation scheme, the identification still might be difficult in case of rearrangements of the structure upon transformation. For both types of unknowns the same scheme of structure identification can be followed, which nowadays is a combination of the classic "by-hand" method and the usage of tools provided on the internet.

The first step is the correct assignment of the molecular ion [81]. In modern non-target analysis the molecular ion usually is given from the peak detection. However, in ESI, adducts are detected with the protonated (positive ESI) or deprotonated (negative ESI) molecule being the most simple adduct. In addition, other adducts (e.g. sodium, formiate etc.) can be formed too, but also the detection of a M^+- or M^--ion is possible in case there already was a charge before ionization [81]. This has to be kept in mind for the second, even more important step: the assignment of the molecular formula. The molecular formula can be obtained by the exact mass of the neutral substance by using tools provided on the internet, e.g. ChemCalc. However, some basic rules have to be followed described by Kind and Fiehn (2007) as the Seven Golden Rules [82]. They include restrictions on element numbers, filtering by the isotopic pattern and element ratio checks to find the most probable molecular formula. The isotopic pattern provides a good measure for the presence of a heteroatom such as chlorine or bromine. Not included in the Seven Golden Rules is the classical nitrogen rule which states that an odd nominal molecular mass contains an odd number of nitrogen atoms. This rule can only be applied to nominal masses and might cause false results of exact masses [82]. However, for targeted unknowns such as transformation products from nitrogen containing micropollutants this rule helps for fast determination on the loss of a nitrogen from of the molecule.

By the molecular formula many possible structures are obtained for an unknown. Observation of the fragmentation pattern here might give some more information about specific functional groups. Over several decades of mass spectrometric analysis, general rules for the fragmentation were established to assist interpretation of the spectra. Most of them are based on electron ionisation (EI) fragmentation reaction [81, 83] which are more specific than ESI-fragmentation. But also for ESI-MS there is ongoing work to assign specific neutral losses and characteristic fragments for several functional groups [81, 84]. Next

to this "by-hand" approach for the structure identification, several spectral databases are available nowadays for LC-MS data. The exact masses and the fragmentation patterns can be searched in databases such as mzCloud or MassBank to find substances that fit the pattern. By the in-silico fragmentation tool MetFrag, huge databases such as PubChem but also more specific ones such as the KEGG or NORMAN libraries can be searched and the algorithm provides a measure for the fit of observed and theoretical fragmentation.

However, although there are, compared to earlier times, improved tools and databases for the identification of newly detected micropollutants, this remains a difficult task which still requires expert knowledge on the plausibility of proposed structures.

1.4 Knowledge gaps

Within the last decades a lot of research was done on the identification of micropollutants, their fate during water treatment, formation of TPs and in turn their fate. But due to the immense number of chemicals in the market the development of new pesticides, pharmaceuticals etc. and the changing occurrence patterns of micropollutants in the environment there is still a huge knowledge gap.

TPs can be formed by biotic and abiotic processes during water treatment but also in the receiving waters and during drinking water production. Not only TPs should be viewed more closely but also metabolites which are formed in human or animal bodies, are excreted via urine or feces and which reach the water cycle by the same route as their precursors. For several pharmaceuticals, metabolites as well as TPs are known and some of them should have even a higher relevance than their precursors. However, in most monitoring and efficiency studies mainly precursors are included in the target methods while the metabolites and TPs are left out.

Since the metabolites and TPs are scarcely viewed, knowledge about underlying degradation mechanisms for some treatment techniques is scarce. Particularly natural processes such as SAT are still considered as "black-boxes"since only little is known about the degradation mechanisms in the soil. Most studies dealing with SAT and other MAR techniques applying a soil passage are done in lab-scale or pilot-scale column experiments with controllable settings and under ideal conditions. However, results differ when moving to full-scale applications since removal efficiencies for micropollutants not only depend on the substance's characteristics but also on the site-specific soil characteristics.

It is agreed that quality of the feed water for natural MAR techniques is a major

influence. Since it is known that the conventional secondary treatment of WWTPs does not efficiently remove micropollutants, advanced treatment usually has to performed. A widely used technique for water reuse in combination with SAT is ozonation. A wide range of micropollutants can be attenuated by ozonation, directly or indirectly. Particularly for olefins and activated aromatics a lot of research was already done on removal kinetics and degradation mechanisms. However, for some functional groups, for example aliphatic amines there is still a lack of knowledge concerning degradation mechanisms and formation of TPs. This knowledge is required to evaluate the overall efficiency, e.g., of the ozone-SAT combination for the attenuation of micropollutants.

1.5 Objectives

The goal of this work was to implement the simultaneous analysis of precursors and TPs in monitoring studies by the development and validation of a targeted multi-residue analysis method, to assess the fate of these precursors and TPs during natural treatment techniques in pilot- and full-scale and to study the efficiency of ozonation on the removal of micropollutants containing an aliphatic amine moiety.

As a first step, a literature survey had to be performed to prepare a list of frequently detected micropollutants in WWTP influents, effluents and surface waters. For each of the selected micropollutants it had to be searched for already known metabolites and TPs, biological and oxidative ones, for which reference standards were commercially available. A multi-residue analysis method for the detection of these micropollutants by LC-ESI-MS/MS had to be developed and validated. Scheduled multiple reaction monitoring (sMRM) should be used due to the high number of analytes. For this kind of analysis parameters such as the cycle time and the scan time have to be defined by the analyst and these parameters influence the quality of analysis. Thus, the effect of varying the parameters as well as the resulting dwell time for analysis had to be determined prior to the validation of the multi-residue method for the detection of the selected micropollutants in WWTP influent, effluent, surface water and bank filtrate.

In the second part of the work this multi-residue analysis method was applied to samples from two natural treatment techniques: i) an engineered above-ground sequential biofiltration (SBF) system with intermediate aeration and ii) a full-scale SAT system. Since the target list of the multi-residue analysis method contained substances with different physico-chemical properties, the fate of differently charged micropollutants should be followed. In addition, it was aimed towards the gathering information about underlying degradation mechanisms by the simultaneous analysis of TPs to aid the understanding of the natural treatment techniques. Furthermore, suggestions for a reduction of the target list to a smaller set of process-based indicator substances was made by considering the physico-chemical properties of the micropollutants and their removal in the studied systems.

Finally, ozonation experiments on a nitrogen-containing micropollutant was performed. A micropollutant was selected, which frequently was detected at elevated concentrations in the first and second part of this work and for which there is nearly no further information about occurrence and attenuation during water treatment. The pharmaceutical sitagliptin was selected, since it contains an aliphatic primary amine moiety and thus was used as

a role model for other micropollutants containing such a functional group. The fate of sitagliptin during ozonation was studied in lab-scale experiments with elucidation of the pH-dependent reaction kinetics and identification of TPs. Furthermore, the fate of sitagliptin and its identified TPs was also followed in pilot-scale ozonation plant with subsequent MBBR polishing. Thus, also preliminary information about the fate of the TPs during subsequent biological treatment was assessed.

1.6 Thesis Outline

Quantification of more than 150 micropollutants including transformation products in aqueous samples by liquid chromatography-tandem mass spectrometry using scheduled multiple reaction monitoring

Chapter 2 describes the development and validation of a multi-residue analysis method. This target method was developed for the monitoring of pre-selected micropollutants as well as already known metabolites and TPs, for which reference standards could be obtained commercially. The method was validated for different water matrices (influent and effluent of WWTPs, surface water and groundwater from a bankfiltration site).

Indirect Potable Reuse: removal efficiencies in sequential biofiltration (SBF) and soil aquifer treatment (SAT) and deduction of indicator substances

In chapter 3, the multi-residue analysis method was applied to samples from a pilot-scale sequential biofiltration (SBF) application and a full-scale soil aquifer treatment (SAT) site to study the fate of trace organic chemicals and their metabolites and TPs. The results were compared to each other to obtain information about underlying attenuation mechanisms and suggestions were made for the selection of performance-based indicator substances.

Ozonation of sitagliptin: removal kinetics and elucidation of oxidative transformation products

Chapter 4 shows the ozonation of the antidiabetic drug sitagliptin. In lab-scale experiments the pH dependant removal kinetics were determined and transformation products were identified. Furthermore, by a monitoring campaign at a pilot-scale ozonation plant, results from the lab-scale experiments were transferred to a realistic application.

Final Conclusion

The main outcomes of the previous chapters will be discussed in chapter 5. A final conclusion will be drawn, discussing the aspects for future research.

Chapter 2

Quantification of more than 150 micropollutants including transformation products in aqueous samples by liquid chromatography-tandem mass spectrometry using scheduled multiple reaction monitoring

N.Hermes, K.S. Jewell, A. Wick T.A. Ternes

Abstract

A direct injection, multi residue analytical method separated in two chromatographic runs was developed utilizing scheduled analysis to simultaneously quantify 154 compounds, 84 precursors and 70 transformation products (TPs)/metabolites. Improvements in the chromatographic data quality, sensitivity and reproducibility were achieved by scheduling the analysis of each analyte into pre-determined retention time windows. This study shows the influence of the scan time on the dwell time and the number of data points per peak as well as the effect on the precision of analysis. Lowering the scan time decreased dwell time to a minimal value, however, this had no negative effects on the precision. Increasing the number of data points per peak by decreasing the scan time led to more accurate peak shapes. A final set of parameters was chosen to obtain a minimum of 10 data points per peak to guarantee accurate peak shapes and thus reproducibility of analysis. A validation of the method was performed for different water matrices yielding very good linearity for all substances, with limits of quantification mainly in the lower to mid ng/L-range and recoveries mainly between 70 and 125% for surface water, bank filtrate as well as influents and effluents of wastewater treatment plants. The analysis of environmental samples and wastewater revealed the occurrence of selected precursors and TPs in all analysed matrices: 95% of the compounds of the target list could be quantified in at least one sample. The relevance of TPs and metabolites such as valsartan acid and clopidogrel acid was also confirmed by their detection in all aqueous matrices. Wastewater indicators such as acesulfame and diclofenac were detected at elevated concentrations as well as oxypurinol which so far were not in the focus of monitoring programs. The developed method can be used for rapid analysis of various water matrices without any sample enrichment and can aid the assessment of water quality and water treatment processes.

2.1 Introduction

Intensive studies during the last decades have found that contamination of the aquatic environment by anthropogenic organic micropollutants is wide-spread. Several reviews summarize the findings and outline challenges and future trends [22, 85–93]. Pharmaceuticals, ingredients of personal care products, pesticides, and industrial chemicals are discharged into the aquatic environment by several routes, including effluents of municipal and industrial wastewater treatment plants (WWTPs), sewer overflows, inappropriate disposal of substances, as well as various diffuse sources. As a consequence, these anthropogenic organic substances can be detected in surface water, ground water and even in drinking water [86, 87, 89, 93, 94]. For certain micropollutants harmful effects on biota and humans are known [85, 95–97]. For many micropollutants no regulations exist, although a potential risk to health and environment cannot be ruled out. These micropollutants are also named contaminants of emerging concern (CECs) [85, 87, 90, 98, 99]. The term refers to precursor compounds as well as human metabolites and transformation products (TPs). Many studies primarily focus of the analysis of precursor substances if the removal of CECs has to be determined in technical processes. However, during water treatment processes as well as in environmental matrices, TPs may be formed by biotic and abiotic processes. The TP formation is relevant for process evaluation, since TPs can have a higher toxicity and/or are often more persistent and mobile than the precursor substances [22, 85, 86, 92, 93, 98, 100]. Evgenidou et al. (2015) [22] published a review about the presence of TPs of pharmaceuticals and illicit drugs in wastewater. The number of reported TPs already showed the necessity of including these substances into multi-residue analysis methods. Petrie et al. (2015) [91] identified the determination of metabolites and TPs as an understudied field, since most studies focus on precursor substances or include only a small number of metabolites [37, 63, 100–116]. Due to continuously improving sensitivity in mass spectrometry, the number of CECs that can be found in the aquatic environment is permanently increasing [86, 87, 93, 98, 99]. Multi-residue methods based on liquid chromatography-mass spectrometry (LC-MS) are applied to simultaneously monitor and quantify an increasing number of CECs. A common instrument configuration used for this purpose is tandem quadrupole MS (LC-ESI-QqQ-MS), referred to here as LC-MS/MS. For target analysis via LC-MS/MS, in general multiple reaction monitoring (MRM) is used. Liu et al. (2011) [117] showed the advantages of a scheduled MRM (sMRM) algorithm over conventional MRM (cMRM). By scheduled MS analysis, i.e. measuring each compound

only during a defined time window with automatic adjustment of the time each transition is monitored (dwell time, t_{Dwell}), the time needed to complete all transitions (cycle time, t_{Cycle}) can be considerably reduced to achieve a better signal-to-noise (S/N) ratio and a higher number of data points per peak. This way the number of analytes can be increased, enabling the analysis of more than 500 CECs in one LC-MS/MS run [115]. The limiting factor of QqQ-instruments is the number of contemporary transitions as well as the limits of the instrument itself regarding detection frequency and lowest possible t_{Dwell}, since these determine t_{Cycle} and number of data points per peak. In general, t_{Dwell} should be as high as possible to increase the sensitivity of the detection method. Thus, t_{Cycle} should be as high as possible, too. However, for accurate recording of chromatographic peaks about 10 data points are required [118] and with the chosen t_{Cycle} this requirement must be fulfilled to obtain a sufficient number of data points even for very narrow peaks. Hence, a major challenge of multi-residue LC-MS/MS methods based on sMRM is to adjust the time windows according to the peak width of each compound and to find a compromise for the t_{Cycle} to maximize the t_{Dwell}, while also enabling sufficient data coverage for each chromatographic peak.

The objective of this study was the development of an LC-MS/MS multi residue analysis method, split into two chromatographic runs, for analysis of 154 CECs and thereby considering also the optimal parameters for the sMRM algorithm. To the best of our knowledge, no literature can be found showing the influence of the definable parameters such as t_{Cycle} on analysis results in practice.

The selected CECs include both precursors and metabolites/TPs of substances of different classes, including pharmaceuticals, pesticides, personal care products and industrial chemicals. The target list contains 84 precursors and 70 metabolites/TPs for which standard solutions are commercially available (with the exception of iopromide-TPs, which were generated according to Schulz et al. (2008) [119]). The influence of t_{Cycle} and the number of contemporary transitions on t_{Dwell} as well as on the number of data points per peak and precision of analysis was evaluated. Validation of the developed analytical method was performed and the applicability on different water matrices (e.g. surface water, bank filtrate, WWTP influent and effluent) was confirmed by the analysis of environmental water samples from German WWTPs as well as rivers and streams.

2.2 Experimental

2.2.1 Chemicals and reagents

A list of the 154 target compounds including the corresponding CAS registry number, supplier and analysis parameters is given in Table A1.1-A and a list of the labelled internal standards (IS) is given in Table A1.1-B. The precursors (84) were selected on the basis of their frequency of detection in literature studies, persistence in urban water cycles as well as their suitability as indicators for the evaluation of water treatment processes [21, 120]. The selection of TPs and metabolites (70) was performed by a literature survey on known metabolites as well as biological and oxidative TPs for the selected precursors. For each substance an individual stock solution at a concentration of 1 g/L was prepared in an appropriate solvent (mainly methanol). Grouped standard solutions of 20 - 30 analytes per group were prepared by dilution of the stock solutions to a concentration of 1 mg/L in methanol. Of those standard solutions all other dilutions were made. Three stock solutions of the internal standards were prepared in methanol at a concentration of 0.1 g/L for each labelled standard. All standard solutions were stored at $-20\,°$C. LC-MS grade methanol and acetonitrile (both LiChrosolv) were supplied by Merck (Darmstadt,Germany). Formic acid and acetic acid as eluent additives for LC-MS were purchased from Sigma Aldrich (Seelze, Germany).

2.2.2 LC-MS/MS

An LC 1260 infinity series by Agilent Technologies (Waldbronn, Germany) was used, consisting of a degasser, binary pump, isocratic pump, autosampler and column oven. Chromatographic separation was achieved on a Zorbax Eclipse Plus C18 column (Narrow Bore RR, 2.1 x 150 mm, 3.5 µm) with a Zorbax Eclipse XDB-C8 Guard Column (2.1 x 12.5 mm, 5 µm), both obtained from Agilent. Aliquots of 80 µL of each sample were injected into the LC-MS/MS system. Two detection methods were used: method 1 (M1) used 0.1% formic acid (A) and acetonitrile (B) as mobile phase. The gradient started at 100% A for 1 min, decreased to 80% for another minute and then was further decreased to 0% for 14.5 min. This was kept for 5.5 min. Within 0.1 min A was increased to 100% and this was kept until the end of analysis. Method 2 (M2) used 0.1% acetic acid (A) and acetonitrile (B) as mobile phases. The gradient started at 98% A, the rest of the gradient was the same as for M1. Total analysis time for both methods was 25 min. Analytes were assigned to the

detection methods by preliminary experiments on the response and peak widths.

Mass spectrometric analysis was performed with a QqQ-MS (Sciex Triple Quad 6500+) with an ESI source. In M1 positive ionization was used, M2 switched between the polarities. The analysis was performed with the advanced scheduled MRM algorithm. For each substance two transitions were monitored for quantification and confirmation purposes. For tramadol and its TPs (except for tramadol-N-oxide) only one transition could be monitored due to poor fragmentation. For all labelled internal standards one transition was used. Optimization of declustering potential (DP) and collision energy (CE) for each mass transition was performed by direct infusion of a standard solution of the individual compounds. Retention times and peak widths were determined in advance by LC-MS/MS analysis of mixed solutions of a smaller number of substances without scheduling. By the results, the detection windows (t_{Window}) for scheduling were defined. A complete list of mass transitions and MS parameters as well as retention times and detection windows is given in A1.1-A. It should be noted that in the control software (Analyst 1.6.3) a target scan time (t_{Target}) has to be defined. For methods using only one polarity such as M1 t_{Target} equals t_{Cycle}. For methods like M2 t_{Target} is defined for each polarity and t_{Cycle} is the sum of both. During MS method development three different t_{Target} were tested for both methods. The final set of sMRM parameters is given in Table 2.1.

Table 2.1: sMRM parameters for both methods; Settling time: time to switch between the polarities; Pause time: time between analysis of two MRM transitions

Parameter	Method 1 (M1)	Method 2 (M2)
Polarity	positive	positive + negative
Target Scan time (t_{Target})	0.3 s	0.2 s each
Settling time	-	15 ms
Pause time	5 ms	4 ms
Number of mass transitions	235	206

Instrument control and data acquisition were performed in Analyst 1.6.3, for the evaluation and integration of the chromatograms and peaks, MultiQuant 3.0.2 was used. The calculation of the contemporary number of transitions, the actual t_{Target}, t_{Dwell} and the number of data points per peak was performed with the software R 3.3.0. For this, the extracted ion chromatograms (EICs) of all transitions of a standard solution were exported from the Analyst software and merged into one table. In R the average frequency (f) of data acquisition within each detection window was calculated by:

$$f\left[s^{-1}\right] = \frac{data\,points}{(t_{max} - t_{min})} \tag{2.1}$$

t_{max} and t_{min} are the actual start and end points of each transition window. From this frequency and the peak widths the number of data points per peak could be calculated according to:

$$data\,points\,per\,peak = Peak\,width\,[s] * f \tag{2.2}$$

The EIC table was sorted by time and the actual $t_{Target,act}$ could be calculated by the time difference between one data point to the next. For the switching method, the settling time, i.e. the time to switch between the polarities, was subtracted from $t_{Target,act}$. For each time point in the sorted EIC table the number of analysed transitions were counted giving the contemporary transitions. The t_{Dwell} could then be calculated as:

$$t_{Dwell}\,[ms] = \left(\frac{t_{Target,act}\,[ms]}{contemporary\,transitions}\right) - pause\,time\,[ms] \tag{2.3}$$

2.2.3   Validation

Validation was performed for the application of the method to bank filtrate, surface water and WWTP influent and effluent. LOQ determination and recovery was performed on at least three replicates per matrix of samples taken at different locations. For all analysed influent samples, concentrations of several substances were expected to exceed the spiking and calibration range. Thus, the influent samples were diluted by a factor of four prior to spiking and the LOQ values as well as the recovery values were determined in these diluted samples.

Calibration samples were prepared in the concentration range of 0.1 - 15,000 ng/L (17 points including 0 ng/L) in ultra-pure water. For acesulfame it was 20-fold and for the iodinated X-ray contrast media (RCMs), their TPs and oxypurinol it was the ten-fold concentration. The internal standards were added to a final concentration of 200 ng/L (acesulfame 4000 ng/L, contrast media and oxypurinol 2000 ng/L) in each calibration standard.

Precision was determined at two levels of the calibration: 100 and 1000 ng/L (acesulfame: 2000 and 20,000 ng/L; RCMs and oxypurinol: 1000 and 10,000 ng/L). For the intra-day measurement the calibration solutions were injected three times each. For the

determination of the inter-day precision the calibration samples were injected on six non-consecutive days. Precision was determined as the relative standard deviation (RSD) of the multiple injections.

Limit of quantification (LOQ) was determined for bank filtrate, surface water, WWTP influent and effluent. A signal-to-noise ratio (S/N) of 10 was used for the most sensitive transition and confirmed by a S/N of 3 for the second transition. Spiked matrix samples at spike levels 10 and 100 ng/L as well as the non-spiked samples were evaluated. The software PeakView 2.2 was used to determine the S/N ratios based on the intensities of noise and peaks in the samples and the corresponding concentrations at an S/N ratio of 10 and 3 were calculated.

Recovery experiments were performed on environmental samples spiked to a level of 100 and 1000 ng/L for each analyte (acesulfame 2000 and 20,000 ng/L, contrast media and oxypurinol 1000 and 10,000 ng/L). IS was added to a final concentration of 200 ng/L (acesulfame 4000 ng/L, contrast media and oxypurinol 2000 ng/L). The relative recovery as a measure of the accuracy was calculated as follows:

$$rel.Recovery\,[\%] = \frac{c_{sample,spike} - c_{sample}}{c_{spike-level}} * 100 \tag{2.4}$$

where $c_{sample,spike}$ is the concentration in the spiked sample, c_{sample} the concentration of the original sample and $c_{spike-level}$ the added concentration.

Since no sample preparation was used, the absolute recovery was used as a measure for the matrix effects (ME) and was calculated by the ratio

$$abs.Recovery\,[\%] = \frac{Area_{sample,spike} - Area_{sample}}{Area_{calibrationspike}} * 100 \tag{2.5}$$

where $Area_{sample,spike}$ is the peak area of the spiked sample, $Area_{sample}$ the peak area of the original sample and $Area_{calibration,spike}$ the peak area of the calibration sample corresponding to the spike level. A value higher than 100% indicated signal enhancement, while a value below 100% indicated signal suppression.

2.2.4   Analysis of environmental samples and wastewater

The method was applied to environmental samples of different matrices: surface water, bank filtrate, WWTP effluent and influent. Details on the samples are given in Table 2.2. The samples were filtered (Whatman, glass fibre filters, pore size 0.45 µm) and stored at

$-20\,°C$ until analysis. The influent samples were diluted with ultrapure water by a factor of four. A mix of internal standards was added prior to analysis, yielding a concentration of 200 ng/L for each IS (acesulfame 4000 ng/L, contrast media and oxypurinol 2000 ng/L).

Table 2.2: Description of environmental samples analysed; all samples taken in Germany; bio = biological treatment, PAC = Powered activated carbon, GAC = granulated activated carbon

Matrix	Sample type	Details
Surface water	grab samples	SW1: Landgraben (stream, Darmstadt)
(SW)	(n = 4)	SW2: Rhine (river, km 590.3, Koblenz)
		SW3: Moselle (river, km 2.0, Koblenz)
		SW4: Lake Tegel (lake, Berlin)
Bank filtrate	grab samples	(depth below ground/retention time/redox potential)
(BF)	(n = 3)	BF1: 12 m / 1 months / 238 mV
		BF2: 19 m / 3 months / 138 mV
		BF3: 25 m / 5 months / 120 mV
WWTPs	24h composite samples	WWTP1: influent + bio + PAC
	(n = 4)	WWTP2: influent + bio + GAC
		WWTP3: influent + bio

2.3 Results and discussion

2.3.1 Optimization of the scheduled MRM method

Due to the high number of substances to be analysed, the detection method was split into two chromatographic runs. Method 1 (M1) included 235 transitions and ran on positive ionization. Deviations of the retention times were below 0.2 s and peak widths were rather small (10 - 20 s). Therefore, for these substances relatively small detection windows (t_{Window}) of 40 s were sufficient for complete coverage of the chromatographic peaks, even for long sample series of more than 100 samples. Only for 8 transitions the t_{Window} was increased to 80 s due to relatively broad peak widths. Method 2 (M2) included 206 transitions and switched between the polarities. Also in M2, the majority of t_{Window} were set to 40 s. A further 18 transitions required higher t_{Window}, between 60 and 120 s.

The main challenge using the sMRM algorithm is that t_{Dwell} is not set by the user, but is automatically adjusted for each compound and depends on the chosen t_{Target} as well as the number of contemporary transitions. The higher the number of contemporary transitions the lower t_{Dwell}. This has a huge influence on the quality of the mass spectra, since lower t_{Dwell} leads to more noise on the baseline and the peaks. Since noise usually

is electronically generated and statistical, it can be reduced by increased acquisition times for the transitions and therefore by higher t_{Dwell} [121]. Thus, the highest possible t_{Dwell} usually is favoured in MS analysis. Furthermore, if t_{Dwell} reaches the lowest possible t_{Dwell} of the instrument, t_{Target} is increased by the system automatically, until the number of contemporary transitions decreases. This also determines the number of data points per peak: The higher t_{Target}, the less data points per peak. The influence of data points per peak is well described in a review by Dyson (1999) [122] for very narrow peaks of fast chromatography or capillary electrochromatography. Integration of chromatographic peaks is usually performed by the trapezoidal rule or the Simpson's rule. For both rules the measurement error increases with decreasing number of data points per peak. Thus, the peak integration is less reproducible leading to higher RSD and therefore to a decrease of precision. This principle is transferable to all chromatographic peaks. As a rule of thumb, 6 - 10 data points per peak [121] are required for good peak shape and reproducible peak evaluation. In this study, a minimum of 10 data points per peak was defined as a requirement for a sufficient coverage of the chromatographic peak.

However, optimization of t_{Target} for guaranteeing a minimum of 10 data points per peak could not be performed easily since this information is not provided by the software. In addition, lowering t_{Target} also lowers t_{Dwell} down to a minimum value and changes in t_{Dwell} are not recorded. Therefore, different t_{Target} values (0.3 s, 0.6 s and 0.9 s for M1, 0.2 s, 0.4 s and 0.5 s for M2) were tested and t_{Dwell} as well as the number of data points per peak were calculated from the raw data by formulas 2.1 - 2.3 (see chapter 2.2.2). It was studied how and if t_{Dwell} affects precision of analysis by a fivefold injection of a 100 ng/L calibration standard by calculation of the relative standard deviation (RSD) of the concentrations. Highest numbers of contemporary transitions for M1 were reached between 5 and 6.5 min of the chromatographic run (see Figure A1.2-A). For all three t_{Target} the lowest t_{Dwell} was reached in this period (Figure 2.1A). With t_{Target} of 0.3 s a minimum of around 5 ms for the calculated t_{Dwell} could be observed. The vendor of the mass spectrometer specifies a minimum of 3 ms thus the difference might be due to rounding errors after exporting of the EICs since the Analyst software provides time values in minutes only to the fourth decimal place. As mentioned, t_{Target} is increased by the system as soon as the minimum t_{Dwell} is reached. This is the case for $t_{Target} = 0.3$ s between 5 - 6.5 min. (Figure A1.2-A). For the other two tested t_{Target} no increase was observed. The effect of the selected t_{Target} on the number of data points per peak is shown in Figure 2.1B-D. With increasing t_{Target} the number of transitions falling below the minimum requirement of 10 data points per

peak increases. For $t_{Target} = 0.3$ s only a limited number of 16 transitions showed less than 10 data points per peak, while for $t_{Target} = 0.9$ s about half of the transitions were below the requirement. A similar result was obtained for M2, which switched between both polarities. The minimal t_{Dwell} was not reached and no corrections of the t_{Target} occurred (Figure 2.2A). All transitions showed more than 10 data points per peak for $t_{Target} = 0.2$ s, while by an increase of the t_{Target} the number of transitions falling below the minimum requirement increased (Figure 2.2B-2D).

Both methods clearly showed the influence of the t_{Target} on t_{Dwell} and data points per peak: an increase of t_{Target} led to an increase in t_{Dwell} but a decrease in data points per peak. Reaching the minimum t_{Dwell} of the instrument did not affect the analysis negatively. Precision of a 100 ng/L calibration standard was good in both methods and for all t_{Target} as can be seen in the boxplots in Figure 2.1E and Figure 2.2E. This might be due to the fact that even with the highest t_{Target} still a minimum of 6 data points per peak was achieved. A rule of thumb states, that this is the least number of data points for which an accurate peak shape can be obtained. However, with increasing t_{Target}, peak shape became more inaccurate and in several cases the top of the peak and therefore the real peak height was not detected. This can be seen at the chromatograms of gabapentin and hydroxyl-atenolol for M1 as well as for sulpiride and O-DM-metoprolol in M2 (Figure A1.2-B). For trace analysis, as in this study, the number of data points per peak was seen as critical for analysis. With the lowest tested t_{Target} nearly all transitions showed more than 10 data points per peak, including the internal standards. Further optimization could be performed to decrease the t_{Window} thereby reducing the number of contemporary transitions. However this may increase the chance of a signal moving out of t_{Window} due to retention time drift and so reduce the robustness of the method.

The influence of the MS parameters on analysis clearly could be seen. For multi-residue analysis methods the optimization of t_{cycle}, t_{window} and t_{Dwell} is important to guarantee accurate peak shape and quality of analysis during the whole chromatographic run time. However, these parameters are rarely reported in the literature and comparison of analytical methods solely based on chromatographic aspects is insufficient in mass spectrometric methods. Thus, reporting of those parameters would be strongly recommended.
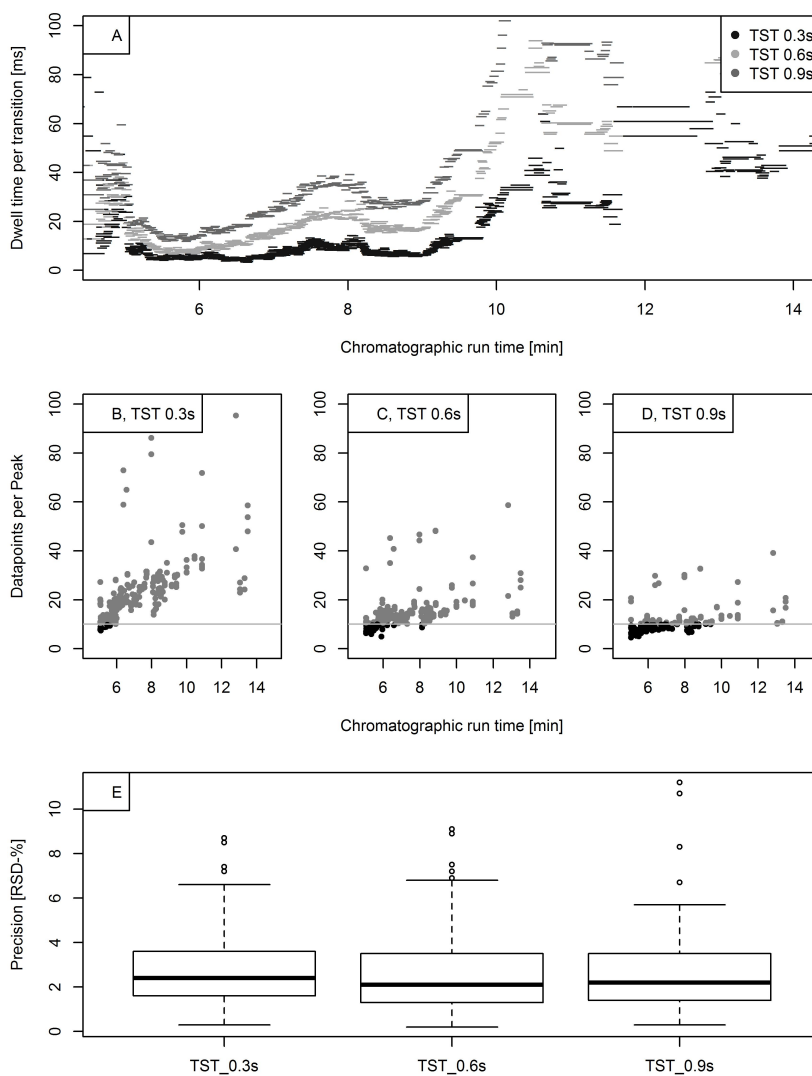
Figure 2.1: Method data M1. TST = t_{Target}. A: Calculated dwell time per transition over the chromatographic run time. B-D: Correlation of data points per peak and chromatographic run time, straight line at data points per peak = 10. E: Boxplot over precision values for the selected t_{Target} with the box showing the interquartile range (IQR) and the median (horizontal line), the whiskers give the range and the circles the outliers which are beyond 1.5 x IQR from the nearest quartile
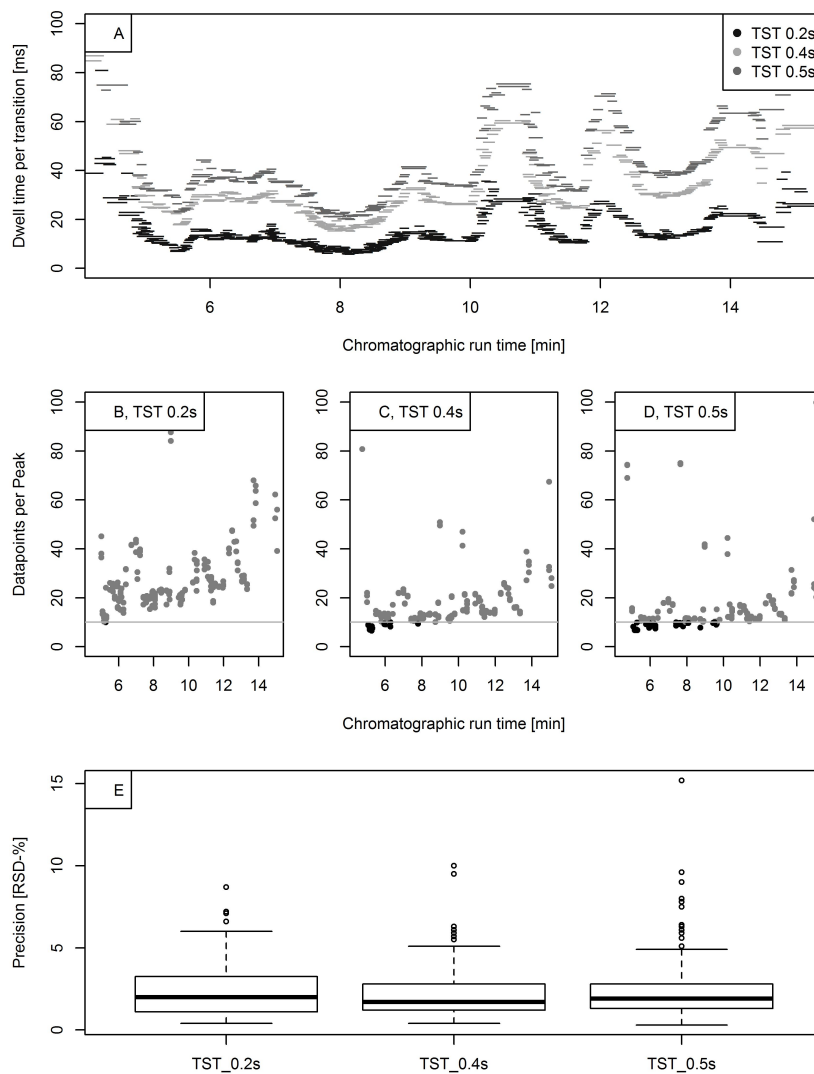
Figure 2.2: Method data M2. TST = t_{Target}. A: Calculated dwell time per transition over the chromatographic run time. B-D: Correlation of data points per peak and chromatographic run time, straight line at data points per peak = 10. E: Boxplot over precision values for the selected t_{Target} with the box showing the interquartile range (IQR) and the median (horizontal line), the whiskers give the range and the circles the outliers which are beyond 1.5 x IQR from the nearest quartile

2.3.2 Validation

Calibration curves were generated using a 1/x weighted linear regression analysis. Linearity was determined by means of the correlation coefficients (R^2) for each substance in the working range (see Table A1.3). For both detection methods no analytes were below $R^2 = 0.97$ and for both methods the average value was 0.997. Therefore, very good linear fits were obtained for all analytes in the methods. Calibration was performed for each measurement series and quality control samples were included after every 15 - 20 injections. A summary of validation results is given in Table 2.3, the complete lists for all 154 compounds can be found in Tables A1.3 to A1.5.

Precision was determined for two concentration levels: 100 ng/L and 1000 ng/L (acesulfame: 2000 and 20,000 ng/L; contrast media and oxypurinol: 1000 and 10,000 ng/L). Intra-day precision (n = 3 for each concentration level) was below 20% RSD for all analytes in both methods with average values of less than 4%. Inter-day (n = 6 for each concentration level) precision was slightly higher with average values of about 7 - 8% in both methods. This was mainly due to higher maximal values for some analytes. 9-carboxylic acid-acridine showed highest values up to 43% RSD. This substance is a TP of carbamazepine and was evaluated by the IS of the precursor compound. It was observed that for 9-carboxylic acid-acridine the recovery values and the assignment of an appropriate IS had to be controlled in every new measurement series.

LOQs ranged from 0.5 - 50 ng/L for the majority of substances in both methods with average values of about 10 - 30 ng/L depending on the matrix. Only a few exceptions exceeded this range, such as oxypurinol and sucralose. However, these substances usually can be found in concentrations much higher than the LOQs. Furthermore, some TPs showed higher LOQs, e.g. iopromide-TPs and 2-hydroxy-ibuprofen, possibly due to poor ionization. Lowest LOQs were observed in bank filtrate, while the highest LOQs were in WWTP influent and effluent.

Since no sample preparation was used prior to analysis, the absolute recovery was a measure for the matrix effect. In both methods most of the substances showed signal suppression with lowest absolute recovery values in the more complex matrices of WWTP influent and effluent. In M1 average absolute recoveries were about 85% in ground- and surface water and about 70% in WWTP influent and effluent. Therefore, an average negative matrix effect of 15 - 30% was observed and thus evaluation of the results could also be performed without IS for several compounds. However, in a few cases absolute recovery

Table 2.3: Summary of validation results; SW = Surface water, BF = Bank filtrate, Inf = WWTP influent, Eff = WWTP effluent.

Parameter	Details	Detection method 1			Detection method 2		
		average	min	max	average	min	max
Linearity (R2)		0.997	0.972	0.999	0.997	0.974	0.999
Precision (% RSD) Instrument precision	Intra-day (100 ng/L)	3.8	0.2	16.0	2.8	0.1	17.5
	Intra-day (1000 ng/L)	2.2	0.1	8.2	2.5	0.3	16.8
	Inter-day (100 ng/L)	8.1	1.7	34.3	8.1	1.2	42.9
	Inter-day (1000 ng/L)	6.9	1.5	28.7	6.8	0.3	40.8
LOQ (ng/L)	SW	29	0.5	200	14	0.5	150
	BF	25	0.5	200	11	0.5	150
	Inf	31	0.5	200	20	1	150
	Eff	28	0.5	200	23	1	150
Abs. Recovery (%)	SW	89	50	137	112	60	170
Spike-level 1000 ng/L	BF	86	55	139	91	63	121
	Inf	73	32	169	61	29	134
	Eff	72	25	167	56	29	104
Rel. Recovery (%)	SW	98	72	121	94	42	136
Spike-level 1000 ng/L)	BF	100	69	126	98	61	123
	Inf	112	69	153	112	80	149
	Eff	106	64	149	103	70	132
Precision (SD) (%)	SW	14	1	39	29	2	61
Method precision	BF	5	1	37	6	1	18
Spike-level 1000 ng/L	Inf	11	4	56	11	3	42
	Eff	8	1	30	11	1	60

went down to less than 50%, i.e. a negative matrix effect of more than 50%. Lamotrigine and O-desmethyl-venlafaxine for example showed an absolute recovery of about 40% in WWTP influent and effluent at a spiking level of 1000 ng/L. In M2 average absolute recovery values of 90 - 100% were reached for ground- and surface waters, while it was just 60% for WWTP influent and effluent. Therefore, matrix effects of ground- and surface waters were minimal for the majority of substances but were about 40% in WWTP influent and effluent. Absolute recovery of less than 50% for a spiking level of 1000 ng/L in WWTP influent and effluents were observed for example for the carbamazepine TPs/metabolites, diphenhydramine and most of the pesticides. For a few substances positive matrix effects, i.e. absolute recoveries higher than 100%, could be observed in single matrices, e.g. for

flecainide and fexofenadine. The matrix effects could be compensated by using isotopically labelled IS.

For both methods average relative recovery values of around 100% were achieved and the majority of substances showed values in the acceptable range of 70 - 125% of relative recovery. Only a few exceptions occurred in the more complex matrices of WWTP influent and effluent. For example, in WWTP influent the demethylated tramadol-TPs and two of the demethylated venlafaxine-TPs showed higher recovery values of around 130%. Method precision was determined as the intra-day precision of recovery experiments using the standard deviation (SD) of absolute recovery. In both methods, average SD values were below 30% for all matrices for both spiking levels. At the lower spiking level of 100 ng/L the precision was less than for the higher spiking level of 1000 ng/L which mainly was caused by the background concentrations of substances. Hydrochlorothiazide for example showed a precision of about 60% in effluents at the lower spiking level due to background concentrations of more than 1000 ng/L in the samples. It has to be emphasized that replicates of samples taken at different locations were used for recovery experiments. The excellent average SD values therefore highlight that both methods can be applied to samples of different sources.

2.3.3   Analysis of environmental water samples and wastewater

The applicability of the methods and the relevance of TPs for monitoring were assessed by analysing samples from surface waters (SW), bank filtrate (BF) and from three WWTPs. Of the 154 substances of the target list, 94% could be quantified in at least one sample. In Figure 2.3 the distribution of precursors and TPs in the samples is shown. A summary of results per sample is given in Table 2.4. Detailed lists are in Tables A1.6-A and A1.6-B.

Highest numbers of substances could be quantified in the WWTP samples. In both influents and effluents, 94% of the precursors and 82% of the TPs could be found at concentrations above LOQ in at least one sample. All included pharmaceutical precursors appeared in at least one sample with concentrations above their LOQs. In all WWTP samples concentrations ranged from < 0.02 µg/L (e.g. phenytoin, propiconazol, tebuconazol) to more than 1 µg/L (e.g. carbamazepine, gabapentin, hydrochlorothiazide, irbesartan). The highest concentrations (more than 5 µg/L) were found for levetiracetam, pregabalin and iopromide in influents. Median concentrations of all measured compounds were 0.1 - 0.2 µg/L in influents, 0.6 - 0.8 µg/L after biological treatment and around 0.02 µg/L after
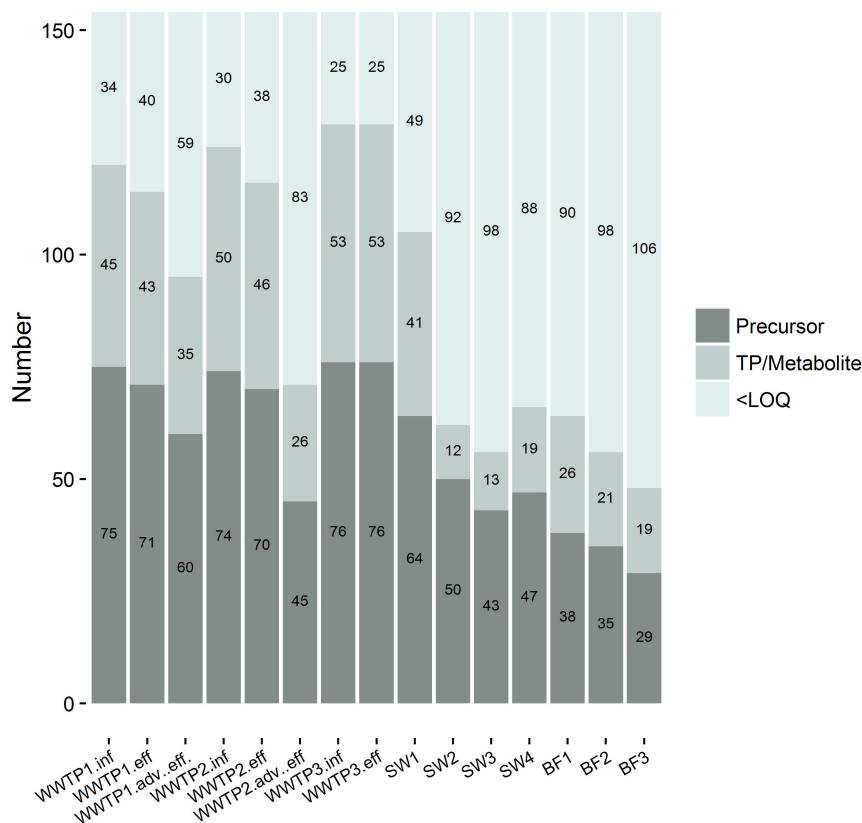
Figure 2.3: Overview of the number of detected CECs in each sample, grouped into for precursors and TPs/metabolites. The method analyzes in total 154 compounds, 84 precursors and 70 TPs/metabolites; inf = influent, eff = effluent, adv.eff = effluent of advanced treatment step.

advanced treatment (activated carbon filtration). As can be seen from the median concentration as well as from the number of substances with concentrations above 1 µg/L, a general reduction of concentrations was observed at every treatment step. However, even after treatment with powdered or granulated activated carbon (WWTP1 and WWTP2 respectively), concentrations above 1 µg/L could still be observed for some substances such as valsartan acid, oxypurinol and sucralose.

In surface waters analysed, 81% of the precursors and 60% of the TPs were found at concentrations above LOQ. SW1 showed the highest numbers of quantifiable substances with 75% of the precursors and 58% of the TPs of the target list above LOQ, while SW2 - 4

had fewer detects - around 55% of the precursors and 20% of the TPs in the method were detected. This was due to a higher percentage of effluent in SW1 (more than 90%) than in the other surface waters. Concentrations above 0.5 µg/L were found for gabapentin and iomeprol. Highest concentrations were found for sucralose(> 20 µg/L in SW1, 0.8 µg/L in SW4) and oxypurinol (> 10 µg/L in SW1, 1.6 µg/L in SW4).

The BF samples were taken from a bank filtration site where SW4 is the corresponding surface water. BF1 and BF2 were taken at the same distance but at different depths from SW4 (travel times 1 and 3 months, respectively), the travel time of the water at the BF3 location is about 5 months. The average concentration of substances in BF1 was nearly twice as high as in SW4, however, at the time of the sampling campaign rainfall occurred at the site, therefore dilution effects may have lowered the concentrations at SW4. Of all measured samples, the BF samples showed the lowest numbers of substances above LOQ, 52% of the analysed precursors and 39% of the analysed TPs. During soil passage the total number of quantifiable substances decreased from 42% in SW4 to 30% in BF3. Concentrations above 0.5 µg/L were found for carbamazepine, gabapentin and sucralose. Highest concentrations were detected for oxypurinol (3 µg/L in BF1) and the TP valsartan acid (3.3 µg/L in BF1).

Oxypurinol is the active metabolite of the anti-gout agent allopurinol. Even after advanced treatment with powdered and granulated activated carbon as in WWTP1 and WWTP2 it was still detected at elevated concentrations of more than 3 µg/L. This is in accordance with the elevated concentrations found in bank filtrate, and drinking water, in a previous study by Funke et al. (2015) [23]. In Germany a health-related orientation level [123] of 0.3 µg/L in drinking water is used. This value was exceeded in some of the bank filtrate samples measured in this study.

Valsartan acid, a biological TP of the sartan-group [124] has a similar health related orientation level of 0.3 µg/L. It is frequently detected in surface waters and WWTP effluents [124–126]. However, there was limited published data on the occurrence of valsartan acid in bank filtrate at the time of writing. Nödler et al. (2013) [124] analysed groundwater samples and Huntscha et al. (2012) [126] samples from a bank filtration site, but in both studies valsartan acid could not be quantified above LOQ. In this study it was the TP with the highest concentrations in bank filtrate (2.5 - 3 µg/L). In WWTP influents, concentrations around 0.1 µg/L were detected, while it was 2 - 5 µg/L in effluents. Also in surface waters, concentrations of more than 1 µg/L were detected. All these results are in accordance with findings of Nödler et al. (2013) [124]. Advanced treatment with

Table 2.4: Summary of quantitation results from the analysis of raw wastewater, tertiary and advanced treatment effluents, surface waters and bank filtrate partially impacted by wastewater.

Sample	Detected > LOQ (Total = 154)	Conc. range (µg/L)	Substance with highest conc.	Median conc. (µg/L)	Average conc. (µg/L)	Substance with conc. > 1 µg/L
WWTP1 influents	120 (78%)	0.01 - 97	Caffeine	0.1	3	30 (19%)
WWTP1 tert. eff	114 (74%)	0.01 - 20	Iomeprol	0.08	0.6	20 (13%)
WWTP1 adv. eff	95 (62%)	0.003 - 7	Iomeprol	0.025	0.3	15 (10%)
WWTP2 influents	124 (81%)	0.005 - 74	Caffeine	0.1	2	30 (19%)
WWTP2 tert. eff	116 (75%)	0.005 - 10	Sucralose	0.06	0.4	16 (10%)
WWTP2 adv. eff	71 (46%)	0.005 - 5	Sucralose	0.015	0.2	6 (4%)
WWTP3 influents	129 (84%)	0.005 - 155	Caffeine	0.2	4.3	38 (25%)
WWTP3 tert. eff	129 (84%)	0.002 - 25	Benzotriazole	0.1	1	24 (16%)
SW1	105 (68%)	0.004 - 30	Sucralose	0.035	0.5	13 (8%)
SW2	62 (40%)	0.004 - 0.4	Acesulfame	0.01	0.03	-
SW3	56 (36%)	0.002 - 0.7	Oxipurinol	0.01	0.03	-
SW4	66 (43%)	0.002 - 1.6	Oxipurinol	0.01	0.065	3 (2%)
BF1	64 (42%)	0.004 - 3.3	Valsartan acid	0.01	0.1	4 (3%)
BF2	56 (36%)	0.003 - 2.7	Valsartan acid	0.01	0.07	2 (1%)
BF3	48 (31%)	0.004 - 2.4	Acesulfame	0.005	0.015	2 (1%)

powdered activated carbon as in WWTP1 did not reduce the concentration of the TP, usage of granulated activated carbon filtration as in WWTP2 reduced the concentration by 50%. The determination of this TP together with the corresponding sartan precursors can allow the assessment of performance at these different treatment processes.

Clopidogrel is a prodrug which is rapidly transformed after administration to the active metabolite. However, about 85% of the drug is hydrolysed to the inactive metabolite clopidogrel acid [127]. In many monitoring campaigns only clopidogrel itself is determined [97, 103]. In this study, concentrations for clopidogrel acid were much higher than for the precursor and reflected the metabolism of the prodrug, i.e. clopidogrel acid made up about 90% of the summed concentrations of clopidogrel and the acid. Furthermore, conventional treatment in WWTPs did not lead to a reduction in concentration of the acid. This is in accordance with findings of Oliveira et al. (2015) [105] who included clopidogrel acid into their study on hospital effluents as well as WWTP influents and effluents observing no reduction in concentration. Furthermore, in contrast to clopidogrel, the acid could also be detected above LOQ in bank filtrate. To the best of our knowledge this is the first study on the occurrence of clopidogrel acid in bank filtrate.

The high number of substances detected, including TPs, and the fact that the substances could be quantified in all analysed matrices showed the relevance of the selected targets. The target list includes substances, which can aid in water quality assessment and the evaluation of performance or stability of engineered water treatment systems since

many of the compounds fulfil the requirements for indicator substances as outlined in assessment strategies (Jekel et al. (2015) [120]; Ternes et al. (2017) [21]). Furthermore, as regulatory frameworks become more complex, cf. health-related orientation levels [123] and the WFD watch list [128], the advantages of a multi-residue determination in a single analysis becomes evident.

2.4 Conclusions

A direct injection multi-residue analysis method using a sMRM analysis was found to be suitable for the quantification of 84 precursor substances as well as 70 TPs/ metabolites of different substance classes. Evaluation of the effect of target scan time on dwell time and number of data points per peak revealed that reaching the minimum dwell time of the instrument did not affect the precision negatively, but a decrease in data points per peak led to inaccurate peak shapes. To guarantee an accurate peak shape and thus quality of analysis, a low target scan time was chosen to gain a minimum of 10 data points per peak. Sensitivity of the method was shown at the validation in real matrices (bank filtrate, surface water, influent and effluent of WWTPs) with LOQs in the lower and mid ng/L range for the majority of substances, low to medium matrix effects of around 15 - 50% in all matrices and relative recoveries of around 100%. In environmental samples, 94% of the target list could be detected at concentrations higher their LOQ in at least one sample, with the highest numbers of findings in WWTP influents and effluents (94% of analysed precursors, 82% of TPs) and the lowest numbers in bank filtrate (52% of precursors and 39% of TPs). Next to frequently detected substances other substances not in the focus of current multi-residue analysis methods could be quantified at elevated concentrations, such as oxypurinol, through-out the water cycle. In addition, the relevance of monitoring TPs next to precursors could be shown in findings of valsartan acid at elevated concentrations even in bank filtrate and the occurrence of the metabolite clopidgrel acid at higher concentrations than its precursor clopidogrel. The developed method allows for direct, rapid routine analysis on trace organic chemicals in various water matrices without any sample enrichment. The simultaneous analysis of the broad set of precursors and TPs/metabolites allows for following degradation pathways and can aid the assessment of water quality and water treatment processes.

Acknowledgments

Chapter 3

Elucidation of removal processes in sequential biofiltration (SBF) and soil aquifer treatment (SAT) by analysis of a broad range of trace organic chemicals (TOrCs) and their transformation products (TPs)

N.Hermes, K.S. Jewell, M. Schulz,J. Müller, U. Hübner, J. Drewes, T.A. Ternes

Abstract

Many chemicals with different physico-chemical properties are present in municipal wastewater. In this study, the removal of a broad range of trace organic chemicals (TOrCs) was determined in two biological treatment processes differing in hydraulic retention time: sequential biofiltration (SBF) and soil-aquifer treatment (SAT), operated in Germany and Spain. Occurrence and the degree of removal of more than 150 TOrCs with different physico-chemical properties were analysed, including precursors as well as human metabolites and environmental transformation products (TPs). Ninety TOrCs were detected in the feed water of the SBF system, 40% of these showed removal efficiencies of higher than 30% during biological treatment. In SAT, 70 TOrCs were detected in the feed water, 60% of these could be reduced by more than 30% after approximately 3 days of subsurface treatment. For uncharged and negatively charged TOrCs biological degradation was mainly responsible for the removal, while positively charged TOrCs were most likely also removed by ionic interactions. The detections of TPs confirmed that biodegradation was a major removal process in both systems. The analysis of positively and negatively charged, neutral and zwitterionic TOrCs and the simultaneous analysis of precursors and their biologically formed TPs enabled a detailed understanding of underlying mechanisms of their removal in the two systems. On this basis, criteria for site-specific indicator selection were proposed.

3.1   Introduction

World-wide depletion of drinking water sources, for example groundwater aquifers, is of growing concern. For countries suffering from water scarcity, the use of reclaimed water via soil-aquifer treatment (SAT) might be an attractive way to augment aquifers and thus overcome the depletion of drinking water sources [7]. Here, an effluent of a municipal wastewater treatment plant (WWTP) is infiltrated after advanced treatment into an unsaturated (vadose) zone and is further purified by biological and physical processes occurring during soil passage. SAT is seen as a cost-effective treatment technology with stable performance. It has the ability to remove certain trace organic chemicals (TOrCs) as well as pathogens [7, 58, 60]. However, in full-scale applications a variety of factors influence the attenuation of TOrCs such as pH, redox conditions, biodegradable dissolved organic carbon (BDOC), temperature, flow rates, soil composition, etc. [60, 129]. There is a strong interest in the elucidation of processes to optimize attenuation capabilities. Studies on specific behaviour of TOrCs during SAT were performed using lab- and pilot-scale column studies fed with artificial and real wastewaters. Biodegradation, sorption and combinations there of were studied [60, 62, 130, 131]. Biodegradation can be a removal process for a variety of TOrCs, but efficiencies were shown to be influenced by the effluent organic matter composition and concentration of the feed waters, predominant redox conditions, and the specific microorganisms present in the systems [58, 64, 132]. These findings were transferred to full-scale studies introducing the sequential managed aquifer recharge technology (SMART) concept [70]. Here, short-term managed aquifer recharge (MAR) (either via bank filtration or SAT) was performed, the reclaimed water was then recovered and re-aerated by surface spreading prior to a second infiltration step. By this method, oxic conditions can be maintained during the second subsurface treatment step. For further optimization of this sequential treatment, the concept of sequential biofiltration (SBF) was introduced [133]. This engineered above-ground treatment system is designed as two sequential filter stages with intermediate aeration or oxidation steps [133, 134]. It was found that the biodegradation of several moderately degradable TOrCs was enhanced by maintaining fully oxic and carbon-starving conditions in the second filter stage and that travel times could be reduced drastically compared to conventional MAR applications. However, retardation by sorption can also play an important role for the removal of specific TOrCs in MAR. Hydrophobicity of TOrCs enhanced sorption and ionic interactions were found responsible for retardation of partially positively charged TOrCs [135].

However, variations in prevailing conditions and soil characteristics limit the prediction of removal for individual compounds in MAR systems. Thus, indicator chemicals were proposed for process evaluations representing certain physico-chemical or biological properties of an entire family of chemicals. Dickenson et al. (2009) [136] and Jekel et al. (2015) [120] proposed indicator chemicals for different treatment systems as for conventional and advanced techniques as well as for bank filtration and SAT. Funke et al. (2015) [23] proposed the use of oxypurinol which is partly excreted by humans and formed in WWTPs from transformation of the anti-gout allopurinol and its conjugates. Recently, a multi-disciplinary indicator concept to highlight the efficiencies of municipal WWTPs to remove TOrCs as well as pathogens was reported by Ternes et al. (2017) [21].

However, none of the studies allowed to derive a more fundamental understanding of underlying removal mechanisms during aquifer passage. To address the huge number of TOrCs used world-wide, it is furthermore crucial to consider the large variety of different biological and physico-chemical properties, being positively or negatively charged, zwitterionic or not charged at all or being well, moderately or poorly degradable. In this study, the removal of more than 150 TOrCs, including human metabolites and TPs was studied in two biological systems, i) an engineered above-ground SBF system with intermediate aeration and ii) a natural full-scale SAT system. While compound removal in the SBF system filled with anthracite and technical sand is dominated by biodegradation, different mechanisms might contribute to TOrC removal in the natural SAT system. Compounds with different physico-chemical properties, i.e. positively, negatively charged, neutral and zwitterionic compounds, as well as pairs of precursors and TPs were included to enable a detailed understanding of underlying mechanisms for compound removal in these two systems and to derive potential candidates for future indicator selection.

3.2 Materials and Methods

3.2.1 Chemicals and Reagents

A list of the target chemicals including CAS registry numbers and supplier can be found in Hermes et al. (2018) [137]. LC-MS grade methanol and acetonitrile (both LiChrosolv) were supplied by Merck (Darmstadt, Germany). Formic acid and acetic acid as eluent additives for LC-MS were purchased from Sigma Aldrich (Seelze, Germany).

3.2.2 Pilot-scale SBF

The SBF system is described in detail by Müller et al. (2017) [133] (Figure 3.1). In brief, a back-washable filter column (A) was operated with anthracite as filter material (grain sizes 1.4 - 2.5 mm) as a first stage filter. The filters of the second stage (S1, S2) were filled with technical sand (grain sizes 0.2 - 1.0 mm) and inoculated with 5% aquifer material from a bank filtration site. First- and second-stage filters had a filter bed height of 1.05 m and 0.95 m and an inner diameter of 0.15 m and 0.1 m, respectively. Between the filters an aeration step with pressurized air was implemented. The filter train was fed with tertiary effluent from the WWTP Garching, Germany. Empty bed contact times (EBCTs) were adjusted by the flow rate of the water to 90 min in the anthracite filter A, 200 min in S1, and 2000 min in S2. A few TOrCs were spiked into the feed water to follow their attenuation processes: caffeine, carbamazepine, citalopram, diclofenac, diphenhydramine, iopromide, metoprolol, phenytoin, primidone, sulfamethoxazole, tramadol, venlafaxine, trimethoprim, atenolol, and climbazole. TOrCs were spiked to concentrations ranging from 0.5 to 3 µg/L. Three sampling campaigns were performed for the SBF system within three weeks by collecting corresponding samples from the feed water and after each treatment column.

3.2.3 Full-scale SAT

The full-scale SAT site was located in a small town (~1000 inhabitants) in the Costa Brava region of Spain. The local WWTP applies conventional secondary treatment, followed by advanced treatment by dual media filtration, UV-disinfection and GAC filtration. During the monitoring campaign the GAC was by-passed a week before the sampling campaign to only observe the effect of the soil passage. The treated wastewater was transferred to an elevated storage tank, from here it was conveyed by gravity to the infiltration basin. The basin had a depth of 1 m and had a 40 cm thick layer of technical sand at the bottom. Two observation wells were located downgradient of the infiltration basin (see Figure 3.1): the first at a distance of 3 m with a travel time of about 30 h, and the second at a distance of about 20 m with a travel time of about 3 d [138]. The well for drinking water production was located at a distance of about 1 km downstream of the recharge basin with water travel times of about 1.5 years and was not sampled in this study. Subsurface geology was composed of rocks at gravel size and a matrix of sand and silt. Drillings for the observation wells, identified also regions with plastic clays. A groundwater level of 8 m below the surface of the observation wells, SAT_1 and SAT_2, close to the infiltration basin indicated that
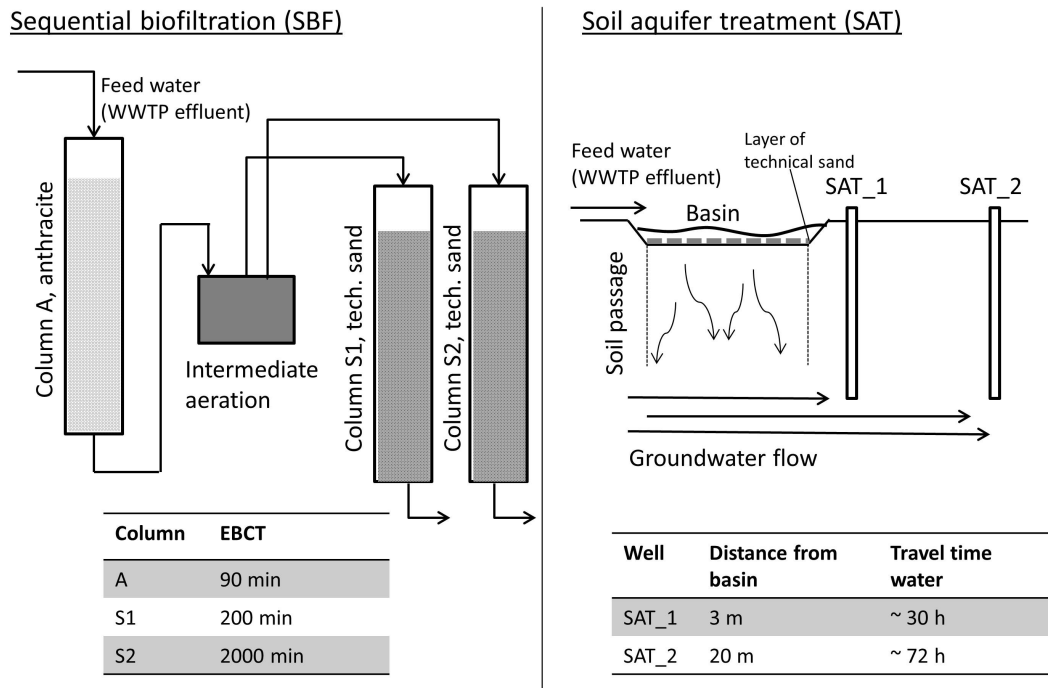
Figure 3.1: Schemes of the studies systems, drawn accoding to Müller et al. (2017) [133] and Amy and Drewes (2007) [56]

initial infiltration was characterized by vertical infiltration under unsaturated conditions. Sampling was carried out at three consecutive days by taking grab samples at the basin and the two observation wells and in total four samples were taken for each sampling point. Water samples were immediately filtered by 0.45 µm regenerated cellulose filters and samples were stored in a freezer ($-20\,°C$) pending analysis.

3.2.4 Analytical method

The analytical method for quantification of more than 150 TOrCs including TPs is described in detail in Hermes et al. (2018) [137]. In brief, direct-injection LC-MS/MS analysis, split into two detection methods, was performed on a HPLC 1260 Infinity Series equipped with a Zorbax Eclipse Plus C18 column (150 mm x 2.1 mm, 3.5 µm, Agilent Technologies)

coupled to a TripleQuad mass spectrometer (6500+, Sciex). A water-acetonitrile gradient was used; for detection method 1, the aqueous phase was buffered with 0.1% formic acid while detection method 2 was buffered with 0.1% acetic acid. Analysis was performed in scheduled MRM mode using deuterium labelled surrogates as internal standards for quantification. Detailed information on MRM transitions and assignment of internal standard to the analytes and validation parameters are reported in Hermes et al. (2018) [137].

3.3 Results and Discussion

3.3.1 Selection of TOrCs

A wide range of TOrCs with different properties and uses are present in WWTP effluents [22, 110, 113]. To get a comprehensive overview, the chemical selection was based on a variety of criteria. Pharmaceuticals, personal care products, industrial chemicals, artificial sweeteners as well as pesticides were included. Furthermore, human metabolites and TPs were targeted. Consumption of chemicals in Germany [139] was considered as well as the occurrence of TOrCs in world-wide monitoring studies. Furthermore, the (bio)degradability of TOrCs in conventional WWTPs was a crucial criterion. The selected TOrCs cover different physico-chemical properties in terms of pK_a and $\log K_{OW}/D$ and thus substances being negatively or positively charged, zwitterionic or not charged at pH 7 were addressed. All selected TOrCs are detectable with the same analytical method. A complete list of monitored chemicals including the usage, physico-chemical properties, degradability in conventional WWTPs, and limit of quantification (LOQ) for the analysis method can be found in the appendix (Table A2.1). Some of the included TOrCs were not considered in monitoring studies so far. Gabapentin lactam for example is a rather new TP [140] which, to the best of our knowledge, has not yet been included in current monitoring studies. The TP valsartan acid has been known for several years [124], but information about its environmental fate is scarce. And further substances, for example sitagliptin or denatonium, were identified as potential water contaminants with higher concentrations only recently [137].

3.3.2 Fate and removal in SBF

The SBF system was fed with tertiary effluent from the municipal WWTP located in Garching, Germany, having a capacity of 31,000 people equivalents. More than 90 TOrCs

were detected in the feed water with concentrations above the LOQ. Detected concentrations ranged from 0.0004 µg/L (phenytoin) to 15.0 µg/L (oxypurinol). More than 10 TOrCs showed concentrations of higher than 1.0 µg/L such as the artificial sweeteners sucralose and acesulfame, the corrosion inhibitor benzotriazole, the pharmaceuticals sitagliptin, diclofenac, gabapentin, and valsartan as well as the TPs/metabolites of pharmaceuticals acyclovir carboxylic acid, valsartan acid, and O-desmethyl-venlafaxine. Pesticides were mainly detected at lower concentration levels, except for mecoprop which exhibited a high variability with concentrations ranging from 0.37 to 2.2 µg/L.
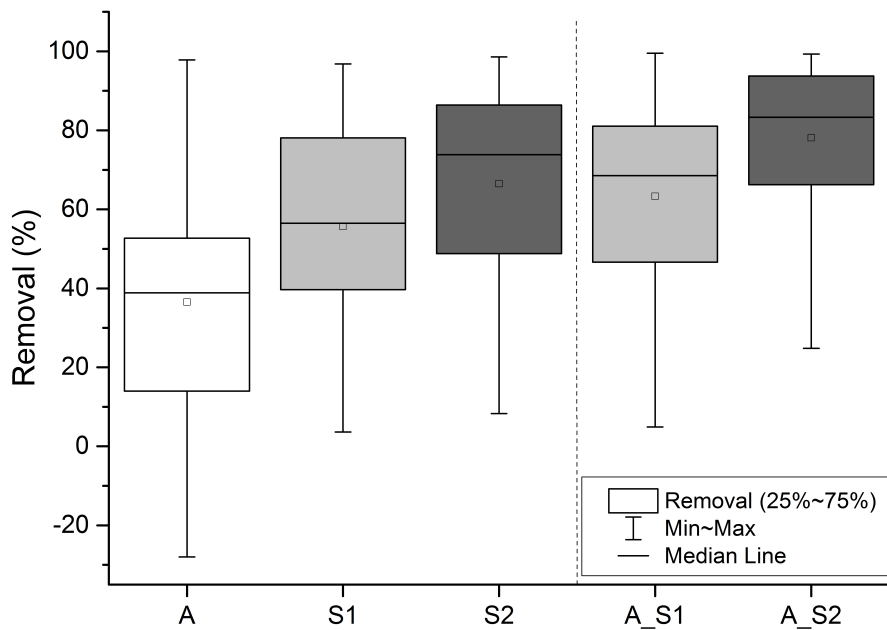
Figure 3.2: Removal in the single columns (A, S1 and S2) and in the SBF system (A_S1, A_S2) for 40 selected TOrCs, which showed a removal of higher than 30% in A_S2 and did not reach LOQ. Column A: EBCT of 90 min, column train A_S1: EBCT 200 min, column train A_S2: EBCT 2,000 min.

The strength of the SBF system compared to SAT is the enhancement of the oxic biodegradation potential by establishing controlled oxic conditions within the second filter at substantially shorter hydraulic retention times (HRTs). Figure 3.2 shows a boxplot of the achieved averaged removal of TOrCs in a single column (A, S1 and S2) and in the

overall SBF systems combining two columns (A_S1, A_S2). Here only those TOrCs were considered which showed a removal of greater than 30% in the second filter stage of the SBF system (40 TOrCs in total).

As expected, there was a reduction in removal with decreasing EBCT: the median removal of TOrCs in S2 with an EBCT of 2,000 min was 75%, while it was 55% for S1 with an EBCT of 200 min. This behaviour was also reported by Müller et al. (2017) [133] and explained by the difference in EBCT but might also be related to the reduced redox conditions in the columns, i.e. a change from oxic to suboxic conditions (Figure A2.2). Column A was characterized by a rapid consumption of dissolved oxygen (DO), yet still maintaining oxic conditions (DO > 2 mg/L) at the outlet. By re-aeration, oxic conditions could be established in the influent of columns S1 and S2, but DO concentrations dropped rapidly within the first 10 cm of the columns. For S1 DO remained at about 3 mg/L, while in S2 a constant decrease to less than 1 mg/L DO was observed. Thus, in S1 oxic conditions prevailed, while S2 dropped to suboxic conditions. Decreasing DO concentrations might adversely affect the degradation of certain TOrCs.
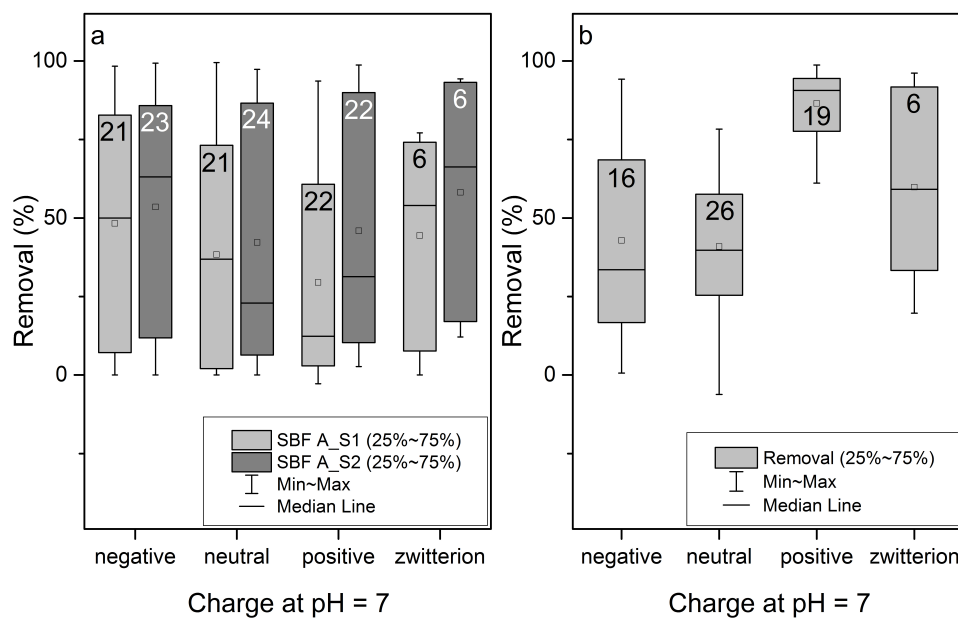
Figure 3.3: Boxplot over the removal of TOrCs in SBF (a) and SAT (b), grouped by their speciation at pH = 7. Only TOrCs were considered that showed a detectable removal, the number of analyte per group is indicated by the numbers in the single bars.

Looking at the overall removal of all detected TOrCs in the SBF system grouped by their charge at pH 7 (Figure 3.3a), it seemed as if negatively charged and zwitter ionic compounds could be removed more effectively (as indicated by the median values) in comparison to neutral and positively charged ones. However, the range of removal values was the same for all groups and spanned over no removal at all to complete attenuation.

In Table 3.1 the concentrations of selected TOrCs (those showing concentration of 10 times higher than the LOQ in the influent to the system) and in Figure 3.4 the removal of all detected substances in the systems are shown (for concentrations and removal of all TOrCs, see Table A2.3) Less than 50% of all detected TOrCs exhibited a moderate to good removal ($> 30\%$). Removal in SBF could mainly be attributed to (bio)degradation. Removal by sorption is negligible since the columns were filled with anthracite and technical sand. Furthermore, the systems were run continuously for three years prior to this study, thus sorption equilibria were assumed to be reached for most TOrCs as reported by Müller et al. (2017) [133].

More than 50% of the non-charged TOrCs were persistent during the SBF treatment. For several of them, e.g. carbamazepine and primidone, this was expected from previous studies [60, 110]. For compounds showing removal $> 30\%$, biodegradation could be verified as the major removal mechanism by the detection of respective TPs in the column effluents (Figure 3.5). Although carbamazepine was persistent, its metabolite 10-OH-carbamazepine was removed by 50% in column A and up to 90% in system A_S2. Its biodegradation was confirmed by the detection of its zwitterionic TP 9-carboxy-acridine [141]. The transformation pathway from 10-OH-carbamazepine to 9-carboxy-acridine involves oxidative steps and thus, the prevalence of oxic conditions enhanced its transformation (Figure 3.5a). The mass balance was closed, when considering that 10-OH-carbamazepine was removed and 9-carboxy-acridine was formed. However, there might be a gap in the mass balance for A_S2, where the removal of 10-OH-carbamazepine could not only be explained by the formation of 9-carboxy-acridine as it was possible in A_S1. Either further degradation processes, possibly taking place under suboxic conditions were involved or sampling frequencies were not sufficient for these TOrCs.

Even more pronounced were the effects of redox conditions and EBCTs on the behaviour of climbazole (Figure 3.5b). In column A only a minor removal of climbazole was observed, but the closed mass balance indicated that climbazole-OH was the main TP. In the sequential approach (A_S1) the removal of climbazole was enhanced and the formation of the TPs was more pronounced. However, the gap in the mass balance indicated a further removal of

3.3. RESULTS AND DISCUSSION

Table 3.1: Effluent concentrations for the TOrCs detected at feed water concentrations of at least ten times the LOQ in the SBF system (n = 3). Concentrations given in µg/L. A list with results for all TOrCs can be found in Table A2.3

Substance	Abbrev	LOQ (µg/L)	Feed (spike)	A	A_S1	A_S2
				Concentrations (µg/L) in the effluent of the columns		
Substances uncharged at pH 7						
Primidone	PRIM	0.02	1.13 ± 0.05	1.1 ± 0.5	1.17 ± 0.05	1.13 ± 0.06
Phenytoin	PHEN	0.001	0.96 ± 0.05	0.9 ± 0.5	0.94 ± 0.02	0.85 ± 0.05
Carbamazepine	CBZ	0.001	1.13 ± 0.05	1.2 ± 0.4	1.17 ± 0.06	1.10 ± 0.01
10-Hydroxy-CBZ	CBZ-10OH	0.01	0.34 ± 0.02	0.17 ± 0.09	0.06 ± 0.02	0.02 ± 0.01
10,11-Dihydro-10,11-10,11-dihydroxy-CBZ	CBZ-DHDH	0.01	0.94 ± 0.04	0.9 ± 0.1	0.91 ± 0.04	0.89 ± 0.06
9-Carboxylic acid-Acridine	CA-ACRI	0.01	0.35 ± 0.04	0.37 ± 0.03	0.46 ± 0.03	0.35 ± 0.09
Lamotrigine	LAM	0.035	1.07 ± 0.07	1.19 ± 0.25	1.20 ± 0.01	1.23 ± 0.06
Hydrochlorothiazide	HCT	0.015	3.1 ± 0.1	3.2 ± 0.2	3.17 ± 0.06	3.1 ± 0.1
Chlorothiazide	CT	0.005	0.12 ± 0.01	0.13 ± 0.01	0.15 ± 0.01	0.15 ± 0.01
4-amino-6-chloro-1,3-benzenedisulfonamide	HCT-TP	0.01	0.39 ± 0.02	0.40 ± 0.18	0.42 ± 0.02	0.42 ± 0.02
Climbazole	CLIM	0.005	0.72 ± 0.08	0.6 ± 0.3	0.35 ± 0.04	0.020 ± 0.001
Hydroxy-Climbazole	CLIM-OH	0.02	0.07 ± 0.01	0.14 ± 0.03	0.25 ± 0.02	0.10 ± 0.02
Aciclovir	ACI	0.025	0.17 ± 0.06	0.10 ± 0.05	0.06 ± 0.03	0.03 ± 0.01
Carboxy-Aciclovir	ACI-COOH	0.03	1.8 ± 0.1	1.8 ± 0.3	1.9 ± 0.3	1.90 ± 0.35
Clopidogrel	CLP	0.001	0.010 ± 0.001	0.010 ± 0.001	< LOQ	< LOQ
Clopidogrel acid	CLP-COOH	0.005	0.16 ± 0.01	0.14 ± 0.01	0.150 ± 0.001	0.15 ± 0.01
Iopromide	IOPR	0.05	1.7 ± 0.9	0.58 ± 0.44	0.10 ± 0.09	0.050 ± 0.001
Iopromide-TP-701A	IOPR-701A	0.05	0.13 ± 0.07	0.13 ± 0.07	0.23 ± 0.18	0.34 ± 0.31
Iopromide-TP-819	IOPR-819	0.2	0.30 ± 0.21	0.3 ± 0.2	0.24 ± 0.06	0.20 ± 0.01
Iopromide-TP-729A	IOPR-729A	0.08	046 ± 0.30	0.36 ± 0.20	0.56 ± 0.38	0.7 ± 0.5
Iopromide-TP-759	IOPR-759	0.2	0.30 ± 0.21	0.4 ± 0.2	0.9 ± 0.9	1.2 ± 1.4
Iomeprol	IOME	0.05	1.73 ± 0.80	0.9 ± 0.6	0.18 ± 0.12	0.11 ± 0.10
Isoproturon	ISO	0.001	0.25 ± 0.11	0.21 ± 0.14	0.21 ± 0.12	0.20 ± 0.11
Terbutryn	TERB	0.001	0.10 ± 0.05	0.09 ± 0.05	0.08 ± 0.04	0.06 ± 0.02
Benzotriazole	BENZ	0.09	5.4 ± 0.57	3.80 ± 1.12	0.86 ± 0.34	0.96 ± 0.91
Caffeine	CAF	0.002	1.24 ± 0.44	0.04 ± 0.03	0.010 ± 0.001	0.08 ± 0.13
Sucralose	SUC	0.06	8.1 ± 0.7	8.1 ± 0.9	8.0 ± 0.8	7.6 ± 0.9
Substances negatively charged at pH 7						
Torsemide	TORA	0.005	0.11 ± 0.01	0.11 ± 0.01	0.11 ± 0.01	0.10 ± 0.01
Valsartan	VAL	0.005	1.88 ± 0.64	0.07 ± 0.04	0.02 ± 0.01	0.01 ± 0.01
Valsartan acid	VALac	0.005	1.85 ± 0.30	2.47 ± 0.38	0.72 ± 0.16	0.86 ± 1.17
Irbesartan	IRB	0.005	0.67 ± 0.08	0.65 ± 0.08	0.62 ± 0.05	0.60 ± 0.05
Candesartan	CAN	0.002	1.200 ± 0.001	1.200 ± 0.001	1.23 ± 0.06	1.200 ± 0.001
Telmisartan	TEL	0.005	0.27 ± 0.05	0.26 ± 0.06	0.18 ± 0.03	0.17 ± 0.08
Olmesartan	OLM	0.02	0.75 ± 0.04	0.76 ± 0.12	0.76 ± 0.01	0.75 ± 0.01
Bezafibrate	BZF	0.002	0.26 ± 0.04	0.19 ± 0.11	0.04 ± 0.04	0.02 ± 0.03
Sulfamethoxazole	SMX	0.01	0.86 ± 0.10	0.7 ± 0.3	0.19 ± 0.05	0.15 ± 0.03
Diatrizoic acid	DIA	0.015	0.2 ± 0.1	0.2 ± 0.1	0.18 ± 0.13	0.18 ± 0.12
Diclofenac	DCF	0.002	4.80 ± 0.01	4.6 ± 1.9	4.47 ± 0.12	4.2 ± 0.3
4-Hydroxy-DCF	DCF-4-OH	0.002	0.99 ± 0.03	0.9 ± 0.3	0.87 ± 0.03	0.5 ± 0.2
DCF lactam	DCFlac	0.001	0.04 ± 0.01	0.05 ± 0.01	0.07 ± 0.01	0.07 ± 0.04
Oxypurinol	OXY	0.15	14.7 ± 1.7	15.0 ± 2.2	15 ± 1	16 ± 0
Mecoprop	MEC	0.01	1.64 ± 0.87	1.35 ± 1.03	0.58 ± 0.42	0.4 ± 0.4
Acesulfame	ACE	0.01	2.6 ± 0.6	1.01 ± 0.55	0.6 ± 0.3	0.14 ± 0.08
Saccharine	SAC	0.005	0.29 ± 0.12	0.010 ± 0.001	0.010 ± 0.001	0.04 ± 0.05
Substances with positive charge or zwitter ionic form at pH 7						
Tramadol	TRAM	0.002	1.13 ± 0.05	1.17 ± 0.48	1.13 ± 0.06	0.99 ± 0.11
O-desmethyl-TRAM	TRAM-O-DM	0.01	0.25 ± 0.01	0.25 ± 0.03	0.25 ± 0.01	0.25 ± 0.01
N,O-didesmethyl-TRAM	TRAM-DDM	0.015	0.16 ± 0.01	0.17 ± 0.01	0.17 ± 0.01	0.170 ± 0.001
Gabapentin	GABA	0.02	1.6 ± 0.1	1.0 ± 0.4	0.18 ± 0.05	0.10 ± 0.04
Gabapentin lactam	GABAlac	0.01	0.13 ± 0.03	0.18 ± 0.06	0.15 ± 0.03	0.14 ± 0.02
Sulpiride	SULP	0.005	0.12 ± 0.01	0.120 ± 0.001	0.12 ± 0.01	0.11 ± 0.01
Amisulpride	AMIS	0.005	0.061 ± 0.02	0.6 ± 0.1	0.65 ± 0.05	0.63 ± 0.03
Citalopram	CIT	0.01	2.35 ± 0.25	2.17 ± 1.07	0.29 ± 0.15	0.030 ± 0.001
Venlafaxine	VLX	0.002	1.33 ± 0.05	1.3 ± 0.5	1.27 ± 0.06	0.55 ± 0.16
O-desmethyl-VLX	VLX-O-DM	0.01	1.70 ± 0.08	1.67 ± 0.10	1.67 ± 0.06	1.600 ± 0.001
N,O-didesmethyl-VLX	VLX-DDM	0.01	0.16 ± 0.01	0.15 ± 0.01	0.15 ± 0.01	0.14 ± 0.01
Metoprolol	METO	0.005	2.1 ± 0.1	1.8 ± 0.8	0.83 ± 0.25	0.6 ± 0.3
Atenolol	ATE	0.01	0.70 ± 0.04	0.70 ± 0.04	0.04 ± 0.02	< LOQ
Atenolol acid	ATE-COOH	0.015	1.70 ± 0.08	1.43 ± 0.66	0.75 ± 0.23	0.60 ± 0.26
Trimethoprim	TMP	0.005	1.15 ± 0.06	0.6 ± 0.4	0.3 ± 0.2	0.03 ± 0.01
Sitagliptin	SITA	0.01	2.28 ± 0.05	2.3 ± 0.5	2.2 ± 0.1	1.800 ± 0.001
Diphenhydramine	DIP	0.005	0.57 ± 0.06	0.5 ± 0.2	0.02 ± 0.01	0.020 ± 0.001
Cetirizine	CET	0.005	0.14 ± 0.01	0.14 ± 0.09	0.13 ± 0.02	0.11 ± 0.01
Fexofenadine	FEX	0.005	0.25 ± 0.01	0.16 ± 0.06	0.02 ± 0.01	0.01 ± 0.01
Denatonium	DEN	0.001	0.24 ± 0.04	0.23 ± 0.05	0.23 ± 0.02	0.23 ± 0.02
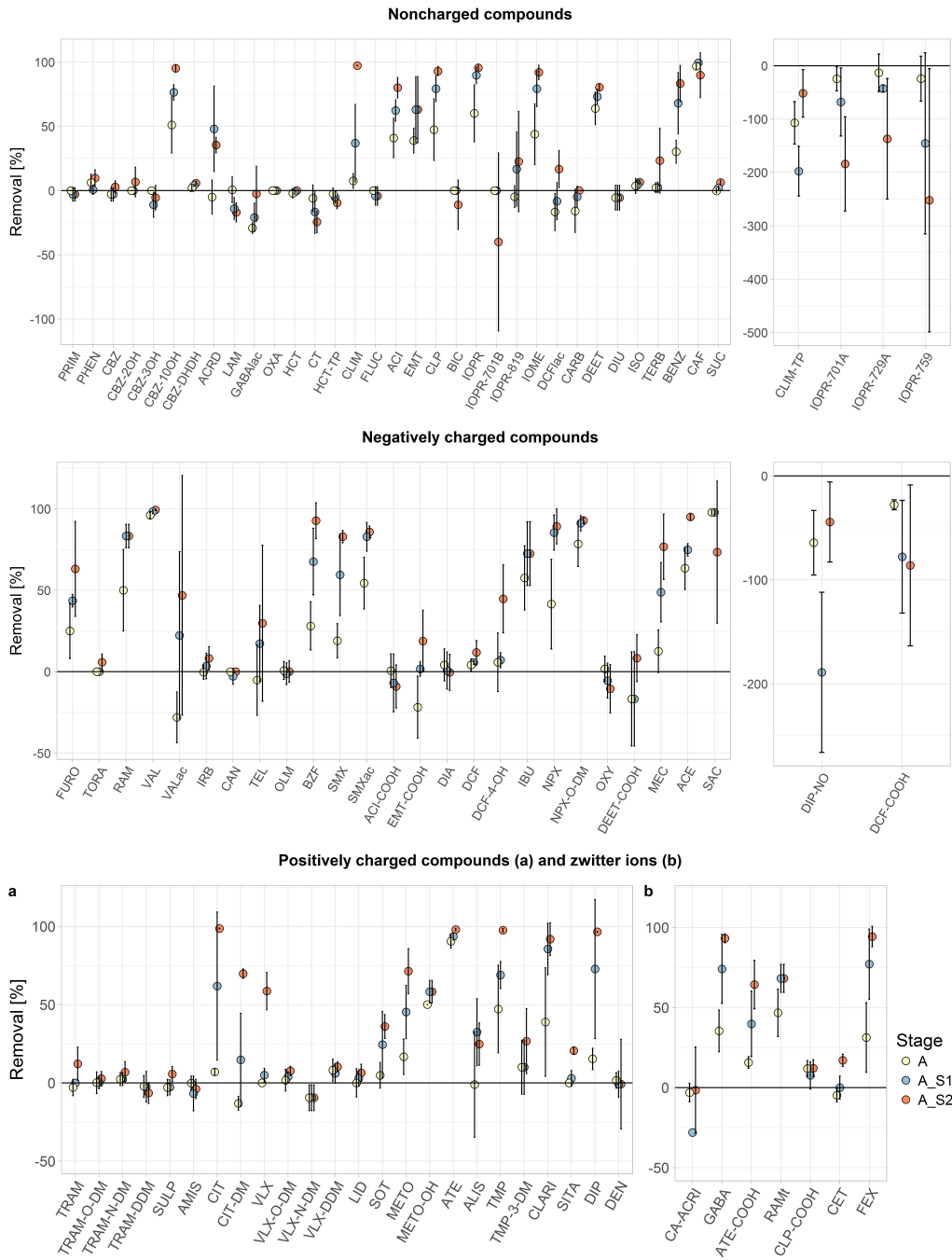
Figure 3.4: Removal of TOrCs in percent during SBF treatment. Column A: EBCT of 90 min, column train A_S1: EBCT 200 min, column train A_S2: EBCT 2000 min. The right graph of the noncharged and negatively charged compounds shows formation of TPs of higher than 50%.
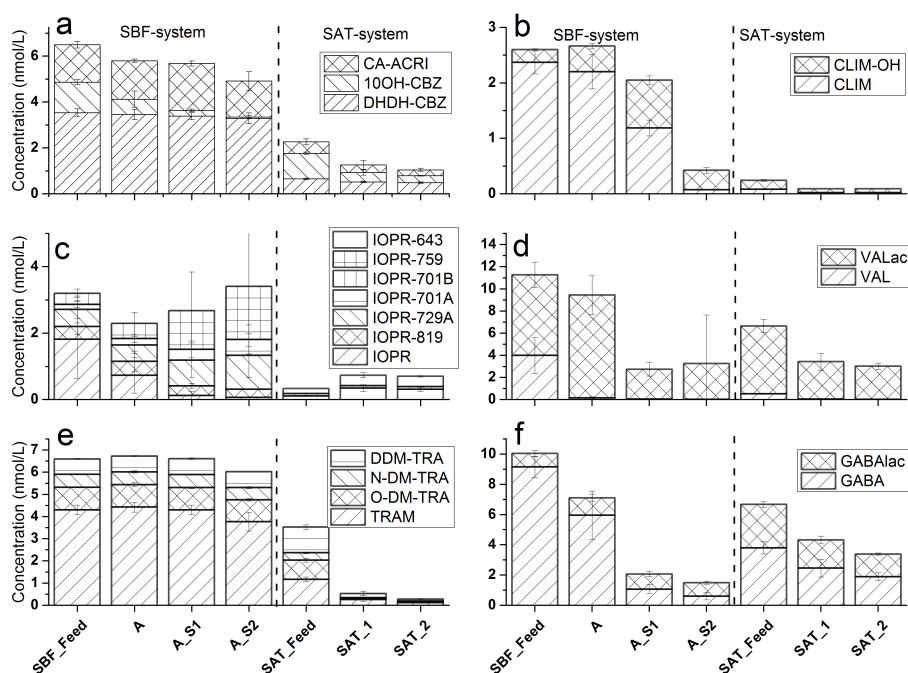
Figure 3.5: Molar concentrations of TOrCs with analyzed TPs; a) 10-hydroxy carbamazepine (10OH-CBZ) and 10,11-dihydro-10,11-dihydroxy carbamazepine (DHDH-CBZ); b) climbazole* (CLIM) and climbazole hydroxyl (CLIM-OH); c) iopromide* (IOPR) and its TPs; d) valsartan (VAL) and valsartan acid (VALac); e) tramadol* (TRA) and its demethylated TPs; and f) gabapentin (GABA) and gabapentin lactam (GABAlac); *spiked in SBF.

either the TPs or the formation of unknown TPs. A_S2 representing longer EBCTs exhibited the lowest concentrations of climbazole and the highest for the TP climbazole-OH and in sum only 15% of the initial concentration remained. Brienza and Chiron (2017) [142] stated that the (bio)degradation of climbazole can occur under anaerobic conditions thus processes under suboxic conditions at longer EBCT of A_S2 might have contributed to the enhanced degradation compared to the fully oxic conditions of A_S1 column. For the X-ray contrast medium iopromide (initial concentration 0.05 mg/L (0.06 nmol/L), spiked at > 1 mg/L (1.26 nmol/L)) concentrations were reduced by more than 80% in A_S1 and by more than 90% in A_S2. Degradation of iopromide under oxic conditions was studied in detail by Schulz et al. [119] and seven of the major TPs were included into this analytical method as isolated reference standards were available. Five of these iopromide TPs were

detected during SBF studies: all of them could be already detected in the feed water. The final stable TP of the oxic transformation pathway was not detected, and thus, the transformation of iopromide was incomplete. The mass balance for iopromide and its TPs (Figure 3.5c) reveals the formation of TPs 729A, 759 and 701A during SBF treatment. These results support the findings of Müller et al. (2019) [143].

The concentrations of the majority of the negatively charged substances were significantly reduced and the formation of TPs confirmed that biodegradation played a major role for the removal. However, some negatively charged substances were also persistent, e.g. diclofenac. Of the sartan group only valsartan was removed by more than 90% already in column A, highlighting the rapid biodegradability of this substance. Bayer et al. (2014) [144] suggested that the biodegradability was due to the amide moiety and the aliphatic carboxyl moiety. The mass balance for valsartan and its TP valsartan acid (Figure 3.5d) indicated a reduction of the precursor in column A and formation of the TP. In A_S1 and A_S2 effluents, valsartan was not detected anymore. Although a high variation of concentration was observed in A_S2 for valsartan acid a clear decrease in concentration compared to column A showed a biodegradability of this TP. Also in A_S1 removal was achieved and comparable mean values between A_S1 and A_S2 were observed.

For positively charged substances and zwitterionic TOrCs a similar pattern as seen for non-charged substances was observed: about half of the substances were persistent. Tramadol and its metabolites for example did not exhibit any reduction of their concentrations (except for a slight reduction in A_S2 as can be seen in the mass balance Figure 3.5e). Similar results were obtained for sitagliptin and cetirizine. Biodegradation, on the other hand, could be confirmed for citalopram due to the formation of desmethyl citalopram and for gabapentin due to the formation of gabapentin lactam. Both precursor substances showed an increased removal with increased residence time in both second stages, S1 and S2, and for citalopram a removal could only be achieved after aeration. For gabapentin, an increased removal was observed with increasing EBCT. Recently, Henning et al. (2018) [140] observed an enhanced biodegradability of gabapentin under oxic conditions and identified gabapentin lactam as its major TP. In SBF, partial removal of gabapentin and a slight formation of its TP was also observed in column A (see Figure 3.5f). In the SBF trains A_S1 and A_S2, however, equal TP concentrations could be detected in the effluents of the column trains despite further removal of gabapentin. As a consequence, the mass balance was incomplete in all cases with only 15% of the initial summed concentration left, showing that either the TP was removed during treatment or that other, not-analysed TPs, were

formed.

These results indicate that, although in tendency the removal in sum was higher in A_S2 than in A_S1, redox conditions besides EBCT, played an important role for an efficient removal of certain TOrCs. The concentrations of TOrCs such as the insect repellent DEET, caffeine and valsartan could be efficiently reduced already in column A, while for others such as mecoprop and citalopram the longest EBCT was essential to achieve a removal of higher than 70%. These results emphasize the importance of studying the behaviour of a larger number of TOrCs to identify suitable indicators for process evaluation.

3.3.3   Comparative assessment of fate and removal in SAT

More than 70 TOrCs were detected in the feed water to the infiltration basin with concentrations up to 9.0 mg/L (oxypurinol). Similar to the SBF system, oxypurinol showed the highest concentrations of all TOrCs studied. Additional four substances were detected at concentrations exceeding 1.0 mg/L, which also were amongst the highest concentrations found in the feed water of the SBF system: sucralose (7.4 mg/L), hydrochlorothiazide (1.7 mg/L), acesulfame (1.7 mg/L), and valsartan acid (1.6 mg/L). In comparison to the SBF system which was fed with municipal WWTP effluent from an urban sewershed, pesticides were detected at higher frequency and higher concentrations in the feed water of the SAT system located in a Spanish rural area. Particularly substances being used as algicides (i.e., diuron, terbutryn and irgarol) were found at elevated concentrations. The system was operated in an area impacted by agricultural activities adjacent to the WWTP and the infiltration site. Furthermore, the site was located close to the Mediterranean Sea and a small marina was close by. Thus, the detected pesticides might have reached the sampled water by urban run-off and leaching.

The overall removal of all detected TOrCs in the SAT system grouped by their charge at pH 7 (Figure 3.3b) showed a clearly better removal of positively charged and zwitterionic TOrCs compared to neutral and negatively charged ones. For the latter two groups the attenuation ranged from no removal at all to a good removal of more than 70%, while the positively charged TOrCs could be attenuated nearly completely and the zwitterionic ones up to 100%.

The concentrations and removal values are illustrated in Table 3.2 for selected TOrCs with feed water concentration at least 10 times the LOQ and Figure 3.6 for all detected TOrCs, respectively (for concentrations and removal of all TOrCs, see Table A2.3). The

Table 3.2: Effluent concentrations for the TOrCs detected at feed water concentrations of at least ten times the LOQ in the SAT system (n = 3). Concentrations given in µg/L. A list with results for all TOrCs can be found in Table A2.3

Substance	Abbrev	LOQ (µg/L)	Concentrations (µg/L) in the effluent of the columns		
			Feed	SAT_1	SAT_2
Substances uncharged at pH 7					
Phenytoin	PHEN	0.001	0.07 ± 0.01	0.060 ± 0.001	0.050 ± 0.001
Carbamazepine	CBZ	0.001	0.020 ± 0.001	0.030 ± 0.001	0.030 ± 0.001
10-Hydroxy-CBZ	CBZ-10OH	0.01	0.28 ± 0.01	0.10 ± 0.03	0.080 ± 0.001
10,11-Dihydro-10,11-dihydroxy-CBZ	CBZ-DHDH	0.01	0.17 ± 0.01	0.14 ± 0.01	0.13 ± 0.01
9-Carboxylic acid-Acridine	CA-ACRI	0.01	0.11 ± 0.03	0.07 ± 0.04	0.06 ± 0.02
Acridone	ACRD	0.001	<LOQ	0.010 ± 0.001	0.010 ± 0.001
Lamotrigine	LAM	0.035	0.029 ± 0.04	0.24 ± 0.04	0.21 ± 0.01
Oxazepam	OXA	0.005	0.07 ± 0.01	0.05 ± 0.01	0.040 ± 0.001
Hydrochlorothiazide	HCT	0.015	1.7 ± 0.2	1.3 ± 0.2	1.07 ± 0.03
Chlorothiazide	CT	0.005	0.07 ± 0.01	0.13 ± 0.01	0.13 ± 0.01
4-amino-6-chloro-1,3-benzenedisulfonamide	HCT-TP	0.01	0.46 ± 0.04	0.46 ± 0.03	0.41 ± 0.01
Aciclovir	ACI	0.025	0.040 ± 0.001	0.030 ± 0.001	0.030 ± 0.001
Carboxy-Aciclovir	ACI-COOH	0.03	0.38 ± 0.07	0.17 ± 0.06	0.11 ± 0.03
Clopidogrel	CLP	0.001	0.001 ± 0.001	0.001 ± 0.001	0.001 ± 0.001
Clopidogrel acid	CLP-COOH	0.005	0.09 ± 0.02	0.02 ± 0.01	0.010 ± 0.001
Iopromide	IOPR	0.05	< LOQ	< LOQ	< LOQ
Iopromide-TP-643	IOPR-643	0.1	0.100 ± 0.0001	0.20 ± 0.05	0.20 ± 0.001
Iopromide-TP-701A	IOPR-701A	0.05	0.07 ± 0.01	0.24 ± 0.07	0.22 ± 0.04
Iopromide-TP-701B	IOPR-701B	0.05	0.050 ± 0.001	0.050 ± 0.001	0.050 ± 0.001
Carbendazim	CARB	0.002	0.040 ± 0.001	0.040 ± 0.001	0.030 ± 0.001
DEET	DEET	0.001	0.04 ± 0.01	0.03 ± 0.01	0.020 ± 0.001
Hydroxy-DEET	DEET-OH	0.005	0.100 ± 0.001	0.07 ± 0.01	0.060 ± 0.001
Diuron	DIU	0.002	0.19 ± 0.02	0.11 ± 0.02	0.08 ± 0.01
N-Demethoxylinuron	DCPMU	0.001	< LOQ	0.010 ± 0.001	0.010 ± 0.001
Terbutryn	TERB	0.001	0.14 ± 0.01	0.06 ± 0.02	0.04 ± 0.01
Irgarol	IRG	0.001	0.070 ± 0.001	0.03 ± 0.01	0.020 ± 0.001
Benzotriazole	BENZ	0.09	0.11 ± 0.02	0.11 ± 0.01	0.11 ± 0.01
Caffeine	CAF	0.002	0.02 ± 0.01	0.03 ± 0.03	0.01 ± 0.01
Sucralose	SUC	0.06	7.4 ± 0.7	7.1 ± 0.4	6.3 ± 0.2
Substances negatively charged at pH 7					
Furosemide	FURO	0.01	0.08 ± 0.02	0.05 ± 0.01	0.040 ± 0.001
Valsartan	VAL	0.005	0.23 ± 0.01	0.02 ± 0.01	0.010 ± 0.001
Valsartan acid	VALac	0.005	1.6 ± 0.2	0.9 ± 0.2	0.79 ± 0.07
Irbesartan	IRB	0.005	0.49 ± 0.07	0.37 ± 0.09	0.33 ± 0.03
Candesartan	CAN	0.002	0.16 ± 0.01	0.15 ± 0.01	0.140 ± 0.001
Telmisartan	TEL	0.005	0.15 ± 0.02	0.010 ± 0.001	0.010 ± 0.001
Olmesartan	OLM	0.02	0.22 ± 0.01	0.20 ± 0.02	0.19 ± 0.01
Sulfamethoxazole	SMX	0.01	0.09 ± 0.01	0.20 ± 0.02	0.25 ± 0.01
Diclofenac	DCF	0.002	0.20 ± 0.02	0.04 ± 0.02	0.010 ± 0.001
4-Hydroxy-Diclofenac	DCF-4-OH	0.002	0.04 ± 0.03	0.03 ± 0.01	0.010 ± 0.001
Diclofenac Lactam	DCFlac	0.001	0.010 ± 0.001	0.010 ± 0.001	0.010 ± 0.001
Oxypurinol	OXY	0.15	9.1 ± 1.1	7.1 ± 0.6	5.4 ± 0.3
Acesulfam	ACE	0.01	1.7 ± 0.03	1.5 ± 0.2	1.4 ± 0.1
Saccharine	SAC	0.005	0.21 ± 0.03	0.010 ± 0.001	0.010 ± 0.001
Substances with positive charge or zwitter ionic form at pH 7					
Tramadol	TRAM	0.002	0.31 ± 0.03	0.07 ± 0.02	0.030 ± 0.001
O-desmethyl-Tramadol	TRAM-O-DM	0.01	0.21 ± 0.02	< LOQ	< LOQ
N-desmethyl-Tramadol	TRAM-N-DM	0.01	0.08 ± 0.01	< LOQ	< LOQ
N,O-didesmethyl-Tramadol	TRAM-DDM	0.015	0.27 ± 0.02	0.04 ± 0.02	0.020 ± 0.001
Gabapentin	GABA	0.02	0.65 ± 0.07	0.42 ± 0.10	0.32 ± 0.04
Gabapentin Lactam	GABAlac	0.01	0.44 ± 0.03	0.28 ± 0.04	0.023 ± 0.01
Sulpiride	SULP	0.005	0.100 ± 0.001	0.010 ± 0.001	0.010 ± 0.001
Citalopram	CIT	0.01	0.09 ± 0.01	0.010 ± 0.001	0.010 ± 0.001
Desmethyl-Citalopram	CIT-DM	0.001	0.05 ± 0.01	< LOQ	< LOQ
Venlafaxine	VLX	0.002	0.16 ± 0.02	< LOQ	< LOQ
O-desmethyl-Venlafaxine	VLX-O-DM	0.01	0.52 ± 0.05	< LOQ	< LOQ
N-desmethyl-Venlafaxine	VLX-N-DM	0.005	0.030 ± 0.001	< LOQ	< LOQ
Lidocaine	LID	0.001	0.040 ± 0.001	0.020 ± 0.001	< LOQ
Sotalol	SOT	0.045	0.09 ± 0.01	0.050 ± 0.001	0.050 ± 0.001
Atenolol	ATE	0.01	0.14 ± 0.02	0.010 ± 0.001	0.010 ± 0.001
Aliskiren	ALIS	0.02	0.26 ± 0.06	0.020 ± 0.001	0.020 ± 0.001
Sitagliptin	SITA	0.01	0.17 ± 0.01	0.010 ± 0.001	0.010 ± 0.001
Cetirizine	CET	0.005	0.06 ± 0.01	0.010 ± 0.001	0.010 ± 0.001
Fexofenadine	FEX	0.005	0.130 ± 0.001	0.010 ± 0.001	0.010 ± 0.001
Imidacloprid	IMI	0.025	0.11 ± 0.01	0.9 ± 0.1	0.8 ± 0.1
Denatonium	DEN	0.001	0.030 ± 0.001	0.001 ± 0.001	0.001 ± 0.001
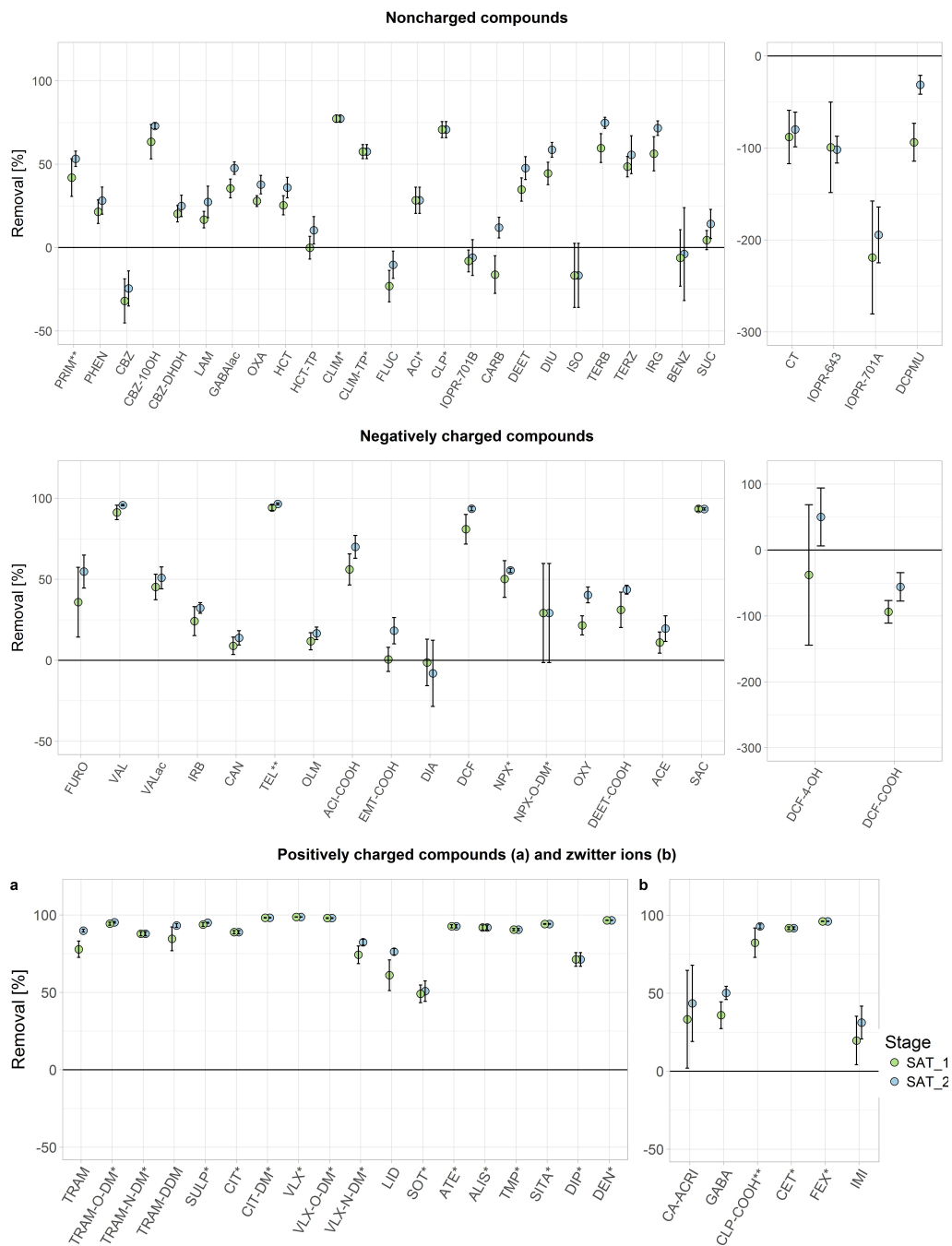
Figure 3.6: Removal of TOrCs during SAT treatment for a travel time of 30 and 72 h, respectively. TOrCs reaching the LOQ of the concentration are marked with * for LOQ in SAT_1 and with ** for reaching LOQ in SAT_2. The right graph of the noncharged and negatively charged compounds shows formation of TPs of higher than 50%.

HRT in the SAT system was comparable to the SBF system (HRT of SAT_1 compared to column-system A_S2). For all substances detected, it can be assumed that the major removal occurred during travel through the vadose zone to the first observation well (SAT_1). The groundwater passage to reach SAT_2 had only minor additional improvement of TOrC removal. By measurements of oxygen in the sampled water of SAT_1, it could be observed that oxic conditions prevailed in the vadose zone and the concentrations of about 60% of all detected TOrCs decreased during the soil passage. It is noteworthy that the studied SAT site was in operation for only three years [138] prior to the sampling campaign and that the infiltration was not continuously operated during this period. Baumgarten et al. (2011) [145] reported that adaptation for the microbial community to remove certain TOrCs such as sulfamethoxazole might take up to several years. With longer operation time the biodegradation of certain TOrCs might improve.

Thirty of the non-charged TOrCs were present in the feed water. Of these, 11 TOrCs exhibited removal efficiencies of higher than 30% in SAT_2 after 72 h of retention time, while none were removed by more than 80%. Several TOrCs were neither removed during SAT nor during SBF, e.g. carbamazepine, lamotrigine, and oxazepam, since they are neither biodegradable nor having elevated sorption affinities to soil/aquifer particles. Hydrochlorothiazide was detected at elevated concentrations in the feed water of both systems (> 3.0 µg/L (> 10 nmol/L) in SBF, > 1.5 µg/L (> 5 nmol/L) in SAT). In contrast to SBF, a removal of hydrochlorothiazide was observed during SAT (25 - 35%), while the concentrations of the TP chlorothiazide doubled during soil passage. For the total concentrations of hydrochlorothiazide and chlorothiazide (see Figure A2.4g) a clear decrease and an incomplete mass balance were observed during SAT. The sweetener sucralose also was found at elevated concentrations in both systems (> 5 µg/L for both). Neither in SBF nor in SAT a removal was achieved. Scheurer et al. (2009) [146] studied the occurrence of sweeteners in wastewater and after SAT. In WWTPs only a minor removal was observed, and at an SAT site even a travel time of more than a month did not support removal of sucralose by more than 50%, indicating the high mobility and elevated persistence of the artificial sweetener. Based on sucralose measurements, dilution with native groundwater in SAT_1 and SAT_2 can be characterized as < 5% and < 15%, respectively. The antithrombotic agent clopidogrel was detected at very low concentrations (< 0.001 µg/L (< 0.01 nmol/L)). In both systems a removal of more than 70% was observed. The metabolite clopidogrel carboxylic acid (zwitterionic at pH 7) was detected at concentrations of around 0.10 µg/L (0.24 nmol/L) in the feed water of both systems. In contrast to SBF, a removal efficiency

of higher than 90% was found in SAT (see Figure A2.4h). The positively charged site of the zwitter ion might have a major influence on the removal in soil, as explained later in this section. Similar to the SBF system, iopromide was degraded, but other TPs were detected (Figure 3.5c). While in SAT mainly TPs were found which are formed in the last reactions of the described transformation pathways (e.g., TP 701A and TP 643), after SBF mainly TPs were found which are formed at the beginning of the transformation pathway. The most obvious difference was the formation of the final TP 643 during SAT. In SBF, iopromide was spiked into the feed water to follow its degradation process, whereas in the feedwater of the SAT system only the iopromide TPs were detected. Thus, no further formation of the early stage TPs occurred in SAT in contrast to SBF, but a further transformation of already formed TPs towards the final iopromide TP 643. The herbicides/algicides diuron, terbutryn and irgarol were detected with concentrations of around 0.10 µg/L in the feed water of the SAT system. All three herbicides were removed by about 50% during the soil passage. Stasinakis et al. (2009) [147] and Luft et al. (2014) [148] already showed the biodegradability of these substances in WWTPs under oxic conditions. They also identified TPs for all three substances. However, these TPs were not included into the monitoring campaign of this study except for two diuron TPs which were detected at low concentrations (< 0.01 µg/L) after SAT.

Of the negatively charged TOrCs, 20 compounds were detected in the feed water. Of these, 12 TOrCs were reduced in concentration either by transformation or sorption by more than 30% in SAT_2, four even above 90%. In both systems (SAT and SBF), oxypurinol was detected at elevated concentrations (> 9 µg/L). It was frequently detected in water samples at this concentration range and was stable during wastewater treatment [23]. It is a highly mobile substance and can thus reach drinking water wells. In the SBF system, no removal at all was observed for oxypurinol indicating its persistence in biological processes. In the SAT system, a minor change of the concentrations (approx. 20%) during soil passage (SAT_1) and an overall removal of 40% in SAT_2 was observed, which is higher than expected from the limited (bio)degradability reported by Funke et al. (2015) [23]. Diclofenac was removed by more than 80% in SAT. In SBF, its reduction was negligible and only a slight formation of its TP diclofenac carboxylate [149] was observed. In SAT, no TPs were found, neither in the feed water nor after soil passage. Rühmland et al. (2015) [63] observed a removal of diclofenac by photodegradation in in-situ degradation experiments and Muntau et al. (2017) [150] confirmed this at a full-scale SAT site in northern Germany. During the sampling campaign for this study, samples of the feed water were taken at the

pumping station prior to the basin. Thus, it cannot be ruled out that photodegradation occurred in the basin where feed water was exposed to sunlight during operation. The observed removal for diclofenac is also in accordance with other SAT studies [60, 150, 151]. The compounds of the sartan group showed a very different behaviour to each other during soil passage. While valsartan was removed very well in both systems, irbesartan and telmisartan indicated a moderate to good removal during SAT but were stable in SBF. Olmesartan and candesartan remained stable in both systems. In both SBF and SAT, the concentrations of the TP valsartan acid were reduced (see Figure 3.5d). Neither Nödler et al. (2013) [124] nor Kern et al. (2010) [152] observed a removal of valsartan acid in bank filtration and in sludge treatment. Sorption effects in SAT seem to be unlikely due to the very low log D value ($<$ -1) and thus it is assumed that removal in SAT was due to biological degradation as it was also observed during SBF. The sweetener acesulfame was detected at concentrations $>$ 1.5 µg/L in both systems. In contrast to the good removal in SBF, no removal was observed during SAT. Contradictory results have also been observed in literature showing elevated removal [153] as well as persistent behaviour [120] of acesulfame in sand filtration and managed aquifer recharge systems. The persistent behaviour in some systems including the investigated SAT site might be explained by a lack of an adopted microbial community appropriate for degradation of acesulfame.

In total, 24 TOrCs detected in the feed water were positively charged or zwitterionic. All of them showed a removal of higher than 80% in SAT_2, except for six TOrCs which were removed between 30 and 80%. In contrast to the SBF system, gabapentin was not efficiently removed in SAT. For its TP gabapentin lactam (noncharged compound) the same behaviour was observed. Both substances exhibited a removal of only up to 35% (see also Figure 3.5f). Tramadol and venlafaxine as well as their metabolites/TPs were efficiently removed to more than 80% (for tramadol mass balance, see Figure 3.5e). During SBF, removal was only observed for venlafaxine at longer EBCTs. However, other studies also showed an efficient removal of these compounds in column experiments [154, 155]. Considering that also the other positively charged TOrCs showed a similar behaviour and no TPs were detected, sorption by ionic interactions, i.e. cation exchange, might be a plausible reason for the elevated removal during SAT. The importance of cation exchange as an attenuation process in SAT systems is already described by He et al. (2016) [60], but so far it was only reported for a small number of TOrCs. Here, in total 33 positively charged TOrCs (18 of these could be detected in the feed water of the SAT system), and eight zwitterionic substances (six detected in the feed water) showed a similar removal
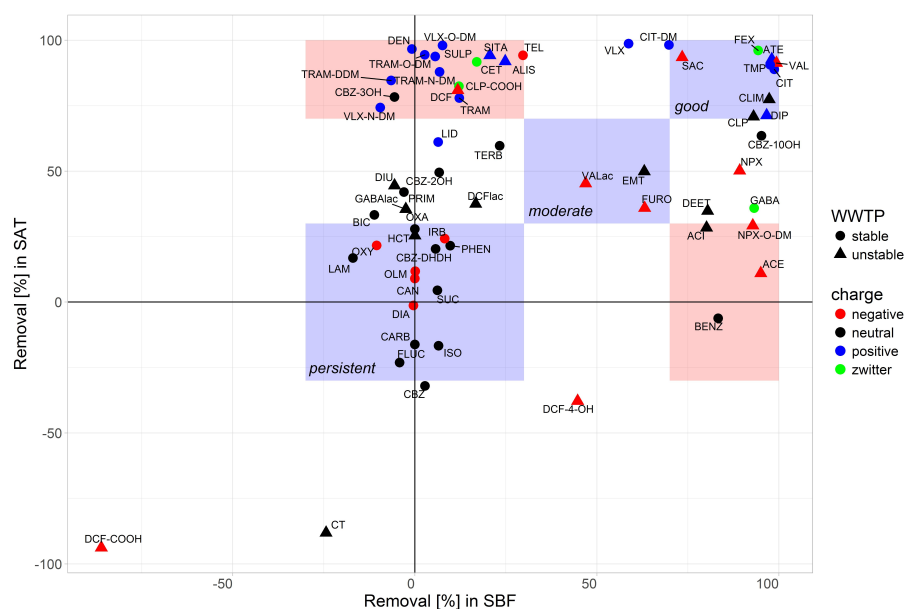
Figure 3.7: Comparison of removal values in SBF and SAT. Inserted blue boxes illustrate regions of similar behaviour, red boxes illustrate a different behaviour for the same hydraulic retentions time (SAT_1 vs. A_S2). Assignment of "stable" and "unstable" in WWTPs is based on literature research on the behaviour in conventional WWTPs reported in literature (see Table A2.1).

behaviour. These results in combination with the fact, that no major TPs from these substances could be detected in this nor in other studies, support the assumption of a removal by sorption, probably due to cation exchange during soil passage.

3.3.4 Direct comparison of removal in SBF and SAT

In this study, two different treatment systems, an engineered above-ground biological system (SBF) and a natural below-ground soil passage system (SAT), were studied. The removal of a broad set of TOrCs and TPs with different physico-chemical properties was utilized for water quality evaluation. For the SBF system, redox conditions changed from oxic to suboxic by adjusting the HRT, while in the SAT system oxic conditions prevailed. For the direct comparison of results from SAT and SBF systems in Figure 3.7 treatment options SAT_1 and A_S2 were chosen due to comparable HRTs.

Approximately 70 TOrCs were detected in the feed water of both systems. By classification of the removal results, process-based indicator chemicals can be deduced meeting the following criteria: persistent (removal < 30%), moderate removal (30 - 70%), and good

removal (> 70%). These classes are highlighted by blue boxes in Figure 3.7. Furthermore, two areas of TOrCs with a completely different behaviour are marked as red boxes.

The compounds in the blue boxes represent candidates for process evaluation of natural and biological treatment systems as they show consistent behaviour in both systems. Several TOrCs which are known to be persistent in conventional WWTPs (declared as "stable" in Figure 3.7) were also found to be persistent in SBF and SAT. Amongst these were carbamazepine and candesartan, but also human metabolites/TPs such as 10,11-dihydroxy-carbamazepine. In the group of moderately removable TOrCs, the TP valsartan acid can be found together with emtricitabine and furosemide. An elevated removal was observed in both systems for 10 TOrCs such as valsartan, fexofenadine and citalopram, probably due to biological degradation.

However, no single dominant transformation of specific compound moieties was observed. Rather, removal could be partly attributed to different transformation reactions such as hydrogenation/ dehydrogenation, amide hydrolysis and demethylation. Climbazole for example is transformed by the reduction/hydrogenation of the keto-function to an alcohol moiety [142], while for fexofenadine oxidation/ dehydrogenation of the secondary alcohol to a keto-moiety can be assumed [156]. Amide hydrolysis is involved in the transformations of atenolol to atenolol acid and valsartan to valsartan acid [157]. Trimethoprim has been stated to be degraded by demethylation of a methoxy group followed by hydroxylation and oxidation [158]. Consistently, in literature these mechanisms were found to proceed rather fast, however, no generalized conclusion about a dependency between specific compound moieties and the degradation efficiency in both systems can be drawn. Aliskiren for example contains a primary amide which might be expected to hydrolyse quickly as found for atenolol, however, no removal could be observed in SBF. Similarly, acyclovir was degraded in SBF to more than 90% and the formation of acyclovir acid confirmed the proposed mechanism of oxidation of primary alcohols [159]. In SAT, removal of acyclovir was very low with about 30% during the sampling campaign. A considerable higher removal in SBF compared to SAT was also observed for DEET which has been reported to be transformed by a dealkylation of the tertiary amine and an oxidation of the methyl moiety [157]. Further examples for inconsistent behaviour in SAT and SBF are acesulfame and gabapentin which is in accordance with a high variability of degradation reported in literature [140, 160, 161]. For all compounds with at least partly positively charged amine moieties at ambient pH, e.g. tramadol, venlafaxine, sitagliptin and denatonium, a considerable higher removal was observed in SAT. However, while removal of individual compounds

such as venlafaxine and tramadol might also be attributed to biodegradation, the consistent behaviour of 18 detected positively charged and zwitterionic compounds supports the assumption of cation exchange as an additional removal mechanism. In summary, it was found that no generalized moiety-specific conclusion could be drawn on the underlying attenuation mechanisms and emphasizes the need of a multi-compound method applied in this study.

Based on Figure 3.7, a list of possible candidates for indicator substances are proposed in Table 3.3 grouping TOrCs with a similar behaviour in both studied SBF and SAT or a completely contrary behaviour. Nevertheless, for all proposed TOrCs their occurrence needs to be confirmed, to choose them as site specific indicator substances.

3.4 Conclusions

Based on the occurrence and removal of more than 100 TOrCs, human metabolites and transformation products in two different biological treatment systems, a sequential biofiltration system with dominant compound removal by biodegradation and a soil-aquifer treatment system with HRT of a few days, where also sorption and dilution effects are relevant, the following conclusions can be drawn:

- In both systems, human metabolites and environmental TPs were sometimes detected in higher concentrations than the precursors (e.g., clopidogrel acid via clopidogrel). Since certain TPs exhibit a higher polarity and are rather persistent, they should be considered when designing monitoring concepts for process evaluation.

- Both systems demonstrated their capability as effective treatment steps. Since attenuation in SBF is only achieved by biodegradation, removal efficiency depends on redox conditions and HRT, while non-biodegradable TOrCs will always persist. In SAT, a combination of biotransformation and sorption effects was able to remove a broader set of TOrCs. However, the efficiency depends on site characteristics, for example soil properties or the adaption stage of the microbial community. In addition, TOrCs breakthrough might occur after longer operation periods triggering the need for long-term monitoring of potentially sorbed substances as removal capacities in the soil are mostly unknown.

- Results confirmed that the analysis of parent compounds and their major TPs pro-

Table 3.3: Candidate substances for the selection of indicators depending on the specific site conditions. Categories 1: physico-chemical properties at environmental pH (7 to 9): 0 = non-charged, + = positively charged, − = negatively charged, +/− = zwitterionic; 2: removal degrees (removal by transformation processes or sorption): i) good removal (> 70%), ii) moderate removal (30 - 70%), iii) persistent (< 30%); 3: feed water concentrations of more than 10 times the LOQ.

			Categories				
Substance	pK_a	LogD		SBF		SAT	
			1	2	3	2	3
persistent in both (removal < 30%)							
Oxazepam	10.61, < 1	2.92	0	iii		ii	•
Hydrochlorothiazide	9.1	- 0.58	0	iii	•	ii	•
Irbesartan	5.85, 4.12	4.40	-	iii	•	ii	•
Phenytoin	8.5	2.14	0	iii	•	iii	•
Carbamazepine (CBZ)	> 13.5	2.77	0	iii	•	iii	•
DHDH-CBZ	12.8	0.81	0	iii	•	iii	•
Oxypurinol	5.28, < 1	- 3.13	-	iii	•	iii	•
Lamotrigine	> 13.5, 5.89	1.89	0	iii	•	iii	
Olmesartan	0.89, 5.33	- 0.75	-	iii	•	iii	•
Candesartan	3.51, 1.25	0.92	-	iii	•	iii	•
Sucralose	11.9	- 0.47	0	iii	•	iii	•
Diatrizoic acid	2.2	- 0.62	-	iii	•	n.d.	
Carbendazim	9.7, 4.28	1.80	0	n.d.		iii	•
Isoproturon	> 13.5	2.57	0	iii	•	iii	•
Fluconazole	12.68, 2.3	0.56	0	iii	•	iii	
moderate removal in both (removal 30 - 70%)							
Valsartan acid	4.03, < 1	- 0.73	-	ii	•	ii	•
Emtricitabine	> 13.5	- 0.90	0	ii		ii	
Furosemide	4.25, < 1	- 0.94	-	ii	•	ii	
good removal in both (removal > 70%)							
Fexofenadine	4.04, 9.01	2.94	+/-	i	•	i	•
Atenolol	> 13.5, 9.67	- 2.14	+	i		i	•
Valsartan	4.35, < 1	1.49	-	i	•	i	•
Citalopram	9.8	1.14	+	i	•	i	
Trimethoprim	7.2	0.92	+	i	•	i	•
Saccharine	1.9	- 0.49	-	i	•	i	•
Climbazole	6.5	4.25	0	i	•	i	
good removal in SAT, persistent in SBF							
Tramadol	> 13.5, 9.23	0.24	+	iii	•	i	•
O-DM-Tramadol	9.62, 8.97	0.10	+	iii	•	i	•
N-DM-Tramadol	> 13.5, 9.89	- 0.66	+	iii	•	i	
N,O-DDM-Tramadol	9.22, 10.02	- 0.74	+	iii	•	i	•
O-DM-Venlafaxine	10.11, 8.87	0.69	+	iii	•	i	•
N-DM-Venlafaxine	> 13.5, 9.78	- 0.30	+	iii	•	i	
Diclofenac	4.0	1.37	-	iii	•	i	•
Clopidogrel acid	1.81, 7.53	1.21	+/-	iii	•	i	•
Telmisartan	3.62, 5.86	5.09	-	iii	•	i	•
Sulpiride	10.24, 8.39	- 1.07	+	iii	•	i	•
Aliskiren	> 13.5, 9.57	0.68	+	iii		i	•
Sitagliptin	8.8	- 0.51	+	iii	•	i	•
Cetirizine	3.59, 7.42	0.77	+/-	iii	•	i	•
Denatonium	12.1	0.41	+	iii	•	i	•
persistent in SAT, good removal in SBF							
Aciclovir	11.99, 3.02	- 1.03	0	i		ii	
Benzotriazole	8.63, < 1	1.29	0	i	•	iii	•
Acesulfame	3.0	- 1.49	-	i	•	iii	•
Gabapentin	4.63, 9.91	- 2.7	+	i	•	ii	•

vides an efficient measure to understand driving removal mechanisms in natural and biological systems. Increased TP concentration in effluents or monitoring wells confirmed biodegradation as a major mechanism for neutral (e.g. climbazole, iopromide) and negatively charged (valsartan) compounds.

- The selection of a large range of different TOrCs revealed additional information: while most positively charged compounds were persistent in SBF, consistently good removal was observed in SAT indicating cation exchange as major removal mechanism.

A selection of performance-based indicator chemicals and TPs must be adapted to site-specific conditions and should contain representatives of the following criteria:

1. TOrCs with different physico-chemical properties at environmental pH (7 - 9): i) non-charged, ii) positively charged, iii) negatively charged, iv) zwitterionic.

2. TOrCs with different removal degrees (removal by transformation processes or sorption): i) good removal ($> 70\%$), ii) moderate removal (30 - 70%), iii) persistent ($< 30\%$)

3. TOrCs with feed water concentrations of more than 10 times the LOQ

4. Pairs of precursor substances and their major human metabolites and TPs

Furthermore, the location of the treatment site and thus the likelihood of the appearance of substance classes (e.g.pharmaceuticals or pesticides) has to be considered. For instance, different TOrCs were present in urban (SBF) and rural (SAT) areas. Therefore, a pre-monitoring of the influent is mandatory to identify the TOrCs relevant for a specific area and country.

Acknowledgments

Chapter 4

Ozonation of sitagliptin: removal kinetics and elucidation of oxidative transformation products

N.Hermes, K.S. Jewell, P. Falås, H. V. Lutze, A. Wick T.A. Ternes

Abstract

Due to increasing use and high excretion rates high quantities of the antidiabetic drug sitagliptin (STG) enter wastewater treatment plants (WWTPs). In conventional biological treatment only a moderate removal was achieved and thus, STG can be detected in WWTP effluents with concentrations in the higher ng/L range. Ozonation is a widely discussed technique for advanced wastewater treatment. In lab-scale experiments STG showed pH dependent removal kinetics with a maximum apparent rate constant of k $\sim$ 1 x 10^4 M^{-1} s^{-1} at pH $\geq$ 9. With an apparent rate constant of k_{O3} = (1.8 $\pm$ 0.7) 10^3 M^{-1} s^{-1} at pH 8 STG can be considered to be readily degraded in ozonation of WWTP effluents. Ozone attacks the primary amine moiety of STG leading to nitro-STG (TP 437) (the primary amine moiety is transformed into a nitro group). Furthermore, a diketone (TP 406) was formed which can be further degraded by ozone. Lab-scale and pilot-scale experiments on ozonation of WWTP effluents confirmed that the ozone attack of STG was incomplete even at high ozone doses of 1.7 and 0.9 mg O_3/mg DOC, respectively. These experiments confirmed that nitro-STG was formed as the main TP in the wastewater matrix. Two other TPs, TP 421c and TP 206b, were also detected, albeit with low intensities.

4.1 Introduction

For many micropollutants it is known that conventional biological water treatment is insufficient for their removal [89, 162] and thus, advanced treatment processes such as ozonation and activated carbon are under investigation [163] to improve their removal. However, ozonation of wastewater treatment plant (WWTP) effluents usually does not lead to a complete mineralization of micropollutants, but rather to the formation of oxidative transformation products (TPs) [68]. Oxidative transformation through ozonation occurs via two pathways: (i) reactions with the ozone and (ii) reactions with intrinsically formed hydroxyl (OH) radicals, e.g., by ozone decay or reactions with organic matter [42]. The direct reaction with ozone is a selective reaction, since ozone primarily attacks electron-rich moieties such as double bonds, amines and activated aromatic rings [42].

Certain TPs might be more toxic than their precursors [164, 165] and some TPs, such as N-oxides, are known to be persistent in biological post-treatments and thus can reach receiving waters [43]. Therefore, identification of TPs is a key factor to understand the reaction of ozone with micropollutants. Many studies deal with reaction mechanisms of micropollutants containing ozone-reactive moieties such as olefins and aromatic compounds [40, 42, 166, 167]. However, information about reaction mechanisms of nitrogen-containing micropollutants is diverse: for aromatic amines, reactions preferably occur at the aromatic ring [43], mechanistic studies on the reaction of ozone with tertiary amines showed the formation of N-oxides and N-dealkylated products [43, 168], while for secondary amines hydroxylamines and N-dealkylated products were detected [43]. For aliphatic primary amines there is only scarce information provided in the literature. There are indications of the formation of hydroxylamines and oximes from aliphatic primary amines [169] as well as the conversion into nitro compounds during dry ozonation [170]. Recently, the knowledge about the mechanistic aspects of ozonation of aliphatic amines was deepened by the study of Lim et al. (2019) [44] on the aqueous ozonation of simple aliphatic amines. They used ethylamine, diethylamine and triethylamine as model substances, determined their removal kinetics and elucidated the chemical structure of TPs formed by the reaction with ozone. They determined species-specific secondary rate constants for the neutral compounds ranging from 9.3 x 10^4 - 2.2 x 10^6 M^{-1} s^{-1}. All amines were transformed into TPs via an attack on the amine. In particular, nitroalkanes were identified during ozonation and it was found that their reactivity towards further ozonation was very low. Formation of nitroalkanes was also found by Shi and McCurry (2020) [171] in the ozonation of N-

methylamines, i.e. secondary aliphatic amines such as ephedrine, fluoxetine and sertraline. To the best of the author's knowledge, there is no mechanistic study on the ozonation of environmentally relevant micropollutants containing an aliphatic primary amine as the main molecule site of reaction with ozone. Sitagliptin (STG) is a dipeptidyl peptidase 4 (DDP 4) inhibitor which is administered for the treatment of diabetes mellitus type 2 [172]. On the German market the antidiabetic STG was launched in 2007 and is either applied in combination with metformin (preparation Janumet and Velmetia) or as an individual pharmaceutical (e.g. Januvia and Xelevia) [139, 172]. Since 2007 STG-containing products were increasingly administered (Figure A3.1) [139]. Its human metabolisation rate is very low; about 80% of the administered antidiabetic is excreted via urine [172, 173] and thus a portion of administered STG enters WWTPs. Due to its elevated persistence and increasing consumption it is discharged in significant quantities by WWTPs with concentrations up to 1.0 µg/L in WWTP effluents [156, 174–176]. To the best of our knowledge, Henning et al. (2019) [156] performed the first study on the degradability of STG during biological wastewater treatment. They found that neither during conventional nor during advanced biological treatment in a moving bed biofilm reactor (MBBR) a degradation higher than 50% could be achieved. The main transformation reactions were found to be conjugation reactions to the primary amine moiety and amide hydrolysis.

Since the biodegradability in conventional and advanced biological treatment is low, additional advanced treatment is necessary for the abatement of STG during wastewater treatment. A widely discussed option for advanced treatment is ozonation. So far, there are no studies dealing with the transformation of STG during ozonation and thus, it was the aim of this study to elucidate the removal of STG by reactions with ozone and OH radicals. The reaction kinetics were determined and the chemical structures of TPs were elucidated. Laboratory batch experiments with WWTP effluents and analysis of effluents of an ozonation pilot plant were performed to confirm the transferability of the laboratory results with pure water to conditions occurring in WWTPs.

4.2 Materials and methods

Chemicals and Reagents: STG, STG-d4, TP 406 (1-[3-(trifluoromethyl)-6,8-dihydro-5H-[1,2,4]triazolo[4,3-a]pyrazin-7-yl]-4-(2,4,5-trifluorophenyl)butane-1,3-dione) and TP 192 (3-(trifluoromethyl)-5,6,7,8-tetrahydro-[1,2,4]triazolo[4,3-a]pyrazine hydrochloride) were purchased from TRC (Toronto, Canada). Trifluoroacetic acid (TFA, 99%, ReagentPlus®) and

13C$_2$-TFA were obtained from Sigma Aldrich (Seele, Germany). Phosphoric acid (purity 85 - 88%), indigo (5,5',7-Indigotrifulfonic acid potassium salt) as well as sodium bicarbonate (NaHCO$_3$) and sodium carbonate (Na$_2$CO$_3$) as eluent concentrate for ion chromatography (IC) (both 0.1 M in water) were purchased from Sigma Aldrich (Seelze, Germany). Sodium hydroxyide (NaOH pellets for analysis, Emsure® ISO), tertiary butanol (t-BuOH) (Emsure®), acetonitrile (LiChrosolv® hypergrade for LC-MS) and formic acid as eluent additive (LiChropur® for LC and Suprapur® for IC, both 98 - 100%) were obtained from Merck (Darmstadt, Germany). Ultrapure water was prepared with a Milli-Q system (Millipore, Merck).

Ozonation: Ozone was generated by silent discharge from oxygen using a Fischer Technology 500 ozone generator (Germany). The ozone-containing gas was sparged through an ice-cooled bottle with ultrapure water to produce an ozone stock solution. The ozone concentration of this stock solution was measured photometrically by direct analysis of ozone at a wavelength of $\lambda = 258$ nm with a molar absorption coefficient [177] of $\epsilon = 2950$ M^{-1} cm^{-1} and was found to be c$_{O3} \approx 1.2$ - 1.3 mM.

Removal kinetics: The removal kinetics of STG were determined under pseudo-first order conditions, i.e. under excess of ozone (molar stoichiometry O$_3$:STG $\geq$ 20). An analyte solution of STG (c$_0$ = 2.5 µmol/L) was prepared in 50 mM phosphate buffer. The pH was adjusted by addition of a 1 M NaOH solution. Experiments were performed at different pH values ranging from pH 4 to pH 9. A total volume of 250 mL was used for the kinetic experiments. The sample volume was 237 mL for pH values 6 - 9 with an addition of 13 mL of ozone stock solution (molar stoichiometry O$_3$:STG $\approx$ 20:1). For the lower pH values the O$_3$:STG stoichiometric ratio was increased to 30:1. A sample volume of 230 mL was used and 20 mL of the ozone stock solution was added. Experiments were performed with and without the addition of t-BuOH (1% v/v) as radical scavenger. After the addition of the ozone stock solution, samples (3 mL) were taken at defined time points by a dispenser and transferred to a vial which contained 250 µL of a 1 mM indigo solution for ozone quenching. Residual ozone was analysed photometrically by the removal of indigo at a wavelength of $\lambda = 600$ nm [178]. Samples for analysis of STG removal by liquid chromatography-quadrupole time-of-flight mass spectrometry with electrospray ionization (LC-ESI-QTOF) were diluted 1:1 with ultrapure water and an isotopically labelled internal standard (STG-d4) was added to a final concentration of 200 ng/L.

TP identification: Determination of potential TPs was performed with the time series samples of the kinetic experiments which were analysed by LC-ESI-QTOF. Changes

in the intensity of detected masses over time were observed by peak picking and alignment of the results in the software R [179]. Potential TPs were isolated for further investigation if they appeared in at least three samples of a time series as well as in replicates of the experiments and if MS^2 spectra were recorded. Structure elucidation was based on assigning neutral losses and identification of characteristic fragments in the MS^2 spectra of the TPs. Furthermore, using the exact mass of the potential TP sum formulas were predicted using the online tool ChemCalc (given an MF range of C 0 - 16, H 0 - 100, N 0 - 5, O 0 - 10 and F 0 - 6 with a mass range of 5 mDa). In parallel, a search in the online in-silico fragmentation tool MetFrag was performed with the exact mass and the MS^2 data using the PubChem data base.

Ozonation in WWTP effluent matrix: The behaviour of STG as well as formation and fate of its TPs under realistic conditions were studied in lab-scale batch experiments with effluent from a German WWTP and in an ozonation pilot plant located in Lundåkra, Sweden. For the batch experiments effluent from the biological treatment (suspended sludge compartments for denitrification and nitrification, dissolved organic carbon (DOC) $\approx$ 12 mg/L, pH $\approx$ 8) was taken at the WWTP of Koblenz, Germany and was filled into 30 mL bottles to achieve a final volume (matrix + ozone stock) of 30 mL. Experiments were performed at room temperature. A preliminary analysis by LC-ESI-QTOF confirmed the occurrence of STG in the effluent. One experimental set-up was performed with the non-spiked WWTP effluent (to follow the attenuation of STG at realistic concentrations) and a second set-up was spiked to a final concentration of 2.5 µmol/L STG (to follow the formation of TPs in the effluent matrix). Different ozone doses were added to samples of both set-ups yielding specific ozone doses in the range from 0.1 to 1.7 mg O$_3$/mg DOC. For the calculation of the ozone dose, the dilution of DOC by the sample preparation was considered. The samples were allowed to stand for 2 h after addition of ozone and closing of the bottles. Prior to sampling the bottles were opened and placed into the fume hood for a few minutes to evaporate residual ozone.

The pilot plant at the WWTP in Lundåkra, Sweden was fed with clarified wastewater from an activated sludge process with a biodenipho configuration for nitrification, denitrification, and biological phosphorous removal ($>$ 95% of the flow) and a parallel trickling filter ($<$ 5% of the flow). To study the influence of the ozone concentration, four different specific ozone doses were applied: 0.3, 0.5, 0.7 and 0.9 mg O$_3$/mg DOC. The applied ozone dose was controlled by a PLC system through automated measurements of the water flow, gas flow, and ozone concentration in the in-gas. The specific ozone dose was determined

through normalization with the DOC concentration in the inlet to the ozone pilot. Residual ozone concentrations in the reactor outlet had been determined prior to the sampling with AccuVac ampules (Hach) and did not exceed 0.01 mg O_3/L. The concentration of ozone in the off-gas could be expected to be limited as no smell of ozone could be detected during sampling. A static mixer was used to disperse the ozone gas in the water before entering the reaction tank. The hydraulic retention time (HRT) in the ozonation plant was 10 min for all doses, the temperature was 11 - 12 °C for all experiments. Time-proportional samples over 24 h were taken at the influent and effluent of the ozone pilot at three consecutive days for each ozone dose for analysis of STG and associated TPs. Temperature and pH were recorded onsite and all composite samples were analysed with Hach cuvettes for DOC, $COD_{dissolved}$, NO_2^--N, NO_3^--N, and NH_4^+-N (Table A3.3).

Analytical methods: To simultaneously analyse the degradation of STG and the formation of TPs a non-target approach was used and two analysis methods were applied: liquid chromatography (LC) and ion exchange chromatography (IC) coupled to a quadrupole time-of-flight mass spectrometer (QTOF) with electrospray ionization (ESI). For LC-ESI-QTOF, the LC (1260 Infinity series, Agilent Technologies) was coupled to a high resolution QTOF (AB SCIEX 5600 QTOF). Chromatographic separation by LC was performed on a Synergi Hydro-RP column (250 x 3 mm, 4 µm, Phenomenx) in a gradient elution (eluent based on water (A) and acetonitrile (B), both with 0.1% formic acid, Table A3.1) with a total run time of 30 min. Injection volume for bench scale experiments was 50 µL. For all other samples 80 µL was injected. Mass spectrometric detection was performed either in positive or in negative ESI mode. A mass range from 100 to 1000 Da was scanned. For the eight most intense masses per cycle MS_2 spectra were triggered. For quantification, STG-d4 was added to the samples of the kinetic lab-scale experiments (for calibrations of STG and TP 406 see Figure A3.2). For the IC-ESI-QTOF methods, an IC (940 Professional IC Vario, Metrohm) was coupled to the aforementioned QTOF instrument. Chromatographic separation by IC was performed on a A Supp 5 column (100 x 4 mm, Metrohm). As eluents ultrapure water (A) and an aqueous solution of 8 mM Na_2CO_3/2.5 mM $NaHCO_3$ (B), both mixed with 20% acetonitrile, were used in a gradient elution (Table A3.2) with a total run time of 30 min. The flow rate of the mobile phase was 0.8 mL/min and 50 µL of sample was injected. The IC system was equipped with a suppressor module. By a divert valve the flow of the IC was split by half after the suppressor. One part of the flow was led into the conductivity detector of the IC system for controlling the system's basic performance and the second part of the flow was directed in

the QTOF system. Mass spectrometric detection was carried out in negative ESI mode. For screening the formation of potential TPs and recording of MS^2 spectra, a data dependent mode was used with an accumulation time of 0.1 s. Collision energy (CE) was set to 25 eV and MS^2 spectra were recorded for the eight most intense masses per cycle. Analysis of TFA formation was done by the IC-ESI-QTOF method but with product ion scans for TFA and 13C2-TFA at two different CEs (-18 and -40) (for calibration curves of TFA see Figure A3.3). Data evaluation for STG and TFA was done by isolating their mass traces and integrating peaks using MultiQuant 3.0.2 software (Sciex). For the TP search a non-target approach was used by peak picking using the Software R [179] (see TP identification).

4.3 Results and Discussion

Removal kinetics: Attenuation of STG was achieved for both set-ups, with and without the addition of the radical scavenger t-BuOH (Figure A3.3). Without the radical scavenger the attenuation was faster than with the addition of t-BuOH and for both cases a clear dependency on the pH was observed.

STG contains several moieties which are either activated (increased electron density) or non-activated (reduced electron density) for an ozone attack [42] (Figure 4.1a): for instance, the benzyl moiety is deactivated by the three substituted and electron-withdrawing fluorine atoms. Also the trifluoromethylated triazole moiety is rather non-reactive to ozone. The electron density in the piperazine moiety is reduced due to the electron-withdrawing amide group. Thus, primarily the aliphatic primary amine moiety is likely to be attacked by ozone. Since ozone only reacts fast with the deprotonated nitrogen, reaction kinetics largely depend on speciation and thus on pH, i.e. reaction kinetics increase with increasing pH (Figure 4.1b,c) [42]. Furthermore, at increasing pH values the decay of ozone is enhanced due to the promoting effect of hydroxide ions [42]. In a chain reaction ozone decays to form OH radicals, which react rather unselectively and faster than the ozone molecule. Therefore, if no radical scavenger is added, a combination of direct reactions with the ozone molecule and indirect reactions caused by the radicals leads to a faster attenuation and, therefore, to higher observed reaction rate constants (Figure 4.1c). The pH dependent reaction kinetics can be extrapolated to determine the species-specific reaction rate constants [44] for the STG species (Table 4.1).

The species specific rate constant for the reaction of the neutral species of STG with
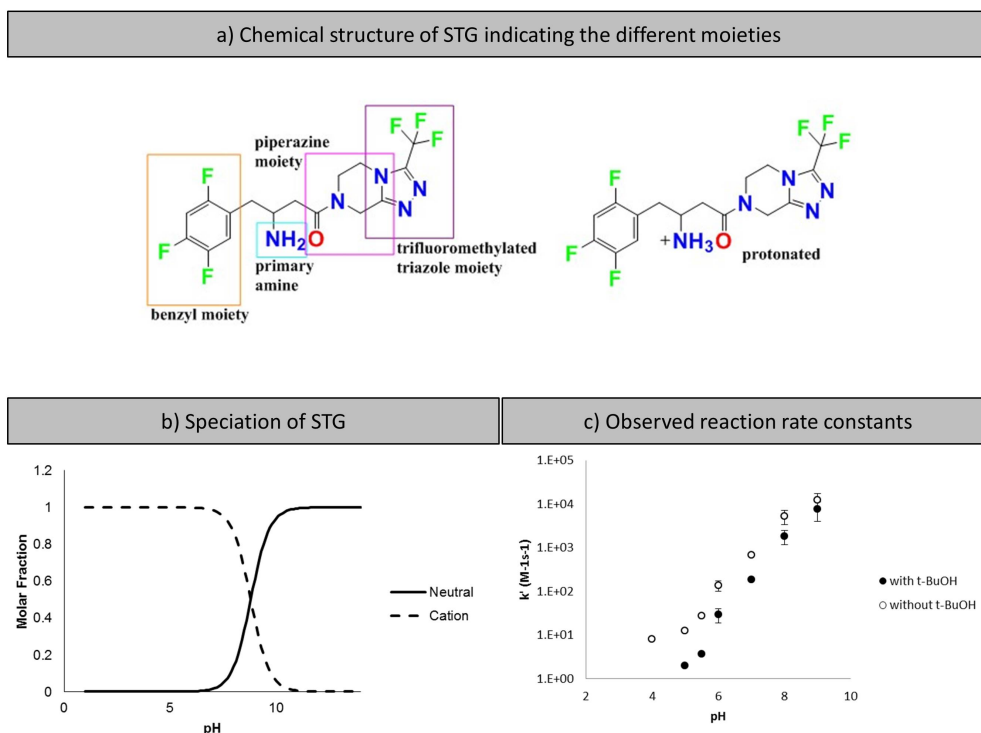
Figure 4.1: Chemical structure of STG indicating the different moieties (a). Speciation (b) and observed reaction rate constants (c) at pH 4 - 9 in a 50 mM phosphate buffer with and without t-BuOH (1% v/v).

ozone is close to other primary amines, for example alanine (k_{O3} = 6.4 x 10^4 M^{-1} s^{-1}) [42], s-butylamine (k_{O3} = 5.2 x 10^4 M^{-1} s^{-1}) [42] and ethylamine (k_{O3} = 9.3 x 10^4 M^{-1} s^{-1}) [42, 44]. Since STG is a rather complex molecule compared to the three mentioned primary amines the difference in rate constants might be explainable by the structural elements as well as by the experimental set-ups used in the different studies. The observed reaction rate constant of STG at typical pH values of water treatment (pH 6 to 8) ranges between 10 and 10^3 M^{-1} s^{-1} (Table 4.1). Since micropollutants with k $\geq$ 10^3 M^{-1} s^{-1} can be considered to be readily degraded in wastewater ozonation [168], STG may only be fully degraded at elevated pH values (i.e., > 8) or elevated ozone doses. Thus, is can be assumed that the pH-dependent attenuation strongly influences the STG removal in real applications.

TP identification: The non-target approach applied in LC-ESI-QTOF and IC-ESI-QTOF revealed several TPs, which appeared after STG attack by ozone. In total, 32

Table 4.1: Apparent second order rate constants for the reaction of STG with ozone in absence and presence of t-BuOH at different pH values and extrapolated species specific rate constants for the neutral and cationic species. The number of experimental replicates is given as n.

	with t-BuOH	without t-BuOH
pH 4 (n = 3)	No reaction observed	7.9 ± 0.2 $M^{-1}s^{-1}$
pH 5 (n = 1)	1.9 $M^{-1}s^{-1}$	12.5 $M^{-1}s^{-1}$
pH 6 (n = 3)	30 ± 10 $M^{-1}s^{-1}$	$(1.4 \pm 0.4) \times 10^2$ $M^{-1}s^{-1}$
pH 7 (n = 1)	1.8×10^2 $M^{-1}s^{-1}$	6.7×10^2 $M^{-1}s^{-1}$
pH 8 (n = 3)	$(1.8 \pm 0.7) \times 10^3$ $M^{-1}s^{-1}$	$(5.3 \pm 1.9) \times 10^3$ $M^{-1}s^{-1}$
pH 9 (n = 2)	$(7.5 \pm 3.5) \times 10^3$ $M^{-1}s^{-1}$	$(1.3 \pm 0.5) \times 10^4$ $M^{-1}s^{-1}$
Species-specific, neutral	1.4×10^4 $M^{-1}s^{-1}$	5.0×10^4 $M^{-1}s^{-1}$
Species-specific, cation	5.3×10^1 $M^{-1}s^{-1}$	3.0 $M^{-1}s^{-1}$

potential TPs were found by the analytical methods (Tables A3.4 and A3.5) in the presence (12 TPs) and the absence (all 32 TPs) of t-BuOH (1% v/v) in 50 mM phosphate buffer at different pH values in the kinetic experiments. The majority of these potential TPs had very small intensities, indicating that they were probably formed in small yields. For determining the most relevant TPs, lab-scale experiments (pure water with phosphate buffer) were compared with lab-scale experiments using WWTP effluent spiked with STG (examples in Figure 4.2). Those TPs which were formed under both conditions were further investigated. In all performed experiments (in 50 mM phosphate buffer at all pH values as well as in WWTP effluent), TP 437 was the quantitatively most relevant TP based on measured intensities. All other TPs were detected at less than 10% of the initial intensity for STG.

STG was detected by LC-ESI-QTOF in positive and in negative mode (retention time (RT) 10 min, $[M+H]^+$ 408.1263, $[M-H]^-$ 406.1103, Figure A3.6). The MS^2 spectrum of STG in positive mode showed certain characteristic fragments: m/z 391.10 was attributed to the loss of NH_3. The fragments m/z 235.08 and m/z 193.07 were assigned to the triazole-piperazine moiety of STG, while m/z 171.04 and 174.05 indicated the benzyl site with the primary amine. In negative mode the formiate adduct of STG (m/z 452.11) exhibited the highest intensity, the fragment m/z 191.06 of the triazole-piperazine moiety provided the base peak in the MS_2 spectrum.

TP 437 (Nitro-STG) was detected by LC-ESI-QTOF in negative and positive mode (RT 14 min, $[M+H]^+$ 438.0999, $[M-H]^-$ 436.0854, Figure A3.7) as well as by IC-ESI-QTOF (RT 4.4 min, $[M-H]^-$ 436.0819) indicating a negative charge at the pH of the mobile phase in IC analysis (pH 10). The even mass of the pseudo-molecular ion indicated an uneven number of nitrogen atoms. In the MS^2 spectrum of LC-ESI(pos)-
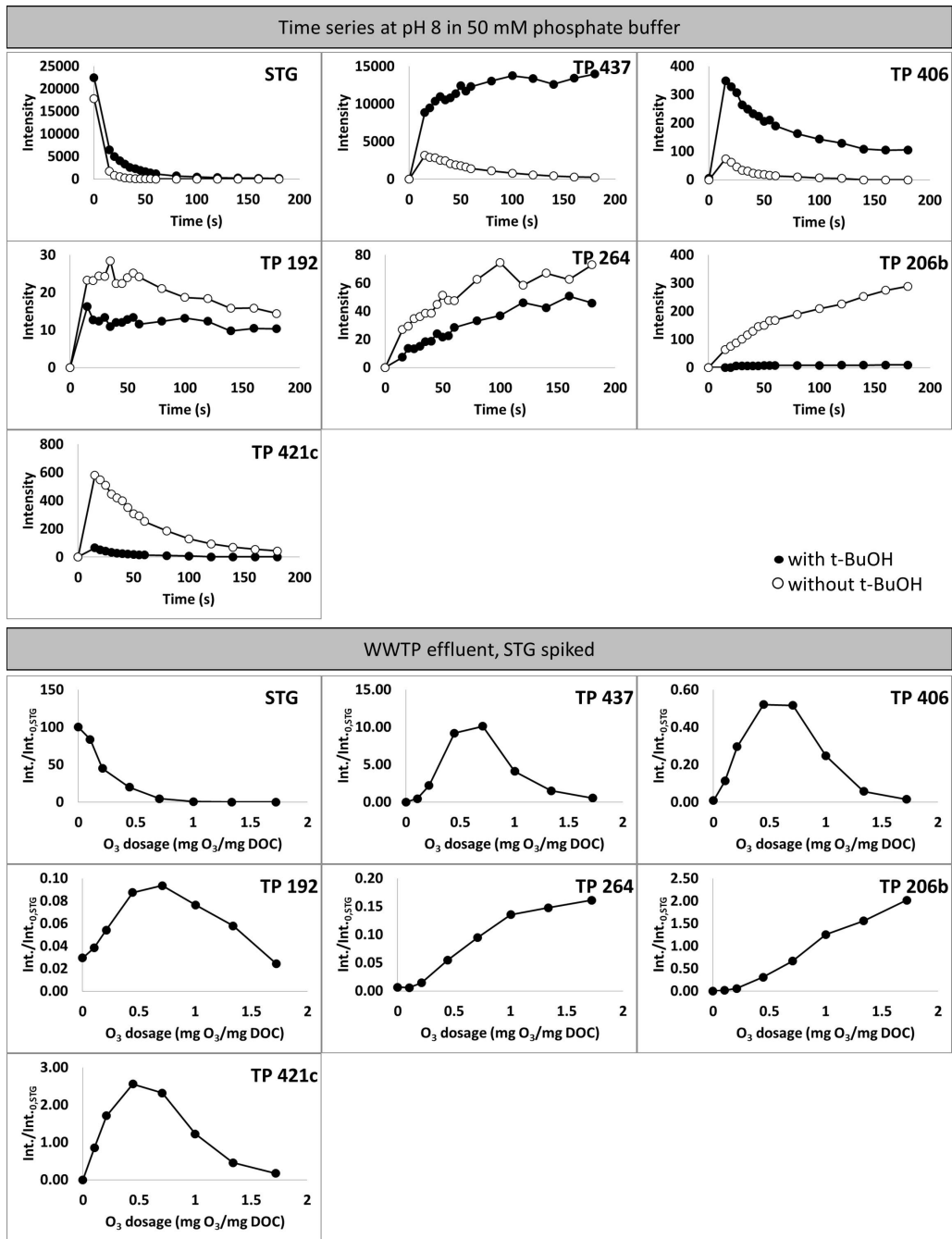
Figure 4.2: Behavior of STG and selected TPs during the batch experiments at pH 8 in phosphate buffer and during batch experiments by ozonation of spiked WWTP effluent (spike of STG = 1 mg/L) at different ozone doses. Plots for all potential TPs are in Figures A3.4 and A3.5.

QTOF a specific loss of -47.00 could be attributed to a loss of HNO_2 leading to fragment m/z 391.10 already known from STG after a loss of NH_3. Due to the appearance of the fragments m/z 193.07 (triazole-piperazine moiety) and m/z 171.04 (benzyl moiety, additionally m/z 145.03 could be assigned to the benzyl moiety) in LC-ESI(pos)-QTOF as well as the identification of fragment m/z 191.08 as the base peak in LC-ESI(neg)-QTOF and IC-ESI-QTOF, it was obvious that the basic structure of STG was maintained during transformation, while the primary amine moiety was converted into a nitro moiety. This structure was also suggested by a MetFrag search with the obtained MS^2 data ((3S)-3-nitro-1-[3-(trifluoromethyl)-6,8-dihydro-5H-[1,2,4]triazolo[4,3-a]pyrazin-7-yl]-4-(2,4,5-trifluorophenyl)butan-1-one, PubChem-ID: 89575803) and is consistent with the results of Lim et al. (2019) [44] for the ozonation of primary amines, finding nitroalkanes as the main TPs in the ozonation of aliphatic primary amines. Although an authentic standard was not commercially available for final verification of the structure, the obtained evidence strongly points towards the nitro structure.

TP 406 (diketo-STG) was detected in LC-ESI-QTOF in positive and negative mode (RT 13 min, $[M+H]^+$ 407.0943, $[M-H]^-$ 405.0794, Figure A3.8). It could not be detected by IC-ESI-QTOF indicating that there was no negative charge at the molecule in the pH range of the mobile phase used for IC analysis (pH = 10). The uneven mass of the quasi-molecular ion indicated an even number of nitrogen atoms in the molecule, thus, one nitrogen atom was lost in the transformation process. Since the fragments m/z 193.07 (triazole-piperazine moiety) and m/z 145.03 (benzyl moiety) appeared in the MS^2 spectrum of the positive ionization and the fragment m/z 191.05 again was the base peak in negative mode, also for TP 406 the basic structure of STG was maintained. The mass difference of -1.03 to STG indicated a replacement of the primary amine moiety by a keto moiety. This chemical structure was verified by a MetFrag search (1-[3-(trifluoromethyl)-6,8-dihydro-5H-[1,2,4]triazolo[4,3-a]pyrazin-7-yl]-4-(2,4,5-trifluorophenyl)butane-1,3-dione, Pub-Chem-ID: 9887588) as well as by comparison with a commercially available reference standard.

Ozonation of STG and TP 406 yielded **TP 192** (trifluoromethyl-triazole-pyrazine, TFTP) to a minor amount. It was detected in LC-ESI-QTOF only in positive mode (RT 4.2 min, $[M+H]^+$ 193.0696, Figure A3.8). It could be identified as the triazole-piperazine moiety by a MetFrag search with the MS^2 data. The structure was verified by a commercially available reference standard (3-(trifluoromethyl)-5,6,7,8-tetrahydro-[1,2,4]triazolo[4,3-a]pyrazine hydrochloride).

TP 264 (TFTP-amide-acid) was detected in LC-ESI-QTOF in positive and negative

mode (RT 7.6 min, $[M+H]^+$ 265.0546, $[M-H]^-$ 263.0396, Figure A3.9) and in IC-ESI-QTOF (RT 3.3 min, $[M-H]^-$ 263.0386). The appearance of the fragments m/z 193.07 in LC-ESI(pos)-QTOF and m/z 191.06 in LC-ESI(neg)- and IC-ESI-QTOF as well as the uneven mass of the quasi-molecular ion led to the assumption that the triazole-piperazine moiety was not altered. The quasi-molecular ion was completely fragmented, indicating its good ionizability, and a loss of CO_2 was detected in the MS^2 spectra in both LC- and IC-ESI-QTOF. This indicated that a carboxylic moiety was formed in α-position to the amide moiety under the loss of the benzyl moiety. That assumption was confirmed by a MetFrag search, yielding the carboxylated triazole-piperazine (2-oxo-2-[3-(trifluoromethyl)-6,8-dihydro-5H-[1,2,4]triazolo[4,3-a]pyrazin-7-yl]acetic acid, PubChem-ID: 64575096).

TP 206b (oxo-TFTP) was detected in LC-ESI-QTOF in positive and negative mode (RT 8.6 min, $[M+H]^+$ 207.0491, $[M-H]^-$ 205.0348, Figure A3.10). Fragments m/z 138.03 and m/z 118.02 in positive ESI were known as fragments of the triazole-piperazine moiety (see TP 192, Figure A3.8). However, since the characteristic fragment of the triazole-piperazine moiety was missing, it seemed to be transformed. An unspecific loss of -18 from the quasi-molecular ion was observed leading to a low intensity fragment mass. Thus, an oxygen atom might have been inserted into the structure causing the loss of H_2O upon fragmentation. In negative ESI hardly any fragmentation occurred. To identify the precursor substance of this TP, ozonation experiments (with and without addition of t-BuOH at pH 8) were also performed on commercially available standards of TP 406 and the TP 192. The formation of TP 206b was observed for both precursor substances, with and without addition of t-BuOH. Thus, the triazole-piperazine moiety must be the precursor of TP 206b. Results of a MetFrag search with the obtained MS^2 data indicated either a breakage of the piperazine moiety and rearrangement of the resulting structure, or an addition of an oxygen atom to the piperazine moiety at the α-carbon to the secondary amine, forming a keto group. However, no exact structure could be proposed with information of the high resolution m/z values.

A similar problem occurred for **TP 421c** (STG-O) which also was detected in LC-ESI-QTOF in negative and positive mode (RT 12.6 min $[M+H]^+$ 422.1048, $[M-H]^-$ 420.0894, Figure A3.11). The even mass of the quasi-molecular ion indicated an uneven number of nitrogen atoms, as with STG and TP 437. The MS^2 spectrum of TP 421c in positive ESI contained characteristic fragments for the benzyl moiety (m/z 145.03) as well as for the triazole-piperazine moiety (m/z 193.07). However, in negative mode the characteristic fragment m/z 191.06 for the triazole-piperazine moiety could not be observed but fragment

m/z 136.01 was known from the MS^2 of other TPs and there is a corresponding mass (m/z 138.03) in positive mode which could be assigned to a fragment of the triazole-piperazine moiety. The mass difference of +13.97 to STG could be assigned to the addition of an oxygen atom and loss of two hydrogen atoms.
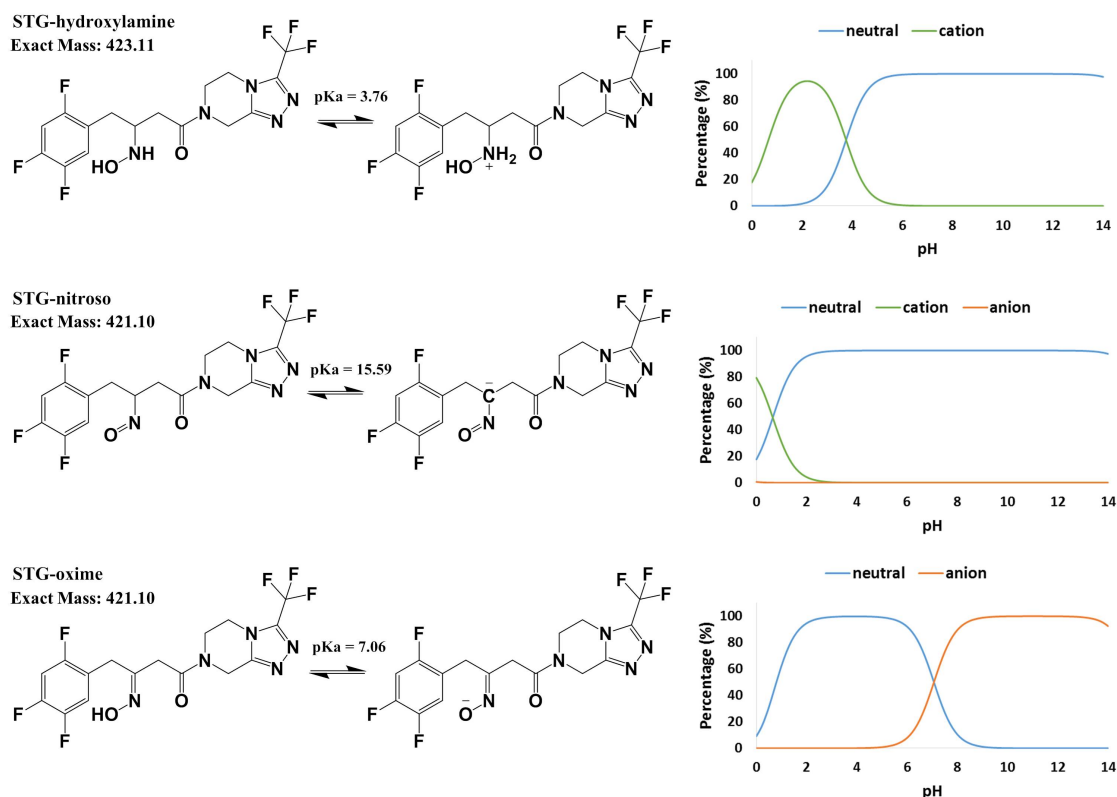
Figure 4.3: Structures for STG-hydroxylamine, STG-nitroso and STG-oxime. Species distribution and pK$_a$ values were determined from the structures in MarvinSketch

Two more potential TPs with the same exact mass but different retention times and different MS^2 spectra were detected for which this oxygen addition could also be assumed: TP 421a (RT 9.9 min, [M+H]$^+$ 422.092, Figure A3.13) and TP 421b (RT 12.2 min, [M+H]$^+$ 422.1047, Figure A3.12). The exact mass of the TPs would fit an oxime or nitroso structure (Figure 4.3) which were postulated to be intermediates in the ozonation of primary aliphatic amines [44, 170] (Figure 4.4. Of these three TPs only TP 421c showed characteristic fragments for the benzyl and the triazole-piperazine moiety and was also de-

tected during IC-ESI-QTOF analysis. Thus, it must carry a negative charge at the pH of the IC eluent (pH 10) which is only true for the oxime structure (Figure 4.3). It therefore is assumed that TP 421c is STG-oxime. For TP 421a and b no definite assumption for the structure can be made based on the MS^2 spectra. However, it could be presumed that one of them shows the STG-nitroso while the other one was formed by a so far unknown reaction mechanism.

Two more TPs containing a nitro group could be identified by observing the characteristic loss of the nitro group and the presence of characteristic fragments for the triazole-piperazine moiety: TP 293 (debenzyl-nitro-STG, Figure A3.14) and TP 453 (hydroxyl-nitro-STG, Figure A3.15). Furthermore, TP 390 (deamino-STG, Figure A3.16) was identified by the characteristic fragments for the benzyl and the triazole-piperazine moiety.

Several other TPs were detected. Some of them showed characteristic fragments for the benzyl or the triazole-piperazine moiety in the MS^2 spectra, while nine TPs did not contain any of the characteristic fragments. Data for all other potential TPs, including the described ones, are listed and described in Figures A3.17 - A3.35.

Scheurer et al. (2017) [180] found that during ozonation of substances carrying a trifluoromethyl-group TFA can be formed. However, only for substances with the trifluoromethylgroup attached to a benzene ring were significant amounts of TFA formed while for STG only low yields of TFA were observed. To analyze low concentrations of TFA, a more sensitive method based on IC-MS/MS was used. TFA was formed with t-BuOH within the first 15 s at all pH values with similar concentrations (Figure A3.36) and remained constant. It is yet unclear why TFA was formed at pH 4 and 6 since ozone is stable under acidic conditions. However, it cannot be ruled out that contaminations in the used stock solutions (STG, buffer, NaOH, t-BuOH) initially reacted with ozone leading to the formation of radicals. Without the addition of t-BuOH a clear dependence of TFA formation on the pH value was observed with increasing concentrations of TFA at higher pH values (> pH 8) and with time (Figure A3.36). Thus, the formation of TFA was caused by reactions with OH radicals. Concentration of OH radicals increases with pH as well as with time causing the observed development in TFA formation since ozone decay into OH radicals is enhanced at higher pH values due to the promoting effect of hydroxide ions [42]. However, only a maximum concentration of 0.2 µmol/L (20 µg/L) of TFA was detected. Considering the initial STG concentration of 2.5 µmol/L, the yield of TFA amounted to 7% at pH 9.

Degradation Pathway: For eight TPs from the LC-ESI-QTOF and one TP from the IC-QTOF analyses chemical structures could be proposed and a degradation pathway of

STG was postulated (Figure 4.4).
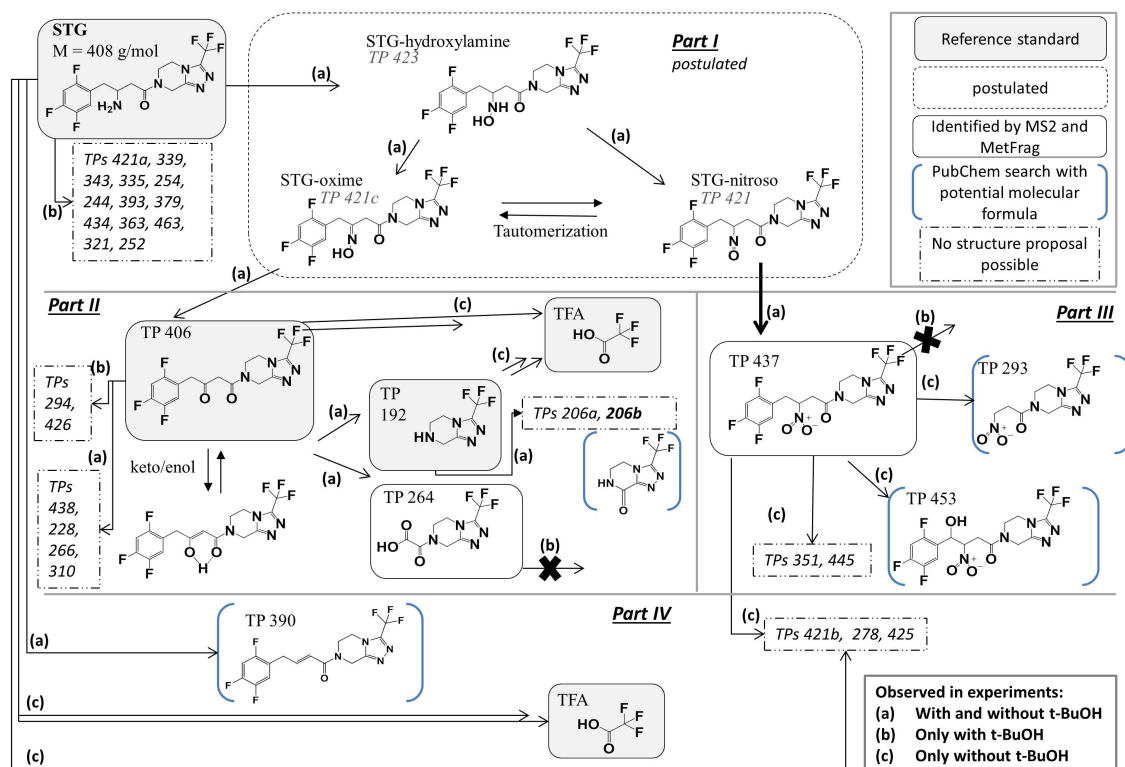
Figure 4.4: Proposed pathway of STG transformation during ozonation. Assignment of arrows indicates the observation of the TPs in lab-scale experiments (50 mM phosphate buffer, pH 8): (a) with and without addition of t-BuOH, (b) only with t-BuOH, (c) only without t-BuOH. Postulated structures of Part I either were not observed (TP 423, TP 421) or only tentatively identified based on the theory (TP 421c)

The electrophilic attack of ozone occurred at the lone electron pair of the nitrogen of the primary amine. Lim et al. (2019) [44] and Keinan and Mazur (1977) [170] postulated that the ozone attack at primary amines leads to the formation of an hydroxylamine which is further oxidized to the tautomeric nitroso and oxime structure (Figure 4.4, Part I). STG-hydroxylamine could not be detected in this study. However, Lim et al. (2019) [44] reported that the reaction kinetics of hydroxylamine TPs of aliphatic amines were much higher than for the amine itself and reacted very fast with ozone. STG-hydroxylamine has a much lower pK$_a$ value than STG (Figure 4.3) and appears in neutral form at all tested pH-values in this study. Thus, it might not be detectable here due to its fast reaction with ozone. TP 421c could tentatively be identified as STG-oxime, however, evidence for

STG-nitroso is scarce, although TP 421a or b would be plausible candidates. STG-nitroso appears in neutral form in the pH range 2 - 14 (Figure 4.3) and in studies on the ozonation of aromatic and aliphatic amines it was detected as an intermediate [44, 45, 170, 181]. But since no reference standards for any of the compounds, STG-hydroxylamine, STG-oxime nor STG-nitroso are commercially available this proposed pathway could not be verified and is based on information from the literature [44, 170].

In further reactions the pathway divides into a main and a side reaction. Figure 4.4, Part II illustrates the side reaction initiated by a further oxidation of the oxime structure to form the diketone TP 406. However, it might also be possible that TP 406 is formed directly from STG by an oxidative dealkylation leading to a deamination as found in the biological degradation [156]. The keto-enol tautomerism leads to the enolate form, where the C=C-double bond can be attacked by ozone according to the well-known Criegee-mechanism [46] leading to TP 264. In addition to TP 264, ozonation experiments on a reference standard of TP 406 showed also the transformation to TP 192. The mechanism is still unknown, since this transformation should be based on a cleavage of an amide bond which is a very slow reaction in ozonation [42]. However, further transformation, with and without addition of t-BuOH, led to the formation of TFA and further TPs with TP 206b being the main TP based on the detected peak intensity.

The main degradation route seemed to be via the nitroso structure (Figure 4.4, Part III). In a further ozone attack the nitroso group was converted into a nitro group. This is in accordance with Lim et al. (2019) [44] who reported that nitro groups are formed as the main products in the direct ozonation of simple aliphatic primary and secondary amines. No further removal of TP 437 with the addition of t-BuOH was observed. However, when OH radicals were involved in the reaction (experiments without t-BuOH) TP 437 could be further transformed (Figure 4.2). Two TPs were identified by their MS^2 spectra possibly carrying a nitro-group since both show characteristic losses for the nitro-group. TP 453 might be formed by a hydroxylation of the β-carbon of the nitro-group, possibly due to a partial charge at this carbon atom by the negative inductive effects of the nitro group and fluorinated benzyl moiety. For TP 293 cleavage of the benzyl unit could be assumed, maintaining the nitro group. Two further TPs showed a loss of -47, i.e. HNO$_2$, in their MS^2 spectra but could not be characterized yet (TP 351 and TP 445).

Several further TPs were detected. TP 390 was formed with and without addition of t-BuOH from STG by cleavage of the primary amine and formation of a C=C-double bond (Figure 4.4, Part IV). For several other, yet unidentified TPs the precursor cannot be

identified unambiguously. However, the ones being formed in the ozonation experiments on reference standards of TP 406 and TP 192 are named in Figure 4.4, Part II. TPs not formed by TP 406 and TP 192 but by STG in presence of t-BuOH can be found in Figure 4.4, Part IV of the pathway, while those being formed in absence of t-BuOH were collected in Figure 4.4, Part III. Formation of TFA could be observed in ozonation experiment on STG, TP 406 and TP 192. The mechanism of TFA formation is yet unclear. Results indicate that it is formed by reaction with OH radicals which must attack the α-carbon to the trifluoromethyl moiety or at one of the adjacent nitrogen atoms causing an N-dealkylation reaction. However, based on the results the mechanisms of TFA formation could not be identified.

Ozonation at realistic conditions: Under realistic conditions, i.e. ozonation of WWTP effluent, ozonation is performed at an ambient pH of 6 - 8. Due to the ozone decay in this pH range and the reaction of ozone with dissolved organic matter (DOM), OH radicals form under these conditions and there will always be a combination of direct and indirect reactions during the ozonation of wastewater leading to the attenuation of micropollutants. In Figure 4.5 and Figure A3.37 results from the laboratory batch experiments in non-spiked WWTP effluent (DOC = 12 mg/L, pH = 8, T = room temperature) and from studies at an ozonation pilot plant (DOC = 10 mg/L, pH = 7, T = 14 °C, continuous ozonation) for different ozone doses are shown. STG showed a moderate removal compared to other selected substances (Figure A3.37); attenuation was low compared to fexofenadine and candesartan but faster than gabapentin and similar to denatonium. In the lab-scale experiments faster attenuation could be observed for all substances leading to complete removal of all of them at the highest ozone dose (1.7 mg O_3/mg DOC) while residuals were detected in the pilot-scale for candesartan and STG (5 - 10%) as well as for denatonium and gabapentin (20 - 30%) at an ozone dose of 0.9 mg O_3/mg DOC. The faster attenuation during the lab-scale experiments indicate higher concentrations of OH radicals, possibly due to the higher pH value of the samples (pH 8) or a higher content of DOM compared to the WWTP effluent treated in the ozone pilot plant. The results for gabapentin are indicative for this, too. At ambient pH values the protonated amine and the deprotonated carboxylic acid moieties of gabapentin are not highly reactive with ozone and thus, removal mainly can be attributed to the reaction with OH radicals [182].

In both lab-scale experiments in WWTP effluent and ozonation in a pilot plant, the same TPs were detected but the occurrence patterns differed (Figure 4.5a and b). TP 192 and TP 406 were already present in the WWTP effluents. Both were recently identified
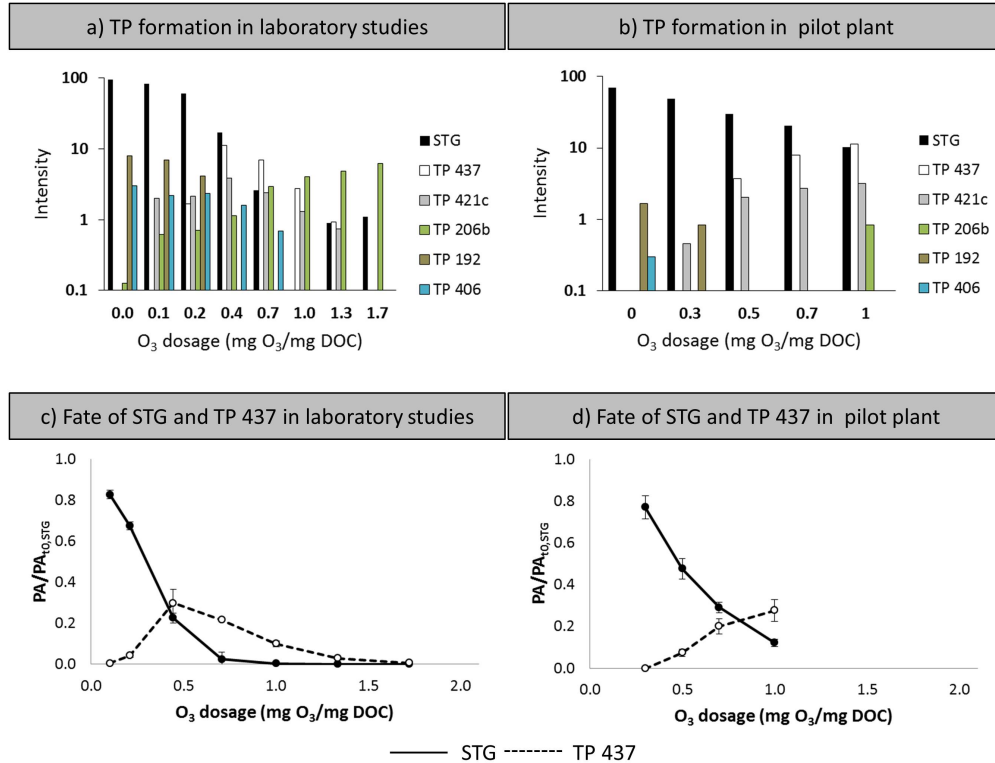
Figure 4.5: Fate of STG during ozonation under natural conditions in lab-scale experiments with non-spiked WWTP effluent and in a WWTP pilot plant. Formation of TPs in batch experiments (a) and in the pilot plant (b) and comparison of the fate of STG and TP 437 in batch experiments (c) and pilot plant (d) (PA = Peak area)

as biological TPs auf STG in the activated sludge treatment [156] and both were removed completely during ozonation. TP 421c was formed in both set-ups already at the lowest ozone dose and showed increasing peak intensities with increasing ozone dose in the pilot plant, while it was removed in lab-scale experiments at higher doses. TP 206b, which was found to be the main TP of the side reaction (Figure 4.4, Part II), showed increasing concentrations in the batch experiments and could not be removed even at ozone dosages close to 2.0 mg O_3/mg DOC. In the pilot plant, TP 206b appeared only at the highest ozone doses. Based on the detected intensities, TP 437 was the main TP formed in both set-ups. In the pilot plant a steady formation could be observed, while in lab-scale experiments a further transformation occurred at ozone doses higher than 0.5 mg O_3/mg DOC (Figure 4.5c and d). In the time-series experiments TP 437 was found to be persistent when a radical scavenger was added. Thus, attenuation of TP 437 is due to OH radicals.

It was already noted above that the radical's concentration seemed to be higher during the lab-scale experiments than in the pilot-plant. Furthermore, comparison of the results in Figure 4.5c and Figure 4.5d led to the assumption that further transformation of TP 437 only could be observed when STG was depleted and no further formation of TP 437 could be expected. In the pilot plant there was no depletion of STG and the continuous formation of TP 437 could have masked its slow transformation. Thus, in real applications, with ozone doses being typically in the range of 0.5 - 0.9 mg O_3/mg DOC [163] STG attenuation possibly will be incomplete and TPs will be formed that are persistent towards further transformation, such as TP 437.

Concerning TFA formation, only the lab-scale batch experiments were considered, comparing the experimental runs for WWTP effluent spiked with STG and non-spiked samples (Figure A3.37). In both, a formation of TFA was observed and TFA concentrations increased with increasing ozone doses to a maximum of 70 µg/L and 75 µg/L in non-spiked and spiked samples, respectively. The low difference of the maximum concentrations indicated that the presence of STG had only a minor influence on the overall TFA formation which is in accordance with Scheurer et al. [180]. Therefore, there are obviously other more important precursor substances transformed to TFA during ozonation.

Ozonation is frequently not applied as a stand-alone technique in wastewater treatment, but in combination with subsequent polishing treatment processes [65, 68, 69, 165, 183]. In preliminary laboratory tests of the biological degradability of the main product TP 437 in a MBBR system (Text A3.4 and Figure A3.38) only a minor removal was observed after three days of treatment. Also in the pilot plant no removal of TP 437 was observed in subsequent MBBR treatment with a HRT of 6 h. Due to the electron withdrawing characteristics of the nitro group direct oxidation of the molecule is hindered but studies on other nitroaromatic compounds do show degradability under anaerobic conditions [184, 185], where the nitro moiety is converted to a hydroxylamine and further to the amine moiety. Thus, assuming a biodegradability of TP 437, STG could be formed back during biological treatment. However, a biodegradation of TP 437 was not observed, neither in the preliminary laboratory batch experiment nor in a subsequent MBBR treatment at the ozonation pilot plant (Figure A3.38). Thus, TP 437 might pass subsequent biological treatment without significant reduction in concentration and reach the receiving water.

Acknowledgments

Chapter 5

Final Conclusions

5.1 General conclusions

Water scarcity is a global and an omnipresent challenge and will increase in the future due to climate change and population growth. Reuse of existing water resources such as reclaimed wastewater could ease the situation, e.g., by the recharge of groundwater aquifers. However, the water cycle is in some cases contaminated by anthropogenic micropollutants. Following the fate of these micropollutants during water treatment and within the water cycle is therefore crucial when assessing the quality of water and the efficiency of water treatment techniques. Not only precursor substances are of importance but also human metabolites and TPs which are formed by biotic and abiotic mechanisms.

Thousands of micropollutants are known but only a small subset is monitored in wastewater, surface water and groundwater. Therefore, multi-residue analysis methods are crucial to get a better overview of the contamination. However, the quality of analysis results depends on the interplay between different MS parameters, which are defined by the analyst during method development. In the current literature, these parameters are scarcely reported. During the development of the multi-residue analysis method presented in Chapter 2 it was found that the cycle time of MS analysis as well as the defined target scan time strongly influence the dwell time, i.e. the accumulation time for each transition within a cycle. The MS instrument adjusted the target scan time automatically in case the minimum dwell time was reached. This affected the number of data points per peak, which is a measure of the quality of analysis. A minimum number of 6 to 10 data points per peak was maintained in the developed method and no negative effects on precision and

accuracy were observed. Nevertheless, it became clear that in target analysis method there is an upper limit of micropollutants that can be analysed without the loss of data quality.

Thus, the selection of compounds to be monitored by multi-residue analysis methods is a critical point. The substance selection performed in Chapter 2 proved to be of relevance for the environmental water analysis since 95% of the target list was detected in at least one sample. The results showed that the selection should be based on:

- toxicity for humans and ecotoxicity for aquatic and terrestric organisms

- the understanding and control of the efficiency of the processes applied for wastewater treatment such as SAT as well as sorption by activated carbon or the use of ozonation

- the potential formation of toxic or persistent TPs which may pose risks to humans and biota.

It was observed that, in accordance with the literature, conventional biological wastewater treatment was not able to remove the majority of micropollutants and also for activated carbon treatment persistent compounds were observed. Thus, it became clear that further treatment steps are necessary for wastewater treatement.

Natural processes such as SAT and SBF have the potential to reduce the burden of micropollutants by attenuation of the micropollutants due to biological, chemical, and physical attenuation processes as shown in Chapter 3. However, they are not able to remove all micropollutants completely due to diverse physico-chemical properties of the micropollutants, and their elevated quantities. By the results, the selection criteria for micropollutants to be monitored were refined to the selection of:

- micropollutants with different physico-chemical properties at environmental pH

- micropollutants with different removal degrees and different main removal mechanisms (biodegradation, sorption) by wastewater treatment processes and

- pairs of precursor substances with their major TP.

It could be shown that the quality of the source water for these techniques, which is reclaimed water, has to be improved by the implementation of advanced treatment techniques to WWTPs prior to treatment by the natural processes.

Innovative processes such as ozonation are capable of oxidizing micropollutants that are recalcitrant to biological degradation. However, the formation of persistent TPs needs to be checked and if these are toxic to humans or biota. Especially, it is crucial to investigate if the TPs have the potential to contaminate drinking water. It is known that in ozonation small and polar TPs are formed which are likely to pass processes at waterworks. Although there is a high number of studies in the ozonation of diverse micropollutants containing olefins and aromatic rings, information is scarce when it comes to substances carrying an aliphatic amine moiety. Chapter 4 shows the first study on the ozonation of a pharmaceutical containing a primary aliphatic amine moiety as the main site for the ozone attack. The pH-dependent kinetics of the ozonation of the antidiabetic sitagliptin revealed the incomplete removal under environmental pH. Furthermore, TPs were identified by non-target analysis, which were persistent towards subsequent biological polishing techniques. The main TP was a nitro-compound, which is not prone to biodegradation but might be transformed back to sitagliptin under anaerobic conditions. Thus, effluent from the ozonation might contain sitagliptin as well as its persistent TPs (e.g. the nitro-compound and TFA) which then may reach the source water for drinking water production.

The results of this thesis show that going forward, a combination of both target and non-target analysis might be an option to evaluate water treatment processes and assess the quality of water. By the target methods quantification of wide range of micropollutants is possible. This is crucial for regulated micropollutants such as pesticides. However, the limitations of MS instruments concerning the number of analysed transitions requires a careful selection of micropollutants. Combining this with non-target analysis methods facilitates the detection of newly emerging micropollutants as well as the formation of previously unknown TPs.

5.2 Outlook

With this thesis, the understanding of the presence of micropollutants, precursors as well as metabolites and TPs in the environment was deepened, for example by the detection of valsartan acid in bank filtrate. The simultaneous measurement of substance pairs, i.e. precursors and their TPs, allows conclusions to be drawn about the predominant transformation and removal mechanisms in different treatment methods. For example, the attenuation of venlafaxine in the SAT could be attributed to ionoc interactions since none of the biological TPs were detected. However, target methods, such as the multi-

residue analysis method used in chapters 2 and 3, can only provide excerpts of the overall picture. Often micropollutants are also measured which have no relevance for the system under investigation. A selection of suitable, universally applicable indicator substances for a process-based evaluation could help here to obtain a quick quantitative overview of the removal performance.

But even this reduced target list would only be suitable to a limited extent. New micropollutants are discovered continuously which can strongly influence the overall picture, for example through the formation of potentially toxic TPs. These would not be further noticed with indicator-based target methods. Using non-target methods, a monitoring strategy could be created with which newly emerging substances could be quickly detected and subsequently identified. If a relevance for these new substances is determined, for example by persistence in the treatment train, further measures can be taken.

If one takes the results of the ozonation of sitagliptin as an example, different TPs formed during ozonation, e.g. the main TP Nitro-STG as well as TFA, which were stable in subsequent treatment steps. If applied in methods for groundwater recharge, it has to be determined how these TPs behave in the soil passage. Sitagliptin itself is retained by ionic interaction due to its positive charge. Nitro-STG has no charge and has little to no biodegradability. If this substance reaches groundwater, once the toxicological potential of this substance has been established, measures may need to be taken to prevent the transfer of this TP to groundwater.

All in all, water reuse schemes are highly complex systems with various dependencies that can only be moderately estimated. By means of non-target analysis, however, a more general overview could be obtained, which could enable faster intervention in the complex system of water reuse in the event of the appearance of novel micropollutants.

Bibliography

[1] WWAP (UNESCO World Water Assessment Programme). *The United Nations World Water Development Report 2019: Leaving No One Behind*. UNESCO: Paris, 2019.

[2] R. G. Maliva. *Anthropogenic Aquifer Recharge*. Springer Hydrogeology. Springer Nature: Cham, 2020.

[3] T. Fichtner, N. Goersmeyer, and C. Stefan. Influence of soil pore system properties on the degradation rates of organic substances during soil aquifer treatment (SAT). *Appl Sci*, 9(3):496, feb 2019.

[4] A. Gil, L. A. Galeano, and M. A. Vicente, editors. *Applications of Advanced Oxidation Processes (AOPs) in Drinking Water Treatment*, volume 67 of *The Handbook of Environmental Chemistry*. Springer: Cham, 2019.

[5] Use of freshwater resources, https://www.eea.europa.eu/data-and-maps/indicators/use-of-freshwater-resources-3/assessment-4, 2018. accessed 2020-04-15.

[6] M. Arnold, J. Batista, E. Dickenson, and D. Gerrity. Use of ozone-biofiltration for bulk organic removal and disinfection byproduct mitigation in potable reuse applications. *Chemosphere*, 202:228–237, 2018.

[7] S. K. Sharma and M. D. Kennedy. Soil aquifer treatment for wastewater treatment and reuse. *Int Biodeterior Biodegradation*, 119:671–677, 2017.

[8] R. Hofman-Caris, T. ter Laak, H. Huiting, H. Tolkamp, A. de Man, P. van Diepenbeek, and J. Hofmann. Origin, fate and control of pharmaceuticals in the urban water cycle: a case study. *Water*, 11:1034, 2019.

[9] S. D. Richardson and S. Y. Kimura. Emerging environmental contaminants: challenges facing our next generation and potential engineering solutions. *Environ Technol Inno*, 8:40–56, 2017.

[10] S. N. Gosling and N. W. Arnell. A global assessment of the impact of climate change on water scarcity. *Climatic Change*, 134:371–385, 2016.

[11] A. Mehran, A. AghaKouchak, N. Nakjiri, M. J. Stewardson, M. C. Peel, T. J. Phillips, Y. Wada, and J. K. Ravalico. Compounding impacts of human-induced water stress and climate change on water availablity. *Scientific Reports*, 7:6282, 2017.

[12] S. H. A. Koop and C. J. van Leeuwen. The challenges of water, waste and climate change in cities. *Environ Dev Sustain*, 19(2):385–418, 2017.

[13] Population trends 1950 to 2100: globally and within europe, https://www.eea.europa.eu/data-and-maps/indicators/total-population-outlook-from-unstat-3/assessment-1, 2020. accessed 2020-04-15.

[14] D. Bixio, C. Thoeye, J. de Koning, D. Joksimovic, D. Savic, T. Wintgens, and T. Melin. Wastewater reuse in europe. *Desalination*, 187:89–101, 2006.

[15] P Quinteiro, S. Rafael, B. Vicente, M. Marta-Almeida, A. Rocha, L. Arroja, and A. C. Dias. Mapping green water scarcity under climate change: A case study of portugal. *Sci Total Environ*, 696:134024, dec 2019.

[16] A. Gogoi, P. Mazumder, V. K. Tyagi, G. G. T. Chaminda, A. K. An, and M. Kumar. Occurrence and fate of emerging contaminants in water environment: A review. *Groundw Sustain Dev*, 6:169–180, 2018.

[17] J. Rogowska, M. Cieszynska-Semenowics, W. Ratajczyk, and L. Wolska. Micropollutants in treated wastewater. *Ambio*, 49:487–503, 2020.

[18] G. A. Zoumpouli, M. Scheurer, H.-J. Brauch, B. Kasprzyk-Hordern, J. Wenk, and O. Happel. COMBI, continuous ozonation merged with biofiltration to study oxidative and microbial transformation of trace organic contaminants. *Environ Sci: Water Res Technol*, 5:552–563, 2019.

[19] F. Costa, A. Lago, V. Rocha, O. Barros, L. Costa, Z. Vipotnik, B. Silva, and T. Tavares. A review on biological processes for pharmaceuticals wastes abatement - a growing threat to modern society. *Environ Sci Technol*, 53:7185–7202, 2019.

[20] P. Krzeminski, M. C. Tomei, P. Karaolia, A. Langenhoff, C. M. R. Almeida, E. Felis, F. Gritten, H. R. Andersen, T. Fernandes, C. M. Manaia, Rizzo L., and D. Fatta-Kassinos. Performance of secondary wastewater treatment methods for the removal of contaminants of emerging concern implicated in crop uptake and antibiotic resistance spread: a review. *Sci Total Environ*, 648:1052–1081, 2019.

[21] T. A. Ternes, C. Prasse, C. L. Eversloh, G. Knopp, P. Cornel, U. Schulte-Oehlmann, T. Schwartz, J. Alexander, W. Seitz, A. Coors, and J. Oehlmann. Integrated evaluation concept to assess the efficacy of advanced wastewater treatment processes for the elimination of micropollutants and pathogens. *Environ Sci Technol*, 51(1):308–319, 2017.

[22] E. N. Evgenidou, I. K. Konstantinou, and D. A. Lambropoulou. Occurrence and removal of transformation products of PPCPs and illicit drugs in wastewaters: a review. *Sci Total Environ*, 505:905–26, 2015.

[23] J. Funke, C. Prasse, C. Lutke Eversloh, and T. A. Ternes. Oxypurinol - a novel marker for wastewater contamination of the aquatic environment. *Water Res*, 74:257–65, 2015.

[24] N. M. Vieno, H. Härkki, T. Tuhkanen, and L. Kronberg. Occurrence of pharmaceuticals in river water and their elimination in a pilot-scale drinking water treatment plant. *Environ Sci Technol*, 41:5077–5084, 2007.

[25] S. Fekadu, E. Alemayehu, R. Dewil, and B. van der Bruggen. Pharmaceuticals in freshwater aquatic environments: a comparison of the african and european challenge. *Sci Total Environ*, 654:324–337, 2019.

[26] G. Lofrano and J. Brown. Wastewater management through the ages: A history of mankind. *Sci Total Environ*, 408:5254–5264, 2010.

[27] A. N. Angelakis, T. Asano, A. Bahri, B. E. Jimenez, and G. Tchobanoglous. Water reuse: From ancient to modern times and the future. *Front Environ Sci*, 6, may 2018.

[28] E. Idelovitch and M. Michail. Soil-aquifer treatment: A new approach to an old method of wastewater resuse. *Journal WPCF*, 56(8):936–943, 1984.

[29] M. Bourgin, B. Beck, M. Boehler, E. Borowska, J. Fleiner, E. Salhi, R. Teichler, U. von Gunten, H. Siegrist, and C. S. McArdell. Evaluation of a full-scale wastewater treatment plant upgraded with ozonation and biological post-treatments: Abatement of micropollutants, formation of transformation products and oxidative by-products. *Water Res*, 129:486–498, 2018.

[30] T. A. Ternes, A. Joss, and H. Siegrist. Scrutinizing pharmaceuticals and personal care products in wastewater treatment. *Environ Sci Technol*, 2004.

[31] N. H. Tran, M. Reinhard, and K. Y. H. Gin. Occurrence and fate of emerging contaminants in municipal wastewater treatment plants from different geographical region − a review. *Water Res*, 133:182–207, 2018.

[32] M. B. Ahmed, J. L. Zhou, H. H. Ngo, W. Guo, N. S. Thomaidis, and J. Xu. Progress in the biological and chemical treatment technologies for emerging contaminant removal from wastewater: A critical review. *J Hazard Mater*, 323(Pt A):274–298, 2017.

[33] S. K. Maeng, S. K. Sharma, K. Lekkerkerker-Teunissen, and G. L. Amy. Occurrence and fate of bulk organic matter and pharmaceutically active compounds in managed aquifer recharge: a review. *Water Res*, 45(10):3015–33, 2011.

[34] P. H. Howard and D. C. Muir. Identifying new persistent and bioaccumulative organics among chemicals in commerce. *Environ Sci Technol*, 44:2277–2285, 2010.

[35] A. Joss, S. Zabczynski, A. Göbel, B. Hoffmann, D. Löffler, C. S. McArdell, T. A. Ternes, A. Thomsen, and H. Siegrist. Biological degradation of of pharmaceuticals in municipal wastewater treatment: Proposing a classification scheme. *Water Res*, 40(8):1686–1696, 2006.

[36] L. Rizzo, S. Malato, D. Antakyali, V. G. Beretsou, M. B. Đolić, W. Gernjak, E. Heath, I. Ivancev-Tumbas, P. Karaolia, A. R. Lado Ribeiro, G. Mascolo, C. S. McArdell, H. Schaar, A. M. T. Silva, and D. Fatta-Kassinos. Consolidated vs new advanced treatment methods for the removal of contaminants of emerging concern from urban wastewater. *Sci Total Environ*, 655:986–1008, mar 2019.

[37] R. Loos, R. Carvalho, D. C. Antonio, S. Comero, G. Locoro, S. Tavazzi, B. Paracchini, M. Ghiani, T. Lettieri, L. Blaha, B. Jarosova, S. Voorspoels, K. Servaes, P. Haglund, J. Fick, R. H. Lindberg, D. Schwesig, and B. M. Gawlik. EU-wide monitoring survey on emerging polar organic contaminants in wastewater treatment plant effluents. *Water Res*, 47(17):6475–87, 2013.

[38] M. Östmann, B. Björlenius, J. Fick, and Tysklind M. Effect of full-scale ozonation and pilot-scale granular activated carbon on the removal of biocides, antimycotics and antibiotics in a sewage treatment plant. *Sci Total Environ*, 649:1117–1123, 2019.

[39] Alessandro di Biase, Maciej S. Kowalski, Tanner R. Devlin, and Jan A. Oleszkiewicz. Moving bed biofilm reactor technology in municipal wastewater treatment: A review. *J Environ Manage*, 247:849–866, oct 2019.

[40] U. von Gunten. Oxidation processes in water treatment: Are we on track? *Environ Sci Technol*, 52(9):5062–5075, 2018.

[41] S. J. Masten and S. H. R. Davies. The use of ozonation to degrade organic contaminants in wastewaters. *Environ Sci Technol*, 28(4):180A–185A, 1994.

[42] C. von Sonntag and U. von Gunten. *Chemistry of Ozone in Water and Wastewater Treatment*. IWA: London, 2012.

[43] U. Hübner, U. von Gunten, and M. Jekel. Evaluation of the persistence of transformation products from ozonation of trace organic compounds - a critical review. *Water Res*, 68:150–170, 2015.

[44] S. Lim, C. S. McArdell, and U. von Gunten. Reactions of aliphatic amines with ozone: Kinetics and mechanisms. *Water Res*, 157:514–528, 2019.

[45] A. Tekle-Röttering, C. von Sonntag, E. Reisz, C. V. Eyser, H. V. Lutze, J. Türk, S. Naumov, W. Schmidt, and T. C. Schmidt. Ozonation of anilines: Kinetics, stoichiometry, product identification and elucidation of pathways. *Water Res*, 98:147–59, 2016.

[46] R. Criegee. Mechanism of ozonolysis. *Angew Chem internat Edit*, 14(11):745–752, 1975.

[47] J. P. Wibaut, F. L. J. Sixma, L. W. F. Kampschmidt, and H. Boer. The mechanism of the reaction between ozone and aromatic compounds. (preliminary communication). *Recueil des Travaux Chimiques des Pays-Bas*, 69(11):1355–1363, sep 1950.

[48] I. Zucker, H. Mamane, A. Riani, I. Gozlan, and D. Avisar. Formation and degradation of N-oxide venlafaxine during ozonation and biological post-treatment. *Sci Total Environ*, 619-620:578–586, 2018.

[49] S. Merel, S. Lege, J. E. Yanez Heras, and C. Zwiener. Assessment of N-oxide formation during wastewater ozonation. *Environ Sci Technol*, 51:410–417, 51.

[50] A. Tekle-Röttering, E. Reisz, K. S. Jewell, H. V. Lutze, T. A. Ternes, W. Schmidt, and T. C. Schmidt. Ozonation of pyridine and other N-heterocyclic aromatic compounds: Kinetics, stoichiometry, identification of products and elucidation of pathways. *Water Research*, 102:582–593, oct 2016.

[51] Y. Lee, D. Gerrity, M. Lee, A. E. Bogeat, E. Salhi, S. Gamage, R. A. Trenholm, E. C. Wert, S. A. Snyder, and U. von Gunten. Prediction of micropollutant elimination during ozonation of municipal wastewater effluents: use of kinetic and water specific information. *Environ Sci Technol*, 47(11):5872–81, 2013.

[52] D. B. Miklos, C. Remy, M. Jekel, K. G. Linden, J. E. Drewes, and U. Hübner. Evaluation of advanced oxidation processes for water and wastewater treatment – a critical review. *Water Research*, 139:118–131, aug 2018.

[53] P. Dillon, P. Stuyfzand, T. Grischek, M. Lluria, R. D. G. Pyne, R. C. Jain, J. Bear, J. Schwarz, W. Wang, E. Fernandez, C. Stefan, M. Pettenati, J. van der Gun, C. Sprenger, G. Massmann, B. R. Scanlon, J. Xanke, P. Jokela, Y. Zheng, R. Rossetto, M. Shamrukh, P. Pavelic, E. Murray, A. Ross, J. P. Bonilla Valverde, A. Palma

Nava, N. Ansems, K. Posavec, K. Ha, R. Martin, and M. Sapiano. Sixty years of global progress in managed aquifer recharge. *Hydrogeol J*, 27(1):1–30, sep 2019.

[54] P. Dillon. Future management of aquifer recharge. *Hydrogeol J*, 13:313–316, 2005.

[55] K. M. Onesios-Barry, D. Berry, J. B. Proescher, I. K. Ashok Sivakumar, and E. J. Bouwer. Removal of pharmaceuticals and personal care products during water recycling: Microbial community structure and effects of substrate concentration. *Appl Environ Microbiol*, 80(8):2440–2450, 2014.

[56] G. Amy and J. Drewes. Soil aquifer treatment (SAT) as a natural and sustainable wastewater reclamation/reuse technology: fate of wastewater effluent organic matter (EfOM) and trace organic compounds. *Environ Monit Assess*, 129(1-3):19–26, 2007.

[57] Q. Gao, K. M. Blum, P. Gago-Ferrero, K. Wiberg, L. Ahrens, and P. L. Andersson. Impact of on-site wastewater infiltration systems on organic contaminants in groundwater and recipient waters. *Sci Total Environ*, 651:1670–1679, 2019.

[58] J. Regnery, C. P. Gerba, E. R. Dickenson, and J. E. Drewes. The importance of key attenuation factors for microbial and chemical contaminants during managed aquifer recharge: A review. *Crit Rev Environ Sci Technol*, 47:1409–1452, 2017.

[59] V. Martinez-Hernandez, R. Meffe, S. Herrera Lopez, and I. de Bustamante. The role of sorption and biodegradation in the removal of acetaminophen, carbamazepine, caffeine, naproxen and sulfamethoxazole during soil contact: A kinetics study. *Sci Total Environ*, 559:232–241, 2016.

[60] K. He, S. Echigo, and S. Itoh. Effect of operating conditions in soil aquifer treatment on the removals of pharmaceuticals and personal care products. *Sci Total Environ*, 565:672–681, 2016.

[61] R. Kodesova, R. Grabic, M. Kocarek, A. Klement, O. Golovko, M. Fer, A. Nikodem, and O. Jaksik. Pharmaceuticals' sorptions relative to properties of thirteen different soils. *Sci Total Environ*, 511:435–43, 2015.

[62] B. Chefetz, T. Mualem, and J. Ben-Ari. Sorption and mobility of pharmaceutical compounds in soil irrigated with reclaimed wastewater. *Chemosphere*, 73(8):1335–43, 2008.

[63] S. Rühmland, A. Wick, T. A. Ternes, and M. Barjenbruch. Fate of pharmaceuticals in a subsurface flow constructed wetland and two ponds. *Ecol Eng*, 2015:125–139, 2015.

[64] T. Rauch-Williams, C. Hoppe-Jones, and J. E. Drewes. The role of organic matter in the removal of emerging trace organic chemicals during managed aquifer recharge. *Water Res*, 44(2):449–60, 2010.

[65] I. Zucker, H. Mamane, H. Cikurel, M. Jekel, U. Hübner, and D. Avisar. A hybrid process of biofiltration of secondary effluent followed by ozonation and short soil aquifer treatment for water reuse. *Water Res*, 84:315–22, 2015.

[66] A. Lakretz, H. Mamane, H. Cikurel, D. Avisar, E. Gelman, and I. Zucker. The role of soil aquifer treatment (SAT) for effective removal of organic matter, trace organic compounds and microorganisms from secondary effluents pre-treated by ozone. *Ozone Sci Eng*, 39(5):385–394, jun 2017.

[67] M. Gifford, A. Selvy, and D. Gerrity. Optimizing ozone-biofiltration systems for organic carbon removal in potable reuse applications. *Ozone Sci Eng*, 2018.

[68] A. de Wilt, K. van Gijn, T. Verhoek, A. Vergnes, M. Hoek, H. Rijnaarts, and A. Langenhoff. Enhanced pharmaceutical removal from water in a three step bio-ozone-bio process. *Water Res.*, 138:97–105, 2018.

[69] H. El-Taliawy, M. E. Casas, and K. Bester. Removal of ozonation products of pharmaceuticals in laboratory moving bed biofilm reactors (MBBRs). *J Hazard Mater*, 347:288–298, 2018.

[70] J. Regnery, A. D. Wing, J. Kautz, and J. E. Drewes. Introducing sequential managed aquifer recharge technology (SMART) - from laboratory to full-scale application. *Chemosphere*, 154:8–16, 2016.

[71] M. Helmecke, E. Fries, and C. Schulte. Regulating water reuse for agricultural irrigation: risks related to organic micro-contaminants. *Environ Sci Eur*, 32(4), 2020.

[72] J. Hollender, E. L. Schymanski, H. P. Singer, and P. L. Ferguson. Non-target screening with high resolution mass spectrometry in the environment : Ready to go. *Environ Sci Technol*, 51:11505–11512, 2017.

[73] S. D. Richardson. The role of GC-MS and LC-MS in the discovery of drinking water disinfection by-products. *J Environ Monit*, 4:1–9, 2002.

[74] D. Barcelo. Occurrence, handling and chromatographic determination of pesticides in the aquatic environment. *Analyst*, 116:681–689.

[75] M. Krauss, H. Singer, and J. Hollender. LC-high resolution MS in environmental analysis: from target screening to the identification of unknowns. *Anal Bioanal Chem*, 397:943–951, 2010.

[76] A. Balinova. Strategies for chromatographic analysis of pesticide residues in water. *J Chromatogr A*, 754:125–135, 1996.

[77] W. Warner, T. Licha, and K. Nödler. Qualitative and quantitative use of micropollutants as source and process indicators. a review. *Sci Total Environ*, 686:75–89, oct 2019.

[78] R. Helmus, T. Ter Iaak, P. de Voogt, A. van Wezel, and E. Schymanski. Patroon: Open source software platform for environmental mass spectrometry based non-target screening. *Biomed Eng*, 2020.

[79] T. Köppe, K. S. Jewell, C. Dietrich, A. Wick, and T. A. Ternes. Application of a non-target workflow for the identification of specific contaminants using the example of the nidda river basin. *Water Res*, 178:115703, 2020.

[80] A. Müller, W. Schulz, W. K. L. Ruck, and W. H. Weber. A new approach to data evaluation in the non-target screening of organic trace substances in water analysis. *Chemosphere*, 85:1211–1219, 2011.

[81] M. Holcapek, R. Jirasko, and M. Lisa. Basic rules for the interpretation of atmospheric pressure ionization mass spectra of small molecules. *J Chromatogr A*, 1217(25):3908–21, 2010.

[82] T. Kind and O. Fiehn. Seven golden rules for heuristic filtering of molecular formulas obtained by accurate mass spectrometry. *BMC Bioinfomatic*, 8:105, 2007.

[83] J. B. Lambert, S. Gronert, H. F. Shurvell, and D. A. Lightner. *Spektroskopie: Strukturaufklärung in der Organischen Chemie*. Pearson: München, 2012.

[84] A. Weissberg and S. Dagan. Interpretation of ESI(+)-MS-MS spectra - towards the identification of "unknowns". *Int J Mass Spectrom*, 299:158–168, 2011.

[85] M. Farre, S. Perez, L. Kantiani, and D. Barcelo. Fate and toxicity of emerging pollutants, their metabolites and transformation products in the aquatic environment. *Trend Anal Chem*, 27(11):991–1007, 2008.

[86] S. Mompelat, B. Le Bot, and O. Thomas. Occurrence and fate of pharmaceutical products and by-products, from resource to drinking water. *Environ Int*, 35(5):803–14, 2009.

[87] D. J. Lapworth, N. Baran, M. E. Stuart, and R. S. Ward. Emerging organic contaminants in groundwater: A review of sources, fate and occurrence. *Environ Pollut*, 163:287–303, 2012.

[88] R. P. Deo. Pharmaceuticals in the surface water of the USA: A review. *Curr Envir Health Rpt*, 1(2):113–122, 2014.

[89] Y. Luo, W. Guo, H. H. Ngo, L. D. Nghiem, F. I. Hai, J. Zhang, S. Liang, and X. C. Wang. A review on the occurrence of micropollutants in the aquatic environment and their fate and removal during wastewater treatment. *Sci Total Environ*, 473-474:619–41, 2014.

[90] Q. Sui, X. Cao, S. Lu, W. Zhao, Z. Qiu, and G. Yu. Occurrence, sources and fate of pharmaceuticals and personal care products in the groundwater: A review. *Emerging Contaminants*, 1:14–24, 2015.

[91] B. Petrie, R. Barden, and B. Kasprzyk-Hordern. A review on emerging contaminants in wastewaters and the environment: current knowledge, understudied areas and recommendations for future monitoring. *Water Res*, 72:3–27, 2015.

[92] Y. Pico and D. Barcelo. Transformation products of emerging contaminants in the environment and high-resolution mass spectrometry: a new horizon. *Anal Bioanal Chem*, 407(21):6257–73, 2015.

[93] C. Postigo and D. Barcelo. Synthetic organic compounds and their transformation products in groundwater: occurrence, fate and mitigation. *Sci Total Environ*, 503-504:32–47, 2015.

[94] K. Yu, B. Li, and T. Zhang. Direct rapid analysis of multiple PPCPs in municipal wastewater using ultrahigh performance liquid chromatography-tandem mass spectrometry without SPE pre-concentration. *Anal Chim Acta*, 738:59–68, 2012.

[95] G. M. Bruce, R. C. Pleus, and S. A. Snyder. Toxicological relevance of pharmaceuticals in drinking water. *Environ Sci Technol*, 44:5619–5626, 2010.

[96] J. Lienert, K. GÃ$\frac{1}{4}$del, and B. I. Escher. Screening method for ecotoxicological hazard assessment of 42 pharmaceuticals considering human metabolism and excretory routes. *Environ Sci Technol*, 41:4471–4478, 2007.

[97] V. Osorio, A. Larranaga, J. Acena, S. Perez, and D. Barcelo. Concentration and risk of pharmaceuticals in freshwater systems are related to the population density and the livestock units in iberian rivers. *Sci Total Environ*, 540:267–77, 2016.

[98] D. M. Cwiertny, S. A. Snyder, D. Schlenk, and E. P. Kolodziej. Environmental designer drugs: when transformation may not eliminate risk. *Environ Sci Technol*, 48(20):11737–45, 2014.

[99] J. Diamond, K. Munkittrick, K. E. Kapo, and J. Flippin. A framework for screening sites at risk from contaminants of emerging concern. *Environ Toxicol Chem*, 34(12):2671–81, 2015.

[100] R. Lopez-Serna, M. Petrovic, and D. Barcelo. Direct analysis of pharmaceuticals, their metabolites and transformation products in environmental waters using on-line turboflow chromatography-liquid chromatography-tandem mass spectrometry. *J Chromatogr A*, 1252:115–29, 2012.

[101] R. Rosal, A. Rodriguez, J. A. Perdigon-Melon, A. Petre, E. Garcia-Calvo, M. J. Gomez, A. Aguera, and A. R. Fernandez-Alba. Occurrence of emerging pollutants in urban wastewater and their removal through biological treatment followed by ozonation. *Water Res*, 44(2):578–88, 2010.

[102] M. S. Kostich, A. L. Batt, and J. M. Lazorchak. Concentrations of prioritized pharmaceuticals in effluents from 50 large wastewater treatment plants in the US and implications for risk estimation. *Environ Pollut*, 184:354–9, 2014.

[103] M. Huerta-Fontela, M. T. Galceran, and F. Ventura. Occurrence and removal of pharmaceuticals and hormones through drinking water treatment. *Water Res*, 45(3):1432–42, 2011.

[104] S. S. Caldas, C. Rombaldi, J. L. Arias, L. C. Marube, and E. G. Primel. Multi-residue method for determination of 58 pesticides, pharmaceuticals and personal care products in water using solvent demulsification dispersive liquid-liquid microextraction combined with liquid chromatography-tandem mass spectrometry. *Talanta*, 146:676–88, 2016.

[105] T. S. Oliveira, M. Murphy, N. Mendola, V. Wong, D. Carlson, and L. Waring. Characterization of pharmaceuticals and personal care products in hospital effluent and waste water influent/effluent by direct-injection LC-MS-MS. *Sci Total Environ*, 518-519:459–78, 2015.

[106] L. Vergeynst, A. Haeck, P. De Wispelaere, H. Van Langenhove, and K. Demeestere. Multi-residue analysis of pharmaceuticals in wastewater by liquid chromatography-magnetic sector mass spectrometry: method quality assessment and application in a belgian case study. *Chemosphere*, 119 Suppl:S2–8, 2015.

[107] M. E. Dasenaki and N. S. Thomaidis. Multianalyte method for the determination of pharmaceuticals in wastewater samples using solid-phase extraction and liquid chromatography-tandem mass spectrometry. *Anal Bioanal Chem*, 407(15):4229–45, 2015.

[108] F. F. Donato, M. L. Martins, J. S. Munaretto, O. D. Prestes, M. B. Adaime, and R. Zanella. Development of a multiresidue method for pesticide analysis in drinking water by solid phase extraction and determination by gas and liquid chromatography with triple quadrupole tandem mass spectrometry. *J Braz Chem Soc*, 26(10):2077–2087, 2015.

[109] J. P. Meador, A. Yeh, G. Young, and E. P. Gallagher. Contaminants of emerging concern in a large temperate estuary. *Environ Pollut*, 213:254–267, 2016.

[110] R. Gurke, M. Rossler, C. Marx, S. Diamond, S. Schubert, R. Oertel, and J. Fauler. Occurrence and removal of frequently prescribed pharmaceuticals and corresponding metabolites in wastewater of a sewage treatment plant. *Sci Total Environ*, 532:762–70, 2015.

[111] I. Ferrer and E. M. Thurman. Analysis of 100 pharmaceuticals and their degradates in water samples by liquid chromatography/quadrupole time-of-flight mass spectrometry. *J Chromatogr A*, 1259:148–57, 2012.

[112] N. A. Alygizakis, P. Gago-Ferrero, V. L. Borova, A. Pavlidou, I. Hatzianestis, and N. S. Thomaidis. Occurrence and spatial distribution of 158 pharmaceuticals, drugs of abuse and related metabolites in offshore seawater. *Sci Total Environ*, 541:1097–1105, 2016.

[113] B. Petrie, J. Youdan, R. Barden, and B. Kasprzyk-Hordern. Multi-residue analysis of 90 emerging contaminants in liquid and solid environmental matrices by ultra-high-performance liquid chromatography tandem mass spectrometry. *J Chromatogr A*, 1431:64–78, 2016.

[114] B. Huerta, S. Rodriguez-Mozaz, C. Nannou, L. Nakis, A. Ruhi, V. Acuna, S. Sabater, and D. Barcelo. Determination of a broad spectrum of pharmaceuticals and endocrine disruptors in biofilm from a waste water treatment plant-impacted river. *Sci Total Environ*, 540:241–9, 2016.

[115] S. Dresen, N. Ferreiros, H. Gnann, R. Zimmermann, and W. Weinmann. Detection and identification of 700 drugs by multi-target screening with a 3200 Q TRAP LC-MS/MS system and library searching. *Anal Bioanal Chem*, 396(7):2425–34, 2010.

[116] B. Lopez, P. Ollivier, A. Togola, N. Baran, and J. P. Ghestem. Screening of french groundwater for regulated and emerging contaminants. *Sci Total Environ*, 518-519:562–73, 2015.

[117] Y. Liu, C. E. Uboh, L. R. Soma, X. Li, F. Guan, Y. You, and J. W. Chen. Efficient use of retention time for analysis of 302 drugs in equine plasma by liquid chromatography-MS/MS with scheduled multiple reaction monitoring and instant library searching for doping control. *Anal. Chem.*, 83:6834–6841, 2011.

[118] F. C. Poole. *The essence of Chromatography*. Elsevier, Amsterdam, 2003.

[119] M. Schulz, D. Löffler, M. Wagner, and T. A. Ternes. Transformation of the x-ray contrast medium iopromide in soil and biological wastewater treatment. *Environ Sci Technol*, 42:7207–7217, 2008.

[120] M. Jekel, W. Dott, A. Bergmann, U. Dunnbier, R. Gnirss, B. Haist-Gulde, G. Ham-scher, M. Letzel, T. Licha, S. Lyko, U. Miehe, F. Sacher, M. Scheurer, C. K. Schmidt, T. Reemtsma, and A. S. Ruhl. Selection of organic process and source indicator substances for the anthropogenically influenced water cycle. *Chemosphere*, 125:155–67, 2015.

[121] J. H. Gross. *Mass spectrometry*. Springer Cham (CH), 2017.

[122] N. Dyson. Peak distortion, data sampling errors and the integrator in the measurement of very narrow chromatographic peaks. *J Chromatogr A*, 842:321–340, 1999.

[123] Umweltbundesamt. Liste der nach GOW bewerteten Stoffe, 2017 (accessed18 august 2017).

[124] K. Nodler, O. Hillebrand, K. Idzik, M. Strathmann, F. Schiperski, J. Zirlewagen, and T. Licha. Occurrence and fate of the angiotensin ii receptor antagonist transformation product valsartan acid in the water cycle–a comparative study with selected beta-blockers and the persistent anthropogenic wastewater indicators carbamazepine and acesulfame. *Water Res*, 47(17):6650–9, 2013.

[125] T. Letzel, A. Bayer, W. Schulz, A. Heermann, T. Lucke, G. Greco, S. Grosse, W. Schussler, M. Sengl, and M. Letzel. LC-MS screening techniques for wastewater analysis and analytical data handling strategies: Sartans and their transformation products as an example. *Chemosphere*, 137:198–206, 2015.

[126] S. Huntscha, H. P. Singer, C. S. McArdell, C. E. Frank, and J. Hollender. Multiresidue analysis of 88 polar organic micropollutants in ground, surface and wastewater using online mixed-bed multilayer solid-phase extraction coupled to high performance liquid chromatography-tandem mass spectrometry. *J Chromatogr A*, 1268:74–83, 2012.

[127] K. Sangkuhl, T. E. Klein, and R. B. Altman. Clopidogrel pathway. *Pharmacogenet Genomics*, 20(7):463–5, 2010.

[128] R. N. Carvalho, L. Ceriani, A. Ippolito, and T. Lettieri. Development of the firstwatch list under the environmental quality standards directive. Technical report, European Commission, 2015.

[129] S. K. Maeng, E. Ameda, S. K. Sharma, G. Grutzmacher, and G. L. Amy. Organic micropollutant removal from wastewater effluent-impacted drinking water sources during bank filtration and artificial recharge. *Water Res*, 44(14):4003–14, 2010.

[130] S. K. Maeng, S. K. Sharma, C. D. Abel, A. Magic-Knezev, and G. L. Amy. Role of biodegradation in the removal of pharmaceutically active compounds with different bulk organic matter characteristics through managed aquifer recharge: batch and column studies. *Water Res*, 45(16):4722–36, 2011.

[131] K. M. Onesios and E. J. Bouwer. Biological removal of pharmaceuticals and personal care products during laboratory soil aquifer treatment simulation with different primary substrate concentrations. *Water Res*, 46(7):2365–75, 2012.

[132] P. Falas, A. Wick, S. Castronovo, J. Habermacher, T. A. Ternes, and A. Joss. Tracing the limits of organic micropollutant removal in biological wastewater treatment. *Water Res*, 95:240–9, 2016.

[133] J. Müller, J. E. Drewes, and U. Hübner. Sequential biofiltration - a novel approach for enhanced biological removal of trace organic chemicals from wastewater treatment plant effluent. *Water Res*, 127:127–138, 2017.

[134] K. Hellauer, D. Mergel, A. S. Ruhl, J. Filter, U. Hübner, M. Jekel, and J. Drewes. Advancing sequential managed aquifer recharge technology (SMART) using different intermediate oxidation processes. *Water*, 9:221, 2017.

[135] M. Schaffer, N. Boxberger, H. Bornick, T. Licha, and E. Worch. Sorption influenced transport of ionizable pharmaceuticals onto a natural sandy aquifer sediment at different pH. *Chemosphere*, 87(5):513–20, 2012.

[136] E. R. Dickenson, J. Drewes, D. L. Sedlak, E. C. Wert, and S. A. Snyder. Applying surrogates and indicators to assess removal efficiency of trace organic chemicals during chemical oxidation of wastewaters. *Environ Sci Technol*, 43:6242–6247, 2009.

[137] N. Hermes, K.S. Jewell, A. Wick, and T.A. Ternes. Quantification of more than 150 micropollutants including transformation products in aqueous samples by liquid chromatography-tandem mass spectrometry using scheduled multiple reaction monitoring. *J Chromatogr A*, 1531:64–73, 2018.

[138] Demoware. http://demoware.eu/en, 2016.

[139] U. Schwabe, D. Paffrath, W.-D. Ludwig, and J. Klauber. *Arzneiverordnungs-Report 2017*. Springer, Berlin, 2017.

[140] N. Henning, U. Kunkel, A. Wick, and T. A. Ternes. Biotransformation of gabapentin in surface water matrices under different redox conditions and the occurrence of one major TP in the aquatic environment. *Water Res*, 137:290–300, 2018.

[141] E. Kaiser, C. Prasse, M. Wagner, K. Broder, and T. A. Ternes. Transformation of oxcarbazepine and human metabolites of carbamazepine and oxcarbazepine in wastewater treatment and sand filters. *Environ Sci Technol*, 48(17):10208–16, 2014.

[142] M. Brienza and S. Chiron. Enantioselective reductive transformation of climbazole: A concept towards quantitative biodegradation assessment in anaerobic biological treatment processes. *Water Res*, 116:203–210, 2017.

[143] J. Müller, K. S. Jewell, M. Schulz, N. Hermes, T. A. Ternes, J. E. Drewes, and U. Hübner. Capturing the oxic transformation of iopromide - a usefull tool for an improved characterization of predominant redox conditions and the removal of trace organic compounds in biofiltration systems? *Water Research*, 152:274–284, 2019.

[144] A. Bayer, R. Asner, W. Schussler, W. Kopf, K. Weiss, M. Sengl, and M. Letzel. Behavior of sartans (antihypertensive drugs) in wastewater treatment plants, their occurrence and risk for the aquatic environment. *Environ Sci Pollut Res Int*, 21(18):10830–9, 2014.

[145] B. Baumgarten, J. Jahrig, T. Reemtsma, and M. Jekel. Long term laboratory column experiments to simulate bank filtration: factors controlling removal of sulfamethoxazole. *Water Res*, 45(1):211–20, 2011.

[146] M. Scheurer, H. J. Brauch, and F. T. Lange. Analysis and occurrence of seven artificial sweeteners in german waste water and surface water and in soil aquifer treatment (SAT). *Anal Bioanal Chem*, 394(6):1585–94, 2009.

[147] A. S. Stasinakis, S. Kotsifa, G. Gatidou, and D. Mamais. Diuron biodegradation in activated sludge batch reactors under aerobic and anoxic conditions. *Water Res*, 43(5):1471–9, 2009.

[148] A. Luft, M. Wagner, and T. A. Ternes. Transformation of biocides irgarol and terbutryn in the biological wastewater treatment. *Environ Sci Technol*, 48(1):244–54, 2014.

[149] K. S. Jewell, P. Falas, A. Wick, A. Joss, and T. A. Ternes. Transformation of diclofenac in hybrid biofilm-activated sludge processes. *Water Res*, 105:559–567, 2016.

[150] M. Muntau, M. Schulz, K. S. Jewell, N. Hermes, U. Hubner, T. Ternes, and J. E. Drewes. Evaluation of the short-term fate and transport of chemicals of emerging concern during soil-aquifer treatment using select transformation products as intrinsic redox-sensitive tracers. *Sci Total Environ*, 583:10–18, 2017.

[151] B. V. Laws, E. R. Dickenson, T. A. Johnson, S. A. Snyder, and J. E. Drewes. Attenuation of contaminants of emerging concern during surface-spreading aquifer recharge. *Sci Total Environ*, 409(6):1087–94, 2011.

[152] S. Kern, R. Baumgartner, D. E. Helbling, J. Hollender, H. Singer, M. J. Loos, R. P. Schwarzenbach, and K. Fenner. A tiered procedure for assessing the formation of biotransformation products of pharmaceuticals and biocides during activated sludge treatment. *J Environ Monit*, 12(11):2100–11, 2010.

[153] S. Castronovo, A. Wick, M. Scheurer, K. Nodler, M. Schulz, and T. A. Ternes. Biodegradation of the artificial sweetener acesulfame in biological wastewater treatment and sandfilters. *Water Res*, 110:342–353, 2017.

[154] K. Hellauer, J. Uhl, M. Lucio, P. Schmitt-Kopplin, D. Wibberg, U. Hübner, and J. E. Drewes. Microbiome-triggered transformations of trace organic chemicals in the presence of effluent organic matter in managed aquifer recharge (MAR) systems. *Environ Sci Technol*, 52:14342–14351, 2018.

[155] K. Hellauer, S. Martinez Mayerlen, J. E. Drewes, and U. Hübner. Biotransformation of trace organic chemicals in the presence of highly refractory dissolved organic carbon. *Chemosphere*, 215:33–39, 2019.

[156] N. Henning, P. Falas, S. Castronovo, K. S. Jewell, K. Bester, T. A. Ternes, and A. Wick. Biological transformation of fexofenadine and sitagliptin by carrier-attached biomass and suspended sludge from a hybrid moving bed biofilm reactor. *Water Res*, (115034), 2019.

[157] D. E. Helbling, J. Hollender, H. P. Kohler, H. Singer, and K. Fenner. High-throughput identification of microbial transformation products of organic micropollutants. *Environ Sci Technol*, 44(17):6621–6627, 2010.

[158] K. S. Jewell, S. Castronovo, A. Wick, P. Falas, A. Joss, and T. A. Ternes. New insights into the transformation of trimethoprim during biological wastewater treatment. *Water Res*, 88:550–557, 2016.

[159] C. Prasse, M. Wagner, R. Schulz, and T. A. Ternes. Biotransformation of the antiviral drugs acyclovir and penciclovir in activated sludge treatment. *Environ Sci Technol*, 45(7):2761–9, 2011.

[160] V. Burke, L. Schneider, J. Greskowiak, P. Baar, A. Sperlich, U. Dünnbier, and G. Massmann. Trace organic removal during river bank filtration for two types of sediment. *Water*, 10:1736, 2018.

[161] F. R. Storck, H. J. Brauch, C. Skark, F. Remmler, and N. Zullei-Seibert. Acesulfam - ein universeller tracer? *DVGW energie wasser-praxis*, 66:26–31, 2015.

[162] J. Gomes, R. Costa, R. M. Qinta-Ferreira, and R. C. Martins. Application of ozonation for pharmaceuticals and personal care products removal from water. *Sci Total Environ*, 586:265–283, 2017.

[163] G. Knopp, C. Prasse, T. A. Ternes, and P. Cornel. Elimination of micropollutants and transformation products from a wastewater treatment plant effluent through pilot scale ozonation followed by various activated carbon and biological filters. *Water Res*, 100:580–592, 2016.

[164] E. Illes, E. Szabo, E. Takacs, L. Wojnarovits, A. Dombi, and K. Gajda-Schrantz. Ketoprofen removal by O_3 and O_3/UV processes: Kinetics, transformation products and ecotoxicity. *Sci Total Environ*, 472:178–184, 2014.

[165] A. Magdeburg, D. Stalter, M. Schlüsener, and T. Ternes. Evaluating the efficiency of advanced wastewater treatment: Target analysis of organic contaminants and (geno-)toxicity assessment tell a different story. *Water Res*, 50:35–47, 2014.

[166] E. Borowska, M. Bourgin, J. Hollender, C. Kienle, C. S. McArdell, and U. von Gunten. Oxidation of cetirizine, fexofenadine and hydrochlorothiazide during ozonation: Kinetics and formation of transformation products. *Water Res*, 94:350–362, 2016.

[167] J. Kuang, J. Huang, B. Wang, Q. Cao, S. Deng, and G. Yu. Ozonation of trimethoprim in aqueous solution: identification of reaction products and their toxicity. *Water Res*, 47(8):2863–72, 2013.

[168] Y. Lee and U. von Gunten. Advances in predicting organic contaminant abatement during ozonation of municipal wastewater effluent: reaction kinetics, transformation products, and changes of biological effects. *Environ Sci: Water Res Technol*, 2(3):421–442, 2016.

[169] M. Elmghari-Tabib. Ozonation reaction patterns of alcohols and aliphatic amines. *Ozone Sci Eng*, 4(4):195–205, 1982.

[170] E. Keinan and Y. Mazur. Dry ozonation of amines. conversion of primary amines to nitro compounds. *J Org Chem*, 42(5):844–847, 1977.

[171] J. L. Shi and D. L. McCurry. Transformation of N-methylamine drugs during wastewater ozonation: Formation of nitromethane, an efficient precursor to halonitromethanes. *Environ Sci Technol*, 2020.

[172] O. I. G. Khreit, H. M. Grant, and C. Henderson. Identification of novel metabolic pathways of sitagliptin (STG) by LC/MS and LC/MS^2 after incubations with rat hepatocytes. *J Drug Metab Toxicol*, 7(4), 2016.

[173] S. H. Vinvent, J. R. Reed, A. J. Bergmann, C. S. Elmore, B. Zhu, S. Xu, D. Ebel, P. Larson, W. Zeng, L. Chen, S. Dilzer, K. Lasseter, K. Gottesdiener, J. A. Wagner, and G. A. Herman. Metabolism and excretion of the dipeptidyl peptidase 4 inhibitor 14C sitagliptin in humans. *Drug Metab Dispos*, 35(4):533–538, 2007.

[174] J. Martin, W. Buchberger, J. L. Santos, E. Alonso, and I. Aparicio. High-performance liquid chromatography quadrupole time-of-flight mass spectrometry method for the analysis of antidiabetic drugs in aqueous environmental samples. *J Chromatogr B Analyt Technol Biomed Life Sci*, 895-896:94–101, 2012.

[175] D. Krakko, V. Licul-Kucera, G. Zaray, and V. G. Mihucz. Single-run ultra-high performance liquid chromatography for quantitative determination of ultra-traces of ten popular active pharmaceutical ingredients by quadrupole time-of-flight mass spectrometry after offline preconcentration by solid phase extraction from drinking and river waters as well as treated wastewater. *Microchem J*, 148:108–119, 2019.

[176] L. Boulard, G. Dierkes, M. P. Schlüsener, A. Wick, J. Koschorreck, and T. A. Ternes. Spatial distribution and temporal trends of pharmaceuticals sorbed to suspended particulate matter of german rivers. *Water Res*, 171:115366, 2020.

[177] E. Gilbert and J. Hoigne. Messung von ozon in wasserwerken; vergleich der DPD- und indigo-methode. *GWF Wasser-Abwasser*, 124:527–531, 1983.

[178] H. Bader and J. Hoigne. Determination of ozone in water by the indigo method. *Water Res*, 15:449–456, 1981.

[179] C. Dietrich, A. Wick, and T. A. Ternes. Open-source feature detection for non-target LC-MS analytics. *in prep.*, 2020.

[180] M. Scheurer, K. Nödler, F. Freeling, J. Janda, O. Happel, M. Riegel, U. Müller, F. R. Storck, M. Fleig, F. T. Lange, A. Brunsch, and H. J. Brauch. Small, mobile, persistent: Trifluoroacetate in the water cycle - overlooked sources, pathways, and consequences for drinking water supply. *Water Res*, 126:460–471, 2017.

[181] P. S. Bailey. The reactions of ozone with organic compounds. *Chem Rev*, 58(5):925–1010, 1958.

[182] J. Reungoat, M. Macova, B. I. Escher, S. Carswell, J. F. Mueller, and J. Keller. Removal of micropollutants and reduction of biological activity in a full scale reclamation plant using ozonation and activated carbon filtration. *Water Res*, 44(2):625–637, 2010.

[183] B. Domenjoud, A. Gonzalez Ospina, E. Vulliet, and S. Baig. Innovative coupling of ozone oxidation and biodegradation for micropollutants removal from wastewater. *Ozone Sci Eng*, 39(5):296–309, 2017.

[184] M. J. Krzmarzick, R. Khatiwada, C. I. Olivares, L. Abrell, R. Sierra-Alvarez, J. Chorover, and J. A. Field. Biotransformation and degradation of the insensitive munitions compound, 3-nitro-1,2,4-triazol-5one, by soil bacterial communities. *Environ Sci Technol*, 49(9):5681–5688, 2015.

[185] A. K. Ghattas, F. Fischer, A. Wick, and T. A. Ternes. Anaerobic biodegradation of (emerging) organic contaminants in the aquatic environment. *Water Res*, 116:268–295, 2017.

Appendix

Appendix A

Supplementary data for Chapter 2:
Quantification of more than 150 micropollutants including transformation products in aqueous samples by liquid chromatography-tandem mass spectrometry using scheduled multiple reaction monitoring

A1.1-A: Target-list including CAS, sum formula, supplier and MS-parameters

Abbreviations: M = Method, RT = Retention time, DW = Detection window, n.a. = not available

Group	Substance	CAS	Formula	Supplier	M	ESI	RT	DW	Q1	Q3a/Q3b	DP	CEa/CEb
Nervous System	Tramadol	36282-47-0	C16H25NO2	Fluka	1	pos	6.7	40	264.2	58.0	46	45
	O-DM-Tramadol	73986-53-5	C15H23NO2	Sigma Aldrich	1	pos	5.9	40	250.1	58.0	45	20
	N-DM-Tramadol	75377-45-6	C15H23NO2	TRC	1	pos	6.2	40	250.1	44.0	45	20
	N,O-DDM-Tramadol	138853-73-3	C14H21NO2	TRC	1	pos	5.9	40	236.1	44.0	44	20
	Tramadol-N-oxide	147441-56-3	C16H25NO3	TRC	1	pos	6.9	40	280.2	135.0/262.2	60	35/18
	Primidone	125-33-7	C12H14N2O2	Sigma Aldrich	1	pos	7.0	40	219.0	162.0/91.0	40	16/39
	Phenytoin	57-41-0	C15H12N2O2	Sigma Aldrich	2	neg	9.6	40	251.0	102.0/208.0	-45	-28/-25
	Carbamazepine (CBZ)	298-46-4	C15H12N2O	Sigma Aldrich	2	pos	9.5	40	237.1	194.0/179.1	71	27/49
	2-Hydroxy-CBZ	68011-66-5	C15H12N2O2	Novartis	2	pos	7.9	40	253.1	210.2/208.0	71	29/35
	3-Hydroxy-CBZ	68011-67-6	C15H12N2O2	Novartis	2	pos	8.3	40	253.1	210.1/167.0	66	27/51
	10-Hydroxy-CBZ	29331-92-8	C15H14N2O2	Novartis	2	pos	7.6	40	255.2	194.1/179.1	46	27/52
	10,11-Dihydro-10,11-dihydroxy-CBZ	35079-97-1	C15H14N2O3	TRC	2	pos	7.1	40	271.0	180.0/236.0	40	45/19
	9-Carboxylic acid-Acridine	5336-90-3	C14H9NO2	Santa Cruz	2	pos	5.1	40	224.1	196.0/167.0	86	37/57
	Acridone	578-95-0	C13H9NO	Th. Gever	2	pos	8.9	40	196.0	167.1/139.1	96	43/71
	Lamotrigine	84057-84-1	C9H7Cl2N5	TCI	1	pos	6.6	40	256.0	211.0/157.0	80	38/45
	2-N-methyl-Lamotrigine	1152091-69-4	C10H9Cl2N5	TRC	1	pos	7.1	40	270.0	201.0/185.0	80	38/48
	Gabapentin	60142-96-3	C9H17NO2	TRC	1	pos	5.6	40	172.1	154.1/137.1	55	19/22
	Gabapentin Lactam	64744-50-9	C9H15NO	Sigma Aldrich	1	pos	8.4	40	154.1	95.0/67.0	80	30/40
	Levetiracetam	102767-28-2	C8H14N2O2	TRC	1	pos	5.7	40	171.1	154.1/126.1	50	11/19
	Levetiracetam acid	102849-49-0	C8H13NO3	TRC	1	pos	6.3	40	172.1	126.0/69.2	96	19/33
	Pregabalin	148553-50-8	C8H17NO2	TRC	2	pos	5.3	40	160.1	97.0/55.0	41	21/35
	Sulpiride	23672-07-3	C15H23N3O4S	Sigma Aldrich	2	pos	5.2	40	342.2	112.1/214.0	60	35/45
	Amisulpride	71675-85-9	C17H27N3O4S	TRC	1	pos	6.2	40	370.2	424.0/196.0	106	39/59
	O-desmethyl-Amisulpride	148516-54-5	C16H25N3O4S	TRC	1	pos	6.2	40	356.2	112.1/129.1	166	37/31
	Oxazepam	604-75-1	C15H11ClN2O2	Sigma Aldrich	1	pos	10.0	40	287.1	241.0/104.0	61	47/81
	Citalopram	59729-32-7	C20H21FN2O	Labmix24	1	pos	8.4	40	325.2	109.1/262.1	85	37/27
	Desmethyl-Citalopram	97743-99-2	C19H19FN2O	TRC	1	pos	8.3	40	311.1	262.1/109.1	45	26/32
	Didesmethyl-Citalopram	1189694-81-2	C18H17FN2O	TRC	1	pos	8.1	40	297.1	109.0/116.0	60	30/30
	Citalopram-N-oxide	63284-72-0	C20H21FN2O2	TRC	1	pos	8.6	40	341.2	262.1/109.1	60	27/35
	Venlafaxine (VLX)	99300-78-4	C17H27NO2	Promochem	1	pos	7.5	40	278.2	58.0/121.1	36	43/28
	O-desmethyl-VLX	93413-62-8	C16H25NO2	Promochem	1	pos	6.3	40	264.1	58.0/107.0	56	45/45
	N-desmethyl-VLX	149289-30-5	C16H25NO2	Campro Scientific	1	pos	7.3	40	264.1	44.0/121.1	36	55/37
	N.O-didesmethyl-VLX	135308-74-6	C15H23NO2	Campro Scientific	1	pos	6.2	40	250.2	44.2/132.8	36	32/31
	VLX-N-oxide	1094598-37-4	C17H27NO3	TRC	1	pos	7.6	40	294.2	121.1/178.1	50	35/25
	Lidocaine	137-58-6	C14H22N2O	TRC	1	pos	6.3	40	235.2	86.1/58.1	80	23/53
	Nor-Lidocaine	7729-94-4	C12H18N2O	TRC	1	pos	6.0	40	207.1	58.1/122.1	35	30/20
	Flecainide	54143-55-4	C17H20F6N2O3	TRC	1	pos	8.5	40	415.2	398.1/301.0	80	35/50
	m-O-dealkylated Flecainide	83526-33-4	C15H19F3N2O3	TRC	1	pos	6.5	40	333.1	316.1/219.1	60	28/40
	Hydrochlorothiazide	58-93-5	C7H8ClN3O4S2	TRC	2	neg	6.0	40	296.0	268.9/205.0	-120	-26/-32
	Chlorothiazide	58-94-6	C7H6ClN3O4S2	Sigma Aldrich	2	neg	5.8	40	294.0	179.0/214.0	-80	-62/-40
	4-amino-6-chloro-1,3-benzenedisulfonamide	121-30-2	C6H8ClN3O4S2	Sigma Aldrich	2	neg	5.5	40	284.0/ 286.0 [1]	78.0	-70	-50/-50

	Name	CAS	Formula	Source		pol							
Cardiovascular System	Xipamide	14293-44-8	C15H15ClN2O4S	TRC	2	neg	11.3	40	353.1	274.1/127.0	-60	-36/-45
	Furosemide	54-31-9	C12H11ClN2O5S	Sigma Aldrich	2	neg	9.6	40	329.0	205.0/285.0	-90	-30/-20
	Torsemide	56211-40-6	C16H20N4O3S	TRC	2	pos	8.1	40	349.1	264.1/290.1	60	25/20
	Hydroxy-Torsemide	99300-68-2	C16H20N4O4S	TRC	2	pos	6.1	40	365.1	280.1/306.1	50	25/20
	Sotalol	959-24-0	C12H20N2O3S	Dr. Ehrenstorfer	1	pos	5.4	40	273.0	213.0/134.0	46	26/37
	Metoprolol	56392-17-7	C15H25NO3	Sigma Aldrich	2	pos	6.1	40	268.0	74.0/116.0	75	35/27
	Hydroxy-Metoprolol	56392-16-6	C15H25NO4	Sigma Aldrich	2	pos	5.3	40	284.2	74.0/116.0	70	35/28
	O-desmethyl-Metoprolol	62572-94-5	C14H23NO3	TRC	2	pos	5.3	40	254.2	177.0/116.0	70	25/25
	Atenolol	29122-68-7	C14H22N2O3	Sigma Aldrich	1	pos	5.3	40	267.0	145.0/190.0	61	37/27
	Atenolol acid	56392-14-4	C14H21NO4	TRC	1	pos	6.7	40	268.1	191.2/226.1	56	27/25
	Hydroxy-Atenolol	68373-10-4	C14H22N2O4	TRC	1	pos	5.1	40	283.1	116.0/74.0	65	25/40
	Enalapril	76095-16-4	C20H28N2O5	TRC	1	pos	8.0	80	377.2	234.1/91.1	60	28/65
	Enalaprilat	84680-54-6	C18H24N2O5	TRC	1	pos	6.4	80	349.2	206.1/303.2	50	28/25
	Ramipril	87333-19-5	C23H32N2O5	TRC	2	pos	9.0	80	417.2	234.1/343.2	70	28/28
	Ramiprilat	n.a.	C21H28N2O5	TRC	2	pos	7.7	80	389.2	206.4/156.4	70	30/30
	Valsartan	137682-53-4	C24H29N5O3	TRC	2	pos	12.0	40	436.2	235.1/207.1	111	27/35
	Valsartan acid	164265-78-5	C14H10N4O2	TRC	2	pos	8.4	40	267.1	206.1/151.1	80	17/57
	Irbesartan	138402-11-6	C25H28N6O	TRC	2	neg	11.1	40	427.2	193.1/121.0	-70	-35/-80
	Candesartan	139481-59-7	C24H20N6O3	TRC	2	pos	10.5	40	441.2	263.2/207.2	51	17/35
	Telmisartan	144701-48-4	C33H30N4O2	TRC	2	pos	10.5	40	515.2	276.1/497.2	181	61/45
	Olmesartan	144689-24-7	C24H26N6O3	TRC	2	neg	7.8	40	445.2	149.1/167.1	-50	-50/-35
	Aliksiren	173334-57-1	C30H53N3O6	TRC	1	pos	8.8	40	552.4	436.3/534.4	70	28/28
	Bezafibrate	41859-67-0	C19H20ClNO4	Sigma Aldrich	2	neg	11.4	40	360.1	274.1/154.0	-65	-22/-36
	3-[(4-chlorobenzoyl)amino]-propanoic acid	n.a.	C10H10ClNO3	Sigma Aldrich	2	neg	8.0	40	226.0/ 228.0 [1)]	154.1/156.1 [1)]	-45	-20/-20
Antiinfectives for systemic use	Climbazole	38083-17-9	C15H17ClN2O2	Dr. Ehrenstorfer	1	pos	9.5	40	293.0	197.0/69.0	50	23/37
	Climbazole-TP	n.a.		[3)]	1	pos	8.9	80	295.0/ 297.0 [1)]	69.0/69.0	50	23/37
	Trimethoprim	738-70-5	C14H18N4O3	Sigma Aldrich	1	pos	6.0	40	291.1	261.1/230.1	86	35/33
	3-desmethyl-TMP	27653-69-6	C13H16N4O3	TRC	1	pos	5.6	40	277.1	261.1/123.1	86	38/51
	5-(2,4,5-Trimethoxy)-2,4-pyrimidinediamnine	30806-86-1	C14H16N4O4	TRC	1	pos	6.4	40	305.1	244.1/137.0	75	35/35
	Sulfamethoxazole (SMX)	723-46-6	C10H11N3O3S	Sigma Aldrich	2	pos	7.9	40	254.1	156.0/188.0	66	23/21
	Acetyl-SMX	21312-10-7	C12H13N3O4S	EAWAG	2	pos	8.1	40	296.1	134.0/198.0	81	35/25
	Clarithromycin	81103-11-9	C38H69NO13	Abbott	1	pos	9.3	40	748.5	590.4/158.1	86	27/39
	Fluconazole	86386-73-4	C13H12F2N6O	TRC	2	pos	7.0	40	307.1	238.1/220.1	70	20/25
	Aciclovir	59277-89-3	C8H11N5O3	TRC	1	pos	5.1	40	226.1	152.1/135.1	71	17/40
	Carboxy-Aciclovir	80685-22-9	C8H9N5O4	TRC	1	pos	5.1	40	240.1	152.1/135.1	46	19/43
	Emtricitabine	143491-57-0	C8H10FN3O3S	TRC	1	pos	5.4	40	248.0	130.0/113.0	61	19/53
	Emtricitabine carboxylate	1238210-10-0	C8H8FN3O4S	TRC	1	pos	5.2	40	262.0	130.0/113.0	48	23/56
	Emtricitabine-S-oxide	152128-77-3	C8H10FN3O4S	TRC	1	pos	5.1	40	264.0	130.0/113.0	60	27/57
ary Tract and Metabolism / and Blood forming organs / plastic / Respiratory system	Ranitidine	666357-59-3	C13H22N4O3S	Sigma Aldrich	1	pos	5.4	40	315.1	176.0/130.0	50	25/36
	Ranitidine-N-oxide	73857-20-2	C13H22N4O4S	Sigma Aldrich	1	pos	5.4	40	331.1	176.2/124.3	30	25/20
	Desmethyl-Ranitidine	66357-25-3	C12H20N4O3S	TRC	1	pos	5.3	40	301.1	176.0/124.0	50	17/20
	Sitagliptin	654671-78-0	C16H15F6N5O	TRC	1	pos	7.1	40	408.1	235.1/174.0	51	29/33
	Clopidogrel	120202-66-6	C16H16ClNO2S	TRC	1	pos	13.5	40	322.1	212.0/184.0	31	23/31
	Clopidogrel acid	144750-42-5	C15H14ClNO2S	TRC	1	pos	7.3	40	308.0	198.0/152.0	66	23/33
	Bicalutamide	90357-06-5	C18H14F4N2O4S	TRC	2	neg	12.0	40	429.1	255.0/185.0	-55	-22/-50
	Diphenhydramine	147-24-0	C17H21NO	TRC	2	pos	7.6	40	256.2	167.0/152.0	30	20/50
	N-desmethyl-Diphenhydramine	53499-40-4	C16H19NO	TRC	2	pos	7.4	40	242.0	167.0/152.0	30	20/50

	Compound	CAS	Formula	Source								
Aliment Blood a Antineo)	Diphenhydramine-N-oxide	3922-74-5	C17H21NO2	TRC	2	pos	8.0	40	272.2	167.0/88.0	35	25/17
	Cetirizine	83881-52-1	C21H252N2O3	TRC	1	pos	9.4	40	389.1	166.1/262.1	55	60/30
	Fexofenadine	153439-40-8	C32H39NO4	TRC	1	pos	9.2	40	502.3	466.3/171.1	80	38/57
Contrast media	Diatrizoic acid	737-31-5	C11H8I3N2O4	Sigma Aldrich	2	pos	5.0	60	614.8	233.1/361.0	91	63/42
	Iopamidol	60166-93-0	C17H22I3N3O8	TRC	1	pos	5.1	40	777.9	558.8/387.0	106	33/55
	Iopromide	73334-07-3	C18H24I3N3O8	TRC	1	pos	5.5	40	791.9	572.9/558.9	101	33/39
	Iopromide-TP-643	n.a.	C12H12I3N3O4	[3] Schulz et al (2008)	1	pos	5.8	40	643.5	612.5/516.6	61	21/19
	Iopromide-TP-701A	n.a.	C14H14I3N3O6	[3] Schulz et al (2008)	1	pos	5.9	40	701.5	612.7/453.7	66	25/43
	Iopromide-TP-701B	n.a.	C14H14I3N3O6	[3] Schulz et al (2008)	1	pos	5.9	40	701.8	626.6/467.7	81	17/37
	Iopromide-TP-731B	n.a.	C15H16I3N3O7	[3] Schulz et al (2008)	1	pos	5.7	40	731.9	626.4/467.6	91	23/41
	Iopromide-TP-819	n.a.	C18H20I3N3O10	[3] Schulz et al (2008)	1	pos	5.6	40	819.8	586.6/700.4	101	35/29
	Iopromide-TP-729A	n.a.	C15H14I3N3O7	[3] Schulz et al (2008)	1	pos	5.5	40	729.5	612.5/453.6	85	27/43
	Iopromide-TP-759	n.a.	C16H16I3N3O8	[3] Schulz et al (2008)	1	pos	6.0	40	759.5	684.4/670.4	66	23/23
	Iomeprol	78649-41-9	C17H22I3N3O8	TRC	1	pos	5.2	40	777.9	531.9/405.0	106	37/39
Musculo-Skeletal System	Diclofenac (DCF)	15307-79-6	C14H10Cl2NO2	Sigma Aldrich	1	pos	13.1	40	296.0	215.0/250.0	46	27/19
	4-Hydroxy-DCF	64118-84-9	C14H11Cl2NO3	TRC	1	pos	11.0	40	312.0	230.0/231.0	47	46/28
	Carboxy-DCF	13625-57-5	C13H9Cl2NO2	TRC	1	pos	13.3	40	282.0	229.0/264.0	28	37/14
	DCF Lactam	15362-40-0	C14H9Cl2NO	TRC	1	pos	12.8	40	278.0	214.0/215.0	60	39/30
	Ibuprofen (IBU)	15687-27-1	C13H18O2	Sigma Aldrich	2	neg	13.4	40	205.1	161.0/159.0	-30	-10/-6
	2-Hydroxy-IBU	51146-55-5	C13H18O3	TRC	2	neg	8.7	40	303.0/221.0 [2]	177.0/177.0	-50/-30	-20/-11
	Carboxy-IBU	15935-54-3	C13H16O4	TRC	2	neg	8.9	40	191.0/235.0 [2]	73.0/73.0	-40	-20/-20
	Naproxen	22204-53-1	C14H14O3	Sigma Aldrich	2	neg	11.3	40	229.1	170.0/185.0	-50	-22/-11
	O-desmethyl-Naproxen	52079-10-4	C13H12O3	Sigma Aldrich	2	neg	8.9	40	215.0	169.0/171.0	-35	-40/-11
	Oxypurinol	2465-59-0	C5H4N4O2	Sigma Aldrich	2	neg	3.0	80	151.0	42.0/66.0	-70	-32/-50
Fungizides/Herbicides/Insectizides	Carbendazim	10605-21-7	C9H9N3O2	Riedel de Haen	1	pos	5.7	40	192.1	160.1/132.1	61	25/41
	Epoxiconazole	133855-98-8	C17H13ClFN3O	Sigma Aldrich	2	pos	12.8	40	330.1	121.0/75.0	70	35/95
	Propiconazole	60207-90-1	C15H17Cl2N3O2	Dr. Ehrenstorfer	2	pos	13.8	40	342.1/344.1 [1]	159.0/161.0 [1]	76	45/37
	Tebuconazole	107534-96-3	C16H22ClN3O	Dr. Ehrenstorfer	2	pos	13.2	40	308.1	70.0/125.0	81	49/45
	DEET	134-62-3	C12H17NO	Sigma Aldrich	1	pos	10.9	40	192.1	119.1/91.1	51	25/43
	DEET carboxylic acid	72236-23-8	C12H15NO3	TRC	1	pos	8.1	40	222.1	149.1/121.1	60	26/40
	Hydroxy-DEET	72236-22-7	C12H17NO2	TRC	1	pos	7.7	40	208.1	135.1/107.1	60	26/35
	N-ethyl-m-toluamide	26819-07-8	C10H13NO	TRC	1	pos	8.9	40	164.0	72.0/119.0	60	20/25
	Imidacloprid	138261-41-3	C9H10ClN5O2	Sigma Aldrich	1	pos	7.7	40	256.1	209.0/175.1	60	25/30
	Diuron	330-54-1	C9H10Cl2N2O	Dr. Ehrenstorfer	2	neg	10.9	40	231.0/233.0 [1]	186.0/186.0	-60	-25/-25
	Didemethyldiuron (DCPU)	2327-02-8	C7H6Cl2N2O	TRC	2	neg	9.4	40	203.0/205.0 [1]	160.0/162.0 [1]	-50	-20/-18
	N-Demethoxylinuron (DCPMU)	3567-62-2	C8H8Cl2N2O	TRC	2	neg	10.3	40	217.0/219.0 [1]	160.0/162.0 [1]	-40	-18/-18
	Isoproturon	34123-59-6	C12H18N2O	Dr. Ehrenstorfer	1	pos	10.9	40	207.0	72.0/165.1	65	35/22
	Mecoprop	7085-19-0	C10H11ClO3	Dr. Ehrenstorfer	2	neg	11.7	40	215.0/213.0 [1]	143.0/141.0 [1]	-35	-20/-20
	Metamitron	41394-05-2	C10H10N4O	Sigma Aldrich	2	pos	7.2	40	203.1	104.0/175.1	65	33/23
	Desamino-Metamitron	36993-94-9	C10H9N3O	LGC	2	pos	6.7	40	188.1	77.0/104.0	60	28/28
	Metazachlor	67129-08-2	C14H16ClN3O	Sigma Aldrich	2	pos	11.5	40	278.1	210.0/134.1	35	15/30
	Metolachlor	51218-45-2	C15H22ClNO2	Chem Service	2	pos	13.7	40	284.1	252.0/286.1	45	20/35
	Metolachlor ESA	947601-85-6	C15H22NO5S	TRC	2	pos	10.3	80	330.2	298.1/202.1	80	18/35
	Metolachlor OA	152019-73-3	C15H21NO4	TRC	2	pos	10.2	70	280.1	248.1/146.1	80	18/37
	Terbutryn	886-50-0	C10H19N5S	Dr. Ehrenstorfer	2	pos	12.5	40	242.0	186.0/91.0	50	25/38

A1.1-A

	Compound	CAS	Formula	Supplier								
	Terbuthylazine	5915-41-3	C9H16ClN5	Dr. Ehrenstorfer	2	pos	12.3	40	230.1	174.1/104.0	61	25/45
	Terbuthylazine-2-Hydroxy	66753-07-9	C9H16ClN5O	Sigma Aldrich	2	pos	6.2	40	212.2	156.1/97.0	70	18/38
	Irgarol	28159-98-0	C11H19N5S	Riedel de Haen	2	pos	12.7	40	254.0	198.0/83.0	70	26/41
Industrial chemicals/Lifestyle compounds/Disinfectants/Sweetener/Bitterant	Benzotriazole	95-14-7	C6H5N3	Dr. Ehrenstorfer	1	pos	6.6	40	120.0	65.0/39.0	90	29/45
	1-Hydroxy-Benzotriazole	123333-53-9	C6H5N3O	Sigma Aldrich	1	pos	5.8	40	136.0	64.0/91.1	60	45/28
	Tetraglyme	143-24-8	C10H22O5	TRC	2	pos	6.4	40	223.1	103.0/59.0	50	14/28
	Ethyltriphenylphosphonium	1530-32-1	C20H20P	Sigma Aldrich	1	pos	8.5	40	291.2	183.1/108.1	100	61/49
	Methyltriphenylphosphonium	1779-49-3	C19H18P	Sigma Aldrich	1	pos	8.1	40	277.1	183.1/108.1	100	59/51
	Tetrabutyltriphenylphosphonium	2304-30-5	C16H36P	Sigma Aldrich	1	pos	10.5	40	259.3	76.0/90.0	110	53/47
	(Methoxymethyl)triphenylphosphonium	4009-98-7	C20H20OP	Sigma Aldrich	1	pos	8.6	40	307.1	183.1/185.1	85	54/31
	Tetrabutylammonium	1643-19-2	C16H36N	Sigma Aldrich	1	pos	9.8	40	242.3	142.0/100.0	100	34/45
	Tetrapropylammonium	1941-30-6	C12H28N	Sigma Aldrich	1	pos	6.5	40	186.2	114.1/142.1	50	34/28
	Caffeine	58-08-2	C8H10N4O2	Sigma Aldrich	1	pos	6.1	40	195.1	138.0/110.0	70	28/30
	Triclosan	3380-34-5	C12H7Cl3O2	Sigma Aldrich	2	neg	15.1	40	287.0/289.0 [1]	35.0/35.0	-35/-45	-30/-26
	Triclocarban	101-20-2	C13H9Cl3N2O	Sigma Aldrich	2	neg	15.0	40	315.0/317.0 [1]	162.0/160.0 [1]	-60	-20/-18
	Carbanilide	102-07-8	C13H12N2O	Sigma Aldrich	2	neg	11.2	40	211.0	92.0	-40	-15
	Acesulfame	55589-62-3	C4H5NO4S	Sigma Aldrich	2	neg	4.8	120	162.0	82.0/78.0	-50	-22/-38
	Saccharine	81-07-2	C7H5NO3S	Dr. Ehrenstorfer	2	neg	5.7	40	182.0/186.0 [1]	105.8/42.0	-50/-75	-26/-52
	Sucralose	56038-13-2	C12H19Cl3O8	Dr. Ehrenstorfer	2	neg	6.3	40	395.0/401.0 [1]	35.0/35.0	-55	-38/-36
	Denatonium	3734-33-6	C21H29N2O	Sigma Aldrich	1	pos	8.6	40	325.2	86.3/91.2	60	28/50
	Tolylbiguanide	93-69-6	C9H13N5	Sigma Aldrich	1	pos	5.5	40	192.1	60.1/116.0	50	28/40

[1] Isotope used

[2] Source fragmentation

[3] in-house

M. Schulz, D. Löffler, M. Wagner, T.A. Ternes, Transformation of the X-ray Contrast Medium Iopromide In Soil and Biological Wastewater Treatment, Environmental Science & Technology, 42 (2008) 7207-7217

A1.1-B: List of labelled internal standards including CAS, sum formula, supplier and MS-parameters

Abbreviations: M = Method, RT = Retention time, DW = Detection window

Substance	CAS	Supplier	M	ESI	RT	DW	Q1	Q3	DP	CE
Acyclovir-d4	1185179-33-2	TRC	1	pos	5.08	40	230.1	152.1	71	19
Aliskiren d6	1246815-96-2	TRC	1	pos	8.75	40	558.4	436.3	60	31
Amisulpride d5	1216626-17-3	TRC	1	pos	6.15	40	375.2	242.0	106	39
O-desmethyl-Amisulpride-d5	n.a.	TRC	1	pos	6.17	40	361.2	134.1	80	32
Atenolol-d7	1202864-50-3	Dr Ehrenstorfer	1	pos	5.31	40	274.0	145.0	66	37
Hydroxy-Atenolol-d7	n.a.	TRC	1	pos	5.08	40	290.1	123.0	60	38
Benzotriazole-d4	1185072-03-0	TRC	1	pos	6.62	40	124.0	69.0	90	33
Caffeine 13C3	78072-66-9	TRC	1	pos	6.05	40	198.1	140.1	85	28
Carbendazim-d4	291765-95-2	Dr Ehrenstorfer	1	pos	5.73	40	196.2	164.1	70	25
Cetirizine-d8	n.a.	TRC	1	pos	9.41	40	397.2	166.1	55	55
Citalopram-d6	1190003-26-9	TRC	1	pos	8.39	40	331.2	109.1	60	37
Didemethyl Citalopram-d6	1189865-88-0	TRC	1	pos	8.12	40	303.2	266.1	60	22
Clarithromycin-N-methyl-d3	n.a.	TRC	1	pos	9.33	40	751.5	161.2	70	40
Climbazole-d4	1185117-79-6	TRC	1	pos	9.47	40	297.0	201.0	50	23
Clopidogrel-d4	1219274-96-0	TRC	1	pos	13.5	40	326.1	216.1	31	23
Clopidogrel d4 Carboxylic acid	1246814-52-7	TRC	1	pos	7.29	40	312.0	202.0	60	25
DEET-d7	1219799-37-7	Dr Ehrenstorfer	1	pos	10.89	40	199.1	126.1	86	24
Diclofenac-d4	153466-65-0	Dr Ehrenstorfer	1	pos	13.05	40	300.0	219.0	46	27
Dipyridamole-d20	1189983-52-5	TRC	1	pos	8.21	40	525.4	449.4	100	65
Enalapril-d5	349554-02-5	TRC	1	pos	7.98	80	382.2	239.2	60	28
Enalaprilat-d5	1356922-29-6	TRC	1	pos	6.57	80	354.2	308.2	60	25
Fexofenadine-d6	548783-71-7	TRC	1	pos	9.15	40	508.3	472.3	80	40
Flecainide-d3	127413-31-4	TRC	1	pos	8.53	40	418.2	401.2	70	35
Gabapentin-d10	1126623-20-8	Sigma Aldrich	1	pos	5.62	40	182.2	164.2	56	21
Gabapentin-Lactam-d6	n.a.	TRC	1	pos	8.37	40	160.3	101.1	81	33
Imidacloprid-d4	1015855-75-0	TRC	1	pos	7.69	40	260.1	179.1	80	25
Iomeprol-d3	1185146-41-1	TRC	1	pos	5.23	40	780.9	408.0	115	55
Iopamidol-d8	1795778-90-3	Campro Scientific	1	pos	5.1	40	785.9	562.9	86	43
Iopromide-d3	1189947-73-6	TRC	1	pos	5.45	40	794.9	575.9	81	33
Isoproturon-d6	217487-17-7	TRC	1	pos	10.89	40	213.2	78.0	65	30
Lamotrigine-13C, 15N4	n.a.	Sigma Aldrich	1	pos	6.58	40	261.0	46.1	86	79
Levetiracetam-d6	1133229-30-7	TRC	1	pos	5.68	40	177.1	132.1	36	20
Lidocaine-ethyl-d10	1189959-13-4	TRC	1	pos	6.32	40	245.2	96.1	96	23
Nor-Lidocaine-d5	1329497-00-8	TRC	1	pos	5.95	40	212.3	63.3	40	30
Oxazepam-d5	65854-78-6	Sigma Aldrich	1	pos	10	40	292.1	236.0	81	31
Primidone-d5	73738-06-4	TRC	1	pos	7	40	224.0	167.1	56	17
Ranitidine-d6	1185514-83-3	TRC	1	pos	5.35	40	321.1	176.0	50	25
Sitagliptin-d4	n.a.	TRC	1	pos	7.11	40	412.1	239.1	26	27
Sotalol-d6	n.a.	Dr Ehrenstorfer	1	pos	5.35	40	279.0	214.0	46	25
Tramadol-d6	1109217-84-6	TRC	1	pos	6.72	40	270.2	64.0	61	43
O-desmethyl-Tramadol-d6	873928-73-5	TRC	1	pos	5.85	40	256.2	64.0	41	84
N,O-didesmethyl-Tramadol-d3	1261398-22-4	TRC	1	pos	5.9	40	239.1	47.0	47	20
N-desmethyl-Tramadol-d3	1261398-09-7	TRC	1	pos	6.22	40	253.2	47.0	45	20
Trimethorprim-d3	738-70-5	Sigma Aldrich	1	pos	6	40	294.0	123.1	90	33
Venlafaxine-d6	1020720-02-8	TRC	1	pos	7.46	40	284.2	58.0	41	43
N,O-didesmethyl-Venlafaxine-d3	1189468-67-4	TRC	1	pos	6.22	40	253.2	47.0	48	47
N-desmethyl-Venlafaxine-d3	1189980-40-2	TRC	1	pos	7.31	40	267.2	47.0	44	38
O-desmethyl-Venlafaxine-d6	1062605-69-9	TRC	1	pos	6.33	40	270.2	58.0	56	43
Methyl-d3-triphenylphosphonium bromide	1787-44-6	Sigma Aldrich	1	pos	8.08	40	280.1	183.1	100	68
Tetra-d28-propylammonium bromide	284474-84-6	Sigma Aldrich	1	pos	6.41	40	214.4	166.4	80	31
Emtricitabine-13C,15N2	1217820-69-3	TRC	1	pos	5.39	40	251.0	133.0	56	20
Candesartan d5	1189650-58-5	TRC	2	pos	10.45	40	446.2	268.0	66	17
Carbamazepine-15N13C	1173022-00-8	Campro Scientific	2	pos	9.53	40	239.0	192.0	61	29
10-Hydroxy-Carbamazepine-d3	n.a.	TLC	2	pos	7.61	40	258.2	240.1	26	15
Diatrizoic acid-d6	1189668-69-6	TRC	2	pos	5.01	60	620.9	367.1	92	25
Diphenhydramine-d6	1189986-72-8	TRC	2	pos	7.57	40	262.2	152.0	30	55
N-desmethyl-Diphenhydramine-d3	1794759-12-8	TRC	2	pos	7.42	40	245.2	167.0	30	20
Epoxiconazole-d4	n.a.	TRC	2	pos	12.81	40	334.1	125.3	60	35
Fluconazole-d4	1124197-58-5	TRC	2	pos	6.99	40	311.1	223.1	70	25
Irgarol-d9	1189926-01-9	Dr Ehrenstorfer	2	pos	12.62	40	263.0	199.0	40	29

Name	CAS	Supplier								
Metamitron-d5	n.a.	HPC	2	pos	7.23	40	208.1	180.1	60	23
Metazachlor-d6	1246816-51-2	TRC	2	pos	11.52	40	284.1	140.1	45	30
Metolachlor-d6	1219803-97-0	TRC	2	pos	13.71	40	290.1	258.1	45	20
Metoprolol-d7	n.a.	Campro Scientific	2	pos	6.11	40	275.0	123.0	80	27
Hydroxy-Metoprolol-d5	1189934-03-9	TRC	2	pos	5.26	40	289.2	121.1	80	28
O-desmethyl-Metoprolol-d5	1189981-81-4	TRC	2	pos	5.3	40	259.2	182.2	70	28
Pregabalin-d4	1276197-54-6	c/d/n isotopes inc	2	pos	5.27	40	164.1	146.1	61	17
Propiconazole-d5	n.a.	Dr Ehrenstorfer	2	pos	13.84	40	347.2	159.1	80	34
Ramipril-d5	1132661-86-9	TRC	2	pos	8.98	80	422.3	239.2	65	35
Sulfamethoxazole-d4	1020719-86-1	TRC	2	pos	7.92	40	258.0	160.0	66	23
N-Acetyl-Sulfamethoxazole-d4	1215530-54-3	TRC	2	pos	8.08	40	300.0	202.0	81	23
Sulpride-d3	124020-27-5	TRC	2	pos	5.16	40	345.4	112.1	80	36
Tebuconazole-d6	n.a.	Dr Ehrenstorfer	2	pos	13.16	40	314.3	72.1	84	59
Telmisartan-d3	1189889-44-8	TRC	2	pos	10.47	40	518.3	500.2	171	47
Terbutryn-d5	1219804-47-3	Dr Ehrenstorfer	2	pos	12.49	40	247.0	191.0	50	25
Terbutylazine-d5	222986-60-9	Dr Ehrenstorfer	2	pos	12.31	40	235.2	104.0	61	45
Tetraglyme-d6	1216628-15-7	TRC	2	pos	6.42	40	229.1	106.1	60	15
Torsemide-d7	1189375-06-1	TRC	2	pos	8.08	40	356.1	264.1	60	25
Hydroxy Torasemide-d7	1329613-35-5	TRC	2	pos	6.1	40	372.1	306.1	55	20
Valsartan-d3	1331908-02-1	TRC	2	pos	11.96	40	439.2	207.1	111	35
Valsartanic acid-d4	n.a.	TRC	2	pos	8.43	40	271.1	210.1	80	17
Acesulfame-d4	1623054-53-4	TRC	2	neg	4.75	70	166.0	86.0	-50	-22
Bezafibrate-d4	1189452-53-6	TRC	2	neg	11.41	40	364.1	158.0	-65	-38
Bicalutamide-d4	1185035-71-5	TRC	2	neg	11.98	40	433.1	185.0	-55	-50
Diuron-d6	1007536-67-5	Dr Ehrenstorfer	2	neg	10.91	40	237.0	186.0	-70	-25
Furosemide-d5	1189482-35-6	TRC	2	neg	9.55	40	334.0	206.0	-125	-34
Hydrochlorothiazide-13C,d2	1190006-03-1	TRC	2	neg	6.02	40	299.0	269.9	-130	-28
Chlorothiazide-13C,15N2	1189440-79-6	TRC	2	neg	5.78	40	297.0	216.0	-90	-40
Ibuprofen-d3	121662-14-4	c/d/n isotopes inc	2	neg	13.35	40	208.1	164.0	-55	-10
Ibuprofen-2-OH-d6	1217055-71-4	TRC	2	neg	8.74	40	227.1	183.0	-35	-13
Ibuprofen Carboxylic acid d3	1216505-29-1	TRC	2	neg	8.89	40	238.0	194.0	-28	-10
Irbesartan-d7	1329496-43-6	Santa Cruz Biotechnology	2	neg	11.11	40	434.2	200.2	-70	-35
Mecoprop-d3	n.a.	Dr Ehrenstorfer	2	neg	11.72	40	216.0	144.0	-40	-25
Naproxen-d3	n.a.	Dr Ehrenstorfer	2	neg	11.3	40	232.0	173.0	-30	-20
Olmesartan-d6	1420880-41-6	TRC	2	neg	7.79	40	451.2	154.1	-45	-50
Oxypurinol-13C 15N2	1217036-71-9	TRC	2	neg	3.02	80	154.0	111.0	-70	-24
Saccharine-d4	1189466-17-8	TRC	2	neg	5.67	40	186.0	42.0	-75	-52
Sucralose-d6	1459161-55-7	TRC	2	neg	6.28	40	401.0	35.0	-55	-38
Triclocarban-d4	1219799-29-7	c/d/n isotopes inc	2	neg	14.95	40	317.0	160.0	-80	-18
Triclosan-13C12	n.a.	Cambridge Isotopes	2	neg	15.07	40	299.0	35.0	-45	-26
Xipamide-d6	1330262-09-3	TRC	2	neg	11.28	40	359.1	78.0	-80	-55

A1.2-A: Number of contemporary transitions and actual target scan time in the methods

Data provided for a theoretical target scan time of 0.3 s in Method 1 and 0.2 s in Method 2
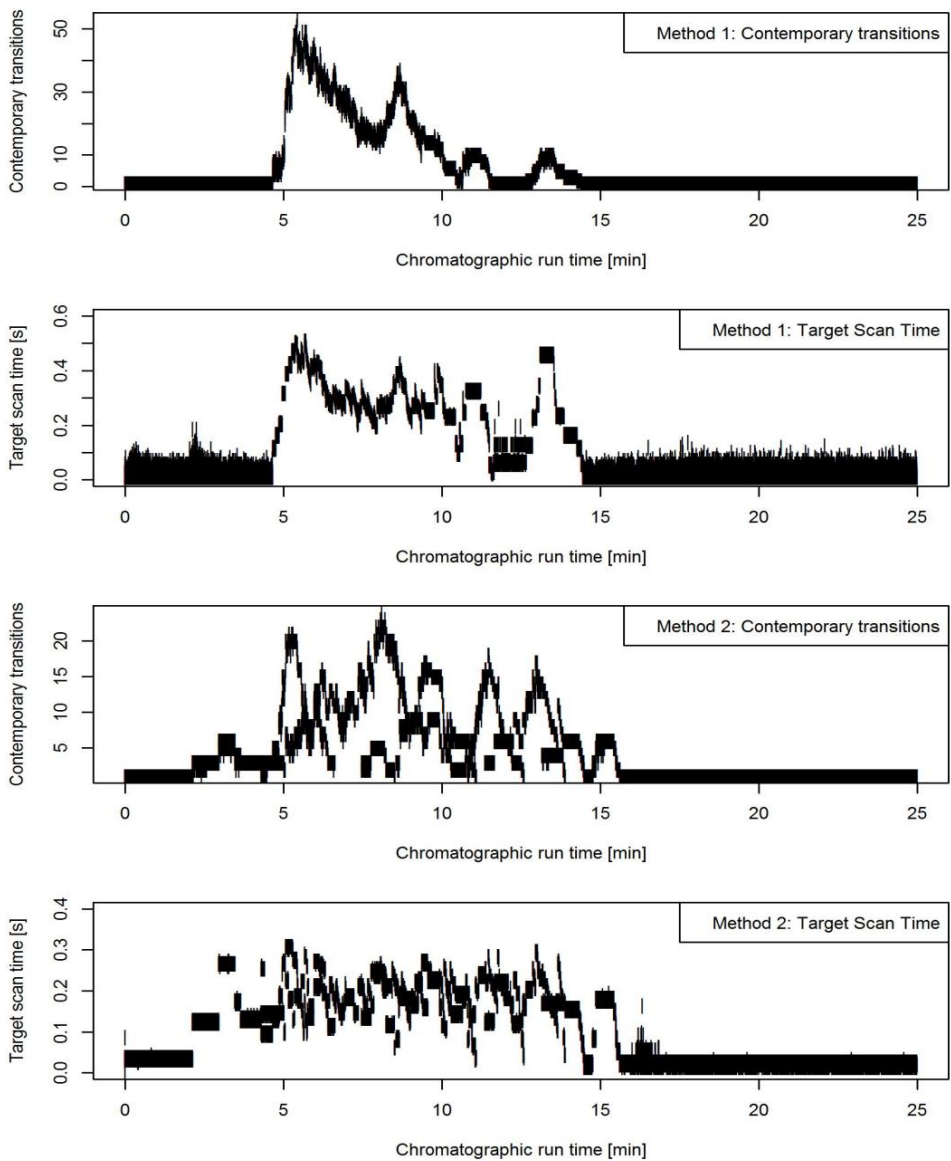
A1.2-B: Comparison of chromatograms at different target scan times
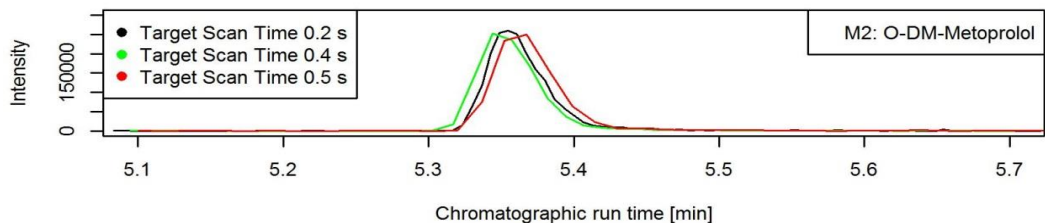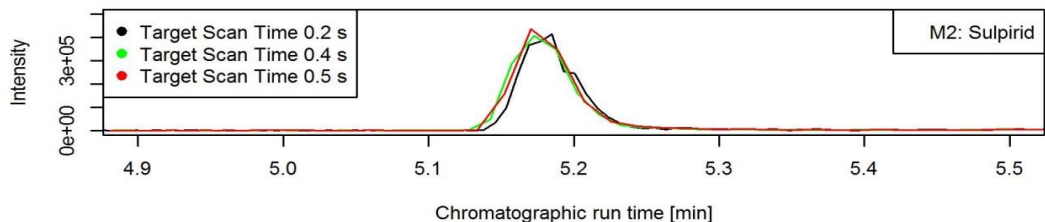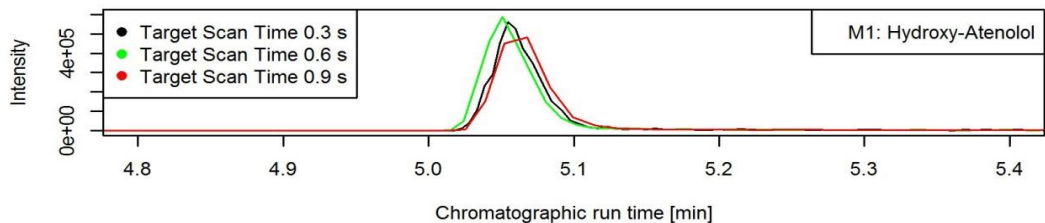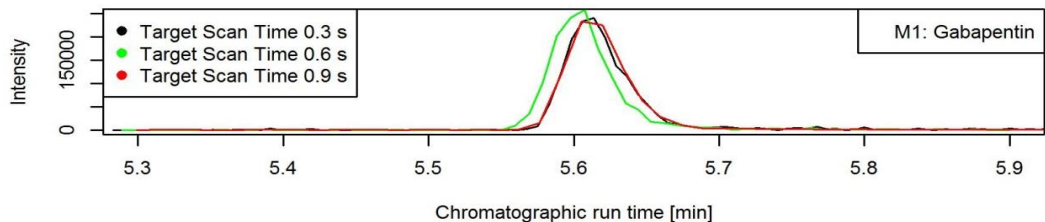
A1.3: Validation, results for working range, LOQ and precision

Abbreviations: M = Method, WR = Working range, LOQ = Limit of Quantification, BF = Bank filtrate, SW = Surface water, Inf = Influent, Eff = Effluent

Substance	M	ESI	IS	WR ng/L	R^2	LOQ BF	LOQ SW	LOQ Inf	LOQ Eff	Intra-day [n=3] 100 ng/L	Intra-day [n=3] 1000 ng/L	Inter-day [n=6] 100 ng/L	Inter-day [n=6] 1000 ng/L
Tramadol	1	pos	Tramadol-d6	5 - 15000	0.9995	2	15	15	15	5.4	2.7	5.4	8.2
O-DM-Tramadol	1	pos	O-DM-Tramadol-d6	1 - 5000	0.9996	10	10	30	10	1.4	1.7	4.1	4.6
N-DM-Tramadol	1	pos	N-DM-Tramadol-d3	1 - 5000	0.9996	10	10	10	20	0.5	1.9	7.0	5.6
N,O-DDM-Tramadol	1	pos	N,O-DD-Tramadol-d3	2 - 15000	0.9998	15	30	20	15	3.0	2.7	7.6	7.2
Tramadol-N-oxide	1	pos	Tramadol-d6	0.5 - 15000	0.9998	15	10	10	10	0.4	0.7	5.1	6.8
Primidone	1	pos	Primidone-d5	5 - 15000	0.9995	20	25	30	35	3.8	3.2	5.7	4.9
Phenytoin	2	neg	Olmesartan-d6	0.5 - 15000	0.9997	1	5	5	5	1.0	4.2	9.4	7.6
Carbamazepine (CBZ)	2	pos	CBZ-15N13C	0.5 - 2000	0.9905	1	1	5	5	0.7	1.0	10.1	1.9
2-Hydroxy-CBZ	2	pos	CBZ-15N13C	0.5 - 15000	0.9997	5	15	25	25	1.3	3.3	12.2	11.6
3-Hydroxy-CBZ	2	pos	CBZ-15N13C	1 - 5000	0.9992	2	5	10	10	2.5	3.9	12.8	16.9
10-Hydroxy-CBZ	2	pos	10-OH-CBZ-d3	1 - 5000	0.9996	10	10	30	30	1.1	0.4	4.5	3.2
10,11-Dihydro-10,11-dihydroxy-CBZ	2	pos	CBZ-15N13C	2 - 15000	0.9991	10	10	30	30	1.4	4.8	12.6	9.0
9-Carboxylic acid-Acridine	2	pos	CBZ-15N13C	1 - 7500	0.9982	10	10	10	10	17.5	1.3	42.9	40.8
Acridone	2	pos	CBZ-15N13C	0.5 - 2000	0.9993	1	1	5	5	1.5	2.2	11.3	16.9
Lamotrigine	1	pos	Lamotrigine-13C, 15N4	2 - 5000	0.9993	35	40	25	35	8.7	3.8	7.7	4.2
2-N-methyl-Lamotrigine	1	pos	Lamotrigine-13C, 15N4	2 - 5000	0.9994	20	20	20	10	2.5	4.6	14.7	10.9
Gabapentin	1	pos	Gabapentin-d10	2 - 15000	0.9991	20	30	30	30	1.4	2.3	4.2	1.8
Gabapentin Lactam	1	pos	Gabapentin-Lactam-d6	2 - 2000	0.9958	10	20	20	20	3.6	1.0	6.2	2.6
Levetiracetam	1	pos	Levetiracetam-d6	5 - 15000	0.9996	15	100	150	30	5.6	5.3	6.5	4.3
Levetiracetam acid	1	pos	Levetiracetam-d6	5 - 2000	0.9925	100	100	150	150	6.1	7.5	7.9	12.5
Pregabalin	2	pos	Pregabalin-d4	2 - 15000	0.9984	20	35	60	90	6.8	7.0	12.4	19.0
Sulpiride	2	pos	Sulpride-d3	0.1 - 5000	0.9986	5	10	10	10	1.3	0.6	3.0	1.6
Amisulpride	1	pos	Amisulprid d5	1 - 2000	0.9990	5	5	5	5	2.3	2.6	5.3	6.3
O-desmethyl-Amisulpride	1	pos	O-DM-Amisulprid-d5	0.5 - 2000	0.9966	5	10	10	10	3.8	0.9	5.7	6.8
Oxazepam	1	pos	Oxazepam-d5	0.5 - 15000	0.9923	5	10	5	10	0.6	0.4	21.8	20.9
Citalopram	1	pos	Citalopram-d4	0.5 - 5000	0.9992	10	10	15	15	3.5	2.2	3.7	2.7
Desmethyl-Citalopram	1	pos	Citalopram-d4	1 - 5000	0.9997	1	5	5	5	4.7	1.3	3.5	4.0
Didesmethyl-Citalopram	1	pos	Didemethyl Citalopram-d6	2 - 15000	0.9999	25	30	25	25	4.1	1.9	3.8	3.9
Citalopram-N-oxide	1	pos	Citalopram-d4	0.5 - 2000	0.9991	5	5	10	5	2.2	2.2	9.3	10.7
Venlafaxine (VLX)	1	pos	Venlafaxine-d6	0.2 - 5000	0.9997	2	2	5	2	1.2	1.6	3.0	4.0
O-desmethyl-VLX	1	pos	O-DM-Venlafaxine-d6	0.5 - 5000	0.9996	10	10	10	20	9.6	1.1	9.1	3.9
N-desmethyl-VLX	1	pos	N-DM-Venlafaxine-d3	0.5 - 15000	0.9998	5	5	10	5	1.5	2.5	6.7	4.8
N.O-didesmethyl-VLX	1	pos	N,O-DM-Venlafaxine-d3	1 - 15000	0.9992	10	10	10	15	6.2	0.9	6.9	1.5
VLX-N-oxide	1	pos	Venlafaxine-d6	0.2 - 2000	0.9968	5	2	5	5	0.6	3.1	7.5	8.6
Lidocaine	1	pos	Lidocain-ethyl-d10	0.1 - 15000	0.9996	1	2	10	5	1.4	1.3	3.7	4.7
Nor-Lidocaine	1	pos	Nor-Lidocaine-d5	1 - 15000	0.9996	5	5	10	10	3.3	1.5	7.6	8.1
Flecainide	1	pos	Flecainid-d3	0.5 - 2000	0.9964	2	2	2	5	2.0	0.5	1.8	2.4
m-O-dealkylated Flecainide	1	pos	Flecainid-d3	0.5 - 2000	0.9935	5	5	10	5	0.4	0.8	14.3	13.5
Hydrochlorothiazide	2	neg	Hydrochlorothiazide-13C,d2	1 - 5000	0.9995	15	20	15	20	2.5	3.9	6.2	5.0
Chlorothiazide	2	neg	Chlorothiazide-IS	1 - 2000	0.9984	5	5	5	5	2.3	2.1	1.9	3.2
4-amino-6-chloro-1,3-benzenedisulfonamide	2	neg	Hydrochlorothiazine-13C,d2	0.5 - 2000	0.9970	10	20	20	60	1.9	2.2	7.9	9.0

Compound			Internal Standard	Range	R²								
Xipamide	2	neg	Xipamide-d6	20 - 15000	0.9951	20	20	2	5	3.4	0.6	27.4	20.9
Furosemide	2	neg	Furosemide-d5	0.5 - 15000	0.9994	10	20	15	20	1.4	1.7	6.6	4.1
Torsemide	2	pos	Torasemide-d7	0.5 - 5000	0.9993	5	2	5	5	0.3	0.8	8.3	2.0
Hydroxy-Torsemide	2	pos	Hydroxy Torasemide-d7	0.1 - 5000	0.9984	2	5	5	5	1.2	2.2	4.9	2.3
Sotalol	1	pos	Sotalol-d6	1 - 15000	0.9995	45	45	30	30	8.5	5.1	7.7	2.5
Metoprolol	2	pos	Metoprolol-d7	1 - 15000	0.9997	5	5	20	15	3.4	2.9	4.0	2.1
Hydroxy-Metoprolol	2	pos	OH-Metoprolol-d5	2 - 5000	0.9998	15	25	30	50	4.0	2.9	5.6	7.7
O-desmethyl-Metoprolol	2	pos	O-DM-Metoprolol-d5	0.5 - 15000	0.9998	5	15	15	40	0.7	4.3	5.6	4.6
Atenolol	1	pos	Atenolol-d7	2 - 15000	0.9992	10	10	10	10	3.2	5.3	3.8	4.8
Atenolol acid	1	pos	Atenolol-d7	2 - 5000	0.9995	15	15	40	40	7.1	2.2	23.2	10.2
Hydroxy-Atenolol	1	pos	Hydroxy-Atenolol-d7	1 - 5000	0.9998	5	5	5	10	4.4	0.3	6.1	4.8
Enalapril	1	pos	Enalapril-d5	1 - 5000	0.9979	5	10	25	10	0.8	1.2	6.2	4.5
Enalaprilat	1	pos	Enalaprilat-d5	5 - 15000	0.9996	20	30	25	35	1.0	0.5	2.2	3.2
Ramipril	2	pos	Ramipril-d5	0.5 - 5000	0.9991	5	10	10	10	5.0	0.5	4.1	3.9
Ramiprilat	2	pos	Ramipril-d5	5 - 5000	0.9992	75	80	100	100	3.8	3.2	19.5	18.8
Valsartan	2	pos	Valsartan-d3	0.5 - 5000	0.9985	5	5	10	10	1.9	2.2	2.1	2.2
Valsartan acid	2	pos	Valsartanic acid-d4	1 - 15000	0.9987	5	10	15	10	1.8	3.7	7.3	5.3
Irbesartan	2	neg	Irbesartan-d7	0.5 - 5000	0.9994	5	5	10	10	1.7	1.6	2.1	1.6
Candesartan	2	pos	Candesartan d5	0.5 - 15000	0.9991	2	2	5	5	0.1	1.4	3.5	6.4
Telmisartan	2	pos	Telmisartan-d3	5 - 2000	0.9975	5	2	10	10	2.1	1.0	4.6	1.9
Olmesartan	2	neg	Olmesartan-d6	5 - 15000	0.9992	20	15	10	20	1.9	1.6	4.7	5.5
Aliksiren	1	pos	Aliskiren d6	2 - 5000	0.9985	20	10	10	15	2.1	3.1	3.8	6.2
Bezafibrate	2	neg	Bezafibrat-d4	1 - 5000	0.9998	2	5	5	5	2.6	2.2	6.2	1.7
3-[(4-chlorobenzoyl)amino]-propanoic acid	2	neg	Bezafibrat-d4	1 - 5000	0.9997	5	10	10	20	5.5	5.8	11.8	3.3
Climbazole	1	pos	Climbazol-d4	0.5 - 2000	0.9990	5	10	10	10	1.3	0.1	4.0	3.7
Climbazole-TP	1	pos	Climbazol-d4	1 - 5000	0.9997	20	10	25	10	1.1	1.1	6.6	7.1
Trimethoprim	1	pos	Trimethorpim-d3	0.5 - 15000	0.9978	5	10	10	10	0.7	0.8	4.1	5.9
3-desmethyl-TMP	1	pos	Trimethorpim-d3	1 - 5000	0.9945	2	5	5	1	3.4	1.2	10.5	7.1
5-(2,4,5-Trimethoxy)-2,4-pyrimidinediamnine	1	pos	Trimethorpim-d3	1 - 2000	0.9978	35	25	15	25	0.8	3.5	13.8	9.2
Sulfamethoxazole (SMX)	2	pos	Sulfamethoxazole-d4	0.5 - 15000	0.9995	10	15	20	35	2.6	2.6	3.3	6.5
Acetyl-SMX	2	pos	N-Acetyl-SMX-d4	2 - 5000	0.9976	20	25	80	50	2.2	8.1	4.8	10.8
Clarithromycin	1	pos	Clarithromycin-N-methyl-d3	0.2 - 1000	0.9998	0.5	5	10	2	2.9	1.5	18.9	8.1
Fluconazole	2	pos	Fluconazole-d4	0.5 - 5000	0.9998	5	5	10	15	1.0	0.3	3.8	1.5
Aciclovir	1	pos	Acyclovir-d4	2 - 5000	0.9993	25	15	20	25	8.0	4.9	8.1	3.7
Carboxy-Aciclovir	1	pos	Acyclovir-d4	1 - 5000	0.9988	30	20	20	25	7.2	8.2	2.2	6.1
Emtricitabine	1	pos	Emtricitabine-d3	1 - 5000	0.9993	20	80	50	50	4.6	4.8	12.0	4.0
Emtricitabine carboxylate	1	pos	Emtricitabine-d3	5 - 5000	0.9969	10	10	50	25	6.1	3.7	9.9	9.8
Emtricitabine-S-oxide	1	pos	Emtricitabine-d3	10 - 5000	0.9995	20	20	80	40	3.7	4.6	7.6	5.4
Ranitidine	1	pos	Ranitidine-d6	2 - 5000	0.9970	10	10	15	20	2.4	0.7	23.2	16.8
Ranitidine-N-oxide	1	pos	Ranitidine-d6	1 - 15000	0.9999	30	30	10	10	4.4	0.3	3.1	10.6
Desmethyl-Ranitidine	1	pos	Ranitidine-d6	2 - 15000	0.9997	10	5	0.5	5	4.6	3.3	10.6	5.8
Sitagliptin	1	pos	Sitagliptin-d4	1 - 15000	0.9996	10	10	10	10	0.6	2.7	3.4	2.4
Clopidogrel	1	pos	Clopidogrel-d4	0.1 - 2000	0.9978	0.5	0.5	0.5	0.5	0.4	0.1	2.4	14.6
Clopidogrel acid	1	pos	Clopidogrel d4 Carboxylic acid	0.5 - 2000	0.9972	5	5	5	10	2.4	0.7	3.5	3.3
Bicalutamide	2	neg	Bicalutamide-d4	0.1 - 2000	0.9996	0.5	1	1	1	0.6	0.6	1.2	2.3
Diphenhydramine	2	pos	Diphenhydramine-d6	1 - 5000	0.9994	5	5	10	10	1.1	2.6	3.5	4.0
N-desmethyl-Diphenhydramine	2	pos	N-DM-Diphenhydramine-d3	0.1 - 5000	0.9995	5	5	10	10	0.7	1.2	2.0	2.3
Diphenhydramine-N-oxide	2	pos	Diphenhydramine-d6	1 - 5000	0.9969	5	5	2	5	3.7	2.2	6.5	6.7
Cetirizine	1	pos	Cetirizine-d8	0.5 - 15000	0.9995	5	10	10	10	3.0	1.9	3.2	2.6

A1.3

Compound													
Fexofenadine	1	pos	Fexofenadin-d6	0.5 - 2000	0.9992	5	2	10	5	0.3	0.4	2.6	2.9
Diatrizoic acid	2	pos	Diatrizoat-d6	5 - 10000	0.9987	15	15	45	50	3.9	0.7	5.3	5.1
Iopamidol	1	pos	Iopamidol-d8	5 - 10000	0.9997	50	50	50	50	5.9	4.2	8.6	4.1
Iopromide	1	pos	Iopromide-d3	10 - 20000	0.9996	50	50	50	50	9.3	1.0	6.7	7.1
Iopromide-TP-643	1	pos	Iopromide-d3	10 - 20000	0.9985	100	100	100	100	15.0	2.1	17.9	12.4
Iopromide-TP-701A	1	pos	Iopromide-d3	10 - 20000	0.9997	50	90	100	80	8.3	2.3	12.8	13.3
Iopromide-TP-701B	1	pos	Iopromide-d3	10 - 20000	0.9999	50	50	100	60	11.7	2.6	9.6	8.7
Iopromide-TP-731B	1	pos	Iopromide-d3	10 - 20000	0.9997	50	50	50	60	12.4	0.8	11.3	7.9
Iopromide-TP-819	1	pos	Iopromide-d3	50 - 20000	0.9982	200	200	200	200	9.8	1.3	10.7	5.3
Iopromide-TP-729A	1	pos	Iopromide-d3	20 - 20000	0.9993	80	200	200	200	16.0	1.3	16.7	13.6
Iopromide-TP-759	1	pos	Iopromide-d3	20 - 20000	0.9997	200	200	200	200	9.7	7.9	18.9	11.7
Iomeprol	1	pos	Iomeprol-d3	20 - 10000	0.9965	50	50	50	50	2.4	3.6	19.0	4.7
Diclofenac (DCF)	1	pos	Diclofenac-d4	5 - 5000	0.9993	2	2	5	2	1.3	0.1		7.8
4-Hydroxy-DCF	1	pos	Diclofenac-d4	0.5 - 2000	0.9857	2	5	2	5	2.9	1.6	3.4	7.3
Carboxy-DCF	1	pos	Diclofenac-d4	0.5 - 2000	0.9997	0.5	2	1	1	1.1	0.9	6.2	2.0
DCF Lactam	1	pos	Diclofenac-d4	0.5 - 2000	0.9948	2	2	2	2	1.9	1.4	3.2	6.2
Ibuprofen (IBU)	2	neg	Ibuprofen-d3	10 - 15000	0.9997	20	20	50	25	3.6	1.9	2.2	2.7
2-Hydroxy-IBU	2	neg	Ibuprofen-2-OH-d6	20 - 2000	0.9975	60	60	100	100	10.5	4.2	17.7	15.7
Carboxy-IBU	2	neg	Ibuprofen Carboxylic acid d3	5 - 15000	0.9994	15	10	30	20	0.3	1.0	5.0	8.3
Naproxen	2	neg	Naproxen-d3	5 - 15000	0.9993	15	20	45	70	3.7	8.7	8.4	6.8
O-desmethyl-Naproxen	2	neg	Naproxen-d3	1 - 5000	0.9990	10	15	20	25	2.3	4.7	10.1	21.7
Oxypurinol	2	neg	Oxypurinol-13C 15N2	1 - 20000	0.9996	150	150	150	150	2.3	3.3	4.5	6.1
Carbendazim	1	pos	Carbendazim-d4	0.5 - 2000	0.9997	2	2	5	5	1.4	1.2	3.5	3.6
Epoxiconazole	2	pos	Epoxiconazol-d4	0.2 - 5000	0.9998	5	5	10	2	0.7	1.3	3.6	0.3
Propiconazole	2	pos	Propiconazole-d5	0.2 - 15000	0.9998	5	5	5	5	0.4	0.6	5.0	2.4
Tebuconazole	2	pos	Tebuconazole-d6	0.5 - 15000	0.9997	1	2	2	2	1.0	0.7	3.2	2.0
DEET	1	pos	DEET-d7	1 - 2000	0.9981	0.5	1	2	1	0.2	0.7	3.0	3.4
DEET carboxylic acid	1	pos	DEET-d7	1 - 2000	0.9994	5	5	10	10	0.7	0.8	6.3	8.5
Hydroxy-DEET	1	pos	DEET-d7	0.1 - 2000	0.9979	5	5	5	5	1.7	2.5	6.7	5.9
N-ethyl-m-toluamide	1	pos	DEET-d7	1 - 2000	0.9980	5	5	2	2	1.4	1.6	8.5	10.2
Imidacloprid	1	pos	Imidacloprid-d4	1 - 15000	0.9997	25	15	15	25	1.6	1.8	6.1	4.0
Diuron	2	neg	Diuron-d6	0.2 - 5000	0.9995	2	2	5	10	1.3	2.1	1.6	2.6
Didemethyldiuron (DCPU)	2	neg	Diuron-d6	1 - 5000	0.9991	10	15	15	10	4.2	1.7	7.5	5.8
N-Demethoxylinuron (DCPMU)	2	neg	Diuron-d6	0.5 - 2000	0.9977	0.5	0.5	1	2	3.0	3.6	5.7	7.3
Isoproturon	1	pos	Isoproturon-d6	0.5 - 2000	0.9988	0.5	1	1	1	0.9	0.7	3.6	3.0
Mecoprop	2	neg	Mecoprop-d3	1 - 2000	0.9951	10	20	5	10	1.8	1.4	1.2	0.8
Metamitron	2	pos	Metamitron-d5	5 - 15000	0.9996	15	30	50	50	5.7	1.4	5.7	5.8
Desamino-Metamitron	2	pos	Metamitron-d5	1 - 15000	0.9995	10	15	15	35	6.3	1.6	27.2	11.5
Metazachlor	2	pos	Metazachlor-d6	0.5 - 15000	0.9995	0.5	0.5	2	2	0.3	1.1	3.0	2.9
Metolachlor	2	pos	Metolachlor-d6	0.5 - 2000	0.9996	1	1	2	2	1.2	0.8	3.4	2.3
Metolachlor ESA	2	pos	Metolachlor-d6	0.5 - 15000	0.9997	5	5	15	10	3.0	2.6	10.0	7.8
Metolachlor OA	2	pos	Metolachlor-d6	1 - 5000	0.9997	10	10	20	15	4.9	0.7	11.5	11.4
Terbutryn	2	pos	Terbutryn-d5	1 - 2000	0.9992	0.5	1	1	1	0.4	0.7	4.0	2.5
Terbuthylazine	2	pos	Terbutylazine-d5	0.2 - 5000	0.9991	2	2	5	2	0.3	1.7	8.2	6.8
Terbuthylazine-2-Hydroxy	2	pos	Terbutylazine-d5	0.5 - 5000	0.9965	2	2	5	10	11.2	16.8	9.8	7.7
Irgarol	2	pos	Irgarol-d9	0.5 - 2000	0.9981	1	1	5	2	1.4	1.2	4.5	3.3
Benzotriazole	1	pos	Benzotriazol-d4	5 - 2000	0.9972	90	75	100	100	1.5	5.4	5.7	3.4
1-Hydroxy-Benzotriazole	1	pos	Benzotriazol-d4	5 - 5000	0.9997	35	40	70	100	3.3	1.1	4.8	5.4
Tetraglyme	2	pos	Tetraglyme-d6	2 - 5000	0.9990	1	10	10	25	3.3	2.8	7.5	2.3

A1.3

Compound			Internal standard	Range	R^2								
Ethyltriphenylphosphonium	1	pos	Methyl-d3-triphenylphosphonium bromide	1 - 5000	0.9994	5	2	2	1	3.0	1.5	2.9	2.8
Methyltriphenylphosphonium	1	pos	Methyl-d3-triphenylphosphonium bromide	0.5 - 2000	0.9969	2	2	2	1	1.4	1.8	1.7	1.7
Tetrabutyltriphenylphosphonium	1	pos	Methyl-d3-triphenylphosphonium bromide	1 - 5000	0.9995	0.5	0.5	0.5	1	1.7	1.3	3.4	6.9
(Methoxymethyl)triphenylphosphonium	1	pos	Methyl-d3-triphenylphosphonium bromide	1 - 5000	0.9997	10	10	5	15	3.7	0.5	5.4	2.3
Tetrabutylammonium	1	pos	Tetra-d28-propylammonium bromide a	5 - 5000	0.9974	0.5	1	0.5	2	5.6	1.9	11.5	5.7
Tetrapropylammonium	1	pos	Tetra-d28-propylammonium bromide a	1 - 2000	0.9991	2	5	2	2	6.0	3.0	3.3	4.6
Caffeine	1	pos	Caffeine 13C3	20 - 5000	0.9976	2	40	40	45	7.2	1.0	12.1	3.7
Triclosan	2	neg	Triclosan-13C12	0.5 - 15000	0.9998	10	10	5	15	1.4	1.2	4.4	3.3
Triclocarban	2	neg	Triclocarban-d4	10 - 5000	0.9990	1	0.5	2	1	2.9	1.0	4.1	2.3
Carbanilide	2	neg	Triclocarban-d4	10 - 2000	0.9961	20	20	10	1	2.3	3.8	17.2	16.5
Acesulfame	2	neg	Acesulfam-d4	2 - 100000	0.9998	10	5	10	10	0.7	4.6	5.0	4.4
Saccharine	2	neg	Saccharine-d4	5 - 15000	0.9999	5	15	45	15	0.5	1.2	6.8	6.6
Sucralose	2	neg	Sucralose-d6	2 - 15000	0.9999	60	100	50	100	5.9	1.7	5.9	2.1
Denatonium	1	pos	Benzotriazol-d4	0.5 - 2000	0.9990	0.5	2	5	2	1.6	2.7	26.4	24.6
Tolylbiguanide	1	pos	Tramadol-d6	1 - 1000	0.9936	5	5	5	5	2.0	1.1	5.7	12.3

A1.4: Validation, results for absolute and relative recovery

Abbreviations: BF = Bank filtrate, SW = Surface water, Inf = Influent, Eff = Effluent

Substance	Abs. Recovery [%] Spike = 100 ng/L				Abs. Recovery [%] Spike = 1000 ng/L				Rel. Recovery [%] Spike = 100 ng/L				Rel. Recovery [%] Spike = 1000 ng/L			
	BF	SW	Inf	Eff	BF	SW	Inf	Eff	BF	SW	Inf	Eff	BF	SW	Inf	Eff
Tramadol	78 ± 8	110 ± 45	2)	89 ± 49	82 ± 4	96 ± 28	59 ± 21	68 ± 11	94 ± 7	93 ± 2	111 ± 12	97 ± 37	97 ± 7	98 ± 16	108 ± 8	106 ± 8
O-DM-Tramadol	53 ± 2	78 ± 25	1)	1)	62 ± 4	79 ± 29	47 ± 17	57 ± 9	106 ± 7	98 ± 20	1)	1)	107 ± 10	104 ± 18	142 ± 5	129 ± 4
N-DM-Tramadol	79 ± 4	83 ± 11	1)	1)	83 ± 5	87 ± 20	50 ± 17	59 ± 11	112 ± 9	101 ± 20	1)	1)	110 ± 5	104 ± 22	135 ± 16	124 ± 4
N,O-DDM-Tramadol	55 ± 6	76 ± 25	1)	1)	65 ± 1	72 ± 9	59 ± 20	56 ± 10	104 ± 12	101 ± 28	1)	1)	105 ± 12	108 ± 41	129 ± 29	116 ± 21
Tramadol-N-oxide	79 ± 1	95 ± 38	71 ± 23	71 ± 22	83 ± 3	96 ± 29	63 ± 22	74 ± 9	100 ± 4	109 ± 10	118 ± 5	100 ± 16	99 ± 11	106 ± 5	115 ± 6	107 ± 11
Primidone	66 ± 8	81 ± 20	70 ± 37	49 ± 27	73 ± 1	76 ± 14	64 ± 21	55 ± 6	90 ± 9	116 ± 56	110 ± 32	94 ± 30	100 ± 6	99 ± 7	115 ± 4	108 ± 15
Phenytoin	85 ± 17	94 ± 42	64 ± 18	49 ± 14	85 ± 11	104 ± 44	70 ± 20	53 ± 14	85 ± 10	80 ± 6	105 ± 17	90 ± 10	81 ± 4	78 ± 4	106 ± 15	90 ± 13
Carbamazepine (CBZ)	71 ± 14	75 ± 28	1)	1)	79 ± 3	93 ± 18	31 ± 11	30 ± 17	93 ± 16	101 ± 12	150 ± 20	130 ± 60	95 ± 6	101 ± 13	140 ± 11	132 ± 6
2-Hydroxy-CBZ	100 ± 7	142 ± 75	42 ± 14	56 ± 7	102 ± 9	148 ± 85	45 ± 9	46 ± 7	113 ± 8	117 ± 45	152 ± 6	119 ± 22	120 ± 10	107 ± 29	144 ± 16	124 ± 13
3-Hydroxy-CBZ	87 ± 3	102 ± 39	35 ± 17	27 ± 21	89 ± 6	110 ± 33	43 ± 10	38 ± 6	113 ± 10	118 ± 27	138 ± 10	93 ± 22	98 ± 5	92 ± 22	119 ± 8	94 ± 17
10-Hydroxy-CBZ	93 ± 6	103 ± 21	2)	1)	94 ± 8	116 ± 42	40 ± 10	33 ± 9	100 ± 5	108 ± 35	120 ± 34	1)	99 ± 5	96 ± 7	117 ± 11	111 ± 8
10,11-Dihydro-10,11-dihydroxy-CBZ	89 ± 21	169 ± 71	1)	1)	99 ± 11	158 ± 78	40 ± 14	1)	89 ± 25	112 ± 76	1)	1)	104 ± 14	112 ± 50	147 ± 20	1)
9-Carboxylic acid-Acridine	54 ± 25	125 ± 96	51 ± 29	1)	71 ± 21	83 ± 65	87 ± 34	66 ± 24	87 ± 38	94 ± 24	126 ± 9	1)	86 ± 21	91 ± 19	121 ± 24	84 ± 14
Acridone	80 ± 4	93 ± 34	38 ± 17	38 ± 8	85 ± 12	109 ± 43	48 ± 17	48 ± 6	97 ± 8	96 ± 23	140 ± 19	114 ± 13	97 ± 7	91 ± 17	135 ± 9	122 ± 24
Lamotrigine	61 ± 3	53 ± 11	1)	1)	75 ± 1	65 ± 6	45 ± 24	37 ± 23	96 ± 10	71 ± 34	1)	1)	97 ± 7	82 ± 40	91 ± 34	91 ± 11
2-N-methyl-Lamotrigine	77 ± 6	87 ± 22	71 ± 22	66 ± 33	83 ± 1	86 ± 16	65 ± 25	76 ± 13	94 ± 11	92 ± 41	131 ± 13	112 ± 20	103 ± 8	89 ± 39	129 ± 36	126 ± 19
Gabapentin	63 ± 25	78 ± 24	1)	1)	83 ± 12	87 ± 7	70 ± 48	48 ± 32	71 ± 51	91 ± 35	1)	1)	96 ± 23	96 ± 10	90 ± 34	107 ± 23
Gabapentin Lactam	86 ± 5	109 ± 28	100 ± 45	1)	91 ± 11	109 ± 13	90 ± 26	80 ± 13	95 ± 13	96 ± 21	116 ± 7	1)	99 ± 9	106 ± 39	117 ± 8	117 ± 11
Levetiracetam	59 ± 10	75 ± 52	1)	55 ± 17	70 ± 10	80 ± 29	63 ± 47	59 ± 1	95 ± 8	91 ± 23	1)	103 ± 23	103 ± 9	100 ± 4	114 ± 6	111 ± 9
Levetiracetam acid	90 ± 18	75 ± 27	1)	83 ± 24	89 ± 11	88 ± 4	64 ± 46	66 ± 6	122 ± 39	92 ± 24	1)	121 ± 36	121 ± 34	109 ± 29	119 ± 45	126 ± 8
Pregabalin	83 ± 10	73 ± 15	1)	1)	95 ± 4	85 ± 19	70 ± 45	41 ± 30	101 ± 30	138 ± 40	1)	1)	114 ± 3	136 ± 38	109 ± 18	98 ± 14
Sulpiride	94 ± 5	2)	59 ± 32	47 ± 26	103 ± 4	2)	67 ± 23	51 ± 20	111 ± 9	110 ± 4	144 ± 22	130 ± 24	110 ± 8	111 ± 16	133 ± 7	124 ± 10
Amisulpride	106 ± 6	121 ± 45	2)	1)	100 ± 3	105 ± 20	55 ± 23	79 ± 28	105 ± 6	102 ± 6	130 ± 14	107 ± 12	101 ± 8	101 ± 9	112 ± 6	108 ± 10
O-desmethyl-Amisulpride	72 ± 9	55 ± 9	40 ± 10	66 ± 19	88 ± 7	70 ± 13	37 ± 11	58 ± 11	81 ± 11	81 ± 12	81 ± 8	83 ± 8	80 ± 12	79 ± 12	79 ± 3	87 ± 5
Oxazepam	88 ± 9	88 ± 15	95 ± 37	91 ± 41	73 ± 6	50 ± 45	32 ± 10	28 ± 4	96 ± 7	84 ± 44	73 ± 8	69 ± 10	90 ± 4	93 ± 46	73 ± 1	72 ± 3
Citalopram	88 ± 2	80 ± 15	83 ± 48	1)	85 ± 3	74 ± 18	76 ± 19	88 ± 12	97 ± 6	104 ± 21	114 ± 11	110 ± 19	97 ± 4	98 ± 9	110 ± 4	111 ± 5
Desmethyl-Citalopram	71 ± 6	60 ± 6	70 ± 34	51 ± 29	77 ± 4	68 ± 8	77 ± 15	80 ± 8	95 ± 8	98 ± 14	110 ± 14	93 ± 14	90 ± 10	96 ± 15	109 ± 3	98 ± 8
Didesmethyl-Citalopram	71 ± 8	70 ± 8	87 ± 29	73 ± 17	80 ± 1	79 ± 7	80 ± 9	78 ± 11	99 ± 12	99 ± 9	103 ± 9	97 ± 9	104 ± 7	96 ± 10	98 ± 8	95 ± 5
Citalopram-N-oxide	78 ± 4	64 ± 14	72 ± 15	65 ± 19	77 ± 3	66 ± 19	70 ± 18	72 ± 9	105 ± 8	107 ± 10	136 ± 23	114 ± 8	91 ± 8	97 ± 6	120 ± 20	104 ± 5
Venlafaxine (VLX)	85 ± 5	128 ± 50	2)	1)	85 ± 2	103 ± 35	72 ± 27	76 ± 24	100 ± 6	105 ± 1	117 ± 3	110 ± 27	98 ± 4	102 ± 8	108 ± 9	102 ± 6
O-desmethyl-VLX	75 ± 3	97 ± 49	1)	1)	82 ± 3	93 ± 29	40 ± 19	48 ± 24	110 ± 10	102 ± 47	172 ± 13	1)	114 ± 14	110 ± 47	135 ± 26	116 ± 9
N-desmethyl-VLX	82 ± 4	91 ± 18	71 ± 30	63 ± 23	85 ± 3	89 ± 19	65 ± 25	71 ± 17	97 ± 7	101 ± 23	102 ± 4	100 ± 6	98 ± 7	94 ± 9	103 ± 11	99 ± 2
N,O-didesmethyl-VLX	68 ± 2	75 ± 8	51 ± 20	51 ± 38	83 ± 6	88 ± 21	49 ± 14	58 ± 8	108 ± 2	101 ± 30	129 ± 23	131 ± 47	112 ± 10	107 ± 27	127 ± 9	124 ± 4
VLX-N-oxide	81 ± 4	97 ± 34	72 ± 23	73 ± 18	87 ± 5	99 ± 26	70 ± 23	75 ± 17	115 ± 7	123 ± 6	138 ± 5	129 ± 12	104 ± 7	109 ± 5	125 ± 12	115 ± 6
Lidocaine	77 ± 4	90 ± 16	60 ± 24	1)	80 ± 1	87 ± 18	54 ± 16	67 ± 8	106 ± 6	100 ± 17	115 ± 15	104 ± 25	107 ± 8	102 ± 19	112 ± 4	108 ± 1
Nor-Lidocaine	75 ± 6	72 ± 6	83 ± 20	82 ± 23	83 ± 4	79 ± 5	66 ± 21	69 ± 6	98 ± 2	103 ± 13	136 ± 15	126 ± 21	99 ± 5	101 ± 9	126 ± 10	117 ± 7
Flecainide	132 ± 28	2)	141 ± 58	150 ± 60	113 ± 17	137 ± 25	140 ± 58	141 ± 14	117 ± 26	115 ± 56	157 ± 33	147 ± 14	126 ± 16	119 ± 41	153 ± 17	146 ± 12
m-O-dealkylated Flecainide	80 ± 5	75 ± 4	76 ± 27	82 ± 20	89 ± 5	83 ± 5	61 ± 22	76 ± 8	106 ± 10	108 ± 5	88 ± 14	91 ± 15	100 ± 11	100 ± 8	76 ± 26	87 ± 6
Hydrochlorothiazide	57 ± 24	98 ± 80	1)	1)	64 ± 22	74 ± 39	50 ± 14	1)	101 ± 11	95 ± 22	1)	1)	102 ± 14	106 ± 33	106 ± 8	99 ± 24
Chlorothiazide	52 ± 27	73 ± 62	54 ± 16	40 ± 17	69 ± 27	90 ± 65	72 ± 17	62 ± 20	100 ± 11	113 ± 26	118 ± 11	109 ± 6	102 ± 2	100 ± 7	113 ± 3	110 ± 5
4-amino-6-chloro-1,3-benzenedisulfonamide	52 ± 36	91 ± 30	54 ± 27	1)	68 ± 29	86 ± 59	62 ± 17	42 ± 24	84 ± 32	66 ± 30	126 ± 59	1)	96 ± 9	87 ± 39	121 ± 4	86 ± 14
Xipamide	77 ± 5	92 ± 33	64 ± 11	54 ± 20	67 ± 4	85 ± 32	56 ± 15	53 ± 16	30 ± 5	67 ± 64	107 ± 3	97 ± 13	85 ± 5	93 ± 12	106 ± 7	104 ± 6
Furosemide	93 ± 13	126 ± 82	78 ± 54	1)	89 ± 5	91 ± 21	88 ± 33	65 ± 20	102 ± 7	98 ± 12	116 ± 35	100 ± 26	96 ± 4	94 ± 12	114 ± 9	107 ± 7
Torsemide	118 ± 7	2)	74 ± 57	2)	115 ± 10	158 ± 84	79 ± 17	73 ± 16	108 ± 9	107 ± 8	121 ± 5	112 ± 7	106 ± 5	104 ± 14	120 ± 6	119 ± 5
Hydroxy-Torsemide	123 ± 10	2)	62 ± 35	60 ± 13	121 ± 13	152 ± 84	81 ± 32	74 ± 20	107 ± 6	101 ± 9	122 ± 11	113 ± 11	99 ± 6	98 ± 7	118 ± 6	113 ± 5
Sotalol	58 ± 3	78 ± 20	52 ± 23	35 ± 18	70 ± 3	80 ± 26	51 ± 16	50 ± 5	103 ± 9	106 ± 26	115 ± 25	111 ± 32	101 ± 6	101 ± 11	110 ± 7	109 ± 6
Metoprolol	80 ± 2	117 ± 61	44 ± 52	1)	88 ± 2	126 ± 72	49 ± 22	44 ± 19	107 ± 7	105 ± 10	112 ± 58	103 ± 44	107 ± 6	105 ± 16	116 ± 4	110 ± 3
Hydroxy-Metoprolol	81 ± 5	101 ± 60	58 ± 42	35 ± 12	98 ± 4	128 ± 79	65 ± 24	48 ± 16	105 ± 10	105 ± 12	125 ± 27	101 ± 21	102 ± 3	99 ± 8	113 ± 6	102 ± 6
O-desmethyl-Metoprolol	72 ± 3	94 ± 52	38 ± 9	39 ± 7	86 ± 6	114 ± 67	52 ± 18	43 ± 13	95 ± 7	100 ± 15	102 ± 11	109 ± 3	96 ± 4	92 ± 8	100 ± 3	96 ± 3
Atenolol	67 ± 2	83 ± 41	2)	2)	78 ± 6	94 ± 32	61 ± 19	54 ± 4	117 ± 14	107 ± 13	109 ± 24	101 ± 22	111 ± 1	103 ± 18	117 ± 7	102 ± 10
Atenolol acid	66 ± 3	76 ± 15	2)	2)	65 ± 4	70 ± 12	63 ± 29	60 ± 13	101 ± 16	96 ± 8	114 ± 28	139 ± 41	90 ± 4	89 ± 3	110 ± 17	108 ± 18
Hydroxy-Atenolol	82 ± 1	89 ± 39	59 ± 17	46 ± 11	86 ± 7	91 ± 33	58 ± 16	50 ± 6	101 ± 5	101 ± 7	114 ± 9	114 ± 15	101 ± 7	100 ± 5	119 ± 8	113 ± 5
Enalapril	107 ± 25	96 ± 41	93 ± 39	93 ± 24	104 ± 21	90 ± 38	85 ± 31	90 ± 17	106 ± 7	102 ± 4	97 ± 7	96 ± 7	103 ± 8	98 ± 6	91 ± 5	92 ± 3
Enalaprilat	118 ± 47	115 ± 39	116 ± 55	100 ± 29	115 ± 38	109 ± 31	88 ± 33	88 ± 5	105 ± 6	109 ± 8	101 ± 18	97 ± 14	112 ± 14	106 ± 6	110 ± 14	107 ± 5
Ramipril	97 ± 6	102 ± 43	68 ± 36	66 ± 17	102 ± 8	111 ± 15	77 ± 27	78 ± 7	100 ± 5	101 ± 9	111 ± 4	101 ± 7	103 ± 6	99 ± 13	109 ± 7	105 ± 2
Ramiprilat	108 ± 10	137 ± 36	2)	1)	107 ± 7	122 ± 67	98 ± 25	84 ± 15	111 ± 12	111 ± 53	115 ± 29	1)	113 ± 9	101 ± 38	102 ± 14	85 ± 4
Valsartan	97 ± 6	103 ± 29	1)	1)	95 ± 6	107 ± 80	1)	69 ± 23	102 ± 8	87 ± 41	1)	1)	99 ± 6	86 ± 29	93 ± 18	95 ± 5
Valsartan acid	1)	1)	51 ± 15	1)	87 ± 19	1)	60 ± 17	1)	1)	1)	101 ± 38	1)	85 ± 44	71 ± 45	105 ± 13	125 ± 68
Irbesartan	115 ± 10	155 ± 80	136 ± 51	1)	115 ± 5	157 ± 57	109 ± 41	93 ± 59	103 ± 9	98 ± 14	126 ± 24	1)	101 ± 5	96 ± 14	132 ± 5	119 ± 12
Candesartan	83 ± 62	2)	105 ± 69	1)	101 ± 7	170 ± 76	92 ± 37	84 ± 56	88 ± 32	96 ± 13	110 ± 22	1)	100 ± 7	100 ± 38	110 ± 4	103 ± 15
Telmisartan	94 ± 12	2)	61 ± 76	79 ± 18	95 ± 19	2)	50 ± 23	54 ± 21	107 ± 5	101 ± 1	115 ± 25	93 ± 30	105 ± 4	103 ± 10	111 ± 3	101 ± 10
Olmesartan	91 ± 32	2)	74 ± 50	1)	100 ± 14	123 ± 79	74 ± 15	61 ± 14	86 ± 12	90 ± 16	100 ± 17	1)	96 ± 4	96 ± 16	106 ± 8	101 ± 6
Aliskiren	2)	2)	2)	2)	2)	2)	2)	2)	101 ± 7	103 ± 19	116 ± 2	112 ± 25	100 ± 5	98 ± 8	112 ± 9	110 ± 10
Bezafibrate	89 ± 10	119 ± 63	90 ± 43	68 ± 26	97 ± 11	139 ± 71	83 ± 28	74 ± 17	102 ± 5	102 ± 8	119 ± 9	106 ± 16	98 ± 7	95 ± 12	108 ± 8	103 ± 5
3-[(4-chlorobenzoyl)amino]-propanoic acid	91 ± 17	2)	66 ± 28	55 ± 16	86 ± 12	106 ± 45	70 ± 24	51 ± 14	109 ± 17	94 ± 17	102 ± 30	97 ± 21	91 ± 6	70 ± 30	93 ± 27	70 ± 5

Climbazole	93 ± 12	110 ± 23	100 ± 39	102 ± 47	89 ± 10	101 ± 19	76 ± 26	85 ± 17	102 ± 8	107 ± 14	128 ± 14	111 ± 12	104 ± 7	102 ± 14	124 ± 5	114 ± 6
Climbazole-TP	91 ± 8	99 ± 12	85 ± 27	76 ± 25	92 ± 10	94 ± 4	81 ± 29	83 ± 15	113 ± 5	127 ± 31	141 ± 26	112 ± 30	109 ± 8	110 ± 12	135 ± 21	114 ± 5
Trimethoprim	78 ± 11	69 ± 2	50 ± 20	56 ± 24	86 ± 5	77 ± 5	46 ± 16	58 ± 13	114 ± 8	105 ± 22	107 ± 36	99 ± 22	96 ± 9	94 ± 8	90 ± 7	84 ± 7
3-desmethyl-TMP	75 ± 11	70 ± 25	48 ± 14	48 ± 13	84 ± 5	80 ± 23	51 ± 14	56 ± 5	129 ± 9	111 ± 8	133 ± 12	95 ± 7	106 ± 10	98 ± 7	119 ± 10	92 ± 11
5-(2,4,5-Trimethoxy)-2,4-pyrimidinediamnine	111 ± 11	100 ± 18	90 ± 29	93 ± 29	113 ± 8	99 ± 14	72 ± 34	84 ± 8	3)	81 ± 36	3)	3)	3)	83 ± 50	3)	3)
Sulfamethoxazole (SMX)	103 ± 13	120 ± 25	2)	1)	96 ± 7	123 ± 50	53 ± 15	41 ± 15	103 ± 6	95 ± 9	102 ± 25	115 ± 30	96 ± 4	93 ± 9	97 ± 8	92 ± 10
Acetyl-SMX	105 ± 10	116 ± 47	1)	2)	100 ± 10	122 ± 44	49 ± 16	41 ± 10	92 ± 15	63 ± 47	124 ± 41	104 ± 52	86 ± 5	59 ± 46	89 ± 23	99 ± 16
Clarithromycin	81 ± 11	84 ± 6	2)	2)	84 ± 12	85 ± 7	169 ± 58	167 ± 43	91 ± 10	98 ± 20	126 ± 20	100 ± 25	88 ± 5	88 ± 10	112 ± 9	97 ± 8
Fluconazole	103 ± 15	2)	94 ± 34	66 ± 12	110 ± 16	2)	92 ± 22	82 ± 10	97 ± 5	102 ± 19	109 ± 4	100 ± 11	98 ± 4	97 ± 8	108 ± 1	106 ± 3
Aciclovir	86 ± 10	83 ± 22	1)	58 ± 5	93 ± 6	87 ± 28	62 ± 25	59 ± 5	104 ± 10	102 ± 27	95 ± 30	99 ± 31	103 ± 5	93 ± 9	98 ± 15	94 ± 9
Carboxy-Aciclovir	69 ± 10	100 ± 22	1)	1)	83 ± 14	85 ± 16	53 ± 10	43 ± 16	73 ± 13	91 ± 23	1)	1)	88 ± 14	86 ± 31	96 ± 21	86 ± 15
Emtricitabine	84 ± 14	89 ± 41	96 ± 44	74 ± 24	97 ± 7	108 ± 43	78 ± 23	70 ± 4	112 ± 4	107 ± 29	98 ± 73	113 ± 13	108 ± 7	98 ± 17	118 ± 43	106 ± 20
Emtricitabine carboxylate	83 ± 19	116 ± 42	97 ± 23	1)	89 ± 8	100 ± 41	64 ± 21	57 ± 7	75 ± 40	91 ± 8	96 ± 69	81 ± 39	91 ± 13	90 ± 10	91 ± 33	83 ± 21
Emtricitabine-S-oxide	72 ± 11	76 ± 36	58 ± 43	53 ± 22	84 ± 5	86 ± 32	52 ± 14	52 ± 6	85 ± 29	90 ± 20	69 ± 49	84 ± 19	89 ± 11	89 ± 16	82 ± 27	82 ± 14
Ranitidine	64 ± 15	117 ± 101	2)	113 ± 47	70 ± 16	96 ± 57	103 ± 33	100 ± 14	73 ± 5	74 ± 23	115 ± 10	104 ± 25	94 ± 9	89 ± 11	145 ± 12	149 ± 14
Ranitidine-N-oxide	63 ± 14	83 ± 64	93 ± 48	75 ± 24	75 ± 8	91 ± 51	78 ± 24	72 ± 9	99 ± 22	96 ± 23	99 ± 14	88 ± 9	111 ± 14	105 ± 11	116 ± 8	112 ± 13
Desmethyl-Ranitidine	46 ± 4	59 ± 36	76 ± 45	48 ± 14	55 ± 6	67 ± 25	62 ± 31	48 ± 7	70 ± 13	77 ± 22	93 ± 29	63 ± 8	82 ± 8	88 ± 8	93 ± 14	75 ± 9
Sitagliptin	105 ± 7	104 ± 19	1)	1)	98 ± 6	102 ± 10	91 ± 54	68 ± 32	104 ± 5	97 ± 15	138 ± 9	122 ± 48	104 ± 7	106 ± 25	121 ± 13	113 ± 3
Clopidogrel	80 ± 4	93 ± 22	75 ± 17	76 ± 11	85 ± 7	93 ± 15	80 ± 24	80 ± 9	112 ± 5	114 ± 6	125 ± 2	120 ± 14	104 ± 4	104 ± 6	116 ± 7	113 ± 6
Clopidogrel acid	104 ± 15	108 ± 13	93 ± 42	2)	99 ± 16	100 ± 9	76 ± 30	71 ± 15	109 ± 8	118 ± 32	128 ± 5	106 ± 27	104 ± 5	104 ± 9	122 ± 8	117 ± 6
Bicalutamide	86 ± 7	103 ± 40	56 ± 13	59 ± 15	84 ± 8	111 ± 40	56 ± 21	59 ± 13	100 ± 5	104 ± 5	110 ± 5	107 ± 8	99 ± 5	98 ± 5	108 ± 5	105 ± 2
Diphenhydramine	89 ± 8	114 ± 50	2)	46 ± 24	93 ± 8	121 ± 50	45 ± 10	46 ± 4	102 ± 7	103 ± 14	112 ± 10	106 ± 10	100 ± 5	97 ± 11	111 ± 1	106 ± 4
N-desmethyl-Diphenhydramine	86 ± 6	106 ± 49	35 ± 12	35 ± 9	90 ± 11	117 ± 53	38 ± 9	40 ± 2	101 ± 3	101 ± 13	94 ± 1	91 ± 5	103 ± 6	97 ± 10	96 ± 6	94 ± 3
Diphenhydramine-N-oxide	90 ± 2	136 ± 92	44 ± 22	47 ± 12	93 ± 8	143 ± 85	49 ± 9	52 ± 6	112 ± 7	112 ± 13	107 ± 5	110 ± 20	110 ± 6	106 ± 18	116 ± 7	112 ± 9
Cetirizine	129 ± 54	139 ± 88	125 ± 10	128 ± 54	121 ± 47	112 ± 46	98 ± 29	109 ± 18	123 ± 4	125 ± 75	110 ± 16	108 ± 14	117 ± 5	103 ± 23	105 ± 29	105 ± 13
Fexofenadine	139 ± 30	144 ± 60	2)	131 ± 75	139 ± 34	132 ± 38	130 ± 48	127 ± 27	110 ± 11	122 ± 58	138 ± 10	132 ± 32	111 ± 8	105 ± 19	127 ± 12	121 ± 7
Diatrizoic acid	102 ± 2	106 ± 38	1)	40 ± 18	109 ± 7	108 ± 56	37 ± 16	29 ± 24	103 ± 5	94 ± 29	103 ± 5	82 ± 24	104 ± 6	90 ± 22	99 ± 8	102 ± 10
Iopamidol	73 ± 21	81 ± 46	2)	2)	73 ± 2	78 ± 32	47 ± 12	49 ± 15	94 ± 25	103 ± 12	102 ± 8	104 ± 20	96 ± 12	95 ± 5	100 ± 3	96 ± 3
Iopromide	82 ± 9	88 ± 41	1)	2)	82 ± 9	84 ± 33	62 ± 21	57 ± 6	94 ± 7	102 ± 9	102 ± 52	81 ± 17	102 ± 7	98 ± 3	99 ± 11	97 ± 3
Iopromide-TP-643	98 ± 4	83 ± 12	156 ± 32	124 ± 15	90 ± 6	75 ± 6	102 ± 27	87 ± 14	119 ± 15	102 ± 31	3)	3)	117 ± 21	103 ± 34	3)	3)
Iopromide-TP-701A	83 ± 8	86 ± 17	106 ± 15	82 ± 18	79 ± 6	72 ± 0	89 ± 12	82 ± 9	93 ± 17	98 ± 4	3)	3)	100 ± 18	97 ± 22	141 ± 17	137 ± 5
Iopromide-TP-701B	76 ± 5	71 ± 9	86 ± 24	71 ± 16	81 ± 7	71 ± 5	68 ± 25	59 ± 6	92 ± 11	103 ± 21	110 ± 9	108 ± 9	99 ± 17	97 ± 23	109 ± 22	98 ± 6
Iopromide-TP-731B	75 ± 3	68 ± 8	90 ± 17	74 ± 11	80 ± 5	71 ± 2	79 ± 20	68 ± 5	92 ± 13	98 ± 13	112 ± 9	110 ± 10	99 ± 18	96 ± 21	122 ± 9	110 ± 3
Iopromide-TP-819	79 ± 6	114 ± 73	88 ± 11	52 ± 20	75 ± 3	83 ± 30	70 ± 20	64 ± 6	69 ± 7	92 ± 27	77 ± 7	61 ± 10	96 ± 14	99 ± 8	112 ± 14	107 ± 2
Iopromide-TP-729A	86 ± 7	96 ± 18	109 ± 27	77 ± 5	86 ± 8	77 ± 7	93 ± 14	69 ± 11	93 ± 11	92 ± 15	122 ± 32	96 ± 34	110 ± 11	98 ± 39	151 ± 20	117 ± 18
Iopromide-TP-759	81 ± 12	89 ± 6	146 ± 35	95 ± 31	87 ± 6	84 ± 7	107 ± 27	83 ± 19	98 ± 14	87 ± 56	3)	137 ± 25	107 ± 20	92 ± 50	3)	136 ± 26
Iomeprol	83 ± 4	107 ± 41	1)	2)	72 ± 4	81 ± 33	57 ± 31	54 ± 7	103 ± 7	106 ± 13	109 ± 37	90 ± 45	105 ± 10	109 ± 13	105 ± 28	99 ± 19
Diclofenac (DCF)	75 ± 16	114 ± 69	1)	1)	61 ± 11	64 ± 8	34 ± 11	25 ± 27	99 ± 19	98 ± 2	102 ± 21	79 ± 42	73 ± 22	72 ± 24	78 ± 3	67 ± 11
4-Hydroxy-DCF	86 ± 17	108 ± 15	1)	1)	73 ± 14	77 ± 20	49 ± 38	40 ± 19	83 ± 22	101 ± 8	1)	1)	69 ± 19	72 ± 22	69 ± 36	64 ± 23
Carboxy-DCF	86 ± 5	103 ± 30	80 ± 24	68 ± 11	89 ± 7	101 ± 20	82 ± 23	77 ± 10	98 ± 6	103 ± 8	120 ± 9	106 ± 30	97 ± 5	99 ± 7	123 ± 4	117 ± 10
DCF Lactam	77 ± 5	88 ± 16	72 ± 21	71 ± 20	80 ± 7	88 ± 14	84 ± 11	80 ± 8	97 ± 8	99 ± 8	129 ± 5	128 ± 22	94 ± 5	96 ± 5	129 ± 20	124 ± 13
Ibuprofen (IBU)	79 ± 13	117 ± 76	1)	57 ± 37	89 ± 9	119 ± 54	76 ± 66	67 ± 24	93 ± 6	104 ± 22	1)	83 ± 26	89 ± 1	86 ± 12	80 ± 22	81 ± 4
2-Hydroxy-IBU	74 ± 16	63 ± 17	1)	68 ± 32	69 ± 10	60 ± 21	1)	69 ± 27	67 ± 8	45 ± 23	1)	168 ± 77	61 ± 7	42 ± 31	1)	111 ± 54
Carboxy-IBU	92 ± 20	103 ± 35	1)	48 ± 16	93 ± 10	98 ± 21	1)	53 ± 7	105 ± 13	95 ± 21	1)	91 ± 13	90 ± 3	74 ± 31	1)	78 ± 3
Naproxen	95 ± 16	104 ± 29	86 ± 18	43 ± 28	107 ± 16	111 ± 11	61 ± 18	57 ± 13	98 ± 9	101 ± 9	112 ± 49	80 ± 33	89 ± 4	84 ± 17	84 ± 7	79 ± 4
O-desmethyl-Naproxen	80 ± 15	84 ± 21	36 ± 28	30 ± 15	90 ± 8	93 ± 16	52 ± 16	48 ± 8	85 ± 7	81 ± 8	78 ± 42	86 ± 64	71 ± 3	67 ± 11	103 ± 2	95 ± 13
Oxypurinol	79 ± 20	1)	1)	1)	85 ± 12	1)	89 ± 43	1)	93 ± 12	89 ± 17	1)	1)	97 ± 4	90 ± 9	116 ± 53	103 ± 34
Carbendazim	75 ± 4	72 ± 7	62 ± 13	66 ± 18	81 ± 5	77 ± 4	57 ± 16	67 ± 7	103 ± 4	103 ± 19	120 ± 6	107 ± 8	102 ± 10	96 ± 11	118 ± 8	107 ± 6
Epoxiconazole	92 ± 12	117 ± 52	70 ± 14	70 ± 17	90 ± 6	2)	67 ± 30	66 ± 14	100 ± 5	100 ± 6	113 ± 3	109 ± 8	100 ± 5	99 ± 8	113 ± 2	109 ± 3
Propiconazole	90 ± 9	133 ± 87	67 ± 15	72 ± 17	97 ± 8	2)	69 ± 28	74 ± 21	100 ± 7	99 ± 9	108 ± 5	103 ± 7	101 ± 5	96 ± 11	108 ± 4	105 ± 4
Tebuconazole	90 ± 11	2)	75 ± 16	71 ± 16	94 ± 7	2)	77 ± 30	77 ± 13	92 ± 7	88 ± 14	101 ± 4	97 ± 8	92 ± 3	86 ± 17	100 ± 2	96 ± 9
DEET	84 ± 4	91 ± 10	1)	74 ± 39	89 ± 6	91 ± 4	77 ± 35	75 ± 15	112 ± 8	117 ± 13	120 ± 22	119 ± 10	99 ± 4	103 ± 7	113 ± 7	108 ± 7
DEET carboxylic acid	84 ± 4	107 ± 48	91 ± 39	71 ± 30	85 ± 7	89 ± 5	73 ± 23	69 ± 9	103 ± 9	104 ± 2	107 ± 6	91 ± 13	94 ± 4	96 ± 7	101 ± 12	95 ± 5
Hydroxy-DEET	97 ± 5	88 ± 7	78 ± 19	66 ± 16	93 ± 3	88 ± 7	73 ± 16	64 ± 13	129 ± 16	117 ± 7	119 ± 21	103 ± 15	104 ± 8	101 ± 7	109 ± 16	96 ± 8
N-ethyl-m-toluamide	75 ± 2	67 ± 7	73 ± 16	63 ± 17	78 ± 2	70 ± 8	72 ± 20	66 ± 11	95 ± 9	93 ± 7	100 ± 18	87 ± 7	88 ± 6	88 ± 7	99 ± 7	91 ± 8
Imidacloprid	91 ± 7	80 ± 3	80 ± 18	62 ± 14	86 ± 4	83 ± 5	70 ± 16	60 ± 9	96 ± 5	97 ± 17	121 ± 11	111 ± 6	94 ± 4	94 ± 13	114 ± 5	111 ± 7
Diuron	77 ± 8	65 ± 16	37 ± 8	29 ± 15	84 ± 7	73 ± 17	38 ± 13	34 ± 13	100 ± 5	103 ± 8	103 ± 6	100 ± 6	99 ± 8	98 ± 6	97 ± 6	95 ± 6
Didemethyldiuron (DCPU)	82 ± 6	78 ± 18	38 ± 15	31 ± 7	84 ± 6	87 ± 16	44 ± 13	35 ± 7	104 ± 6	95 ± 13	97 ± 21	102 ± 28	102 ± 6	94 ± 14	108 ± 9	98 ± 25
N-Demethoxyliuron (DCPMU)	80 ± 4	71 ± 15	33 ± 10	28 ± 5	80 ± 7	80 ± 11	35 ± 11	30 ± 8	106 ± 6	106 ± 2	114 ± 16	124 ± 17	95 ± 6	100 ± 4	108 ± 1	104 ± 19
Isoproturon	87 ± 4	79 ± 15	82 ± 32	77 ± 32	90 ± 7	82 ± 13	76 ± 29	73 ± 16	110 ± 6	113 ± 10	115 ± 6	111 ± 11	100 ± 4	100 ± 6	107 ± 8	103 ± 8
Mecoprop	83 ± 12	110 ± 55	74 ± 17	70 ± 30	91 ± 6	127 ± 56	81 ± 33	74 ± 24	115 ± 10	118 ± 14	127 ± 10	123 ± 24	96 ± 7	95 ± 9	111 ± 7	104 ± 4
Metamitron	106 ± 7	120 ± 49	62 ± 24	63 ± 8	107 ± 9	135 ± 56	68 ± 18	68 ± 9	100 ± 6	99 ± 8	104 ± 4	108 ± 3	99 ± 7	96 ± 14	102 ± 3	104 ± 4
Desamino-Metamitron	98 ± 33	111 ± 51	58 ± 18	52 ± 13	98 ± 27	121 ± 60	63 ± 20	52 ± 8	86 ± 30	87 ± 15	118 ± 14	106 ± 20	92 ± 28	87 ± 16	121 ± 9	103 ± 29
Metazachlor	86 ± 9	89 ± 8	39 ± 9	36 ± 10	89 ± 7	98 ± 7	40 ± 17	40 ± 7	103 ± 6	106 ± 20	114 ± 7	109 ± 10	101 ± 5	99 ± 11	110 ± 5	107 ± 4
Metolachlor	86 ± 10	103 ± 44	42 ± 10	43 ± 7	90 ± 10	119 ± 42	42 ± 20	42 ± 12	99 ± 5	104 ± 10	127 ± 6	115 ± 12	96 ± 6	99 ± 7	115 ± 3	106 ± 11
Metolachlor ESA	74 ± 17	38 ± 70	33 ± 7	29 ± 15	81 ± 9	2)	34 ± 16	29 ± 13	82 ± 12	110 ± 74	118 ± 21	87 ± 26	88 ± 6	84 ± 31	116 ± 5	88 ± 21
Metolachlor OA	88 ± 14	83 ± 20	50 ± 20	49 ± 18	92 ± 7	100 ± 25	56 ± 25	51 ± 10	98 ± 20	100 ± 70	121 ± 31	107 ± 31	98 ± 12	99 ± 37	130 ± 4	110 ± 8
Terbutryn	85 ± 10	120 ± 67	46 ± 12	50 ± 10	82 ± 6	128 ± 73	43 ± 19	48 ± 8	106 ± 7	112 ± 9	126 ± 6	122 ± 12	101 ± 5	102 ± 5	115 ± 1	116 ± 3
Terbuthylazine	80 ± 11	90 ± 33	42 ± 9	44 ± 10	78 ± 6	96 ± 29	42 ± 19	45 ± 8	104 ± 6	106 ± 4	120 ± 7	115 ± 13	96 ± 8	94 ± 8	112 ± 6	104 ± 8
Terbuthylazine-2-Hydroxy	86 ± 7	115 ± 63	51 ± 22	48 ± 11	94 ± 4	136 ± 79	69 ± 25	62 ± 17	136 ± 24	134 ± 28	133 ± 29	115 ± 48	123 ± 12	115 ± 26	149 ± 13	115 ± 29
Irgarol	80 ± 11	119 ± 77	44 ± 11	46 ± 12	79 ± 6	126 ± 76	43 ± 19	45 ± 10	106 ± 5	108 ± 7	122 ± 4	109 ± 20	99 ± 6	98 ± 6	114 ± 7	107 ± 9
Benzotriazole	82 ± 21	1)	1)	1)	88 ± 5	104 ± 48	1)	1)	97 ± 12	1)	1)	1)	106 ± 9	96 ± 34	1)	1)

1-Hydroxy-Benzotriazole	75 ± 15	77 ± 20	83 ± 22	2)	82 ± 4	84 ± 20	68 ± 23	67 ± 6	101 ± 24	100 ± 32	96 ± 59	87 ± 33	101 ± 3	98 ± 6	108 ± 14	109 ± 11
Tetraglyme	76 ± 7	97 ± 39	41 ± 22	31 ± 9	85 ± 3	108 ± 41	44 ± 17	37 ± 9	99 ± 15	100 ± 19	110 ± 6	101 ± 6	102 ± 6	94 ± 15	110 ± 5	103 ± 5
Ethyltriphenylphosphonium	103 ± 8	148 ± 76	140 ± 42	121 ± 37	103 ± 9	137 ± 59	112 ± 36	108 ± 12	111 ± 6	108 ± 25	130 ± 10	121 ± 15	110 ± 9	105 ± 20	123 ± 10	119 ± 7
Methyltriphenylphosphonium	91 ± 6	145 ± 55	116 ± 43	101 ± 31	94 ± 7	123 ± 52	97 ± 30	97 ± 16	103 ± 6	108 ± 9	120 ± 2	112 ± 12	100 ± 7	104 ± 4	108 ± 7	107 ± 5
Tetrabutyltriphenylphosphonium	87 ± 5	121 ± 63	117 ± 44	103 ± 35	93 ± 6	122 ± 53	99 ± 26	95 ± 13	97 ± 4	96 ± 8	119 ± 16	113 ± 19	97 ± 4	96 ± 8	108 ± 14	104 ± 11
(Methoxymethyl)triphenylphosphonium	95 ± 5	177 ± 118	113 ± 31	96 ± 26	93 ± 6	124 ± 45	104 ± 35	98 ± 15	101 ± 4	98 ± 2	118 ± 13	108 ± 17	100 ± 7	103 ± 18	110 ± 12	103 ± 6
Tetrabutylammonium	72 ± 5	87 ± 21	99 ± 21	85 ± 24	90 ± 6	100 ± 20	88 ± 29	85 ± 15	105 ± 7	104 ± 26	124 ± 44	110 ± 19	105 ± 7	97 ± 21	116 ± 18	106 ± 15
Tetrapropylammonium	87 ± 5	104 ± 33	113 ± 33	104 ± 27	89 ± 2	104 ± 31	80 ± 36	86 ± 6	102 ± 8	101 ± 5	115 ± 18	105 ± 10	96 ± 8	96 ± 4	103 ± 19	104 ± 5
Caffeine	64 ± 2	63 ± 5	1)	61 ± 17	79 ± 2	73 ± 6	1)	58 ± 10	84 ± 24	103 ± 22	1)	117 ± 19	93 ± 8	93 ± 5	1)	107 ± 7
Triclosan	88 ± 7	96 ± 29	73 ± 20	73 ± 8	91 ± 4	110 ± 32	71 ± 20	67 ± 13	99 ± 7	97 ± 14	115 ± 9	104 ± 4	101 ± 5	96 ± 13	111 ± 5	110 ± 6
Triclocarban	93 ± 8	93 ± 20	29 ± 11	64 ± 7	95 ± 5	102 ± 15	29 ± 6	57 ± 11	98 ± 6	101 ± 6	107 ± 5	104 ± 9	102 ± 4	99 ± 10	107 ± 8	103 ± 5
Carbanilide	78 ± 8	68 ± 13	33 ± 6	29 ± 9	79 ± 5	74 ± 10	34 ± 9	31 ± 10	75 ± 8	90 ± 19	148 ± 38	58 ± 14	85 ± 8	89 ± 12	149 ± 87	75 ± 20
Acesulfame	86 ± 20	92 ± 11	1)	102 ± 36	109 ± 18	105 ± 46	134 ± 59	104 ± 31	103 ± 7	103 ± 13	119 ± 9	107 ± 8	105 ± 6	97 ± 13	114 ± 12	111 ± 4
Saccharine	77 ± 23	108 ± 79	1)	60 ± 23	85 ± 23	121 ± 90	1)	83 ± 30	96 ± 10	100 ± 8	1)	113 ± 42	96 ± 6	100 ± 7	92 ± 37	115 ± 8
Sucralose	1)	1)	1)	1)	63 ± 25	2)	63 ± 26	1)	1)	1)	1)	1)	90 ± 11	88 ± 10	112 ± 39	103 ± 38
Denatonium	88 ± 4	120 ± 34	95 ± 45	77 ± 34	91 ± 3	105 ± 27	85 ± 26	84 ± 17	109 ± 6	126 ± 36	136 ± 4	127 ± 28	109 ± 7	121 ± 11	134 ± 20	127 ± 27
Tolylbiguanide	64 ± 8	60 ± 42	56 ± 13	56 ± 19	79 ± 5	73 ± 36	58 ± 13	63 ± 6	96 ± 9	110 ± 45	110 ± 10	93 ± 17	85 ± 3	96 ± 20	105 ± 8	91 ± 8

1) concentration in the unspiked sample higher than spike level. Thus no calculation of recovery was performed

2) high fluctuations of analyte area which was compensated by IC. Thus no calculation of recovery and error was performed

3) no appropriate internal standard available or internal standard not needed for evaluation. Thus no calculation of relative recovery was performed

A1.5-A: Boxplots validation results M1

Abbreviations: BF = Bank filtrate, SW = Surface water, Inf = Influent, Eff = Effluent
100, 1000: calibration standard (precision) or spiked concentration (recoveries) in ng/L

A1.5-B: Boxplots validation results M2

Abbreviations: BF = Bank filtrate, SW = Surface water, Inf = Influent, Eff = Effluent
100, 1000: calibration standard (precision) or spiked concentration (recoveries) in ng/L
        (acesulfam 20fold, oxypurinol and contrast media 10fold)

A1.6-A: Mean concentrations in WWTPs

Abbreviations: M = Method, WWTP = Wastewater treatment plant, Inf = Influent, sec.Eff. = secondary effluent, tert. Eff = tertiary effluent

Concentrations in µg/L

Substance	M	ESI	WWTP 1			WWTP 2			WWTP 3	
			Inf.	sec. Eff.	tert. Eff.	Inf.	sec. Eff.	tert. Eff.	Inf.	sec. Eff.
Tramadol	1	pos	0.40 ± 0.02	0.31 ± 0.01	0.11 ± 0.01	0.46 ± 0.05	0.5 ± 0.2	< LOQ	0.42 ± 0.04	0.43 ± 0.04
O-DM-Tramadol	1	pos	0.30 ± 0.02	0.27 ± 0.01	0.11 ± 0.01	0.37 ± 0.04	0.5 ± 0.2	< LOQ	0.34 ± 0.03	0.36 ± 0.02
N-DM-Tramadol	1	pos	0.155 ± 0.006	0.15 ± 0.03	0.10 ± 0.01	0.19 ± 0.03	0.24 ± 0.09	0.05 ± 0.01	0.24 ± 0.02	0.26 ± 0.01
N,O-DDM-Tramadol	1	pos	0.47 ± 0.04	0.50 ± 0.04	0.20 ± 0.02	0.53 ± 0.09	0.7 ± 0.3	0.02 ± 0.01	0.55 ± 0.03	0.55 ± 0.04
Tramadol-N-oxide	1	pos	< LOQ	< LOQ	< LOQ	< LOQ	< LOQ	< LOQ	< LOQ	< LOQ
Primidone	1	pos	0.42 ± 0.03	0.38 ± 0.01	0.29 ± 0.03	0.10 ± 0.01	0.09 ± 0.03	0.04 ± 0.01	0.43 ± 0.02	0.43 ± 0.03
Phenytoin	2	neg	0.01 ± 0.00	0.011 ± 0.001	< LOQ	0.01 ± 0.01	0.02 ± 0.00	< LOQ	< LOQ	0.01 ± 0.00
Carbamazepine (CBZ)	2	pos	*	*	*	*	*	*	1.5 ± 0.4	1.4 ± 0.1
2-Hydroxy-CBZ	2	pos	0.138 ± 0.003	0.09 ± 0.01	0.03 ± 0.00	0.13 ± 0.03	0.13 ± 0.05	< LOQ	0.22 ± 0.03	0.14 ± 0.01
3-Hydroxy-CBZ	2	pos	0.13 ± 0.02	0.089 ± 0.006	0.02 ± 0.00	0.11 ± 0.02	0.09 ± 0.04	< LOQ	0.18 ± 0.02	0.13 ± 0.02
10-Hydroxy-CBZ	2	pos	1.20 ± 0.05	0.78 ± 0.03	0.13 ± 0.03	0.7 ± 0.2	0.27 ± 0.07	0.05 ± 0.01	1.24 ± 0.09	0.79 ± 0.07
10,11-Dihydro-10,11-dihydroxy-CBZ	2	pos	1.79 ± 0.09	1.19 ± 0.05	0.71 ± 0.09	1.6 ± 0.3	1.4 ± 0.6	0.4 ± 0.1	2.6 ± 0.3	2.1 ± 0.1
9-Carboxylic acid-Acridine	2	pos	0.16 ± 0.02	0.15 ± 0.03	0.11 ± 0.01	0.18 ± 0.02	0.3 ± 0.1	0.05 ± 0.01	0.24 ± 0.04	0.23 ± 0.05
Acridone	2	pos	0.01 ± 0.00	0.01 ± 0.00	< LOQ	0.01 ± 0.00	0.009 ± 0.001	< LOQ	0.01 ± 0.00	0.01 ± 0.00
Lamotrigine	1	pos	0.39 ± 0.04	0.61 ± 0.03	0.20 ± 0.02	0.5 ± 0.1	1.1 ± 0.5	0.11 ± 0.03	0.64 ± 0.07	1.31 ± 0.06
2-N-methyl-Lamotrigine	1	pos	< LOQ	0.059 ± 0.002	< LOQ	< LOQ	0.03 ± 0.01	< LOQ	< LOQ	0.02 ± 0.01
Gabapentin	1	pos	5.7 ± 0.4	2.1 ± 0.1	0.9 ± 0.1	2.92 ± 0.05	2.3 ± 0.8	1.8 ± 0.5	8.4 ± 0.5	2.1 ± 0.5
Gabapentin Lactam	1	pos	0.06 ± 0.01	0.74 ± 0.05	0.81 ± 0.08	0.14 ± 0.03	0.8 ± 0.4	0.7 ± 0.2	0.07 ± 0.03	1.0 ± 0.3
Levetiracetam	1	pos	10.1 ± 0.8	0.14 ± 0.01	0.06 ± 0.02	5.2 ± 0.9	0.04 ± 0.01	< LOQ	12 ± 2	0.07 ± 0.03
Levetiracetam acid	1	pos	4.7 ± 0.6	< LOQ	< LOQ	2.4 ± 0.6	< LOQ	< LOQ	5.4 ± 0.8	< LOQ
Pregabalin	2	pos	6.5 ± 0.3	1.87 ± 0.02	0.96 ± 0.06	4.6 ± 0.7	0.44 ± 0.06	0.20 ± 0.02	8.3 ± 0.4	1.3 ± 0.4
Sulpiride	2	pos	0.5 ± 0.3	0.27 ± 0.02	0.03 ± 0.01	0.04 ± 0.01	0.04 ± 0.01	< LOQ	0.43 ± 0.01	0.40 ± 0.03
Amisulpride	1	pos	0.60 ± 0.06	0.43 ± 0.02	0.03 ± 0.01	0.3 ± 0.1	0.2 ± 0.1	< LOQ	0.8 ± 0.1	0.8 ± 0.1
O-desmethyl-Amisulpride	1	pos	< LOQ	< LOQ	< LOQ	< LOQ	< LOQ	< LOQ	< LOQ	< LOQ
Oxazepam	1	pos	0.11 ± 0.01	0.104 ± 0.004	0.04 ± 0.01	0.21 ± 0.03	0.23 ± 0.08	0.04 ± 0.01	0.183 ± 0.006	0.18 ± 0.01
Citalopram	1	pos	0.19 ± 0.01	0.125 ± 0.001	< LOQ	0.24 ± 0.03	0.22 ± 0.07	< LOQ	0.23 ± 0.05	0.21 ± 0.01
Desmethyl-Citalopram	1	pos	0.11 ± 0.02	0.077 ± 0.003	< LOQ	0.14 ± 0.01	0.13 ± 0.04	0.01 ± 0.00	0.13 ± 0.03	0.10 ± 0.01
Didesmethyl-Citalopram	1	pos	< LOQ	< LOQ	< LOQ	< LOQ	< LOQ	< LOQ	0.04 ± 0.01	< LOQ
Citalopram-N-oxide	1	pos	0.01 ± 0.00	< LOQ	< LOQ	0.02 ± 0.00	0.01 ± 0.00	< LOQ	0.02 ± 0.01	0.01 ± 0.00
Venlafaxine (VLX)	1	pos	0.370 ± 0.004	0.303 ± 0.005	0.13 ± 0.02	0.47 ± 0.06	0.5 ± 0.2	0.04 ± 0.01	0.53 ± 0.08	0.49 ± 0.07
O-desmethyl-VLX	1	pos	0.97 ± 0.04	0.95 ± 0.07	0.62 ± 0.07	1.2 ± 0.2	1.5 ± 0.5	0.16 ± 0.05	1.39 ± 0.02	1.60 ± 0.04
N-desmethyl-VLX	1	pos	0.048 ± 0.003	0.046 ± 0.004	0.02 ± 0.00	0.08 ± 0.01	0.07 ± 0.03	0.05 ± 0.02	0.072 ± 0.003	0.075 ± 0.005
N.O-didesmethyl-VLX	1	pos	0.152 ± 0.008	0.15 ± 0.02	0.095 ± 0.007	0.20 ± 0.03	0.2 ± 0.1	0.05 ± 0.01	0.24 ± 0.01	0.25 ± 0.01
VLX-N-oxide	1	pos	< LOQ	< LOQ	< LOQ	< LOQ	< LOQ	< LOQ	< LOQ	< LOQ
Lidocaine	1	pos	0.22 ± 0.05	0.19 ± 0.02	0.05 ± 0.01	0.29 ± 0.05	0.3 ± 0.1	0.01 ± 0.00	0.31 ± 0.06	0.28 ± 0.05
Nor-Lidocaine	1	pos	0.02 ± 0.00	0.01 ± 0.00	< LOQ	0.03 ± 0.01	0.03 ± 0.01	0.013 ± 0.001	0.03 ± 0.00	0.03 ± 0.00
Flecainide	1	pos	0.07 ± 0.01	0.055 ± 0.001	0.01 ± 0.00	0.07 ± 0.01	0.06 ± 0.02	< LOQ	0.88 ± 0.05	0.89 ± 0.05
m-O-dealkylated Flecainide	1	pos	< LOQ	0.01 ± 0.00	< LOQ	< LOQ	0.01 ± 0.00	< LOQ	0.080 ± 0.005	0.09 ± 0.02
Hydrochlorothiazide	2	neg	3.3 ± 0.2	2.83 ± 0.06	1.1 ± 0.1	1.8 ± 0.2	1.8 ± 0.7	0.15 ± 0.02	4.8 ± 0.3	4.4 ± 0.3
Chlorothiazide	2	neg	0.094 ± 0.001	0.114 ± 0.002	0.06 ± 0.01	0.05 ± 0.01	0.06 ± 0.02	0.06 ± 0.02	0.14 ± 0.01	0.15 ± 0.02
4-amino-6-chloro-1,3-benzenedisulfonamide	2	neg	0.5 ± 0.1	0.31 ± 0.04	0.09 ± 0.02	0.30 ± 0.07	0.2 ± 0.1	< LOQ	1.1 ± 0.1	0.89 ± 0.06
Xipamide	2	neg	0.035 ± 0.002	0.029 ± 0.001	0.02 ± 0.00	< LOQ	< LOQ	< LOQ	0.109 ± 0.005	0.094 ± 0.003
Furosemide	2	neg	1.0 ± 0.1	0.4 ± 0.1	0.13 ± 0.03	0.11 ± 0.02	0.03 ± 0.01	< LOQ	0.83 ± 0.05	0.35 ± 0.04
Torsemide	2	pos	0.166 ± 0.008	0.124 ± 0.004	0.08 ± 0.01	0.115 ± 0.004	0.11 ± 0.04	0.03 ± 0.01	0.26 ± 0.02	0.23 ± 0.02
Hydroxy-Torsemide	2	pos	0.149 ± 0.006	0.007 ± 0.001	< LOQ	0.11 ± 0.02	< LOQ	< LOQ	0.23 ± 0.02	< LOQ
Sotalol	1	pos	0.15 ± 0.01	0.135 ± 0.006	0.04 ± 0.01	0.10 ± 0.01	0.10 ± 0.04	< LOQ	0.49 ± 0.03	0.45 ± 0.02
Metoprolol	2	pos	1.01 ± 0.02	0.675 ± 0.003	0.06 ± 0.02	0.27 ± 0.05	0.18 ± 0.06	< LOQ	1.6 ± 0.2	1.1 ± 0.1
Hydroxy-Metoprolol	2	pos	0.9 ± 0.06	0.14 ± 0.01	< LOQ	0.25 ± 0.04	< LOQ	< LOQ	1.7 ± 0.1	0.14 ± 0.02
O-desmethyl-Metoprolol	2	pos	0.04 ± 0.01	< LOQ	< LOQ	< LOQ	< LOQ	< LOQ	0.08 ± 0.01	< LOQ
Atenolol	1	pos	0.21 ± 0.01	0.078 ± 0.001	0.02 ± 0.00	1.1 ± 0.1	0.31 ± 0.07	0.02 ± 0.01	0.39 ± 0.02	0.10 ± 0.02
Atenolol acid	1	pos	0.96 ± 0.09	0.734 ± 0.006	0.08 ± 0.02	0.25 ± 0.04	0.22 ± 0.08	< LOQ	1.4 ± 0.3	1.2 ± 0.1
Hydroxy-Atenolol	1	pos	0.02 ± 0.00	< LOQ	< LOQ	0.039 ± 0.001	0.03 ± 0.01	< LOQ	0.03 ± 0.01	0.012 ± 0.001
Enalapril	1	pos	0.075 ± 0.004	< LOQ	< LOQ	0.06 ± 0.004	< LOQ	< LOQ	0.125 ± 0.007	< LOQ
Enalaprilat	1	pos	0.17 ± 0.01	< LOQ	< LOQ	0.13 ± 0.01	< LOQ	< LOQ	0.28 ± 0.03	< LOQ
Ramipril	2	pos	0.067 ± 0.004	0.030 ± 0.001	< LOQ	< LOQ	< LOQ	< LOQ	0.095 ± 0.006	0.05 ± 0.01
Ramiprilat	2	pos	0.76 ± 0.01	0.37 ± 0.01	< LOQ	< LOQ	< LOQ	< LOQ	1.0 ± 0.1	0.6 ± 0.2
Valsartan	2	pos	6.6 ± 0.1	1.2 ± 0.1	0.20 ± 0.05	7.3 ± 0.7	0.26 ± 0.01	0.02 ± 0.00	13.5 ± 0.6	0.7 ± 0.3
Valsartan acid	2	pos	0.08 ± 0.02	2.2 ± 0.2	2.4 ± 0.1	0.5 ± 0.1	4 ± 2	2.3 ± 0.9	0.10 ± 0.02	6 ± 1
Irbesartan	2	neg	0.73 ± 0.06	0.521 ± 0.008	0.37 ± 0.04	1.1 ± 0.2	1.1 ± 0.4	0.24 ± 0.08	2.1 ± 0.2	2.0 ± 0.3
Candesartan	2	neg	1.00 ± 0.01	0.823 ± 0.007	0.70 ± 0.06	0.93 ± 0.07	0.9 ± 0.3	0.4 ± 0.1	1.6 ± 0.1	1.7 ± 0.1
Telmisartan	2	pos	0.8 ± 0.1	0.53 ± 0.04	0.11 ± 0.02	0.16 ± 0.02	0.13 ± 0.02	0.016 ± 0.001	1.4 ± 0.6	0.9 ± 0.1
Olmesartan	2	neg	0.391 ± 0.002	0.31 ± 0.01	0.28 ± 0.03	0.39 ± 0.06	0.4 ± 0.2	0.21 ± 0.08	0.87 ± 0.06	0.86 ± 0.07
Aliksiren	1	pos	0.34 ± 0.05	0.139 ± 0.006	< LOQ	1.1 ± 0.2	0.6 ± 0.1	0.04 ± 0.00	0.6 ± 0.3	0.5 ± 0.1
Bezafibrate	2	neg	0.35 ± 0.02	0.10 ± 0.01	0.02 ± 0.01	0.31 ± 0.05	0.02 ± 0.00	< LOQ	0.9 ± 0.1	0.17 ± 0.08
3-[(4-chlorobenzoyl)amino]-propanoic acid	2	neg	< LOQ	< LOQ	< LOQ	< LOQ	< LOQ	< LOQ	< LOQ	< LOQ
Climbazole	1	pos	0.17 ± 0.02	0.051 ± 0.003	0.01 ± 0.00	0.19 ± 0.03	0.08 ± 0.02	< LOQ	0.196 ± 0.008	0.099 ± 0.005
Climbazole-TP	1	pos	< LOQ	0.073 ± 0.004	0.02 ± 0.00	< LOQ	0.08 ± 0.03	0.01 ± 0.00	< LOQ	0.08 ± 0.02
Trimethoprim	1	pos	0.26 ± 0.02	0.16 ± 0.01	0.01 ± 0.00	0.33 ± 0.09	0.09 ± 0.04	< LOQ	0.37 ± 0.05	0.16 ± 0.08
3-desmethyl-TMP	1	pos	0.052 ± 0.004	0.020 ± 0.001	< LOQ	0.05 ± 0.01	0.03 ± 0.01	< LOQ	0.07 ± 0.01	0.02 ± 0.01
5-(2,4,5-Trimethoxy)-2,4-pyrimidinediamnine	1	pos	< LOQ	< LOQ	< LOQ	< LOQ	< LOQ	< LOQ	< LOQ	< LOQ
Sulfamethoxazole (SMX)	2	pos	0.22 ± 0.04	0.09 ± 0.01	0.12 ± 0.01	0.30 ± 0.08	0.3 ± 0.1	0.08 ± 0.03	0.82 ± 0.07	0.5 ± 0.1
Acetyl-SMX	2	pos	1.3 ± 0.1	0.21 ± 0.03	0.06 ± 0.01	1.7 ± 0.2	0.08 ± 0.01	< LOQ	1.8 ± 0.2	0.084 ± 0.005
Clarithromycin	1	pos	0.23 ± 0.01	0.066 ± 0.001	0.02 ± 0.01	0.35 ± 0.02	0.18 ± 0.02	0.026 ± 0.002	0.46 ± 0.08	0.26 ± 0.09
Fluconazole	2	pos	0.089 ± 0.006	0.082 ± 0.002	0.05 ± 0.01	0.08 ± 0.01	0.07 ± 0.03	0.03 ± 0.01	0.11 ± 0.01	0.11 ± 0.02
Aciclovir	1	pos	2.3 ± 0.1	0.41 ± 0.04	0.09 ± 0.03	0.031 ± 0.001	0.031 ± 0.001	< LOQ	2 ± 1	0.05 ± 0.01
Carboxy-Aciclovir	1	pos	0.74 ± 0.03	1.54 ± 0.02	1.2 ± 0.1	0.57 ± 0.07	1.2 ± 0.5	0.4 ± 0.1	1 ± 2	1.9 ± 0.2
Emtricitabine	1	pos	0.29 ± 0.04	0.07 ± 0.01	< LOQ	0.45 ± 0.08	0.057 ± 0.004	< LOQ	0.6 ± 0.2	0.122 ± 0.005
Emtricitabine carboxylate	1	pos	< LOQ	0.11 ± 0.01	0.13 ± 0.01	< LOQ	0.3 ± 0.1	0.17 ± 0.04	0.11 ± 0.04	0.32 ± 0.06
Emtricitabine-S-oxide	1	pos	0.21 ± 0.02	< LOQ	< LOQ	0.25 ± 0.03	0.06 ± 0.01	< LOQ	0.18 ± 0.06	0.060 ± 0.005
Ranitidine	1	pos	0.18 ± 0.05	0.07 ± 0.01	< LOQ	0.11 ± 0.01	0.06 ± 0.03	< LOQ	0.6 ± 0.1	0.27 ± 0.02

Compound										
Ranitidine-N-oxide	1	pos	< LOQ	< LOQ	< LOQ	< LOQ	< LOQ	< LOQ	< LOQ	< LOQ
Desmethyl-Ranitidine	1	pos	< LOQ	< LOQ	< LOQ	< LOQ	< LOQ	< LOQ	< LOQ	< LOQ
Sitagliptin	1	pos	3.3 ± 0.2	1.85 ± 0.02	0.2 ± 0.05	2.3 ± 0.3	1.6 ± 0.5	0.06 ± 0.02	3.4 ± 0.2	1.8 ± 0.3
Clopidogrel	1	pos	0.02 ± 0.00	0.01 ± 0.00	0.01 ± 0.00	0.01 ± 0.00	0.01 ± 0.00	< LOQ	0.04 ± 0.01	0.02 ± 0.00
Clopidogrel acid	1	pos	0.27 ± 0.01	0.25 ± 0.01	0.10 ± 0.01	0.16 ± 0.01	0.17 ± 0.06	< LOQ	0.32 ± 0.02	0.32 ± 0.02
Bicalutamide	2	neg	0.02 ± 0.00	0.02 ± 0.00	0.01 ± 0.00	0.01 ± 0.00	0.01 ± 0.00	< LOQ	0.08 ± 0.01	0.073 ± 0.005
Diphenhydramine	2	pos	0.116 ± 0.004	0.044 ± 0.002	< LOQ	0.089 ± 0.004	0.11 ± 0.03	< LOQ	0.19 ± 0.03	0.18 ± 0.02
N-desmethyl-Diphenhydramine	2	pos	0.01 ± 0.00	0.011 ± 0.001	< LOQ	0.017 ± 0.001	0.04 ± 0.01	< LOQ	0.02 ± 0.00	0.022 ± 0.002
Diphenhydramine-N-oxide	2	pos	0.01 ± 0.01	< LOQ	< LOQ	0.02 ± 0.00	< LOQ	< LOQ	0.02 ± 0.01	0.01 ± 0.00
Cetirizine	1	pos	0.085 ± 0.004	0.082 ± 0.005	0.04 ± 0.01	0.07 ± 0.01	0.08 ± 0.03	0.02 ± 0.00	0.21 ± 0.01	0.22 ± 0.03
Fexofenadine	1	pos	0.15 ± 0.01	0.12 ± 0.01	0.05 ± 0.01	0.53 ± 0.08	0.4 ± 0.1	0.11 ± 0.02	0.54 ± 0.06	0.42 ± 0.04
Diatrizoic acid	2	pos	2.0 ± 0.3	3 ± 1	3 ± 1	4 ± 1	5 ± 2	5 ± 2	12.9 ± 0.6	14 ± 3
Iopamidol	1	pos	3 ± 3	2.2 ± 0.6	2.1 ± 0.7	0.4 ± 0.2	0.2 ± 0.2	0.2 ± 0.1	23 ± 6	20 ± 6
Iopromide	1	pos	14 ± 10	4 ± 2	1.0 ± 0.4	6 ± 4	0.3 ± 0.3	0.18 ± 0.05	21 ± 10	6 ± 2
Iopromide-TP-643	1	pos	< LOQ	< LOQ	0.16 ± 0.01	< LOQ	< LOQ	0.26 ± 0.09	0.109 ± 0.005	0.15 ± 0.05
Iopromide-TP-701A	1	pos	< LOQ	0.46 ± 0.02	1.1 ± 0.3	0.3 ± 0.1	0.9 ± 0.5	0.8 ± 0.4	0.16 ± 0.03	1.0 ± 0.4
Iopromide-TP-701B	1	pos	< LOQ	< LOQ	< LOQ	< LOQ	< LOQ	< LOQ	< LOQ	< LOQ
Iopromide-TP-731B	1	pos	< LOQ	< LOQ	< LOQ	< LOQ	< LOQ	0.08 ± 0.02	< LOQ	< LOQ
Iopromide-TP-819	1	pos	< LOQ	0.30 ± 0.06	0.8 ± 0.3	< LOQ	0.9 ± 0.2	0.4 ± 0.1	< LOQ	0.6 ± 0.2
Iopromide-TP-729A	1	pos	< LOQ	< LOQ	< LOQ	< LOQ	< LOQ	< LOQ	< LOQ	0.6 ± 0.4
Iopromide-TP-759	1	pos	< LOQ	1.1 ± 0.4	2.5 ± 0.9	0.26 ± 0.04	2 ± 1	1.3 ± 0.8	< LOQ	1.2 ± 0.6
Iomeprol	1	pos	40 ± 30	20 ± 6	7 ± 2	1 ± 1	< LOQ	< LOQ	30 ± 10	10 ± 4
Diclofenac (DCF)	1	pos	2.9 ± 0.1	1.8 ± 0.2	1.0 ± 0.1	2.3 ± 0.3	2.1 ± 0.1	0.25 ± 0.03	2.6 ± 0.2	1.8 ± 0.1
4-Hydroxy-DCF	1	pos	0.7 ± 0.1	0.3 ± 0.2	0.40 ± 0.03	0.7 ± 0.2	0.7 ± 0.3	0.25 ± 0.05	0.9 ± 0.2	0.5 ± 0.2
Carboxy-DCF	1	pos	0.01 ± 0.00	0.026 ± 0.003	0.016 ± 0.001	0.01 ± 0.00	0.03 ± 0.01	0.08 ± 0.02	0.010 ± 0.001	0.04 ± 0.01
DCF Lactam	1	pos	0.01 ± 0.01	0.01 ± 0.00	< LOQ	0.01 ± 0.00	0.01 ± 0.00	< LOQ	0 ± 0	0.03 ± 0.00
Ibuprofen (IBU)	2	neg	15.2 ± 0.3	0.8 ± 0.1	0.04 ± 0.01	7.4 ± 1.0	< LOQ	< LOQ	24 ± 3	< LOQ
2-Hydroxy-IBU	2	neg	37 ± 2	1.7 ± 0.4	0.15 ± 0.02	18 ± 2	< LOQ	< LOQ	37 ± 2	< LOQ
Carboxy-IBU	2	neg	58 ± 2	< LOQ	< LOQ	27 ± 3	< LOQ	< LOQ	86 ± 7	< LOQ
Naproxen	2	neg	1.2 ± 0.1	0.32 ± 0.06	0.13 ± 0.02	2.6 ± 0.5	0.12 ± 0.03	< LOQ	1.60 ± 0.05	0.17 ± 0.06
O-desmethyl-Naproxen	2	neg	0.15 ± 0.04	< LOQ	0.04 ± 0.01	0.2 ± 0.1	0.07 ± 0.03	< LOQ	0.8 ± 0.2	0.16 ± 0.06
Oxypurinol	2	neg	22 ± 1	10.8 ± 0.4	3.4 ± 0.3	5.6 ± 0.8	6 ± 2	1 ± 0.2	21 ± 6	20.5 ± 0.8
Carbendazim	1	pos	0.05 ± 0.02	0.03 ± 0.01	< LOQ	0.03 ± 0.00	0.02 ± 0.01	< LOQ	1 ± 1	0.02 ± 0.01
Epoxiconazole	2	pos	< LOQ	< LOQ	< LOQ	< LOQ	< LOQ	< LOQ	< LOQ	< LOQ
Propiconazole	2	pos	0.01 ± 0.00	0.01 ± 0.00	< LOQ	0.01 ± 0.00	0.01 ± 0.00	< LOQ	0.01 ± 0.00	0.01 ± 0.00
Tebuconazole	2	pos	0.01 ± 0.00	0.01 ± 0.00	< LOQ	0.01 ± 0.00	0.01 ± 0.00	< LOQ	0.01 ± 0.00	0.01 ± 0.00
DEET	1	pos	0.6 ± 0.1	0.17 ± 0.02	0.09 ± 0.01	2.1 ± 0.5	0.02 ± 0.01	0.022 ± 0.001	1.1 ± 0.3	0.17 ± 0.09
DEET carboxylic acid	1	pos	0.02 ± 0.01	0.036 ± 0.001	0.041 ± 0.002	0.06 ± 0.01	0.07 ± 0.02	0.09 ± 0.02	0.1 ± 0.1	0.08 ± 0.09
Hydroxy-DEET	1	pos	< LOQ	< LOQ	< LOQ	< LOQ	< LOQ	< LOQ	< LOQ	< LOQ
N-ethyl-m-toluamide	1	pos	0.01 ± 0.00	< LOQ	< LOQ	0.02 ± 0.01	0.006 ± 0.001	< LOQ	0.01 ± 0.01	0.01 ± 0.00
Imidacloprid	1	pos	< LOQ	< LOQ	< LOQ	0.02 ± 0.00	< LOQ	< LOQ	0.03 ± 0.00	0.028 ± 0.001
Diuron	2	neg	0.02 ± 0.00	0.02 ± 0.00	< LOQ	0.04 ± 0.02	0.05 ± 0.01	< LOQ	0.02 ± 0.00	0.02 ± 0.00
Didemethyldiuron (DCPU)	2	neg	< LOQ	< LOQ	< LOQ	< LOQ	< LOQ	< LOQ	< LOQ	< LOQ
N-Demethoxylinuron (DCPMU)	2	neg	< LOQ	< LOQ	< LOQ	< LOQ	< LOQ	< LOQ	< LOQ	< LOQ
Isoproturon	1	pos	0.10 ± 0.04	0.08 ± 0.02	0.025 ± 0.002	0.02 ± 0.01	0.02 ± 0.01	0.01 ± 0.00	0.05 ± 0.04	0.05 ± 0.02
Mecoprop	2	neg	0.023 ± 0.002	0.02 ± 0.01	0.02 ± 0.00	0.10 ± 0.03	0.15 ± 0.03	0.085 ± 0.003	0.03 ± 0.01	0.02 ± 0.01
Metamitron	2	pos	< LOQ	< LOQ	< LOQ	< LOQ	< LOQ	< LOQ	< LOQ	< LOQ
Desamino-Metamitron	2	pos	< LOQ	< LOQ	< LOQ	< LOQ	< LOQ	< LOQ	< LOQ	< LOQ
Metazachlor	2	pos	0.01 ± 0.01	0.01 ± 0.00	0.01 ± 0.00	< LOQ	0.01 ± 0.01	0.01 ± 0.00	< LOQ	< LOQ
Metolachlor	2	pos	< LOQ	< LOQ	< LOQ	0.01 ± 0.00	0.01 ± 0.00	0.01 ± 0.00	< LOQ	< LOQ
Metolachlor ESA	2	pos	< LOQ	< LOQ	< LOQ	0.10 ± 0.02	0.08 ± 0.03	0.05 ± 0.01	0.016 ± 0.001	0.01 ± 0.00
Metolachlor OA	2	pos	< LOQ	< LOQ	< LOQ	< LOQ	< LOQ	< LOQ	< LOQ	< LOQ
Terbutryn	2	pos	0.06 ± 0.02	0.06 ± 0.01	0.020 ± 0.001	0.04 ± 0.02	0.04 ± 0.01	0.01 ± 0.00	0.10 ± 0.05	0.07 ± 0.03
Terbuthylazine	2	pos	< LOQ	< LOQ	< LOQ	< LOQ	0.01 ± 0.00	< LOQ	< LOQ	< LOQ
Terbuthylazine-2-Hydroxy	2	pos	0.01 ± 0.00	< LOQ	< LOQ	0.013 ± 0.001	0.03 ± 0.00	< LOQ	0.01 ± 0.00	< LOQ
Irgarol	2	pos	< LOQ	< LOQ	< LOQ	< LOQ	< LOQ	< LOQ	< LOQ	< LOQ
Benzotriazole	1	pos	15 ± 2	7.1 ± 0.6	2.0 ± 0.2	11 ± 2	7 ± 3	0.4 ± 0.1	36 ± 7	25 ± 8
1-Hydroxy-Benzotriazole	1	pos	1.1 ± 0.2	0.32 ± 0.01	0.17 ± 0.02	1.3 ± 0.2	0.19 ± 0.05	< LOQ	1.2 ± 0.1	0.37 ± 0.07
Tetraglyme	2	pos	0.07 ± 0.04	0.028 ± 0.002	0.04 ± 0.01	0.04 ± 0.04	< LOQ	0.05 ± 0.01	0.33 ± 0.05	0.26 ± 0.03
Ethyltriphenylphosphonium	1	pos	< LOQ	< LOQ	< LOQ	< LOQ	< LOQ	< LOQ	< LOQ	< LOQ
Methyltriphenylphosphonium	1	pos	< LOQ	< LOQ	< LOQ	< LOQ	< LOQ	< LOQ	0.01 ± 0.00	0.01 ± 0.00
Tetrabutyltriphenylphosphonium	1	pos	0.01 ± 0.01	0.01 ± 0.00	0.01 ± 0.00	0.01 ± 0.00	0.01 ± 0.00	< LOQ	0.01 ± 0.00	0.008 ± 0.001
(Methoxymethyl)triphenylphosphonium	1	pos	< LOQ	< LOQ	< LOQ	< LOQ	< LOQ	< LOQ	0.01 ± 0.00	< LOQ
Tetrabutylammonium	1	pos	0.03 ± 0.03	0.01 ± 0.00	0.01 ± 0.00	0.01 ± 0.01	0.01 ± 0.01	< LOQ	0.04 ± 0.01	0.04 ± 0.01
Tetrapropylammonium	1	pos	< LOQ	< LOQ	< LOQ	< LOQ	< LOQ	< LOQ	0.03 ± 0.02	0.03 ± 0.02
Caffeine	1	pos	97 ± 7	0.7 ± 0.1	< LOQ	74 ± 8	< LOQ	< LOQ	155 ± 10	0.16 ± 0.03
Triclosan	2	neg	0.05 ± 0.01	< LOQ	< LOQ	0.25 ± 0.04	< LOQ	< LOQ	0.08 ± 0.01	< LOQ
Triclocarban	2	neg	0.01 ± 0.01	< LOQ	< LOQ	0.02 ± 0.01	< LOQ	< LOQ	0.01 ± 0.01	0.01 ± 0.00
Carbanilide	2	neg	0.08 ± 0.06	0.04 ± 0.05	< LOQ	0.05 ± 0.01	0.01 ± 0.01	< LOQ	0.06 ± 0.02	0.01 ± 0.00
Acesulfame	2	neg	27 ± 2	4.7 ± 0.3	3.0 ± 0.3	38 ± 5	1.4 ± 0.2	0.7 ± 0.1	43 ± 2	1.9 ± 0.6
Saccharine	2	neg	25 ± 1	1.6 ± 0.2	0.29 ± 0.04	24 ± 3	0.195 ± 0.006	0.04 ± 0.01	56 ± 5	0.2 ± 0.1
Sucralose	2	neg	4.54 ± 0.06	4.4 ± 0.1	3.5 ± 0.3	10 ± 1	9 ± 3	5 ± 1	9.9 ± 0.5	10 ± 1
Denatonium	1	pos	0.27 ± 0.02	0.21 ± 0.01	0.01 ± 0.00	0.21 ± 0.03	0.2 ± 0.1	0.01 ± 0.00	0.46 ± 0.05	0.45 ± 0.05
Tolylbiguanide	1	pos	< LOQ	< LOQ	< LOQ	< LOQ	0.01 ± 0.00	< LOQ	< LOQ	< LOQ

* carbamazepine could not be evalutated due to background signals

A1.6-B: Concentrations in surface water and bank filtrate

Abbreviations: M = Method, SW = Surface water, BF = Bank filtrate
Concentrations in µg/L

Substance	M	ESI	SW1	SW2	SW3	SW4	BF1	BF2	BF3
Tramadol	1	pos	0.27	0.02	0.04	0.04	0.1	0.04	0.01
O-DM-Tramadol	1	pos	0.2	< LOQ	0.02	< LOQ	0.07	0.05	< LOQ
N-DM-Tramadol	1	pos	0.16	< LOQ	< LOQ	< LOQ	0.01	< LOQ	< LOQ
N,O-DDM-Tramadol	1	pos	0.34	< LOQ	0.04	< LOQ	0.12	0.11	0.03
Tramadol-N-oxide	1	pos	< LOQ	< LOQ	< LOQ	< LOQ	< LOQ	< LOQ	< LOQ
Primidone	1	pos	0.23	< LOQ	< LOQ	0.04	0.1	0.08	0.09
Phenytoin	2	neg	0.01	< LOQ	< LOQ	< LOQ	0.01	0.01	0.001
Carbamazepine (CBZ)	2	pos	0.66	0.03	0.04	0.18	0.73	0.41	0.16
2-Hydroxy-CBZ	2	pos	0.06	< LOQ	< LOQ	< LOQ	0.02	0.02	0.01
3-Hydroxy-CBZ	2	pos	0.06	< LOQ	< LOQ	< LOQ	0.01	0.01	0.001
10-Hydroxy-CBZ	2	pos	0.09	0.02	0.02	0.05	< LOQ	< LOQ	< LOQ
10,11-Dihydro-10,11-dihydroxy-CBZ	2	pos	1.06	0.05	0.06	0.17	0.06	0.11	0.23
9-Carboxylic acid-Acridine	2	pos	0.18	0.01	0.02	0.06	0.98	0.8	0.35
Acridone	2	pos	0.01	< LOQ	< LOQ	0.001	0.001	< LOQ	< LOQ
Lamotrigine	1	pos	0.87	< LOQ	< LOQ	0.09	0.17	0.05	< LOQ
2-N-methyl-Lamotrigine	1	pos	0.04	< LOQ	< LOQ	< LOQ	< LOQ	< LOQ	< LOQ
Gabapentin	1	pos	1.13	0.13	0.19	0.22	0.57	0.54	0.84
Gabapentin Lactam	1	pos	1.35	0.03	0.04	0.07	0.24	0.25	0.15
Levetiracetam	1	pos	< LOQ	< LOQ	< LOQ	< LOQ	0.2	0.04	0.03
Levetiracetam acid	1	pos	< LOQ	< LOQ	< LOQ	< LOQ	< LOQ	< LOQ	< LOQ
Pregabalin	2	pos	0.07	0.06	0.07	0.05	0.06	0.04	0.06
Sulpiride	2	pos	0.36	< LOQ	0.01	0.03	0.02	< LOQ	< LOQ
Amisulpride	1	pos	0.44	0.01	0.01	0.01	< LOQ	< LOQ	< LOQ
O-desmethyl-Amisulpride	1	pos	< LOQ	< LOQ	< LOQ	< LOQ	< LOQ	< LOQ	< LOQ
Oxazepam	1	pos	0.05	< LOQ	0.02	< LOQ	< LOQ	< LOQ	< LOQ
Citalopram	1	pos	0.04	< LOQ	< LOQ	< LOQ	< LOQ	< LOQ	< LOQ
Desmethyl-Citalopram	1	pos	0.03	< LOQ	< LOQ	< LOQ	< LOQ	< LOQ	< LOQ
Didesmethyl-Citalopram	1	pos	< LOQ	< LOQ	< LOQ	< LOQ	< LOQ	< LOQ	< LOQ
Citalopram-N-oxide	1	pos	< LOQ	< LOQ	< LOQ	< LOQ	< LOQ	< LOQ	< LOQ
Venlafaxine (VLX)	1	pos	0.34	0.02	0.01	0.02	< LOQ	< LOQ	< LOQ
O-desmethyl-VLX	1	pos	0.95	0.03	0.02	0.02	0.04	< LOQ	< LOQ
N-desmethyl-VLX	1	pos	0.07	< LOQ	< LOQ	0.01	0.01	< LOQ	< LOQ
N.O-didesmethyl-VLX	1	pos	0.16	< LOQ	< LOQ	< LOQ	< LOQ	< LOQ	< LOQ
VLX-N-oxide	1	pos	0.001	< LOQ	< LOQ	< LOQ	< LOQ	< LOQ	< LOQ
Lidocaine	1	pos	0.13	0.01	0.01	0.01	0.04	0.02	0.01
Nor-Lidocaine	1	pos	0.02	< LOQ	< LOQ	0.01	0.02	0.02	0.01
Flecainide	1	pos	0.24	0.01	0.03	0.02	< LOQ	< LOQ	< LOQ
m-O-dealkylated Flecainide	1	pos	0.01	< LOQ	< LOQ	< LOQ	< LOQ	< LOQ	< LOQ
Hydrochlorothiazide	2	neg	1.7	0.06	< LOQ	< LOQ	0.12	0.05	< LOQ
Chlorothiazide	2	neg	0.09	< LOQ	< LOQ	< LOQ	0.08	0.06	0.04
4-amino-6-chloro-1,3-benzenedisulfonamide	2	neg	0.82	< LOQ	< LOQ	< LOQ	0.2	0.18	0.16
Xipamide	2	neg	< LOQ	< LOQ	< LOQ	< LOQ	< LOQ	< LOQ	< LOQ
Furosemide	2	neg	< LOQ	< LOQ	< LOQ	< LOQ	< LOQ	< LOQ	< LOQ
Torsemide	2	pos	0.13	0.01	0.001	0.01	0.03	0.01	< LOQ
Hydroxy-Torsemide	2	pos	< LOQ	< LOQ	< LOQ	< LOQ	< LOQ	< LOQ	< LOQ
Sotalol	1	pos	0.19	< LOQ	< LOQ	< LOQ	< LOQ	< LOQ	< LOQ
Metoprolol	2	pos	0.15	0.02	0.01	0.01	0.01	< LOQ	< LOQ
Hydroxy-Metoprolol	2	pos	< LOQ	< LOQ	< LOQ	< LOQ	< LOQ	< LOQ	< LOQ
O-desmethyl-Metoprolol	2	pos	< LOQ	< LOQ	< LOQ	< LOQ	< LOQ	< LOQ	< LOQ
Atenolol	1	pos	0.02	< LOQ	< LOQ	< LOQ	< LOQ	< LOQ	< LOQ
Atenolol acid	1	pos	< LOQ	0.02	< LOQ	< LOQ	< LOQ	< LOQ	< LOQ
Hydroxy-Atenolol	1	pos	< LOQ	< LOQ	< LOQ	< LOQ	< LOQ	< LOQ	< LOQ
Enalapril	1	pos	< LOQ	< LOQ	< LOQ	< LOQ	< LOQ	< LOQ	< LOQ
Enalaprilat	1	pos	< LOQ	< LOQ	< LOQ	< LOQ	< LOQ	< LOQ	< LOQ
Ramipril	2	pos	< LOQ	< LOQ	< LOQ	< LOQ	< LOQ	< LOQ	< LOQ
Ramiprilat	2	pos	< LOQ	< LOQ	< LOQ	< LOQ	< LOQ	< LOQ	< LOQ
Valsartan	2	pos	0.03	0.04	0.04	0.03	0.04	0.02	0.01
Valsartan acid	2	pos	2.78	0.11	0.11	1.56	3.27	2.66	2.12
Irbesartan	2	neg	0.35	0.02	0.02	0.01	0.06	0.02	< LOQ
Candesartan	2	pos	1.09	0.03	0.03	0.12	0.31	0.18	0.1
Telmisartan	2	pos	0.36	0.02	0.03	0.09	< LOQ	< LOQ	< LOQ
Olmesartan	2	neg	0.33	0.02	0.03	0.03	0.14	0.13	0.09
Aliksiren	1	pos	0.14	0.01	< LOQ	0.01	< LOQ	< LOQ	< LOQ
Bezafibrate	2	pos	0.01	0.01	< LOQ	< LOQ	< LOQ	0.01	0.01
3-[(4-chlorobenzoyl)amino]-propanoic acid	2	neg	< LOQ	< LOQ	< LOQ	< LOQ	< LOQ	< LOQ	< LOQ
Climbazole	1	pos	0.02	< LOQ	< LOQ	< LOQ	< LOQ	< LOQ	< LOQ
Climbazole-TP	1	pos	0.09	< LOQ	< LOQ	0.02	< LOQ	< LOQ	< LOQ
Trimethoprim	1	pos	0.01	< LOQ	< LOQ	< LOQ	< LOQ	< LOQ	< LOQ
3-desmethyl-TMP	1	pos	< LOQ	< LOQ	< LOQ	< LOQ	< LOQ	< LOQ	< LOQ
5-(2,4,5-Trimethoxy)-2,4-pyrimidinediamnine	1	pos	< LOQ	< LOQ	< LOQ	< LOQ	< LOQ	< LOQ	< LOQ
Sulfamethoxazole (SMX)	2	pos	0.14	< LOQ	< LOQ	< LOQ	< LOQ	< LOQ	< LOQ
Acetyl-SMX	2	pos	< LOQ	< LOQ	< LOQ	< LOQ	< LOQ	< LOQ	< LOQ
Clarithromycin	1	pos	0.08	0.01	0.01	< LOQ	< LOQ	< LOQ	< LOQ
Fluconazole	2	pos	0.06	< LOQ	0.01	0.02	0.04	0.03	0.01
Aciclovir	1	pos	< LOQ	< LOQ	< LOQ	< LOQ	< LOQ	< LOQ	< LOQ
Carboxy-Aciclovir	1	pos	0.64	0.05	0.07	0.15	0.19	0.16	0.07
Emtricitabine	1	pos	< LOQ	< LOQ	< LOQ	< LOQ	< LOQ	< LOQ	< LOQ
Emtricitabine carboxylate	1	pos	0.24	0.02	0.01	0.09	0.22	0.21	0.19
Emtricitabine-S-oxide	1	pos	0.02	< LOQ	< LOQ	< LOQ	< LOQ	< LOQ	< LOQ

Ranitidine	1	pos	0.03	< LOQ	< LOQ	0.02	< LOQ	0.01	< LOQ
Ranitidine-N-oxide	1	pos	< LOQ	< LOQ	< LOQ	< LOQ	< LOQ	< LOQ	< LOQ
Desmethyl-Ranitidine	1	pos	< LOQ	< LOQ	< LOQ	< LOQ	< LOQ	< LOQ	< LOQ
Sitagliptin	1	pos	0.79	0.05	0.07	0.12	< LOQ	< LOQ	< LOQ
Clopidogrel	1	pos	0.001	< LOQ	< LOQ	< LOQ	< LOQ	< LOQ	< LOQ
Clopidogrel acid	1	pos	0.12	0.01	0.01	0.01	0.02	0.01	< LOQ
Bicalutamide	2	neg	0.01	0.001	0.001	0.001	0.001	0.001	< LOQ
Diphenhydramine	2	pos	0.03	< LOQ	< LOQ	< LOQ	< LOQ	< LOQ	< LOQ
N-desmethyl-Diphenhydramine	2	pos	0.01	< LOQ	< LOQ	< LOQ	< LOQ	< LOQ	< LOQ
Diphenhydramine-N-oxide	2	pos	0.01	< LOQ	< LOQ	< LOQ	< LOQ	< LOQ	< LOQ
Cetirizine	1	pos	0.18	< LOQ	< LOQ	0.03	0.01	< LOQ	< LOQ
Fexofenadine	1	pos	0.16	0.08	0.01	0.03	< LOQ	< LOQ	< LOQ
Diatrizoic acid	2	pos	5.32	0.13	0.15	0.15	< LOQ	< LOQ	0.05
Iopamidol	1	pos	0.36	0.34	0.08	1.07	1.39	1.14	0.48
Iopromide	1	pos	0.15	0.14	0.06	0.09	0.13	< LOQ	< LOQ
Iopromide-TP-643	1	pos	0.37	< LOQ	< LOQ	< LOQ	0.12	< LOQ	< LOQ
Iopromide-TP-701A	1	pos	1.36	< LOQ	< LOQ	< LOQ	0.27	0.18	0.33
Iopromide-TP-701B	1	pos	0.17	< LOQ	< LOQ	< LOQ	< LOQ	< LOQ	< LOQ
Iopromide-TP-731B	1	pos	< LOQ	< LOQ	< LOQ	< LOQ	< LOQ	< LOQ	< LOQ
Iopromide-TP-819	1	pos	< LOQ	< LOQ	< LOQ	< LOQ	< LOQ	< LOQ	< LOQ
Iopromide-TP-729A	1	pos	2.38	< LOQ	< LOQ	< LOQ	< LOQ	< LOQ	< LOQ
Iopromide-TP-759	1	pos	0.9	< LOQ	< LOQ	< LOQ	0.2	0.25	0.47
Iomeprol	1	pos	1.2	0.32	0.22	0.59	0.4	0.18	< LOQ
Diclofenac (DCF)	1	pos	< LOQ	0.03	0.03	0.01	0.05	0.03	0.93
4-Hydroxy-DCF	1	pos	0.01	< LOQ	< LOQ	< LOQ	< LOQ	< LOQ	< LOQ
Carboxy-DCF	1	pos	0.02	< LOQ	< LOQ	< LOQ	0.01	0.01	0.001
DCF Lactam	1	pos	0.01	< LOQ	< LOQ	0.001	< LOQ	< LOQ	< LOQ
Ibuprofen (IBU)	2	neg	< LOQ	< LOQ	< LOQ	< LOQ	< LOQ	< LOQ	< LOQ
2-Hydroxy-IBU	2	neg	< LOQ	< LOQ	< LOQ	< LOQ	< LOQ	< LOQ	< LOQ
Carboxy-IBU	2	neg	< LOQ	< LOQ	< LOQ	< LOQ	< LOQ	< LOQ	< LOQ
Naproxen	2	neg	< LOQ	< LOQ	< LOQ	< LOQ	< LOQ	< LOQ	< LOQ
O-desmethyl-Naproxen	2	neg	< LOQ	< LOQ	< LOQ	< LOQ	< LOQ	< LOQ	< LOQ
Oxypurinol	2	neg	11.41	0.38	0.66	1.59	3.09	< LOQ	0.21
Carbendazim	1	pos	0.03	0.02	0.001	0.001	0.01	0.01	0.001
Epoxiconazole	2	pos	< LOQ	< LOQ	< LOQ	< LOQ	< LOQ	< LOQ	< LOQ
Propiconazole	2	pos	< LOQ	< LOQ	< LOQ	< LOQ	< LOQ	< LOQ	< LOQ
Tebuconazole	2	pos	< LOQ	0.001	0.001	< LOQ	< LOQ	< LOQ	< LOQ
DEET	1	pos	0.11	0.02	0.02	0.03	0.03	0.02	0.02
DEET carboxylic acid	1	pos	0.33	0.01	0.01	0.01	< LOQ	< LOQ	0.01
Hydroxy-DEET	1	pos	< LOQ	< LOQ	< LOQ	< LOQ	< LOQ	< LOQ	< LOQ
N-ethyl-m-toluamide	1	pos	< LOQ	< LOQ	< LOQ	< LOQ	< LOQ	< LOQ	< LOQ
Imidacloprid	1	pos	< LOQ	< LOQ	< LOQ	< LOQ	< LOQ	< LOQ	< LOQ
Diuron	2	neg	0.01	0.001	0.001	0.001	0.01	0.01	0.001
Didemethyldiuron (DCPU)	2	neg	< LOQ	< LOQ	< LOQ	< LOQ	< LOQ	< LOQ	< LOQ
N-Demethoxylinuron (DCPMU)	2	neg	< LOQ	< LOQ	< LOQ	0.001	0.001	0.001	< LOQ
Isoproturon	1	pos	0.02	0.01	0.02	0.001	0.001	0.001	0.001
Mecoprop	2	neg	0.05	< LOQ	< LOQ	< LOQ	< LOQ	< LOQ	0.01
Metamitron	2	pos	< LOQ	< LOQ	< LOQ	< LOQ	< LOQ	< LOQ	< LOQ
Desamino-Metamitron	2	pos	< LOQ	< LOQ	< LOQ	< LOQ	< LOQ	< LOQ	< LOQ
Metazachlor	2	pos	0.05	0.01	0.01	< LOQ	< LOQ	< LOQ	< LOQ
Metolachlor	2	pos	0.001	0.01	0.02	0.001	< LOQ	< LOQ	< LOQ
Metolachlor ESA	2	pos	0.03	< LOQ	< LOQ	0.05	0.06	0.04	0.03
Metolachlor OA	2	pos	0.01	< LOQ	< LOQ	0.04	0.05	0.03	0.03
Terbutryn	2	pos	0.02	0.001	0.001	0.001	0.001	0.001	< LOQ
Terbuthylazine	2	pos	0.001	0.01	0.01	0.01	< LOQ	< LOQ	< LOQ
Terbuthylazine-2-Hydroxy	2	pos	0.03	0.01	0.01	0.01	0.02	0.01	0.001
Irgarol	2	pos	0.001	< LOQ	< LOQ	0.001	0.001	0.001	< LOQ
Benzotriazole	1	pos	5.02	0.23	0.2	0.62	1.54	0.73	0.3
1-Hydroxy-Benzotriazole	1	pos	0.04	< LOQ	< LOQ	< LOQ	< LOQ	< LOQ	< LOQ
Tetraglyme	2	pos	0.02	0.06	< LOQ	< LOQ	0.02	0.01	0.04
Ethyltriphenylphosphonium	1	pos	0.03	0.01	< LOQ	< LOQ	< LOQ	< LOQ	< LOQ
Methyltriphenylphosphonium	1	pos	0.35	0.03	< LOQ	< LOQ	< LOQ	< LOQ	< LOQ
Tetrabutyltriphenylphosphonium	1	pos	0.001	0.001	< LOQ	0.001	0.001	0.001	0.001
(Methoxymethyl)triphenylphosphonium	1	pos	0.65	0.05	< LOQ	< LOQ	< LOQ	< LOQ	< LOQ
Tetrabutylammonium	1	pos	0.07	0.03	< LOQ	< LOQ	< LOQ	< LOQ	< LOQ
Tetrapropylammonium	1	pos	< LOQ	0.01	< LOQ	< LOQ	< LOQ	< LOQ	< LOQ
Caffeine	1	pos	< LOQ	0.08	0.13	0.05	0.001	0.001	0.01
Triclosan	2	neg	< LOQ	< LOQ	< LOQ	< LOQ	< LOQ	< LOQ	< LOQ
Triclocarban	2	neg	< LOQ	< LOQ	< LOQ	0.001	< LOQ	< LOQ	< LOQ
Carbanilide	2	neg	< LOQ	< LOQ	< LOQ	< LOQ	< LOQ	< LOQ	< LOQ
Acesulfame	2	neg	0.33	0.41	0.42	0.33	0.5	0.5	2.35
Saccharine	2	neg	0.03	0.06	0.05	0.04	< LOQ	< LOQ	0.04
Sucralose	2	neg	29.93	0.31	0.44	0.79	0.65	0.73	0.65
Denatonium	1	pos	0.22	0.02	0.02	0.03	0.001	0.001	< LOQ
Tolylbiguanide	1	pos	< LOQ	< LOQ	< LOQ	< LOQ	< LOQ	< LOQ	< LOQ

Appendix B

Supplementary data for Chapter 3:
Indirect Potable Reuse: removal efficiencies in sequential biofil-
tration (SBF) and soil aquifer treatment (SAT) and deduction
of indicator substances

Supporting Information

A2.1: Substance data, including name, abbreviation, usage, health related threshold and orientation values, degradability in conventional WWTPs, physicochemical parameters and method LOQ

Substance	Abbreviation	Use	Thresholds µg/L	Degradability in conventional WWTPs	pKa	Charge state	LogD	LOQ µg/L
		Substances uncharged at pH7						
Primidone	PRIM	Antiepileptic	3[1)]	Stable [a),b)]	11.5	neutral	1.12	0.02
Phenytoin	PHEN	Antiepileptic	-	Stable [a)]	8.49	neutral	2.13	0.001
Carbamazepine (CBZ)	CBZ	Antiepileptic	0.3[1)], 100[2),3)]	Stable [a),b)]	>13.5	neutral	2.77	0.001
2-Hydroxy-CBZ	CBZ-2OH	CBZ-metabolite	-	Stable [a),d)]	9.19	neutral	2.46	0.005
3-Hydroxy-CBZ	CBZ-3OH	CBZ-metabolite	-	Stable [a),d)]	9.15	neutral	2.46	0.002
10-Hydroxy-CBZ	CBZ-10OH	CBZ-metabolite	-	Stable [a),d)]	12.84	neutral	1.73	0.01
10,11-Dihydro-10,11-dihydroxy-CBZ	CBZ-DHDH	CBZ-metabolite		Stable [a),d)]	12.84	neutral	0.81	0.01
9-Carboxylic acid-Acridine	CA-ACRI	CBZ-TP	-	Stable [a),d)]	0.75, 6.81	zwitter	0.87	0.01
Acridone	ACRD	CBZ-TP	-	Stable [a),d)]	<1	neutral	4.20	0.001
Lamotrigine	LAM	Antiepileptic	0.3[1)]	Stable [a)]	>13.5, 5.89	neutral	1.89	0.035
2-N-methyl-Lamotrigine	LAM-2N	LAM-metabolite	-	*n.i.*	>13.5, <1	neutral	-0.92	0.02
Oxazepam	OXA	Psycholeptic	-	Stable [b)]	10.61, <1	neutral	2.92	0.005
Hydrochlorothiazide	HCT	Diuretic	-	Degra [e)]	9.09	neutral	-0.58	0.015
Chlorothiazide	CT	HCT-metabolite	-	Formation [a)]	9.19	neutral	-0.45	0.005
4-amino-6-chloro-1,3-benzenedisulfonamide	HCT-TP	HCT-metabolite	-	Stable [a)]	9.19, <1	neutral	-1.04	0.01
Climbazole	CLIM	Antifungal	-	Degra [a)]	6.49	neutral	4.25	0.005
Climbazole-OH	CLIM-OH	CLIM-TP	-	Formation	13.23, 6.53	neutral	3.56	0.02
Fluconazole	FLUC	Antimycotics	-	Degra [a),b)]	12.68, 2.3	neutral	0.56	0.005
Aciclovir	ACI	Antiviral	0.3[1)]	Degra [a)]	11.99, 3.02	neutral	-1.03	0.025
Carboxy-Aciclovir	ACI-COOH	ACI-metabolite/TP	-	Stable	3.44, 2.64	neg	-4.23	0.03
Emtricitabine	EMT	Antiviral	-	Degra [a)]	>13.5	neutral	-0.90	0.02
Emtricitabine carboxylate	EMT-COOH	EMT-TP	-	Formation [a)]	3.3	neg	-3.88	0.01
Emtricitabine-S-oxide	EMT-SO	EMT-TP	-	Degra [a)]	>13.5	neutral	-2.27	0.02
Clopidogrel	CLP	Antithrombotic	-	Degra [a),e)]	4.77	neutral	4.03	0.001
Clopidogrel acid	CLP-COOH	CLP-metabolite	-	Stable [a)]	1.81, 7.53	zwitter	1.21	0.005
Bicalutamide	BIC	Antineoplastic	-	Stable [a)]	11.78	neutral	2.71	0.001
Iopamidol	IOPA	Contrast Medium	1[1)], 400[5)]	Stable [a)]	11, <1	neutral	-0.74	0.05
Iopromide	IOPR	Contrast Medium	750[5)]	Degra [a)]	11.09, <1	neutral	-0.45	0.05
Iopromide-TP-643	IOPR-643	IOPR-TP	-	Formation [a)]	11, <1	neutral	1.75	0.1
Iopromide-TP-701A	IOPR-701A	IOPR-TP	-	Formation [a)]	1.84, <1	negative	-2.07	0.05
Iopromide-TP-701B	IOPR-701B	IOPR-TP	-	Formation	1.74, <1	negative	-2.07	0.05

Name	Abbrev.	Class	Conc.	Behavior	pKa	Charge	logD	
Iopromide-TP-731B	IOPR-731B	IOPR-TP	-	Formation	1.78, <1	negative	-2.55	0.05
Iopromide-TP-819	IOPR-819	IOPR-TP	-	Formation	1.51, <1	negative	-6.84	0.2
Iopromide-TP-729A	IOPR-729A	IOPR-TP	-	Formation	1.27, <1	negative	-1.79	0.08
Iopromide-TP-759	IOPR-759	IOPR-TP	-	Formation [a]	1.46	negative	-5.89	0.2
Iomeprol	IOME	Contrast Medium	-	Degra	11.73, <1	neutral	-1.45	0.05
Carbendazim	CARB	Fungicide	0.1[2], 100[5]	Stable [a]	9.7, 4.28	neutral	1.80	0.002
Epoxiconazole	EPOX	Fungicide	0.1[2]	*n.i.*	2	neutral	3.74	0.005
Propiconazole	PROP	Fungicide	0.1[2]	Stable [a]	1.95	neutral	4.33	0.005
Tebuconazole	TEBU	Fungicide	0.1[2]	Stable [a]	>13.5, 2.01	neutral	3.69	0.001
DEET	DEET	Repellant	-	Degra [a]	<1	neutral	2.50	0.001
Hydroxy-DEET	DEET-OH	DEET-TP	-	*n.i.*	>13.5, <1	neutral	1.22	0.005
N-ethyl-m-toluamide	DEET-TP	DEET-TP	-	*n.i.*	15.09, <1	neutral	1.92	0.005
DEET carboxylic acid	DEET-COOH	DEET-TP	-	*n.i.*	3.88, <1	negative	-1.33	0.005
Diuron	DIU	Herbicide/Algicide	0.1[2], 30[5], 0.2[6]	Degra	13.18	neutral	2.53	0.002
Didemethyldiuron (DCPU)	DCPU	DIU-TP	-	*n.i.*	13.45	neutral	2.09	0.01
N-Demethoxylinuron (DCPMU)	DCPMU	DIU-TP	-	*n.i.*	13.31	neutral	2.31	0.001
Isoproturon	ISO	Herbicide	0.1[2], 0.3[6]	Stable [a]	>13.5	neutral	2.57	0.001
Metamitron	META	Herbicide	0.1[2]	*n.i.*	2.78	neutral	0.44	0.015
Desamino-Metamitron	META-D	META-TP	-	*n.i.*	11.98, 2.19	neutral	1.81	0.01
Metazachlor	METAZ	Herbicide	0.1[2]	Degra [a]	2.34	neutral	2.98	0.001
Metolachlor	METOL	Herbicide	0.1[2], 300[5]	*n.i.*		neutral	3.48	0.001
Metolachlor ESA	METOL-E	METOL-TP	-	*n.i.*	-0.68	negative	-0.26	0.005
Metolachlor OA	METOL-A	METOL-TP	-	*n.i.*	3.21	negative	-0.46	0.01
Terbutryn	TERB	Herbicide/Algicide	0.065[6]	Stable [a]	>13.5, 6.72	neutral	2.66	0.001
Terbuthylazine	TERZ	Herbicide	0.1[2]	Degra	>13.5, 4.18	neutral	2.48	0.002
Terbuthylazine-2-Hydroxy	TERZ-OH	TERZ-TP	-	Formation	12.45, 5.83	neutral	0.25	0.002
Irgarol	IRG	Herbicide/Algicide	0.0025[6]	*n.i.*	>13.5, 6.68	neutral	2.82	0.001
Benzotriazole	BENZ	Industrial	3[1]	Degra [a]	8.63, <1	neutral	1.29	0.09
Tetraglyme	TETR	Industrial	-	*n.i.*		neutral	-0.06	0.001
Caffeine	CAF	Life-style	0.35[5]	Degra [a,c]	<1	neutral	-0.55	0.002
Triclosan	TRIC	Personal care product	0.35[5]	Degra [c]	7.68	neutral	4.98	0.01
Triclocarban	TRICC	Personal care product	-	Degra [a]	11.42	neutral	4.93	0.001
Carbanilide	TRICC-TP	TRICC-TP	-	*n.i.*	11.53	neutral	3.12	0.02
Sucralose	SUC	Sweetener	0.1[5]	Stable [a]	11.91	neutral	-0.47	0.06
Substances with negative charge at pH 7								
Xipamide	XIP	Diuretic	-	Stable [a]	3.66, <1	negative	1.11	0.02
Furosemide	FURO	Diuretic	-	Degra e)	4.25, <1	negative	-0.94	0.01
Torsemide	TORA	Diuretic	-	Stable [a,b,e]	5.92, 4.2	negative	1.22	0.005

Hydroxy-Torsemide	TORA-OH	TORA-TP	-	*n.i.*	5.92, 4.2	negative	-0.06 0.002
Ramipril	RAM	ACE Inhibitor	-	Degra [a)]	3.75, 5.2	negative	0.04 0.005
Ramiprilat	RAMt	RAM-TP	-	Degra [a)]	3.13, 8.05	zwitter	-2.91 0.075
Valsartan	VAL	Angiotensin II Antagonists	0.3[1)]	Degra [a),e)]	4.35, <1	negative	1.49 0.005
Valsartan acid	VALac	VAL-T	0.3[1)]	Formation [a)]	4.03, <1	negative	-0.73 0.005
Irbesartan	IRB	Angiotensin II Antagonist	-	Stable [a),b),c)]	5.85, 4.12	negative	4.40 0.005
Candesartan	CAN	Angiotensin II Antagonist	0.3[1)]	Stable [a),b)]	3.51, 1.25	negative	0.92 0.002
Telmisartan	TEL	Angiotensin II Antagonist	-	Stable [a)]	3.62, 5.86	negative	5.09 0.005
Olmesartan	OLM	Angiotensin II Antagonist	0.3[1)]	Stable [a)]	0.89, 5.33	negative	-0.75 0.02
Bezafibrate	BZF	Lipid modifying agent	300[4)]	Degra [a),b),c),d)]	3.83, <1	negative	0.97 0.002
Sulfamethoxazole	SMX	Antibacterials	35[4)], 0.01[5)]	Degra [a),b),c),d)]	6.16, 1.97	negative	0.15 0.01
Acetyl-Sulfamethoxazole	SMXac	SMX-TP	-	Degra [a)]	5.88, <1	negative	0.10 0.02
Diatrizoic acid	DIA	Contrast Medium	1[1)], 0.35[4)]	Stable [a)]	2.17	negative	-0.62 0.015
Diclofenac	DCF	Antiphlogistic	0.3[1)], 1.8[3),4)]	Degra [a),e)]	4	negative	1.37 0.002
4-Hydroxy-Diclofenac	DCF-4-OH	DCF-TP	-	Degra [a)]	3.76, <1	negative	0.89 0.002
Diclofenac Lactam	DCFlac	DCF-TP	-	Degra [a)]	12.05	neutral	3.80 0.001
Carboxy-Diclofenac	DCF-COOH	DCF-TP	-	Degra [a)]	3.79	negative	2.54 0.002
Ibuprofen	IBU	Antiphlogistic	1[1)], 400[4)]	Degra [a),c),e)]	4.85	negative	1.71 0.02
Carboxy-Ibuprofen	IBU-COOH	IBU-TP	-	Degra [a),d)]	3.97	negative	-2.36 0.015
Naproxen	NPX	Antiphlogistic	220[4)]	Degra [a),c),e)]	4.19	negative	0.25 0.015
O-desmethyl-Naproxen	NPX-O-DM	NPX-TP	-	Degra [a)]	4.34	negative	0.23 0.01
Oxypurinol	OXY	Antigout	0.3[1)]	Stable [a)]	5.28, <1	negative	-3.13 0.15
Mecoprop	MEC	Herbicide	-	Stable [a)]	3.47	negative	-0.25 0.01
Acesulfame	ACE	Sweetener	-	Degra [a)]	3.02	negative	-1.49 0.01
Saccharine	SAC	Sweetener	-	Degra [a)]	1.94	negative	-0.49 0.005
Substances with positive charge or zwitter ionic form at pH 7							
Tramadol	TRAM	Analgesic	-	Stable [a),b),c)]	>13.5, 9.23	positive	0.24 0.002
O-desmethyl-Tramadol	TRAM-O-DM	TRAM-metabolite	-	Stable [a),c)]	9.62, 8.97	positive	0.10 0.01
N-desmethyl-Tramadol	TRAM-N-DM	TRAM-metabolite	-	Stable [a),c)]	>13.5, 9.89	positive	-0.66 0.01
N,O-didesmethyl-Tramadol	TRAM-DDM	TRAM-metabolite	-	Stable [a)]	9.22, 10.02	positive	-0.74 0.015
Tramadol-N-oxide	TRAM-NO	TRAM-TP	-	*n.i.*	>13.5, 4.4	zwitter	1.33 0.015
Gabapentin	GABA	Antiepileptic	1[1)]	Stable [a)]	4.63, 9.91	zwitter	-1.27 0.02
Gabapentin Lactam	GABAlac	GABA-metabolite/TP	1[1)]	Formation [a)]	>13.5, <1	neutral	1.03 0.01
Sulpiride	SULP	Antidepressant	-	Stable [a)]	10.24, 8.39	positive	-1.07 0.005
Amisulpride	AMIS	Antidepressant	-	Stable [a)]	>13.5, 7.05	positive	-0.08 0.005
O-desmethyl-Amisulpride	AMIS-O-DM	AMI-metabolite	-	*n.i.*	6.28, 7.26	zwitter	-0.15 0.005

A2.1

Compound	Abbr.	Class		Stability	pKa	Charge		
Citalopram	CIT	Antidepressant	-	Stable [a),b),c)]	9.78	positive	1.14	0.01
Desmethyl-Citalopram	CIT-DM	CIT-metabolite	-	Stable [a),c)]	10.54	positive	0.32	0.001
Didesmethyl-Citalopram	CIT-DDM	CIT-metabolite	-	n.i.	10.02	positive	0.14	0.025
Citalopram-N-oxide	CIT-NO	CIT-metabolite	-	n.i.	4.48	zwitter	2.64	0.005
Venlafaxine	VLX	Antidepressant	-	Stable [a),c),e)]	>13.5, 8.91	positive	0.84	0.002
O-desmethyl-Venlafaxine	VLX-O-DM	VLX-metabolite	-	Stable [a)]	10.11, 8.87	positive	0.69	0.01
N-desmethyl-Venlafaxine	VLX-N-DM	VLX-metabolite	-	Stable [a)]	>13.5, 9.78	positive	-0.30	0.005
N,O-didesmethyl-Venlafaxine	VLX-DDM	VLX-metabolite	-	Stable [a)]	10.29, 9.57	positive	-0.43	0.01
Venlafaxine-N-oxide	VLX-NO	VLX-TP	-	n.i.	>13.5, 4.34	zwitter	1.61	0.005
Lidocaine	LID	Antiarrhythmic	-	Stable [a)]	>13.5, 7.75	positive	2.02	0.001
Nor-Lidocaine	LIDnor	LID-metabolite	-	Stable [a)]	>13.5, 8.58	positive	0.52	0.005
Sotalol	SOT	Beta-Blocker	-	Stable [a),b),e)]	10.07, 9.43	positive	-2.47	0.045
Metoprolol	METO	Beta-Blocker	25[4)]	Stable [a),b),c)]	>13.5, 9.67	positive	-0.73	0.005
Hydroxy-Metoprolol	METO-OH	METO-metabolite	-	Degra [a)]	>13.5, 9.67	positive	-1.73	0.015
O-desmethyl-Metoprolol	METO-O-DM	METO-metabolite	-	n.i.	>13.5, 9.67	positive	-1.45	0.005
Atenolol	ATE	Beta-Blocker	-	Degra [a),c),e)]	>13.5, 9.67	positive	-2.14	0.01
Atenolol acid	ATE-COOH	ATE-metabolite	-	Stable [a)]	3.54, 9.67	zwitter	-1.24	0.015
Hydroxy-Atenolol	ATE-OH	ATE-metabolite	-	Degra [a)]	12.47, 9.67	positive	-2.86	0.005
Aliksiren	ALIS	Renin-inhibitor	-	Degra [a)]	>13.5, 9.57	positive	0.68	0.02
Trimethoprim	TMP	Antibiotic	70[4)]	Degra [a),e)]	7.16	positive	0.92	0.005
3-desmethyl-TMP	TMP-3-DM	TMP-TP	-	Degradable [a)]	10, 7.16	positive	0.77	0.002
5-(2,4,5-Trimethoxy)-2,4-pyrimidinediamnine	TMP-TP	TMP-TP	-	Degradable	7.34	positive	0.67	0.035
Clarithromycin	CLARI	Antibiotic	250[4)]	Degradable [a),e)]	12.46, 8.38	positive	1.84	0.001
Ranitidine	RANI	H2-receptor antagonsist	-	Degradable [a),c),e)]	7.8	zwitter	0.04	0.01
Desmethyl-Ranitidine	RANI-DM	RANI-metabolite	-	n.i.	8.4	zwitter	-0.80	0.03
Ranitidine-N-oxide	RANI-NO	RANI-TP	-	n.i.	>13.5, 3.76	zwitter	-0.13	0.01
Sitagliptin	SITA	used in diabetes	-	Degradable [a)]	8.78	positive	-0.51	0.01
Diphenhydramine	DIP	Antihistamine	-	Degradable [a)]	8.87	positive	1.69	0.005
N-desmethyl-Diphenhydramine	DIP-N-DM	DIP-metabolite/TP	-	Stable [a)]	9.68	positive	0.69	0.005
Diphenhydramine-N-oxide	DIP-NO	DIP-TP	-	Stable	4.14	zwitter	2.53	0.005
Cetirizine	CET	Antihistamine	-	Stable [a),c)]	3.59, 7.42	zwitter	0.77	0.005
Fexofenadine	FEX	Antihistamine	-	Stable [a),c)]	4.04, 9.01	zwitter	2.94	0.005
Imidacloprid	IMI	Insecticide	-	Stable [a)]	10.6, 6.75	zwitter	0.68	0.025
Denatonium	DEN	Bitterant	-	Stable [a)]	12.14	positive	0.41	0.001
Tolylbiguanide	TOLY	Industrial	-	n.i.	9.01	positive	1.21	0.005
Ethyltriphenylphosphonium	ETP	Industrial	-	n.i.	-	positive	4.98	0.005
Methyltriphenylphosphonium	MTP	Industrial	-	n.i.	-	positive	4.73	0.002
Tetrabutyltriphenylphosphonium	TBTP	Industrial	-	n.i.	-	positive	5.47	0.001

(Methoxymethyl)triphenylphosphonium	MMTP	Industrial	-	*n.i.*	-	positive	4.33	0.01
Tetrabutylammonium	TBA	Industrial	-	*n.i.*	-	positive	1.32	0.001
Tetrapropylammonium	TPA	Industrial	-	*n.i.*	-	positive	-0.45	0.002

n.i . No information

[1] German precautionary health-related orientation values, [2] European Drinking Water Directive, [3] Water quality control policy for potable reuse by the World Health Organization,

[4] Guidelines for water recycling in Australia, [5] Water quality control policy for recycled water of California, [6] environmental quality standards of the Directive 2013/39/EU

[a] Hermes et al. (2018), [b] Gurke et al. (2015), [c] Petrie et al. (2016), [d] Evgenidou et al. (2015), [e] Gros et al. (2012)

A2.2: Redox- and Bulk-Parameters in Sequential Biofiltration (SBF)

A2.3: Concentrations and Removal in Sequential Biofiltration (SBF)

|				SBF							SAT				
			LOQ	Concentrations [µg/L] in the effluent of the columns				Removal [%]			Concentrations [µg/L]			Removal [%]	
Substance	Abbreviation	Use	[µg/L]	Feed (spike)	A	A_S1	A_S2	A	A_S1	A_S2	Feed	SAT_1	SAT_2	SAT_1	SAT_2
				Substances uncharged at pH7											
Primidone	PRIM	Antiepileptic	0.02	1.13 ± 0.05	1.13 ± 0.54	1.17 ± 0.06	1.13 ± 0.06	0 ± 0	0 ± 10	0 ± 10	0.03 ± 0.02	0.02 ± 0.01	0.020 ± 0.001	40 ± 10	50 ± 10
Phenytoin	PHEN	Antiepileptic	0.001	0.96 ± 0.05	0.92 ± 0.46	0.94 ± 0.02	0.85 ± 0.05	10 ± 10	0 ± 0	10 ± 10	0.07 ± 0.01	0.060 ± 0.001	0.050 ± 0.001	20 ± 10	30 ± 10
Carbamazepine (CBZ)	CBZ	Antiepileptic	0.001	1.13 ± 0.05	1.17 ± 0.36	1.17 ± 0.06	1.100 ± 0.001	0 ± 0	0 ± 0	0 ± 0	0.020 ± 0.001	0.030 ± 0.001	0.030 ± 0.001	-30 ± 10	-20 ± 10
2-Hydroxy-CBZ	CBZ-2OH	CBZ-metabolite	0.005	0.05 ± 0.01	0.05 ± 0.01	0.05 ± 0.01	0.04 ± 0.01	0 ± 0	0 ± 0	10 ± 10	< LOQ	< LOQ	< LOQ		
3-Hydroxy-CBZ	CBZ-3OH	CBZ-metabolite	0.002	0.06 ± 0.01	0.06 ± 0.01	0.07 ± 0.01	0.06 ± 0.01	0 ± 0	-10 ± 10	-10 ± 10	< LOQ	< LOQ	< LOQ	-	-
10-Hydroxy-CBZ	CBZ-10OH	CBZ-metabolite	0.01	0.34 ± 0.02	0.17 ± 0.09	0.06 ± 0.02	0.02 ± 0.01	50 ± 20	80 ± 30	100 ± 0	0.28 ± 0.01	0.1 ± 0.03	0.080 ± 0.001	60 ± 10	70 ± 0
10,11-Dihydro-10,11-dihydroxy-CBZ	CBZ-DHDH	CBZ-metabolite	0.01	0.94 ± 0.04	0.93 ± 0.12	0.91 ± 0.04	0.89 ± 0.06	0 ± 0	0 ± 0	10 ± 0	0.17 ± 0.01	0.14 ± 0.01	0.13 ± 0.01	20 ± 0	30 ± 10
9-Carboxylic acid-Acridine	CA-ACRI	CBZ-TP	0.01	0.35 ± 0.04	0.37 ± 0.03	0.46 ± 0.03	0.35 ± 0.09	0 ± 10	-30 ± 30	0 ± 30	0.11 ± 0.03	0.07 ± 0.04	0.06 ± 0.02	30 ± 30	40 ± 20
Acridone	ACRD	CBZ-TP	0.001	0.010 ± 0.001	0.010 ± 0.001	0.001 ± 0.001	0.010 ± 0.001	-10 ± 10	50 ± 30	40 ± 10	0.001 ± 0.000	0.010 ± 0.001	0.010 ± 0.001	-360 ± 110	-140 ± 40
Lamotrigine	LAM	Antiepileptic	0.035	1.07 ± 0.07	1.09 ± 0.25	1.200 ± 0.001	1.23 ± 0.06	0 ± 10	-10 ± 10	-20 ± 10	0.29 ± 0.04	0.24 ± 0.04	0.21 ± 0.01	20 ± 10	30 ± 10
2-N-methyl-Lamotrigine	LAM-2N	LAM-metabolite	0.02	< LOQ	< LOQ	< LOQ	< LOQ	-	-	-	< LOQ	< LOQ	< LOQ	-	-
Oxazepam	OXA	Psycholeptic	0.005	0.030 ± 0.001	0.03 ± 0.01	0.030 ± 0.001	0.030 ± 0.001	0 ± 0	0 ± 0	0 ± 0	0.07 ± 0.01	0.05 ± 0.01	0.040 ± 0.001	30 ± 0	40 ± 10
Hydrochlorothiazide	HCT	Diuretic	0.015	3.13 ± 0.1	3.2 ± 0.17	3.17 ± 0.06	3.1 ± 0.1	0 ± 0	0 ± 0	0 ± 0	1.68 ± 0.19	1.25 ± 0.16	1.07 ± 0.03	30 ± 10	40 ± 10
Chlorothiazide	CT	HCT-metabolite	0.005	0.12 ± 0.01	0.13 ± 0.01	0.15 ± 0.01	0.15 ± 0.01	-10 ± 10	-20 ± 20	-20 ± 10	0.07 ± 0.01	0.13 ± 0.01	0.13 ± 0.001	-90 ± 30	-80 ± 20
4-amino-6-chloro-1,3-benzenedisulfonamide	HCT-TP	HCT-metabolite	0.01	0.39 ± 0.02	0.4 ± 0.18	0.42 ± 0.02	0.42 ± 0.02	0 ± 0	-10 ± 0	-10 ± 0	0.46 ± 0.04	0.46 ± 0.03	0.41 ± 0.01	0 ± 10	10 ± 10
Climbazole	CLIM	Antifungal	0.005	0.72 ± 0.08	0.64 ± 0.31	0.35 ± 0.04	0.020 ± 0.001	10 ± 10	40 ± 30	100 ± 0	0.020 ± 0.001	0.010 ± 0.001	0.010 ± 0.001	80 ± 0	80 ± 0
Climbazole-OH	CLIM-OH	CLIM-TP	0.02	0.07 ± 0.01	0.14 ± 0.03	0.25 ± 0.02	0.1 ± 0.02	-110 ± 40	-200 ± 50	-50 ± 40	0.05 ± 0.001	0.020 ± 0.001	0.020 ± 0.001	60 ± 10	60 ± 0
Fluconazole	FLUC	Antimycotics	0.005	0.08 ± 0.01	0.08 ± 0.01	0.08 ± 0.01	0.08 ± 0.01	0 ± 0	0 ± 10	0 ± 10	0.010 ± 0.001	0.010 ± 0.001	0.010 ± 0.001	-20 ± 10	-10 ± 10
Aciclovir	ACI	Antiviral	0.025	0.17 ± 0.06	0.1 ± 0.05	0.06 ± 0.03	0.03 ± 0.01	40 ± 20	60 ± 10	80 ± 10	0.04 ± 0.001	0.03 ± 0.001	0.030 ± 0.001	30 ± 10	30 ± 10
Carboxy-Aciclovir	ACI-COOH	ACI-metabolite/TP	0.03	1.78 ± 0.13	1.77 ± 0.28	1.93 ± 0.31	1.9 ± 0.35	0 ± 10	-10 ± 20	-10 ± 10	0.38 ± 0.07	0.17 ± 0.06	0.11 ± 0.03	60 ± 10	70 ± 10
Emtricitabine	EMT	Antiviral	0.02	0.07 ± 0.03	0.04 ± 0.02	0.020 ± 0.001	0.020 ± 0.001	40 ± 10	60 ± 30	60 ± 30	0.040 ± 0.001	0.020 ± 0.001	0.020 ± 0.001	50 ± 0	50 ± 0
Emtricitabine carboxylate	EMT-COOH	EMT-TP	0.01	0.35 ± 0.03	0.43 ± 0.17	0.32 ± 0.07	0.29 ± 0.09	-20 ± 20	0 ± 0	20 ± 20	0.37 ± 0.01	0.37 ± 0.02	0.31 ± 0.03	0 ± 10	20 ± 10
Emtricitabine-S-oxide	EMT-SO	EMT-TP	0.02	< LOQ	< LOQ	< LOQ	< LOQ	-	-	-	< LOQ	< LOQ	< LOQ	-	-
Clopidogrel	CLP	Antithrombotic	0.001	0.010 ± 0.001	0.010 ± 0.001	< LOQ	< LOQ	50 ± 20	80 ± 10	90 ± 0	< LOQ	< LOQ	< LOQ	70 ± 0	70 ± 0
Clopidogrel acid	CLP-COOH	CLP-metabolite	0.005	0.16 ± 0.01	0.14 ± 0.01	0.150 ± 0.001	0.14 ± 0.01	10 ± 10	10 ± 10	10 ± 10	0.09 ± 0.02	0.02 ± 0.01	0.010 ± 0.01	80 ± 10	90 ± 0
Bicalutamide	BIC	Antineoplastic	0.001	0.04 ± 0.01	0.04 ± 0.01	0.04 ± 0.01	0.04 ± 0.01	0 ± 0	0 ± 0	-10 ± 20	< LOQ	< LOQ	< LOQ	-	-
Iopamidol	IOPA	Contrast Medium	0.05	< LOQ	< LOQ	< LOQ	< LOQ	-	-	-	< LOQ	< LOQ	< LOQ	-	-
Iopromide	IOPR	Contrast Medium	0.05	1.7 ± 0.92	0.58 ± 0.44	0.10 ± 0.09	0.050 ± 0.001	60 ± 20	90 ± 10	100 ± 0	< LOQ	< LOQ	< LOQ	-	-
Iopromide-TP-643	IOPR-643	IOPR-TP	0.1	< LOQ	< LOQ	< LOQ	< LOQ	-	-	-	0.100 ± 0.001	0.20 ± 0.05	0.20 ± 0.01	-100 ± 50	-100 ± 10
Iopromide-TP-701A	IOPR-701A	IOPR-TP	0.05	0.13 ± 0.07	0.13 ± 0.07	0.23 ± 0.18	0.34 ± 0.31	-20 ± 20	-70 ± 60	-180 ± 90	0.07 ± 0.01	0.24 ± 0.07	0.22 ± 0.04	-220 ± 60	-190 ± 30
Iopromide-TP-701B	IOPR-701B	IOPR-TP	0.05	0.050 ± 0.001	0.050 ± 0.001	0.050 ± 0.001	0.07 ± 0.03	0 ± 0	0 ± 0	-40 ± 70	0.050 ± 0.001	0.050 ± 0.001	0.05 ± 0.01	-10 ± 10	-10 ± 10
Iopromide-TP-731B	IOPR-731B	IOPR-TP	0.05	< LOQ	< LOQ	< LOQ	< LOQ	-	-	-	< LOQ	< LOQ	< LOQ	-	-
Iopromide-TP-819	IOPR-819	IOPR-TP	0.2	0.39 ± 0.22	0.34 ± 0.22	0.24 ± 0.06	0.200 ± 0.001	0 ± 10	20 ± 30	20 ± 40	< LOQ	< LOQ	< LOQ	-	-
Iopromide-TP-729A	IOPR-729A	IOPR-TP	0.08	0.46 ± 0.3	0.36 ± 0.2	0.56 ± 0.38	0.74 ± 0.48	-10 ± 40	-40 ± 10	-140 ± 110	< LOQ	< LOQ	< LOQ	-	-
Iopromide-TP-759	IOPR-759	IOPR-TP	0.2	0.3 ± 0.12	0.35 ± 0.22	0.88 ± 0.88	1.21 ± 1.37	-20 ± 40	-150 ± 170	-250 ± 250	< LOQ	< LOQ	< LOQ	-	-
Iomeprol	IOME	Contrast Medium	0.05	1.73 ± 0.8	0.94 ± 0.64	0.18 ± 0.12	0.11 ± 0.1	40 ± 20	80 ± 10	90 ± 10	< LOQ	< LOQ	< LOQ	-	-
Carbendazim	CARB	Fungicide	0.002	< LOQ	< LOQ	< LOQ	< LOQ	-	-	-	0.040 ± 0.001	0.040 ± 0.001	0.030 ± 0.001	-20 ± 10	10 ± 10
Epoxiconazole	EPOX	Fungicide	0.005	< LOQ	< LOQ	< LOQ	< LOQ	-	-	-	< LOQ	< LOQ	< LOQ	-	-
Propiconazole	PROP	Fungicide	0.005	< LOQ	< LOQ	< LOQ	< LOQ	-	-	-	< LOQ	< LOQ	< LOQ	-	-
Tebuconazole	TEBU	Fungicide	0.001	< LOQ	< LOQ	< LOQ	< LOQ	-	-	-	< LOQ	< LOQ	< LOQ	70 ± 0	70 ± 0
DEET	DEET	Repellant	0.001	0.07 ± 0.02	0.02 ± 0.01	0.02 ± 0.01	0.01 ± 0.01	60 ± 10	70 ± 10	80 ± 0	0.04 ± 0.01	0.03 ± 0.01	0.020 ± 0.001	30 ± 10	50 ± 10
Hydroxy-DEET	DEET-OH	DEET-TP	0.005	0.04 ± 0.01	0.04 ± 0.08	0.03 ± 0.01	0.03 ± 0.01	-20 ± 30	-20 ± 30	10 ± 10	0.100 ± 0.001	0.07 ± 0.01	0.060 ± 0.001	30 ± 10	40 ± 10
N-ethyl-m-toluamide	DEET-TP	DEET-TP	0.005	< LOQ	< LOQ	< LOQ	< LOQ	-	-	-	< LOQ	< LOQ	< LOQ	-	-
DEET carboxylic acid	DEET-COOH	DEET-TP	0.005	< LOQ	< LOQ	< LOQ	< LOQ	-	-	-	< LOQ	< LOQ	< LOQ	-	-
Diuron	DIU	Herbicide/Algicide	0.002	0.010 ± 0.001	0.01 ± 0.01	0.010 ± 0.001	0.010 ± 0.001	-10 ± 10	-10 ± 10	-10 ± 10	0.19 ± 0.02	0.11 ± 0.02	0.08 ± 0.02	40 ± 10	60 ± 10
Didemethyldiuron (DCPU)	DCPU	DIU-TP	0.01	< LOQ	< LOQ	< LOQ	< LOQ	-	-	-	< LOQ	< LOQ	< LOQ	-	-
N-Demethoxylinuron (DCPMU)	DCPMU	DIU-TP	0.001	< LOQ	< LOQ	< LOQ	< LOQ	-	-	-	0.001 ± 0.001	0.01 ± 0.001	0.01 ± 0.001	-90 ± 20	-30 ± 10
Isoproturon	ISO	Herbicide	0.001	0.25 ± 0.11	0.21 ± 0.14	0.21 ± 0.12	0.2 ± 0.11	0 ± 10	0 ± 0	10 ± 0	< LOQ	< LOQ	< LOQ	-20 ± 20	-20 ± 20
Metamitron	META	Herbicide	0.015	< LOQ	< LOQ	< LOQ	< LOQ	-	-	-	< LOQ	< LOQ	< LOQ	-	-
Desamino-Metamitron		META-TP	0.01	< LOQ	< LOQ	< LOQ	< LOQ	-	-	-	< LOQ	< LOQ	< LOQ	-	-
Metazachlor	METAZ	Herbicide	0.001	< LOQ	< LOQ	< LOQ	< LOQ	-	-	-	< LOQ	< LOQ	< LOQ	-	-
Metolachlor	METOL	Herbicide	0.001	< LOQ	< LOQ	< LOQ	< LOQ	-	-	-	< LOQ	< LOQ	< LOQ	-	-
Metolachlor ESA	METOL-E	METOL-TP	0.005	< LOQ	< LOQ	< LOQ	< LOQ	-	-	-	< LOQ	< LOQ	< LOQ	-	-
Metolachlor OA	METOL-A	METOL-TP	0.01	< LOQ	< LOQ	< LOQ	< LOQ	-	-	-	< LOQ	< LOQ	< LOQ	-	-
Terbutryn	TERB	Herbicide/Algicide	0.001	0.1 ± 0.05	0.09 ± 0.05	0.08 ± 0.04	0.06 ± 0.02	0 ± 0	0 ± 0	20 ± 30	0.14 ± 0.01	0.06 ± 0.02	0.04 ± 0.01	60 ± 10	70 ± 0
Terbuthylazine	TERZ	Herbicide	0.002	< LOQ	< LOQ	< LOQ	< LOQ	-	-	-	0.010 ± 0.001	< LOQ	< LOQ	50 ± 10	60 ± 10
Terbuthylazine-2-Hydroxy	TERZ-OH	TERZ-TP	0.002	< LOQ	< LOQ	< LOQ	< LOQ	-	-	-	0.020 ± 0.001	0.020 ± 0.001	0.020 ± 0.001	-10 ± 0	10 ± 10

Substance	Abbr.	Class / TP	LOQ												
Irgarol	IRG	Herbicide/Algicide	0.001	< LOQ	< LOQ	< LOQ	< LOQ	30 ± 10	70 ± 20	80 ± 10	0.070 ± 0.001	0.03 ± 0.01	0.020 ± 0.001	60 ± 10	70 ± 0
Benzotriazole	BENZ	Industrial	0.09	5.4 ± 0.57	3.8 ± 0.11	0.86 ± 0.34	0.96 ± 0.91	30 ± 10	70 ± 20	80 ± 10	0.11 ± 0.02	0.11 ± 0.01	0.11 ± 0.01	-10 ± 20	0 ± 30
Tetraglyme	TETR	Industrial	0.001	0.04 ± 0.01	0.04 ± 0.01	0.04 ± 0.01	0.03 ± 0.01	0 ± 20	-10 ± 10	10 ± 10	0.001 ± 0.001	0.010 ± 0.001	0.03 ± 0.03	-180 ± 190	-890 ± 1030
Caffeine	CAF	Life-style	0.002	1.24 ± 0.44	0.04 ± 0.03	0.010 ± 0.001	0.08 ± 0.13	100 ± 0	100 ± 0	90 ± 20	0.02 ± 0.01	0.03 ± 0.03	0.02 ± 0.01	-90 ± 190	0 ± 90
Triclosan	TRIC	Personal care product	0.01	< LOQ	< LOQ	< LOQ	< LOQ	-	-	-	< LOQ	< LOQ	< LOQ	-	-
Triclocarban	TRICC	Personal care product	0.001	< LOQ	< LOQ	< LOQ	< LOQ	-	-	-	< LOQ	< LOQ	< LOQ	-	-
Carbanilide		TRICC-TP	0.02	< LOQ	< LOQ	< LOQ	< LOQ	-	-	-	< LOQ	< LOQ	< LOQ	-	-
Sucralose	SUC	Sweetener	0.06	8.08 ± 0.67	8.07 ± 0.88	7.97 ± 0.8	7.63 ± 0.86	0 ± 0	0 ± 0	10 ± 0	7.41 ± 0.71	7.05 ± 0.39	6.32 ± 0.19	0 ± 10	10 ± 10
Substances with negative charge at pH 7															
Xipamide	XIP	Diuretic	0.02	< LOQ	< LOQ	< LOQ	< LOQ	-	-	-	< LOQ	< LOQ	< LOQ	-	-
Furosemide	FURO	Diuretic	0.01	0.33 ± 0.05	0.25 ± 0.12	0.16 ± 0.08	0.13 ± 0.12	20 ± 20	40 ± 0	60 ± 30	0.08 ± 0.02	0.05 ± 0.01	0.040 ± 0.001	40 ± 20	50 ± 10
Torsemide	TORA	Diuretic	0.005	0.11 ± 0.01	0.11 ± 0.01	0.11 ± 0.01	0.10 ± 0.01	0 ± 0	0 ± 0	10 ± 10	< LOQ	< LOQ	< LOQ	-	-
Hydroxy-Torsemide	TORA-OH	TORA-TP	0.002	< LOQ	< LOQ	< LOQ	< LOQ	-	-	-	< LOQ	< LOQ	< LOQ	-	-
Ramipril	RAM	ACE Inhibitor	0.005	0.04 ± 0.01	0.02 ± 0.01	0.010 ± 0.001	0.010 ± 0.001	50 ± 30	80 ± 10	80 ± 10	< LOQ	< LOQ	< LOQ	-	-
Ramiprilat	RAMt	RAM-TP	0.075	0.25 ± 0.05	0.14 ± 0.06	0.080 ± 0.001	0.080 ± 0.001	50 ± 10	70 ± 10	70 ± 10	< LOQ	< LOQ	< LOQ	-	-
Valsartan	VAL	Angiotensin II Antagonists	0.005	1.88 ± 0.64	0.07 ± 0.04	0.02 ± 0.01	0.01 ± 0.01	100 ± 0	100 ± 0	100 ± 0	0.23 ± 0.01	0.02 ± 0.01	0.010 ± 0.001	90 ± 0	100 ± 0
Valsartan acid	VALac	VAL-T	0.005	1.85 ± 0.3	2.47 ± 0.38	0.72 ± 0.16	0.86 ± 1.17	-30 ± 20	20 ± 50	50 ± 70	1.63 ± 0.16	0.9 ± 0.02	0.79 ± 0.07	50 ± 10	50 ± 10
Irbesartan	IRB	Angiotensin II Antagonist	0.005	0.67 ± 0.08	0.65 ± 0.08	0.62 ± 0.05	0.60 ± 0.05	0 ± 0	0 ± 10	10 ± 10	0.49 ± 0.07	0.37 ± 0.09	0.33 ± 0.03	20 ± 10	30 ± 0
Candesartan	CAN	Angiotensin II Antagonist	0.002	1.200 ± 0.001	1.2 ± 0.12	1.23 ± 0.06	1.200 ± 0.001	0 ± 0	0 ± 0	0 ± 0	0.16 ± 0.01	0.15 ± 0.01	0.140 ± 0.001	10 ± 10	10 ± 0
Telmisartan	TEL	Angiotensin II Antagonist	0.005	0.27 ± 0.05	0.26 ± 0.06	0.18 ± 0.03	0.17 ± 0.08	-10 ± 20	20 ± 20	30 ± 50	0.15 ± 0.02	0.010 ± 0.001	0.010 ± 0.001	90 ± 0	100 ± 0
Olmesartan	OLM	Angiotensin II Antagonist	0.02	0.75 ± 0.04	0.76 ± 0.12	0.76 ± 0.01	0.75 ± 0.01	0 ± 10	0 ± 10	0 ± 10	0.22 ± 0.01	0.20 ± 0.02	0.19 ± 0.01	10 ± 10	20 ± 0
Bezafibrate	BZF	Lipid modifying agent	0.002	0.26 ± 0.04	0.19 ± 0.11	0.04 ± 0.04	0.02 ± 0.03	30 ± 10	70 ± 20	90 ± 10	< LOQ	< LOQ	< LOQ	-	-
Sulfamethoxazole	SMX	Antibacterials	0.01	0.86 ± 0.1	0.7 ± 0.3	0.19 ± 0.05	0.15 ± 0.03	20 ± 10	60 ± 20	80 ± 0	0.09 ± 0.01	0.20 ± 0.02	0.25 ± 0.01	-130 ± 20	-170 ± 30
Acetyl-Sulfamethoxazole	SMXac	SMX-TP	0.02	0.14 ± 0.03	0.07 ± 0.04	0.020 ± 0.001	0.020 ± 0.001	50 ± 20	80 ± 10	90 ± 0	< LOQ	< LOQ	< LOQ	-	-
Diatrizoic acid	DIA	Contrast Medium	0.015	0.21 ± 0.11	0.18 ± 0.11	0.18 ± 0.13	0.18 ± 0.12	0 ± 10	0 ± 10	0 ± 10	< LOQ	< LOQ	< LOQ	0 ± 10	-10 ± 20
Diclofenac	DCF	Antiphlogistic	0.002	4.80 ± 0.08	4.6 ± 0.2	4.47 ± 0.12	4.2 ± 0.3	0 ± 0	10 ± 0	10 ± 0	0.2 ± 0.01	0.04 ± 0.02	0.01 ± 0.001	80 ± 10	90 ± 0
4-Hydroxy-Diclofenac	DCF-4-OH	DCF-TP	0.002	0.99 ± 0.03	0.93 ± 0.29	0.87 ± 0.03	0.54 ± 0.19	10 ± 20	10 ± 0	40 ± 20	0.04 ± 0.03	0.03 ± 0.01	0.010 ± 0.001	-40 ± 110	50 ± 40
Diclofenac Lactam	DCFlac	DCF-TP	0.001	0.04 ± 0.01	0.05 ± 0.01	0.07 ± 0.04	0.07 ± 0.04	-30 ± 0	-80 ± 50	-90 ± 80	0.010 ± 0.001	0.010 ± 0.001	0.010 ± 0.001	-90 ± 20	-60 ± 20
Carboxy-Diclofenac	DCF-COOH	DCF-TP	0.002	0.040 ± 0.001	0.05 ± 0.01	0.04 ± 0.01	0.03 ± 0.01	-20 ± 10	-10 ± 10	20 ± 10	< LOQ	< LOQ	< LOQ	-	-
Ibuprofen	IBU	Antiphlogistic	0.02	0.1 ± 0.04	0.04 ± 0.03	0.020 ± 0.001	0.020 ± 0.001	60 ± 20	70 ± 20	70 ± 20	< LOQ	< LOQ	< LOQ	-	-
Carboxy-Ibuprofen	IBU-COOH	IBU-TP	0.015	< LOQ	< LOQ	< LOQ	< LOQ	-	-	-	< LOQ	< LOQ	< LOQ	-	-
Naproxen	NPX	Antiphlogistic	0.015	0.4 ± 0.1	0.25 ± 0.18	0.03 ± 0.02	0.05 ± 0.06	40 ± 30	90 ± 10	90 ± 10	0.030 ± 0.001	0.020 ± 0.001	0.020 ± 0.001	50 ± 10	60 ± 0
O-desmethyl-Naproxen	NPX-O-DM	NPX-TP	0.01	0.18 ± 0.02	0.04 ± 0.03	0.02 ± 0.01	0.01 ± 0.01	80 ± 10	90 ± 0	90 ± 0	0.020 ± 0.01	0.01 ± 0.001	0.01 ± 0.001	30 ± 30	30 ± 30
Oxypurinol	OXY	Antigout	0.15	14.75 ± 1.7	15 ± 2	15 ± 1	16 ± 0.001	0 ± 10	-10 ± 10	-10 ± 10	9.08 ± 1.07	7.08 ± 0.61	5.38 ± 0.33	20 ± 10	40 ± 0
Mecoprop	MEC	Herbicide	0.01	1.64 ± 0.87	1.35 ± 1.03	0.58 ± 0.42	0.4 ± 0.4	10 ± 0	50 ± 20	80 ± 20					
Acesulfame	ACE	Sweetener	0.01	2.58 ± 0.59	1.01 ± 0.55	0.6 ± 0.3	0.14 ± 0.08	60 ± 10	70 ± 0	90 ± 0	1.7 ± 0.27	1.51 ± 0.23	1.35 ± 0.13	10 ± 10	20 ± 10
Saccharine	SAC	Sweetener	0.005	0.29 ± 0.12	0.010 ± 0.001	0.010 ± 0.001	0.04 ± 0.05	100 ± 0	100 ± 0	70 ± 40	0.21 ± 0.03	0.010 ± 0.001	0.010 ± 0.001	90 ± 0	90 ± 0
Substances with positive charge or zwitter ionic form at pH 7															
Tramadol	TRAM	Analgesic	0.002	1.13 ± 0.05	1.17 ± 0.48	1.13 ± 0.06	0.99 ± 0.11	0 ± 10	0 ± 0	10 ± 10	0.31 ± 0.03	0.07 ± 0.02	0.030 ± 0.001	80 ± 10	90 ± 0
O-desmethyl-Tramadol	TRAM-O-DM	TRAM-metabolite	0.01	0.25 ± 0.01	0.25 ± 0.03	0.25 ± 0.01	0.25 ± 0.02	0 ± 10	0 ± 0	0 ± 0	0.21 ± 0.02	< LOQ	< LOQ	90 ± 10	100 ± 0
N-desmethyl-Tramadol	TRAM-N-DM	TRAM-metabolite	0.01	0.15 ± 0.01	0.14 ± 0.02	0.15 ± 0.01	0.14 ± 0.01	0 ± 0	0 ± 0	10 ± 10	0.08 ± 0.01	< LOQ	< LOQ	90 ± 0	90 ± 0
N,O-didesmethyl-Tramadol	TRAM-DDM	TRAM-metabolite	0.015	0.16 ± 0.01	0.17 ± 0.01	0.17 ± 0.01	0.17 ± 0.001	0 ± 10	0 ± 10	-10 ± 10	0.27 ± 0.02	0.04 ± 0.02	0.020 ± 0.001	80 ± 10	90 ± 0
Tramadol-N-oxide	TRAM-NO	TRAM-TP	0.015	< LOQ	< LOQ	< LOQ	< LOQ	-	-	-	< LOQ	< LOQ	< LOQ	-	-
Gabapentin	GABA	Antiepileptic	0.02	1.58 ± 0.1	1.02 ± 0.41	0.18 ± 0.05	0.1 ± 0.04	40 ± 10	70 ± 20	90 ± 0	0.65 ± 0.07	0.43 ± 0.1	0.32 ± 0.04	40 ± 10	50 ± 0
Gabapentin Lactam	GABAlac	GABA-metabolite/TP	0.01	0.13 ± 0.03	0.18 ± 0.06	0.15 ± 0.03	0.14 ± 0.02	-30 ± 20	-20 ± 10	0 ± 20	0.44 ± 0.03	0.28 ± 0.04	0.23 ± 0.01	40 ± 10	50 ± 0
Sulpiride	SULP	Antidepressant	0.005	0.12 ± 0.01	0.120 ± 0.001	0.12 ± 0.01	0.11 ± 0.01	0 ± 10	0 ± 0	10 ± 0	0.1 ± 0.01	0.010 ± 0.001	0.010 ± 0.001	90 ± 0	100 ± 0
Amisulpride	AMIS	Antidepressant	0.005	0.61 ± 0.02	0.61 ± 0.1	0.65 ± 0.05	0.63 ± 0.03	0 ± 0	-10 ± 10	0 ± 10	< LOQ	< LOQ	< LOQ	-	-
O-desmethyl-Amisulpride	AMIS-O-DM	AMI-metabolite	0.005	< LOQ	< LOQ	< LOQ	< LOQ	-	-	-	< LOQ	< LOQ	< LOQ	-	-
Citalopram	CIT	Antidepressant	0.01	2.35 ± 0.25	2.17 ± 1.07	0.29 ± 0.15	0.030 ± 0.001	10 ± 0	60 ± 50	100 ± 0	0.09 ± 0.01	0.010 ± 0.001	0.010 ± 0.001	90 ± 0	90 ± 0
Desmethyl-Citalopram	CIT-DM	CIT-metabolite	0.001	0.1 ± 0.01	0.11 ± 0.04	0.07 ± 0.01	0.030 ± 0.001	-10 ± 0	10 ± 30	70 ± 0	0.05 ± 0.01	< LOQ	< LOQ	100 ± 0	100 ± 0
Didesmethyl-Citalopram	CIT-DDM	CIT-metabolite	0.025	< LOQ	< LOQ	< LOQ	< LOQ	-	-	-	< LOQ	< LOQ	< LOQ	-	-
Citalopram-N-oxide	CIT-NO	CIT-metabolite	0.005	< LOQ	< LOQ	< LOQ	< LOQ	-	-	-	< LOQ	< LOQ	< LOQ	-	-
Venlafaxine	VLX	Antidepressant	0.002	1.33 ± 0.05	1.33 ± 0.5	1.27 ± 0.06	0.55 ± 0.16	0 ± 0	0 ± 0	60 ± 10	0.16 ± 0.02	< LOQ	< LOQ	100 ± 0	100 ± 0
O-desmethyl-Venlafaxine	VLX-O-DM	VLX-metabolite	0.01	1.7 ± 0.68	1.67 ± 0.1	1.67 ± 0.06	1.600 ± 0.001	0 ± 0	0 ± 0	10 ± 0	0.52 ± 0.05	< LOQ	< LOQ	100 ± 0	100 ± 0
N-desmethyl-Venlafaxine	VLX-N-DM	VLX-metabolite	0.005	0.070 ± 0.001	0.08 ± 0.01	0.080 ± 0.001	0.08 ± 0.01	-10 ± 10	-10 ± 10	-10 ± 10	0.03 ± 0.001	< LOQ	< LOQ	70 ± 10	80 ± 10
N,O-didesmethyl-Venlafaxine	VLX-DDM	VLX-metabolite	0.01	0.16 ± 0.01	0.15 ± 0.01	0.15 ± 0.01	0.14 ± 0.01	10 ± 10	10 ± 10	10 ± 0	< LOQ	< LOQ	< LOQ	-	-
Venlafaxine-N-oxide	VLX-NO	VLX-TP	0.005	< LOQ	< LOQ	< LOQ	< LOQ	-	-	-	< LOQ	< LOQ	< LOQ	-	-
Lidocaine	LID	Antiarrhythmic	0.001	0.11 ± 0.01	0.11 ± 0.01	0.1 ± 0.01	0.1 ± 0.01	0 ± 10	0 ± 10	10 ± 10	0.040 ± 0.001	0.020 ± 0.001	< LOQ	60 ± 10	80 ± 10
Nor-Lidocaine	LIDnor	LID-metabolite	0.005	< LOQ	< LOQ	< LOQ	< LOQ	-	-	-	< LOQ	< LOQ	< LOQ	-	-
Sotalol	SOT	Beta-Blocker	0.045	0.08 ± 0.01	0.08 ± 0.01	0.050 ± 0.001	0.050 ± 0.001	0 ± 10	20 ± 20	40 ± 10	0.09 ± 0.01	0.050 ± 0.001	0.050 ± 0.001	50 ± 10	50 ± 10
Metoprolol	METO	Beta-Blocker	0.005	2.13 ± 0.1	1.8 ± 0.84	0.83 ± 0.25	0.6 ± 0.3	20 ± 10	50 ± 20	70 ± 10	0.010 ± 0.001	0.010 ± 0.001	0.010 ± 0.0001	30 ± 20	30 ± 20
Hydroxy-Metoprolol	METO-OH	METO-metabolite	0.015	0.04 ± 0.01	0.020 ± 0.001	0.020 ± 0.001	0.20 ± 0.001	50 ± 0	60 ± 10	60 ± 10	< LOQ	< LOQ	< LOQ	-	-
O-desmethyl-Metoprolol	METO-O-DM	METO-metabolite	0.005	< LOQ	< LOQ	< LOQ	< LOQ	-	-	-	< LOQ	< LOQ	< LOQ	-	-

Compound	Abbr.	Class	Relation														
Atenolol	ATE	Beta-Blocker		0.01	0.7 ± 0.04	0.7 ± 0.04	0.04 ± 0.02	0.01 ± 0.01	90 ± 0	90 ± 0	100 ± 0	0.14 ± 0.02	< LOQ	< LOQ	90 ± 0	90 ± 0
Atenolol acid	ATE-COOH		ATE-metabolite	0.015	1.7 ± 0.08	1.43 ± 0.66	0.75 ± 0.23	0.6 ± 0.26	20 ± 0	40 ± 20	60 ± 20	< LOQ	< LOQ	< LOQ	-	-
Hydroxy-Atenolol	ATE-OH		ATE-metabolite	0.005	< LOQ	< LOQ	< LOQ	< LOQ	-	-	-	0.020 ± 0.001	< LOQ	< LOQ	70 ± 10	-
Aliksiren	ALIS	Renin-inhibitor		0.02	0.06 ± 0.01	0.05 ± 0.01	0.03 ± 0.01	0.04 ± 0.02	0 ± 30	30 ± 20	20 ± 10	0.26 ± 0.06	< LOQ	< LOQ	90 ± 0	90 ± 0
Trimethoprim	TMP	Antibiotic		0.005	1.15 ± 0.06	0.6 ± 0.39	0.27 ± 0.19	0.03 ± 0.01	50 ± 30	70 ± 10	100 ± 0	0.05 ± 0.001	0.010 ± 0.001	0.010 ± 0.001	90 ± 0	90 ± 0
3-desmethyl-TMP	TMP-3-DM		TMP-TP	0.002	0.01 ± 0.01	0.01 ± 0.01	0.01 ± 0.01	0.010 ± 0.001	10 ± 20	10 ± 20	30 ± 20	0.010 ± 0.001	< LOQ	< LOQ	80 ± 0	-
5-(2,4,5-Trimethoxy)-2,4-pyrimidinediamnine	TMP-TP		TMP-TP	0.035	< LOQ	< LOQ	< LOQ	< LOQ	-	-	-	< LOQ	< LOQ	< LOQ	-	-
Clarithromycin	CLARI	Antibiotic		0.001	0.04 ± 0.01	0.02 ± 0.02	0.001 ± 0.000	0.001 ± 0.000	40 ± 30	90 ± 20	90 ± 10	< LOQ	< LOQ	< LOQ	-	-
Ranitidine	RANI	H2-receptor antagonsist		0.01	< LOQ	< LOQ	< LOQ	< LOQ	-	-	-	< LOQ	< LOQ	< LOQ	-	-
Desmethyl-Ranitidine	RANI-DM		RANI-metabolite	0.03	< LOQ	< LOQ	< LOQ	< LOQ	-	-	-	< LOQ	< LOQ	< LOQ	-	-
Ranitidine-N-oxide	RANI-NO		RANI-TP	0.01	< LOQ	< LOQ	< LOQ	< LOQ	-	-	-	< LOQ	< LOQ	< LOQ	-	-
Sitagliptin	SITA	used in diabetes		0.01	2.28 ± 0.05	2.27 ± 0.49	2.2 ± 0.1	1.8 ± 0.001	0 ± 0	0 ± 10	20 ± 0	0.17 ± 0.01	< LOQ	< LOQ	90 ± 0	90 ± 0
Diphenhydramine	DIP	Antihistamine		0.005	0.57 ± 0.06	0.48 ± 0.22	0.02 ± 0.01	0.020 ± 0.001	20 ± 10	70 ± 40	100 ± 0	0.020 ± 0.001	0.010 ± 0.001	0.010 ± 0.001	70 ± 0	70 ± 0
N-desmethyl-Diphenhydramine	DIP-N-DM		DIP-metabolite/TP	0.005	0.010 ± 0.001	0.02 ± 0.01	0.020 ± 0.001	0.01 ± 0.001	-70 ± 60	-100 ± 0	20 ± 0	< LOQ	< LOQ	< LOQ	-	-
Diphenhydramine-N-oxide	DIP-NO		DIP-TP	0.005	0.01 ± 0.001	0.01 ± 0.01	0.02 ± 0.01	0.010 ± 0.001	-60 ± 30	-190 ± 80	-40 ± 40	< LOQ	< LOQ	< LOQ	-	-
Cetirizine	CET	Antihistamine		0.005	0.14 ± 0.01	0.14 ± 0.09	0.13 ± 0.02	0.11 ± 0.01	0 ± 0	0 ± 10	20 ± 0	0.06 ± 0.01	0.010 ± 0.001	0.010 ± 0.001	90 ± 0	90 ± 0
Fexofenadine	FEX	Antihistamine		0.005	0.25 ± 0.01	0.16 ± 0.06	0.02 ± 0.01	0.01 ± 0.01	30 ± 20	80 ± 20	90 ± 10	0.130 ± 0.001	0.010 ± 0.001	0.010 ± 0.001	100 ± 0	100 ± 0
Imidacloprid	IMI	Insecticide		0.025	< LOQ	< LOQ	< LOQ	< LOQ	-	-	-	0.11 ± 0.01	0.09 ± 0.01	0.08 ± 0.01	20 ± 20	30 ± 10
Denatonium	DEN	Bitterant		0.001	0.24 ± 0.04	0.23 ± 0.05	0.23 ± 0.02	0.23 ± 0.02	0 ± 10	0 ± 10	0 ± 30	0.030 ± 0.001	< LOQ	< LOQ	100 ± 0	100 ± 0
Tolylbiguanide	TOLY	Industrial		0.005	< LOQ	< LOQ	< LOQ	< LOQ	-	-	-	< LOQ	< LOQ	< LOQ	-	-
Ethyltriphenylphosphonium	ETP	Industrial		0.005	< LOQ	< LOQ	< LOQ	< LOQ	-	-	-	< LOQ	< LOQ	< LOQ	-	-
Methyltriphenylphosphonium	MTP	Industrial		0.002	< LOQ	< LOQ	< LOQ	< LOQ	-	-	-	< LOQ	< LOQ	< LOQ	-	-
Tetrabutyltriphenylphosphonium	TBTP	Industrial		0.001	< LOQ	< LOQ	< LOQ	< LOQ	-	-	-	< LOQ	< LOQ	< LOQ	-	-
(Methoxymethyl)triphenylphosphonium	MMTP	Industrial		0.01	< LOQ	< LOQ	< LOQ	< LOQ	-	-	-	< LOQ	< LOQ	< LOQ	-	-
Tetrabutylammonium	TBA	Industrial		0.001	< LOQ	< LOQ	< LOQ	< LOQ	-	-	-	< LOQ	< LOQ	< LOQ	-	-
Tetrapropylammonium	TPA	Industrial		0.002	< LOQ	< LOQ	< LOQ	< LOQ	-	-	-	< LOQ	< LOQ	< LOQ	-	-

A2.4: Mass Balances
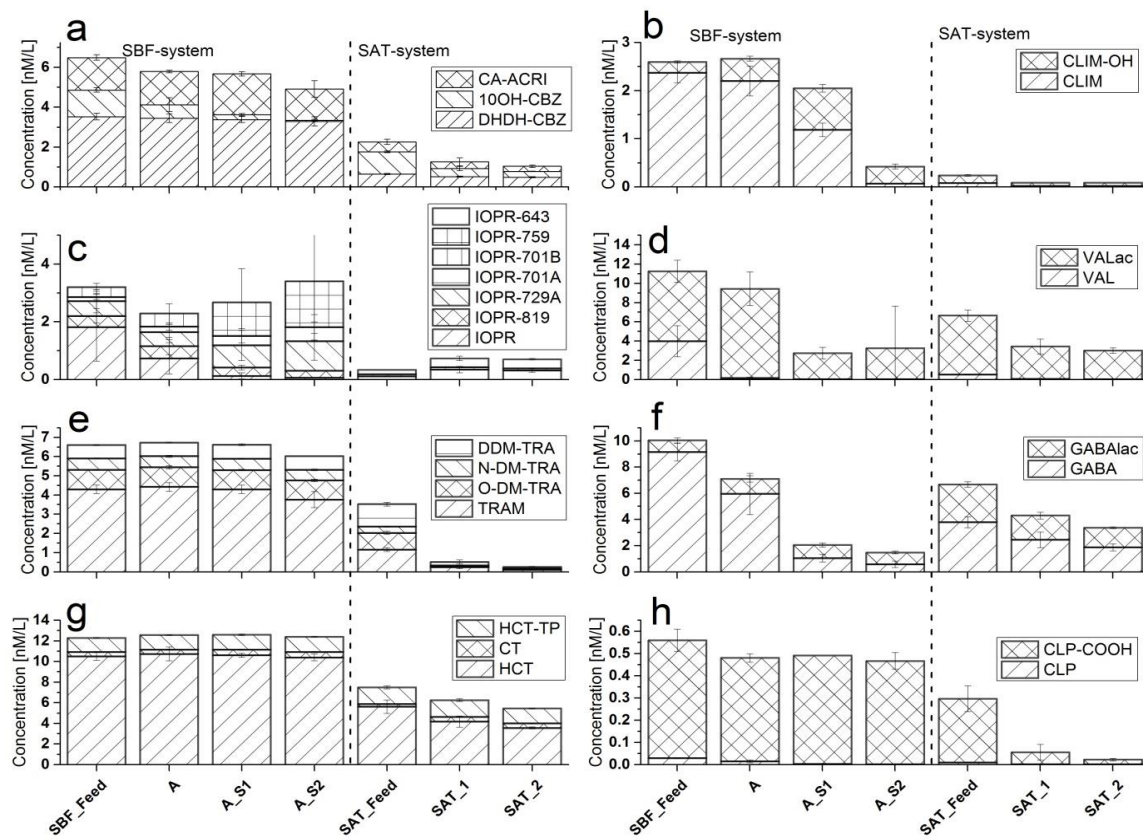
a) 10-OH-carbamazepine, b) Climbazole, c) iopromide, d)valsatan, e) tramadol, f) gabapentin
g) hydrochlorothiazide, h) clopidogrel

Appendix C

Supplementary data for Chapter 4:
Ozonation of sitagliptin: removal kinetics and elucidation of oxidative transformation products
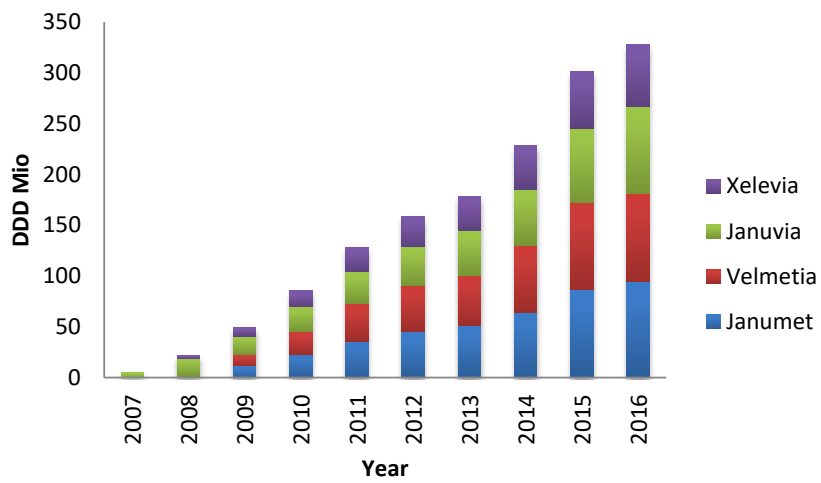
Figure A3.1. Consumption numbers of four STG preparations in Germany for the years 2007 – 2016. Januvia and Xelevia are single agent preparations of STG while Velmetia and Janumet are combination preparations with metformin. Consumption numbers increased steadily over the shown time period.

Table A3.1. Wastewater characteristic before and after ozonation in the ozonation pilot plant at the WWTP Lundakra (average ± standard deviation, n=3)

Matrix	0.3 mg O_3/mg DOC		0.5 mg O_3/mg DOC		0.7 mg O_3/mg DOC		0.9 mg O_3/mg DOC	
	Influent	Effluent	Influent	Effluent	Influent	Effluent	Influent	Effluent
Temperature (°C)	11.0 + 0.6	10.9 + 0.5	11.1 + 0.2	11.1 + 0.1	11.9 + 0.7	11.9 + 0.7	13.4 + 0.4	13.6 + 0.5
pH	7.4 + 0.0	7.3 + 0.1	7.3 + 0.1	7.3 + 0.1	7.3 + 0.0	7.5 + 0.3	7.3 + 0.0	7.2 + 0.0
DOC (mg/L)	10.6 + 0.1	10.5 + 0.9	10.4 + 0.6	10.8 + 0.9	10.4 + 0.2	10.6 + 0.7	10.6 + 0.4	11.0 + 1.2
$COD_{dissolved}$ (mg/L)	25.5 + 0.2	25.5 + 2.2	26.3 + 1.6	26.4 + 2.5	25.0 + 1.7	24.5 + 1.2	26.6 + 1.1	25.4 + 2.3
NH_4-N (mg/L)	4.3 + 0.7	4.4 + 0.7	4.6 + 0.3	4.7 + 0.3	5.1 + 0.3	5.1 + 0.2	3.9 + 0.1	3.9 + 0.1
NO_3-N (mg/L)	1.0 + 0.3	1.6 + 0.2	1.2 + 0.1	1.5 + 0.2	0.8 + 0.2	1.2 + 0.3	0.8 + 0.3	1.1 + 0.2
NO_2-N (mg/L)	0.4 + 0.2	0.1 + 0.1	0.20 + 0.02	< 0.05	0.24 + 0.06	< 0.05	0.3 + 0.1	< 0.05
Suspended solids (mg/L)	24.1 + 18.2	16.0 + 8.9	11.7 + 4.5	12.0 + 1.7	6.7 + 3.1	4.7 + 0.6	5.0 + 1.7	3.7 + 0.6

Table A3.2. Details on the LC-ESI-QTOF analysis method

LC	**Agilent Technologies 1260 Infinity Series**
	Synergie™ Hydro-RP (3 × 250 mm; 4 µm) Temp.: 40°C Flow: 450 µL/min, injection: 50 µL A: Water + 0.1 % HCOOH, B: CH_3CN + 0.1 % HCOOH Run time: 30 min Gradient:
Instr.	QToF-MS 5600 TripleTOF (Sciex), ESI +/-
MS	Accumulation time = 0.2 s, Cycle time = 0.6 s, Scan range = 100 Da –1000 Da
MS^2	**Data dependent** (isolation width = 1 Da) Accumulation time = 0.05 s, CE = 40 eV, CES = 15 eV trigger threshold = 100 cps, max. ions = 8

For evaluation of removal kinetics, quantification of STG was performed. To account for any random uncertainties, STG-d4 was added to the samples. Calibration curves were drawn for the uncorrected peak area as well as for area ratio of STG-STG-d4.

Good linearity was achieved in the concentration range of 0 – 1 mg/L.
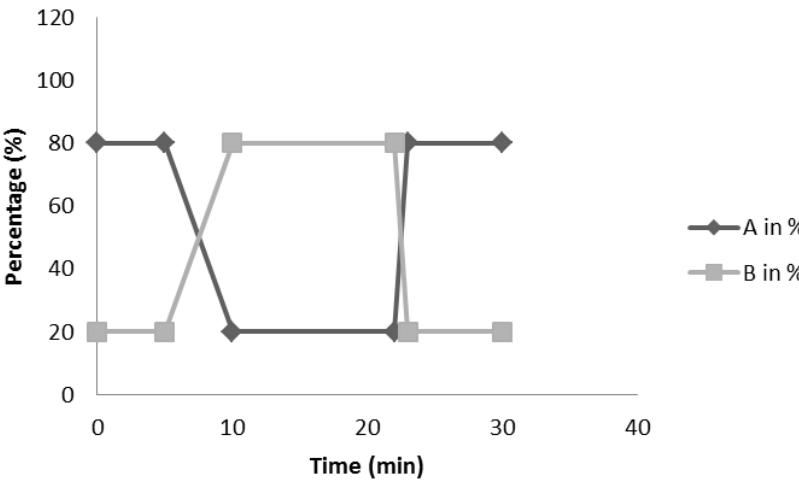
To obtain further information about concentrations of TP 406, also for comparison of ionizability of TP 406 to STG, calibration curves for TP 406 were prepared with the area of TP 406 as well as the area ration TP 406:STG-d4.

Good linearity was achieved in the concentration range of 0 – 0.4 mg/L.
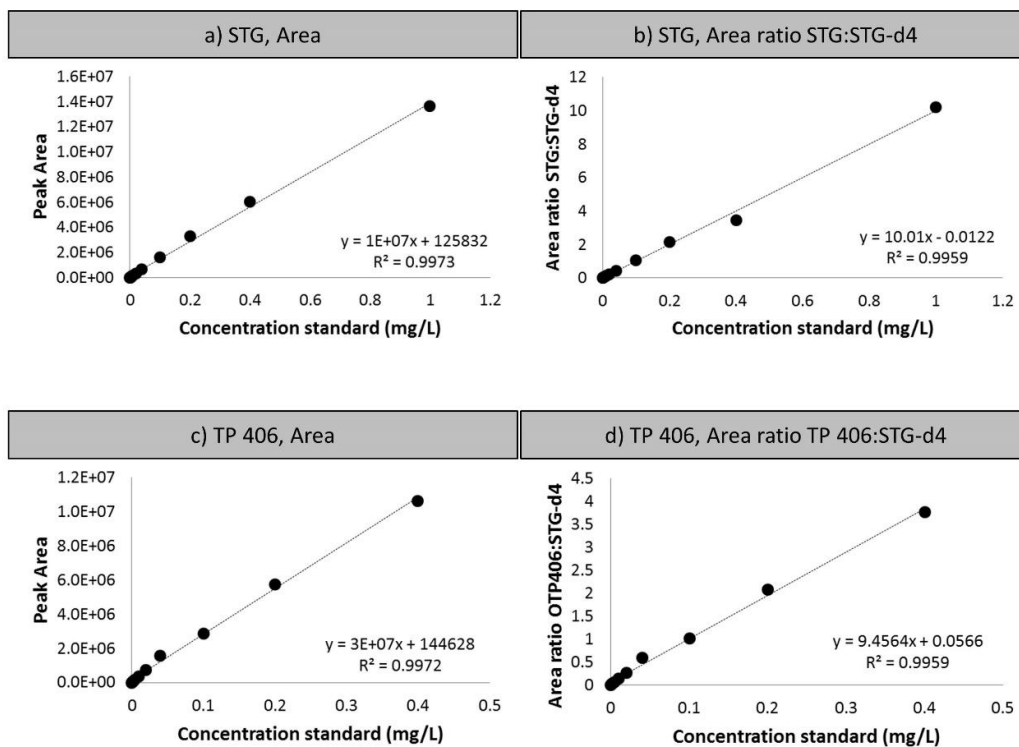
Figure A3.2. External calibration of STG and TP 406 at the LC-ESI-QTOF using STG-d4 as internal standard

Table A3.3. Details on the IC-ESI-QTOF analysis method

IC	940 Professional IC Vario (Metrohm)
	A Supp 5 (4 x 100 mm) Temp. : 45°C Flow: 800 µL/min, injection: 50 µL A: 80% Water + 20 % ACN, B: 8 mM Na_2CO_3/2.5 mM $NaHCO_3$/20% ACN Run time: 30 min Gradient:
Instr.	QToF-MS 5600 TripleTOF (Sciex), ESI -
MS	Accumulation time = 0.2 s, Cycle time = 1 s, Scan range = 50 Da –1200 Da
MS^2	**Data dependent** (isolation width = 1 Da) Accumulation time = 0.1 s, CE = -25 eV trigger threshold = 100 cps, max. ions = 8 Product ion (4 experiments) Accumulation time = 0.1 s, Products of 112.985 Da and 114.9917 Da CE/CES = -18/0 and -40/15

For quantification purposes, calibration curves were prepared for TFA by plotting the area against the concentration of the standards as well as plotting the area ration of TFA:TFA-13C2.

Good linearity was achieved for the concentration range of 0 – 60 µg/L.

| a) TFA, Area | b) TFA, Area ratio TFA:13C2 TFA |

Figure a) TFA, Area: y = 2E+06x + 2E+06, R² = 0.9853

Figure b) TFA, Area ratio TFA:13C2 TFA: y = 0.0862x + 0.0819, R² = 0.9898
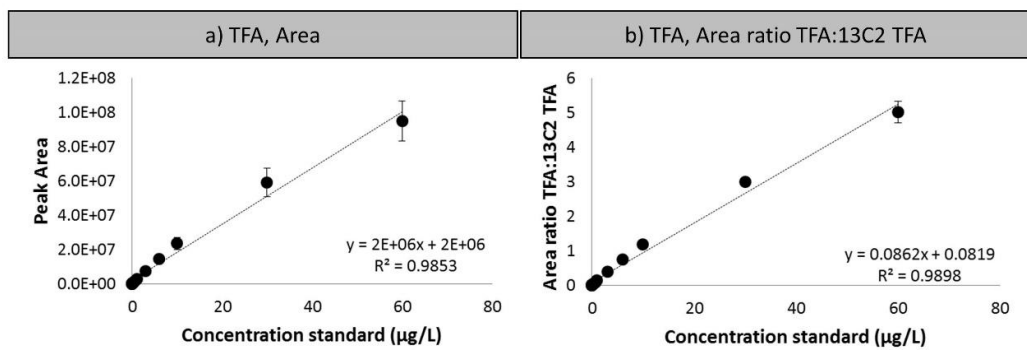
Figure A3.3. External calibration of TFA at the IC-ESI-QTOF using TFA-13C2 as internal standard

a) Attenuation STG with t-BuOH
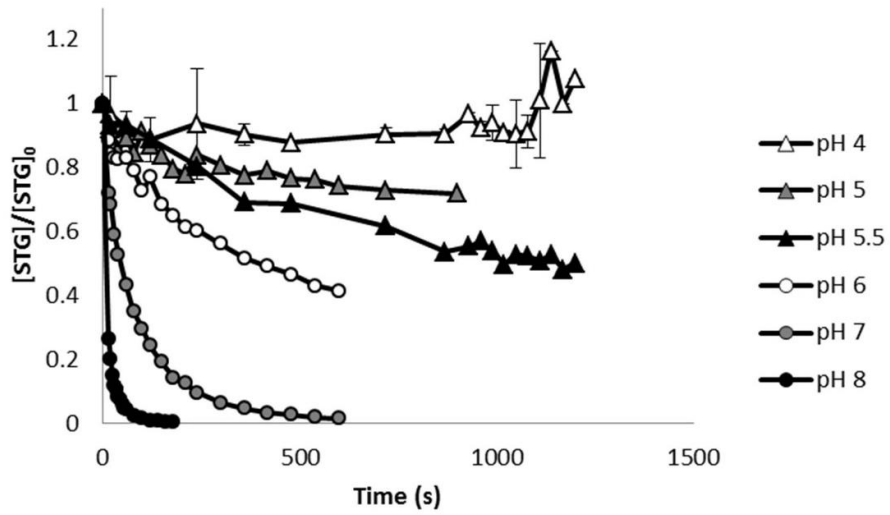
b) Attenuation STG without t-BuOH
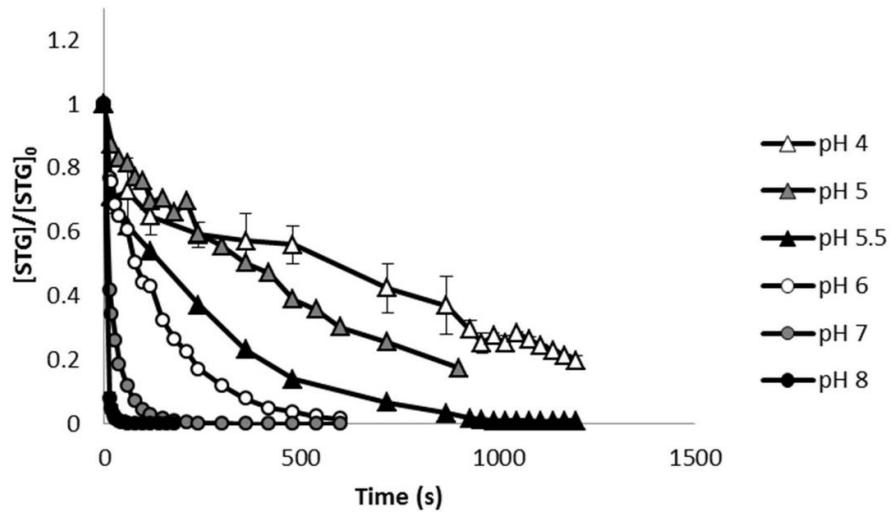
Figure A3.4. Attenuation of STG in in 50 mM phosphate buffer at different pH values in presence and absence of t-BuOH as radical scavenger

Table A3.4. Overview of observed potential TPs in time series experiments (50 mM phosphate buffer). 32 potential TPs could be detected in the time-series experiments. The table contains information about the retention times (RT), exact masses in positive and negative ESI, RT in IC-ESI-QTOF, formation at different pH values and maximum intensities at pH 8

					Formation in time series							
		LC		IC	with t-BuOH			without t-BuOH			highest Intensity pH 8 pos/neg	
TP	RT	[M+H]⁺	[M-H]⁻	RT	pH 4	pH 6	pH 8	pH 4	pH 6	pH 8	with t-BuOH	without t-BuOH
407, STG	10.2	408.126	452.1153	-							22500/10000	17800/8500
Identified TPs or TPs for which proposals for possible structures could be made												
437	14	438.1000	436.0847		x	x	x	x	x	x	14000/10000	4000/4000
406	13.2	407.0940	405.0789	-	-	x	x	-	-	x	350/900	100/300
192	4.2	193.0696	-	-	-	x	x	-	x	x	15/-	25/-
264	7.6	265.0545	263.0394		-	-	x	-	x	x	50/100	80/160
206b	8.6	207.0490	205.0341	2	-	-	-	-	x	x	0/0	300/180
421c	12.6	422.1048	420.0894	3.74	x	x	x	x	x	x	60/0	600/1200
421b	12.2	422.1047	420.0894		-	x	-	x	x	x	0/0	60/110
421a	9.9	422.0920	420.0768	-	-	-	-	x	x	x	0/0	80/160
293	8.3	294.0812	292.0661	-	-	-	-	-	x	x	0/0	10/15
453	13.7	454.0943	452.0796	-	-	-	-	-	-	x	0/0	35/80
390	13.8	391.0990	389.0840	-	-	x	x	-	x	x	160/350	80/150
Unidentified TPs in the order of their appearance in the chromatogram												
310	7.8	311.0602	309.9442	-	-	-	x	-	x	x	15/-	40/-
252	7.8	253.0545	251.0396	-	-	-	-	-	-	x	0/0	30/90
254	7.9	255.0702	253.0564	-	-	-	-	-	x	x	0/8	30/12
294	8.2	295.0652	293.0501	-	-	-	-	x	x	x	5/5	25/25
379	8.2	380.0814	378.0662	-	-	-	-	x	x	x	0/0	30/50
363	8.3	364.0865	362.0713		-	-	-	x	x	x	0/0	20/50
266	8.5	267.0704	-	-	-	-	x	x	x	x	70/-	100/-
206a	8.5	207.0490	205.0341	-	-	-	-	x	x	x	0/0	10/10
393	8.5	394.0970	392.0818	-	-	-	-	x	x	x	0/0	10/25
228	8.6	229.0311	-	-	-	-	x	x	x	x	0/-	300/-
244	8.6	245.0049	-	-	-	-	-	x	x	x	0/-	30/-
335	8.8	336.0917	334.0764		-	-	-	x	x	x	0/0	25/45
278	8.9	279.0704	-	-	-	-	x	-	x	x	40/-	50/-
339	9.6	340.0867	338.0714	-	-	-	-	-	-	x	0/0	60/60
343	9.6	344.0966	342.0814	-	-	-	-	-	x	x	0/0	12/60
351	10.4	352.0868	350.0711	-	-	-	-	x	x	x	10/0	140/7
445	11.1	446.0920	444.0766	-	-	-	-	-	x	x	0/0	90/50
438	11.8	439.0838	437.0693	5.7	-	-	x	-	-	x	80/16	30/10
426	12	427.0833	-	-	-	-	-	-	-	x	10/-	14/-
425	13.4	426.0998	424.0854	-	-	x	x	x	x	x	50/50	400/450
463	13.4	464.0554	462.0583	-	-	-	-	-	x	x	10/120	10/100
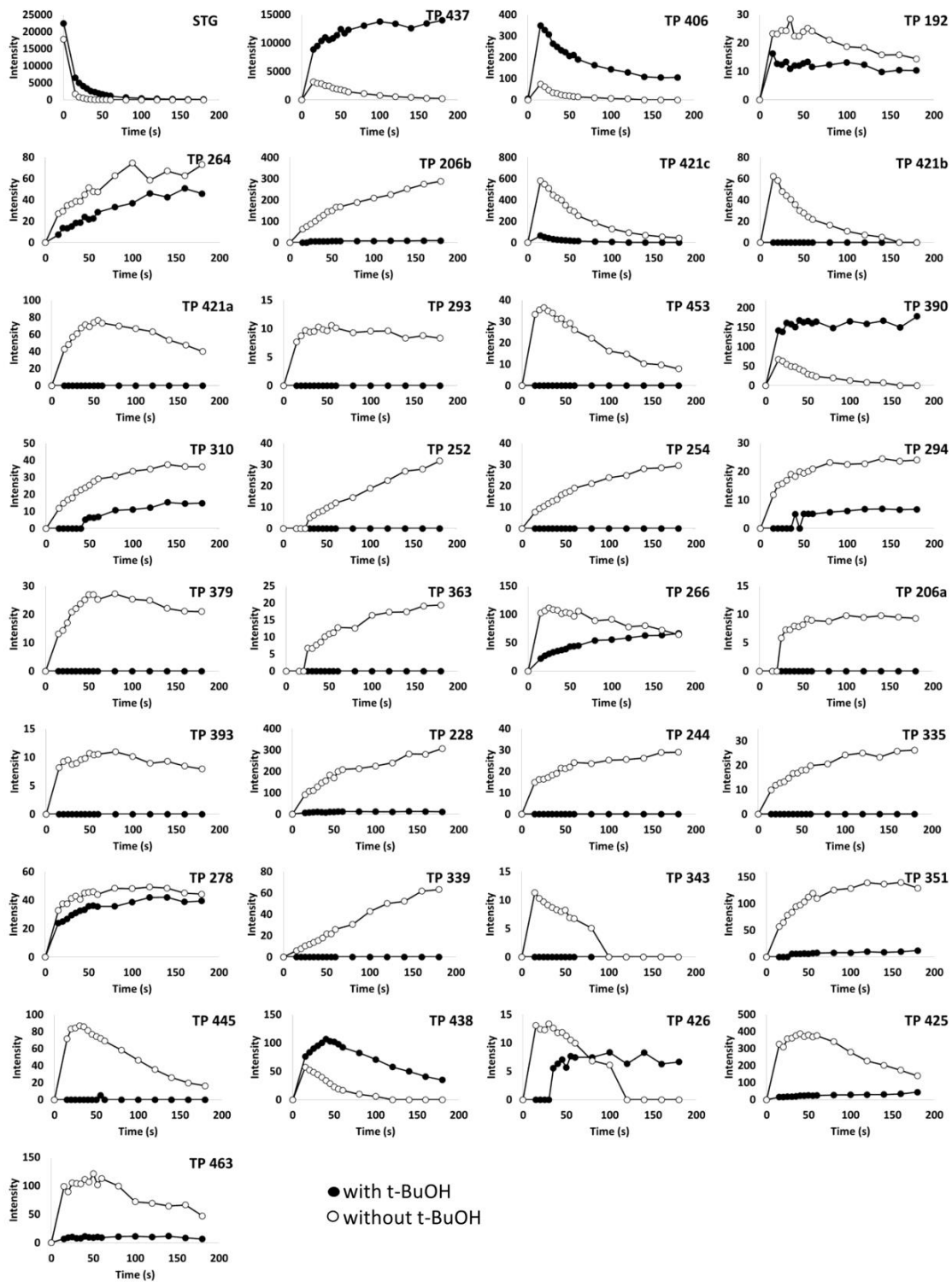
Figure A3.5. Occurrence of TPs in the time series of pH 8, 50 mM phosphate buffer, with and without t-BuOH

Table A3.5. Overview of observed potential TPs in WWTP effluent (batch experiments (WWTP Koblenz): DOC = 12 mg/L, pH = 8, spike STG: 1 mg/L; pilot plant (WWTP Lundakra): DOC = 10 mg/L, pH = 7). The table contains information about the retention times (RT), exact masses in positive and negative ESI and formation of TPs in WWTP effluent

TP	RT	LC		batch experiments		pilot plant
		[M+H]⁺	[M-H]⁻	spike STG	non-spike	
407, STG	10.2	408.126	452.1153			
Identified TPs or TPs for which proposals for possible structures could be made						
437	14	438.1000	436.0847	x	x	x
406	13.2	407.0940	405.0789	x	Influent	Influent
192	4.2	193.0696	-	x	Influent	Influent
264	7.6	265.0545	263.0394	x	x	-
206b	8.6	207.0490	205.0341	x	x	x
421c	12.6	422.1048	420.0894	x	x	x
421b	12.2	422.1047	420.0894	x	x	-
421a	9.9	422.0920	420.0768	x	-	-
293	8.3	294.0812	292.0661	x	-	-
453	13.7	454.0943	452.0796	x	-	-
390	13.8	391.0990	389.0840	x	-	-
Unidentified TPs in the order of their appearance in the chromatogram						
310	7.8	311.0602	309.9442	x	-	-
252	7.8	253.0545	251.0396	x	-	-
254	7.9	255.0702	253.0564	x	-	-
294	8.2	295.0652	293.0501	x	-	-
379	8.2	380.0814	378.0662	x	-	-
363	8.3	364.0865	362.0713	x	-	-
266	8.5	267.0704	-	x	-	-
206a	8.5	207.0490	205.0341	x	-	-
393	8.5	394.0970	392.0818	x	-	-
228	8.6	229.0311	-	x	x	-
244	8.6	245.0049	-	x	-	-
335	8.8	336.0917	334.0764	x	-	-
278	8.9	279.0704	-	x	-	-
339	9.6	340.0867	338.0714	x	-	-
343	9.6	344.0966	342.0814	x	-	-
351	10.4	352.0868	350.0711	x	x	-
445	11.1	446.0920	444.0766	x	-	-
438	11.8	439.0838	437.0693	x	-	-
426	12	427.0833	-	x	-	-
425	13.4	426.0998	424.0854	x	x	x
463	13.4	464.0554	462.0583	x	-	-
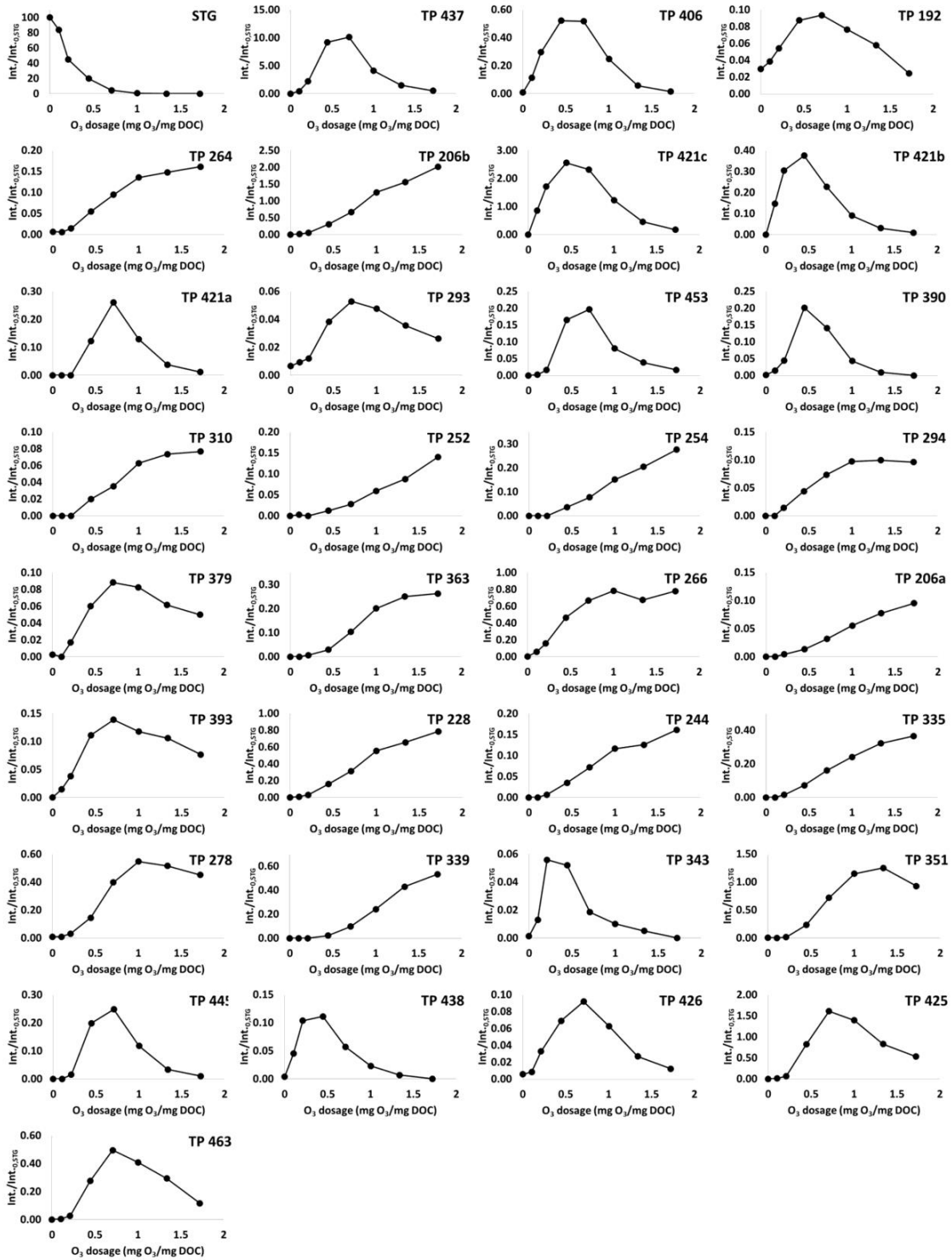
Figure A3.6. Occurrence of TPs in batch experiments in WWTP effluent with spiked STG (DOC = 12 mg/L, pH = 8, spike STG = 1 mg/L)

Text A3.1. Structure elucidation for observed TPs

Structure elucidation was based on the obtained MS^2 data. In a first step the MS^2 spectrum of STG was investigated and structures were assigned to the fragments to identify characteristic fragments. In a seconds step the MS^2 spectra of the TPs were searched for the characteristic fragments as well as for specific losses such as $-H_2NO$ (-47.00), $-NH_3$ (-17.03), $-CO_2$ (-43.99), -COOH (-44.99) etc. The in-silico fragmentation tool MetFrag (https://msbi.ipb-halle.de/MetFragBeta/) was searched for TP structures by calculating the neutral mass from the parent ion of the ionization, using the obtained MS2 data for the fragmentation settings and filtering for structures that obtain only C, N, O, H and/or F. Molecular formulas were derived from the exact masses via ChemCalc (https://www.chemcalc.org/mf_finder), giving an MF range of C 0-16, H 0-100, N 0-5, O 0-10 and F 0-6 with a mass range of 0.5.

STG: In positive ESI the small quasi-molecular ion shows the good fragmentability of STG. The loss of -17 with a change from even to uneven m/z can be attributed to a loss of NH2 leading to fragment m/z 391.098. Fragments m/z 174.053 and 171.042 can be assigned to the benzoyl part of STG, while fragment m/z 193.069 gives the triazole-piperazine unit. In negative ESI STG is detected in the form of an adduct at m/z 452.114. The fragment m/z 406.11 corresponds to STG and it also can be detected with very low intensity in the MS1 spectrum. Base peak of STG in negative ionization is m/z 191.056 which corresponds to the triazole-piperazine unit. This fragment is will be used as characteristic fragment for the identification of TPs in negative ESI.
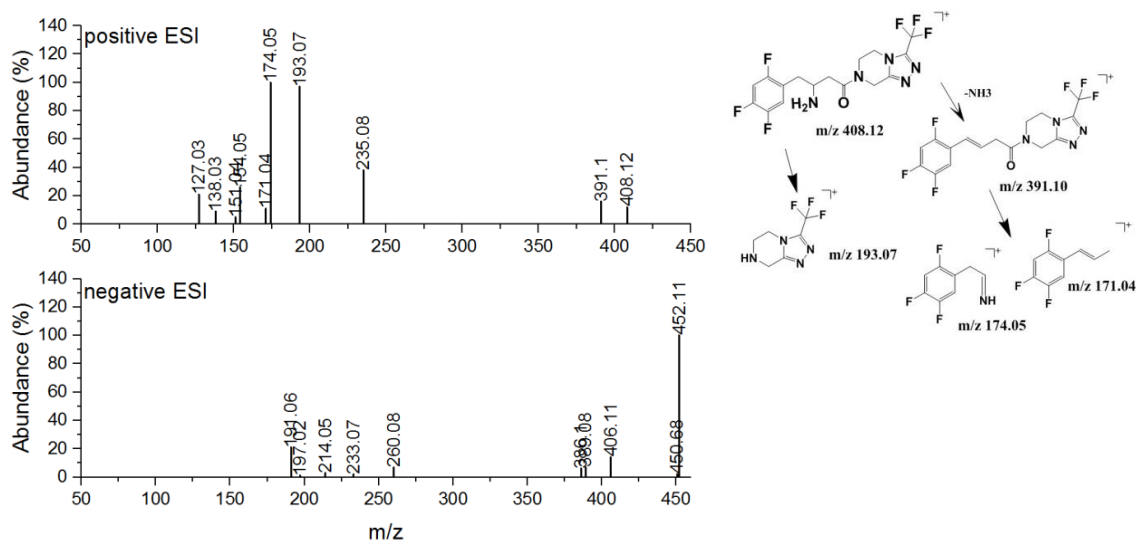
Figure A3.7. MS2 spectra of STG in positive and negative ESI (left) and characteristic fragments in positive ESI (right)

TP 437: In positive ESI the loss of -47 could be observed from the quasi-molecular ion at m/z 438.09 to the fragment m/z 391.10. This loss could be assigned to HNO2 which is characteristic for aliphatic nitro compounds in electron impact and atmospheric pressure ionization[1, 2]. The presence of m/z 193.07, m/z 171.04 and m/z 145.03 confirms that the basic structure of STG was maintained. Thus, the primary amine of STG was converted into a nitro group. The presence of m/z 191.06 as base peak in the MS2 of negative ESI confirms the presence of the unchanged triazole-piperazine unit. The same MS2 spectrum for the same exact mass was also detected in IC-ESI-QTOF at a retention

time of 4.4 min. Retardation in IC can be explained by a partially negatively charged C-atom at the nitro group at the pH of the IC eluent. A search in MetFrag with the obtained MS2 data confirmed the structure, the molecular formula is C16H13F6N5O3.
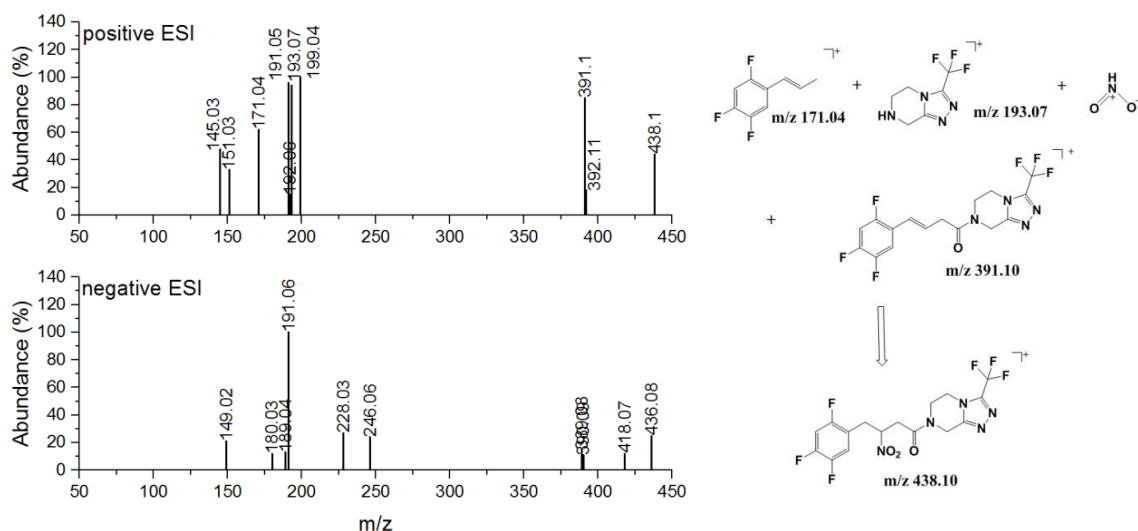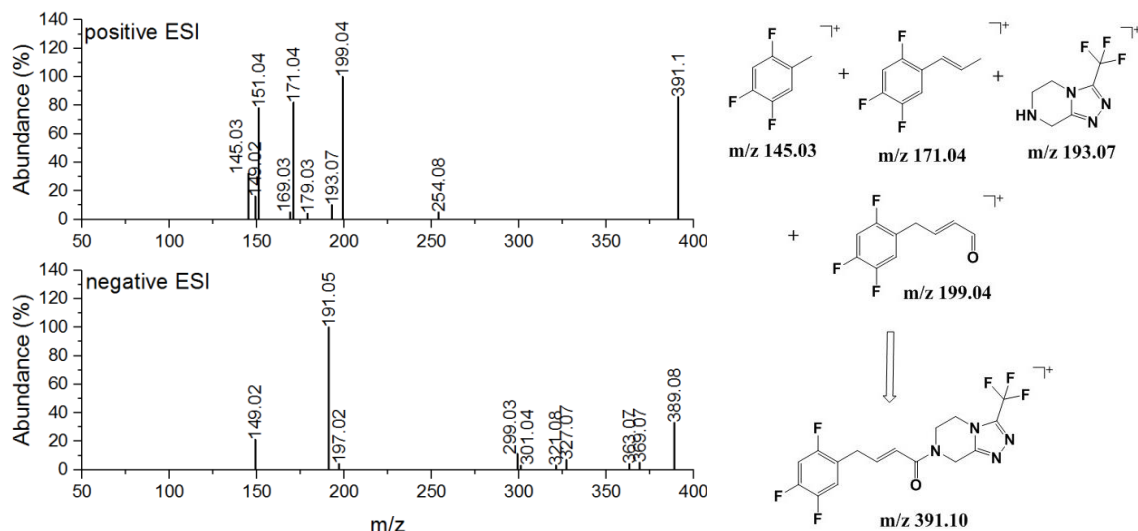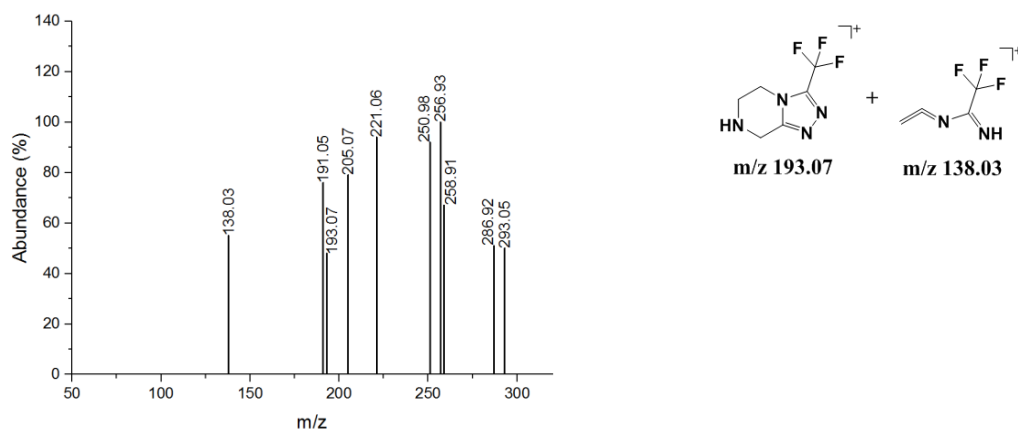

Figure A3.8. MS2 spectra of TP 437 in positive and negative ESI (left) and structure elucidation in positive ESI (right)

TP 406: For TP 406 characteristic fragments for the benzoyl unit (m/z 145.03) and for the triazole-piperazine unit (m/z 193.07) could be detected in positive ESI. Some low intensity, higher mass fragments could be found showing a loss of -18 to the quasi-molecular ion, indicating the presence of oxygen groups. The presence of the unchanged triazole-piperazole unit is confirmed by the fragment m/z 191.06 which, as for STG and TP 437, is the base peak in the MS2 spectrum of negative ionization. A reference standard could be obtained and analysed. The proposed structure of TP 406 could be verified by a commercially available reference standard.
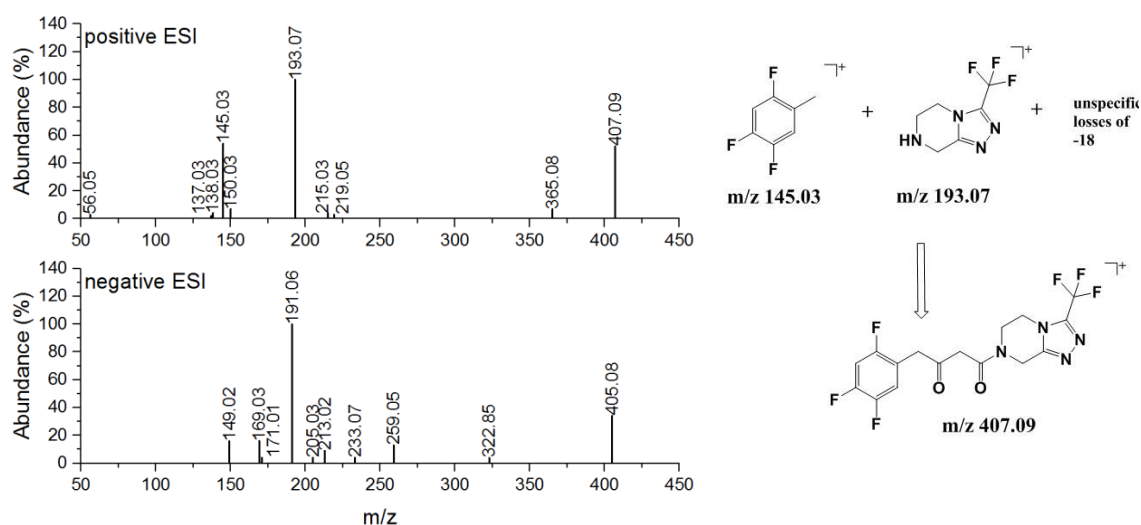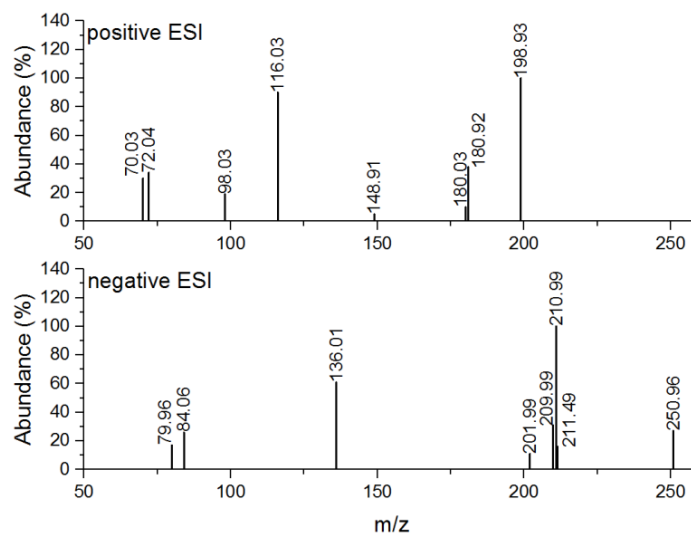

Figure A3.9. MS2 spectra of TP 406 in positive and negative ESI (left) and structure elucidation in positive ESI (right)

TP 192: TP 192 only can be detected in positive ESI and can be identified as the triazole-piperazine unit. Since a reference standard is available commercially, identification can be verified. The detected MS2 spectrum serves as comparison for the other detected TPs.
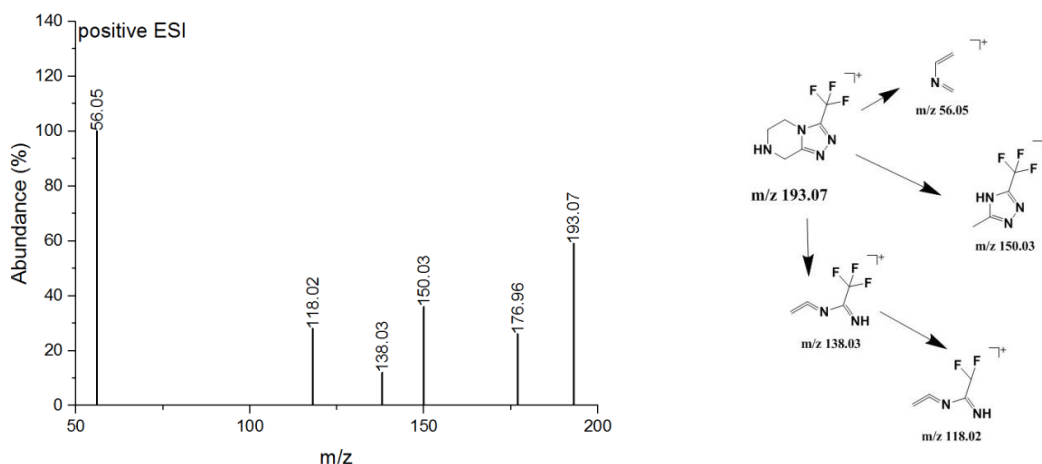
Figure A3.10. MS2 spectra of TP 192 in positive ESI (left) and characteristic fragments in positive ESI (right)

TP 264: A specific loss of -44 could be observed which can be attributed to the loss of CO_2 forming fragment m/z 221.063 in positive ESI. In positive ESI the fragments m/z 193.07, 150.03, 138.03, 118.02 and 56.05 can be attributed to the triazole-piperazine unit which seems to be unchanged. Thus, a carboxy group seems to be attached to the triazole-piperazine unit. The base peak of m/z 191.06 can be assigned to the triazole-piperazine unit. As in pos ESI the quasi-molecular ion cannot be observed. A peak with exactly the same MS2 spectrum at the same exact mass was also obtained in IC-ESI-QTOF. Thus, the molecule contains a negative charge which corresponds to the observed loss of the carbonyl group. A search in MetFrag with the obtained MS2 data confirmed the structure, the molecular formula is $C_8H_7F_3N_4O_3$.
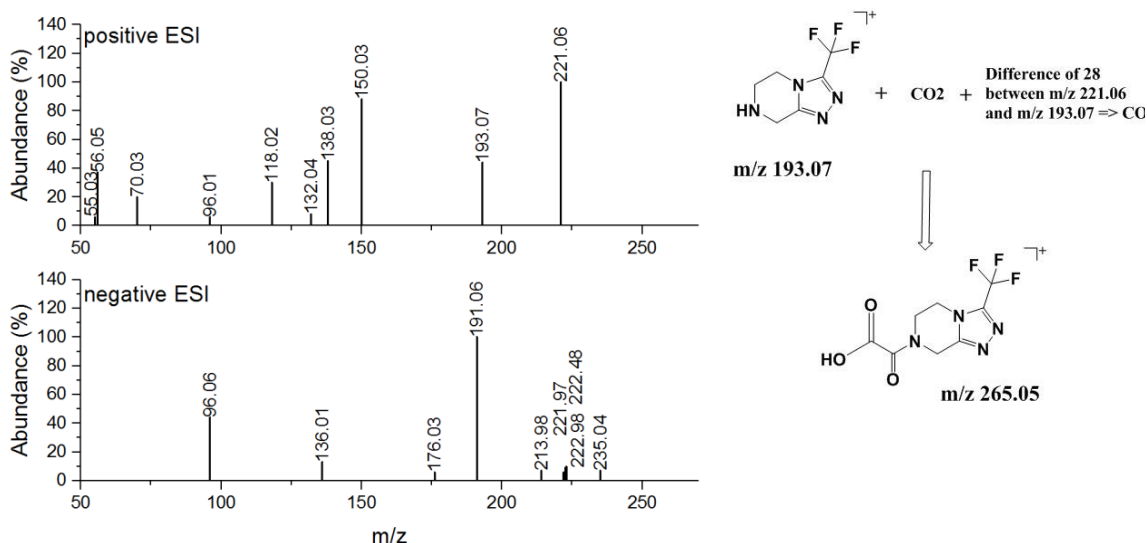
Figure A3.11. MS2 spectra of TP 264 in positive and negative ESI (left) and structure elucidation in positive ESI (right)

TP 206b: Fragments m/z 138.03 and m/z 118.02 are known as fragments of the triazole-piperazine unit (see at TP 192). However, since there is not the characteristic fragment of the triazole-piperazole unit itself, it seems to be altered upon transformation. An unspecific loss of of -18 from the quasi-molecular ion, leading to a low intensity fragment mass, can be detected. Thus, an oxygen might be present in the structure. The MS2 spectrum of the negative ESI confirms that the triazole-piperazole unit must be altered since the characteristic fragment of m/z 191.06 is missing. Searching for possible molecular formulas by the exact mass gave C6H5F3N4O with a double bond equivalent of 5 as possible result. However, the proposed structure could not be verified, neither by a reference standard not by a search in MetFrag.
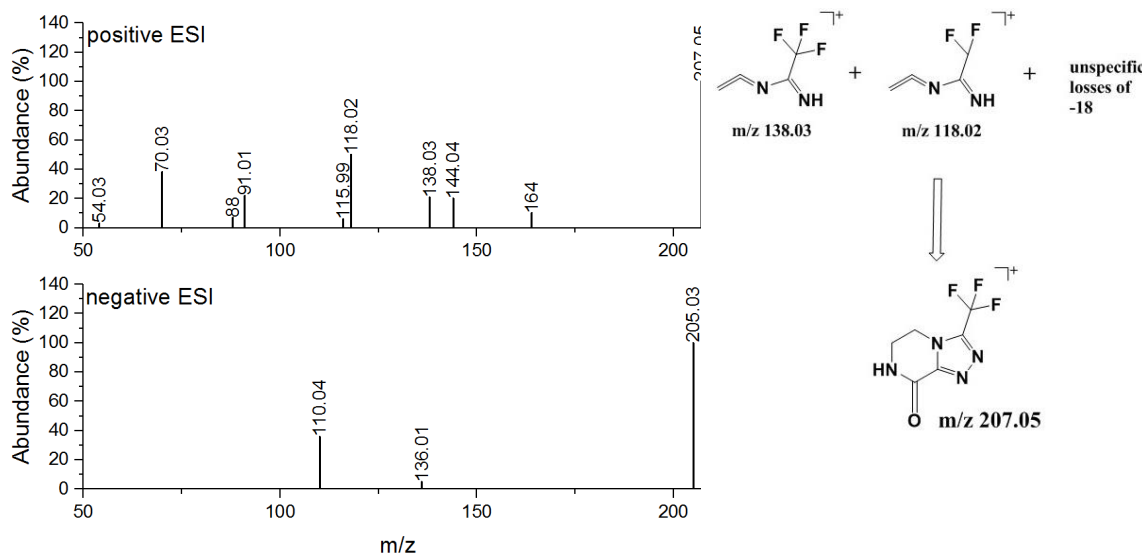
Figure A3.12. MS2 spectra of TP 206b in positive and negative ESI (left) and structure elucidation in positive ESI (right)

TP 421c: The MS2 spectrum of TP 421c in positive ESI contains characteristic fragments for the benzoyl unit (m/z 145.03) as well as for the triazole-piperazine unit (m/z 193.07). Fragment m/z 191.06 also appears as fragment of TP 437 and is thought to be also caused by the triazole-piperazine unit. In contrast to the MS2 spectrum of the positive ionization, the characteristic fragment for the triazole-piperazine unit is not visible in negative ionization. Base peak is m/z 136.01. There is a series of fragments showing losses of -20 (m/z 420.08/400.08 and 377.08/357.08) which might be due to losses of HF. The exact mass leads to a proposed molecular formula of C16H13F6N5O2 with a double bond equivalent of 10. TP 421c also could be detected by IC-ESI-QTOF, thus, a TP must carry a negative charge at the pH of the mobile phase in IC (pH = 10). This would fit to an oxime structure of STG.
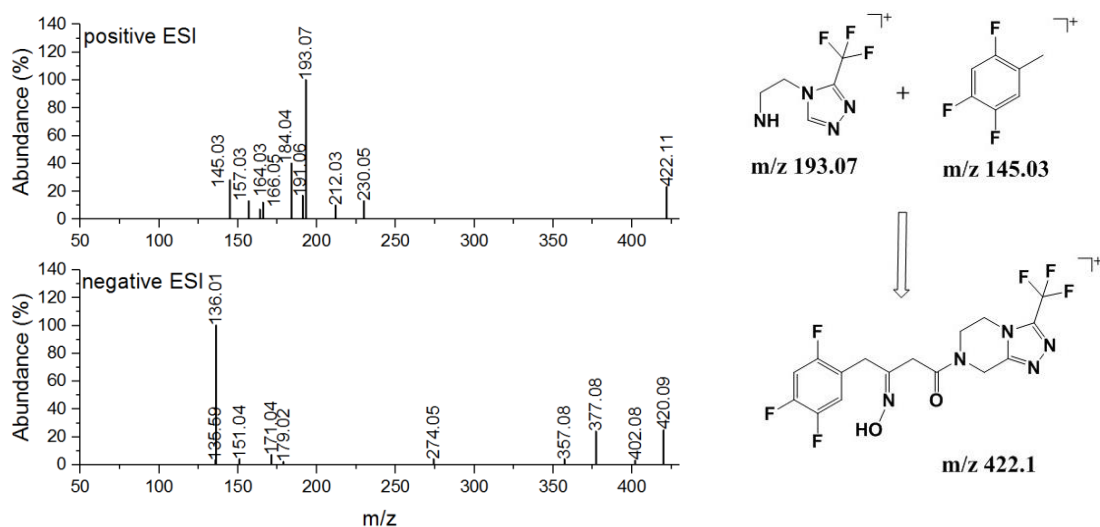
Figure A3.13. MS2 spectra of TP 421c in positive and negative ESI (left) and structure elucidation in positive ESI (right)

TP 421 b: TP 421b shows a complex MS2 spectrum with several fragment masses. The spectrum differs from the ones obtained for TP 421a and 421c. The characteristic fragments for the triazole-piperazine unit cannot be observed, except for m/z 150.03. But the characteristic fragments for the benzyol unit are present. Furthermore, fragment 199.04 is known from TP 437 and was assigned to the benzoyl unit. The high intensity of the [M+H]+ speaks for low fragmentability. The high mass range shows several fragments which makes assignment of neutral losses quite difficult. The MS2 spectrum in negative ESI is more clear than for positive ESI. Losses of -18 and -20 can be observed but there is still no precise information for structure elucidation. The exact mass leads to a proposed molecular formula of C16H13F6N5O2 with a double bond equivalent of 10. However, a structure could not be proposed.
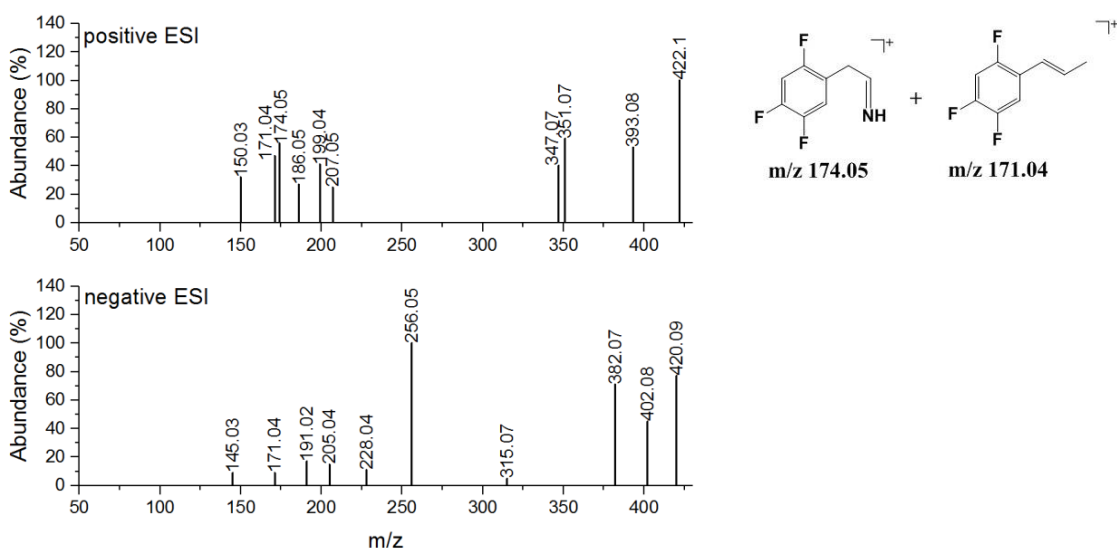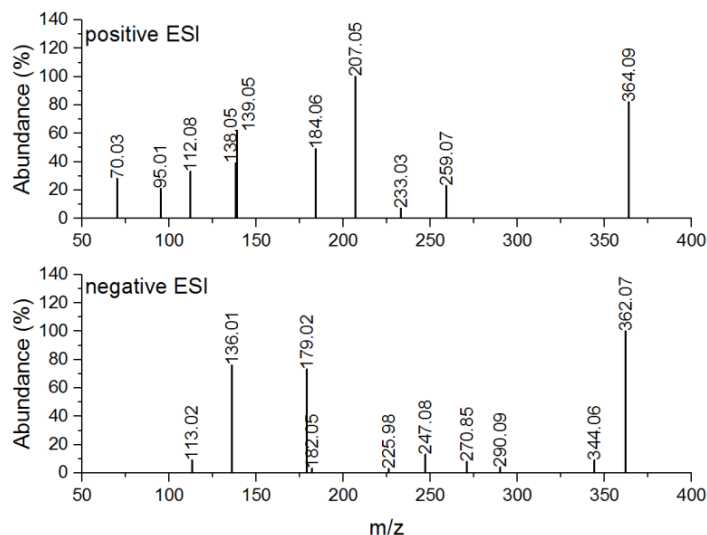

Figure A3.14. MS2 spectra of TP 421b in positive and negative ESI (left) and observed characteristic fragments in positive ESI (right)

TP 421a: The MS2 spectrum of TP 421a contains the characteristic fragment for the triazole-piperazine moiety, m/z 191.05 and m/z 193.07. Characteristic fragments for the benzoyl moiety could not be identified. Base peak is m/z 404.08 which shows a loss of -18 to the quasi-molecular ion which is indicative for the addition of a. OH group to the molecule. In negative ESI higher intensities and MS2 spectra could be obtained. The high intensity for the [M-H]- shows the low fragmentability of the structure. The base peak, m/z 329.09, is nearly at the same height as the quasi-molecular ion. The characteristic fragment of the triazole-piperazine unit can be observed as well as losses of -47 and -44. The exact mass leads to a proposed molecular formula of C16H13F6N5O2 with a double bond equivalent of 10. However, a structure could not be proposed.
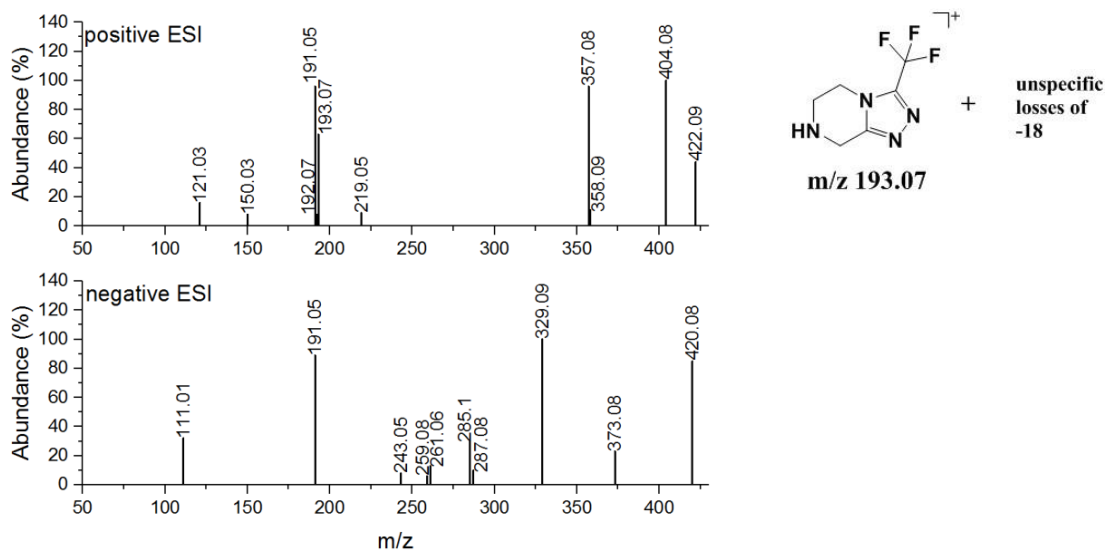
Figure A3.15. MS2 spectra of TP 421a in positive and negative ESI (left) and observed characteristic fragments in positive ESI (right)

TP 293: The MS2 spectrum of TP 293 shows the characteristic fragment for the triazole-piperazine unit (m/z 193.07) and fragments thereof (m/z 150.03, 118.02, additionally 138.02 and 56.05 as low intensity fragments). Highest mass fragments are m/z 277.05 (Δ -17) and m/z 276.07 (Δ -18), possibly showing a loss of OH and H2O respectively. The MS2 spectrum of the negative ESI supports the assumption of the intact triazole-piperazine unit due to the presence of fragment m/z 191.05. The exact mass leads to a molecular formula of C9H10F3N5O3 with a double bond equivalent of 6.
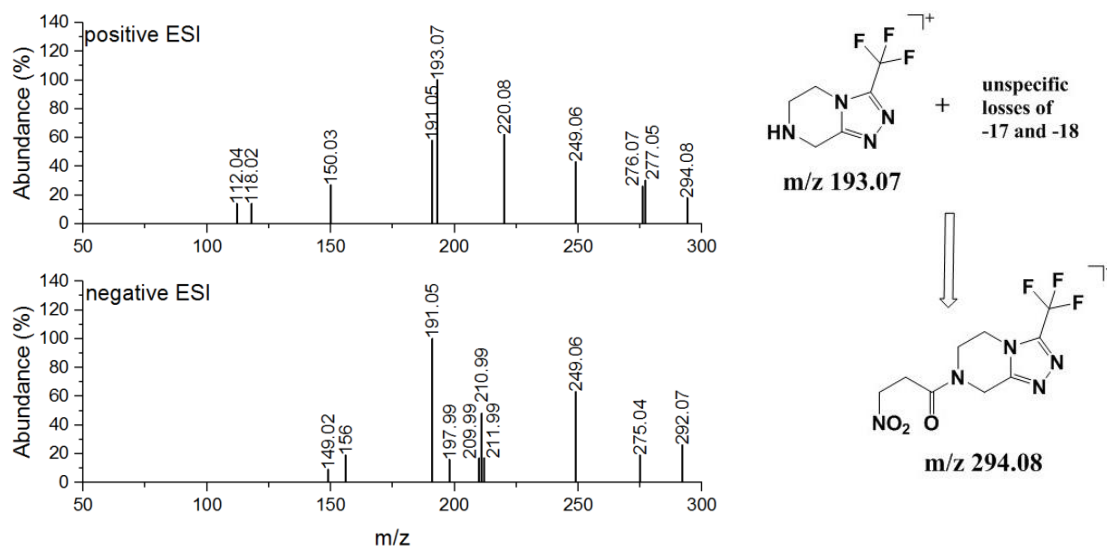
Figure A3.16. MS2 spectra of TP 293 in positive and negative ESI (left) and structure elucidation in positive ESI (right)

TP 453: In positive ESI the MS2 spectrum of TP 453 shows the characteristic fragments for the benzoyl unit (m/z 171.04, 151.04, 145.03). The fragment m/z 191.05 is known from the MS2 spectrum of TP 437 and can be assigned to the triazole-piperazine unit. The spectrum shows a loss of -47 to a low intensity fragment and a further loss of -18, yielding m/z 389.09. Thus, the molecule contains a nitro group and an additional Hydroxyl-Group. In negative ESI again the loss of the nitro group (m/z 452.08 to m/z 405.08) can be observed, giving the base peak of the spectrum. Also the loss of -18 occurs, yielding m/z 387.07. By the exact mass a molecular formula of $C_{16}H_{13}F_6N_5O_4$ with a double bond equivalent of 9 was derived.
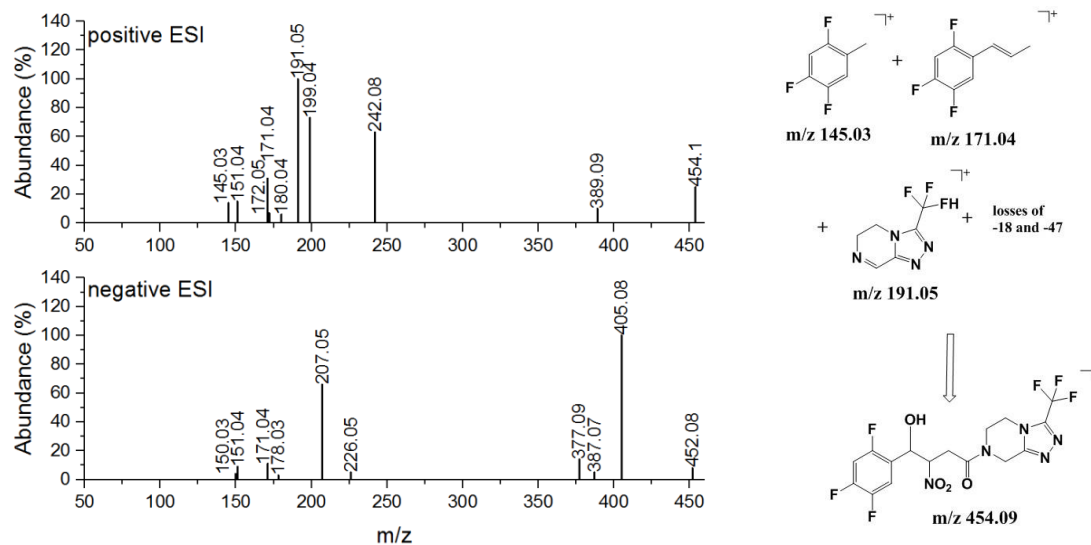
Figure A3.17. MS2 spectra of TP 453 in positive and negative ESI (left) and structure elucidation in positive ESI (right)

TP 390: For TP 390 characteristic fragments for the benzoyl unit (m/z 171.04) as well as for the triazole-piperazine unit (m/z 193.07) could be observed. The same exact mass also can be detected as fragment for STG and TP 437 but TP 390 shows a different RT and therefor also is formed as original TP. The MS2 spectrum of the negative ESI supports the assumption of the intact triazole-piperazine unit due to the presence of fragment m/z 191.05. By the exact mass a molecular formula of C16H12F6N4O with a double bond equivalent of 10 was derived.

Figure A3.18. MS2 spectra of TP 390 in positive and negative ESI (left) and structure elucidation in positive ESI (right)

TP 310: The MS2 spectrum of positive ESI shows a high number of fragment masses with similar intensity. Characteristic fragments for the triazole-piperazine unit can be observed but a structure elucidation is not possible.

Figure A3.19. MS2 spectra of TP 310 in positive ESI (left) and observed characteristic fragments (right)

TP 252: The MS2 spectrum of TP 252 in positive ESI does not show any characteristic fragments for the STG structure. In addition, no specific losses can be observed. However, the fact that the [M+H]+ is not visible speaks for an easily cleaved group within the structure. Also negative ESI does not lead to already known characteristic fragments. Here, the quasi-molecular ion is visible, base peak is the fragment m/z 210.99 (loss of -40). However, a structure elucidation is not possible.

Figure A3.20. MS2 spectra of TP 252 in positive and negative ESI

TP 254: As for TP 252 neither characteristic fragments nor specific losses can be observed in the MS2 spectrum of TP 254. Although also the MS2 spectrum in negative ESI does not show any characteristic fragments, it does show a fragment also occurring at TP 252: m/z 136.01. This fragment also occurs for other TPs and might show some structural similarities. A structure for TP 254 cannot be proposed.
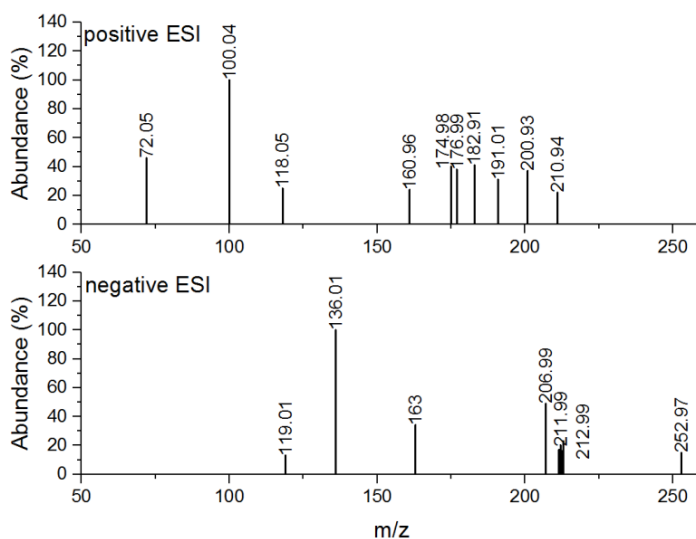
Figure A3.21. MS2 spectra of TP 254 in positive and negative ESI

TP 294: Since all characteristic fragments for the triazole-piperazine unit can be observed for TP 294, this part must be unchanged. In addition, no quasi-molecular ion is observed, speaking for an easy to cleave group, and a specific loss of -44 occurred from the precursor mass to the highest mass fragment of m/z 251.07, being assigned to a loss of CO_2. Further, an unspecific loss of -18 can be observed from m/z 251.07 to m/z 233.06. Both losses together might be an indication for three oxygen atoms in the molecule. The uneven mass of the precursor speaks for an even number of nitrogens. Base peak of the MS2 in negative ESI is fragment m/z 191.06 which corresponds to the

triazole-piperazine unit, confirming its unchanged presence in the molecule. A structure for TP 294 cannot be proposed.
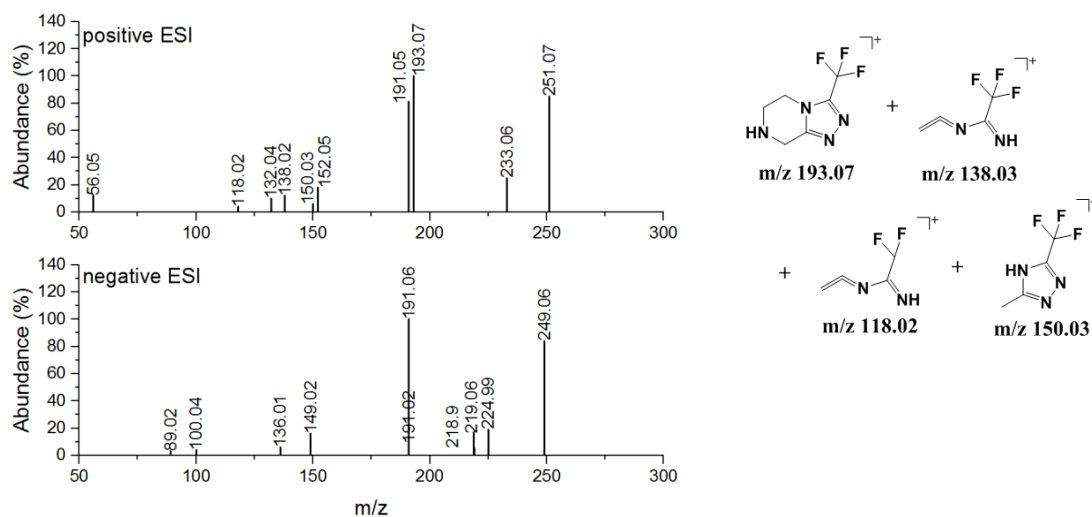
Figure A3.22. MS2 spectra of TP 294 in positive and negative ESI (left) and observed characteristic fragments (right)

TP 379: In positive ESI the quasi-molecular ion is not visible. The mass difference to the highest mass fragment m/z 336.09 is -44, which usually can be assigned to CO_2. Furthermore, unspecific losses of -18 and -28 were observed, possibly showing another oxygen atom. The even m/z of the precursor indicated an uneven number of nitrogens and the triazole-piperazine unit is unchanged due to the appearance of the characteristic fragment m/z 193.07. The MS2 of the negative ionization supports the assumption of the unchanged triazole-piperazine unit since the characteristic fragment m/z 191.05 occurs in the spectrum. A structure for TP 379 cannot be proposed.
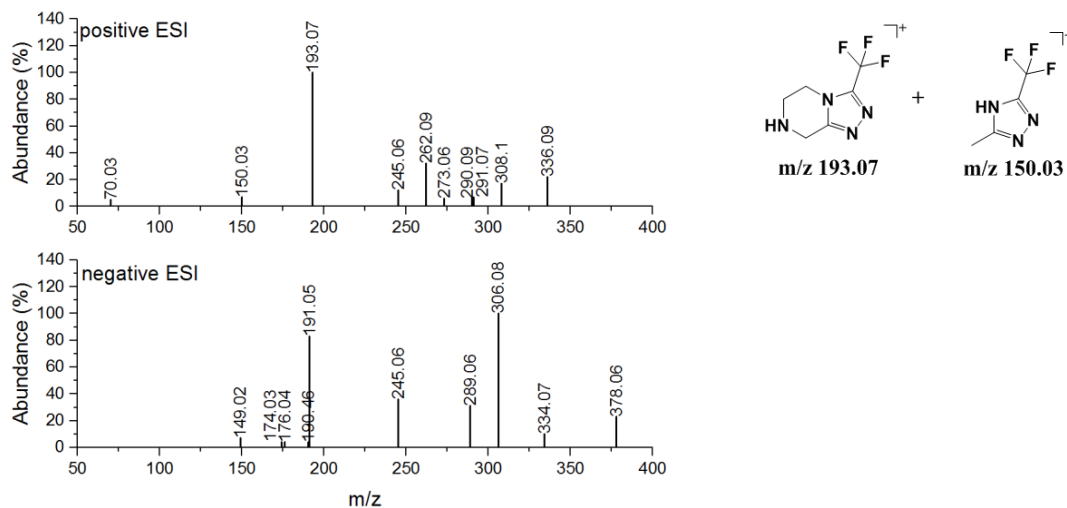
Figure A3.23. MS2 spectra of TP 379 in positive and negative ESI (left) and observed characteristic fragments in positive ESI (right)

TP 363: The MS2 spectrum of TP 363 does not contain any characteristic fragments. The high mass difference of -105 from the [M+H]+ to the highest mass fragment does not allow for any assumption about neutral losses. As for positive ESI, no characteristic fragments were visible in negative ESI.

Here, a lower mass difference from the quasi-molecular ion to the highest mass fragment of -18 could be observed. However, this does not lead to any further conclusions about a possible structure. A structure for TP 363 cannot be proposed.
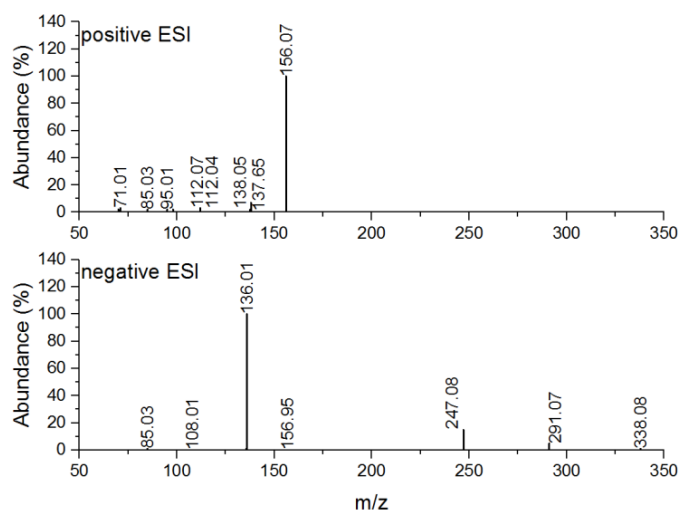

Figure A3.24. MS2 spectra of TP 363 in positive and negative ESI

TP 266: TP 266 shows all characteristic fragments for the triazole-piperazine unit in the MS^2 spectrum of positive ESI. Furthermore, a mass difference of -18 was detected from the $[M+H]^+$ to the highest mass fragment, m/z 249.06, a loss of -28 to fragment m/z 221.07 and a further loss of -28 to m/z 193.07. A similar pattern of fragments already could be observed for TP 264, the carboxylated triazole-piperazine unit. The facts that no specific loss of CO_2 but an unspecific loss of H_2O could be observed and the difference of +2 between the TP masses might indicate basically the same structure, however, a signal for this TP could neither be detected in LC-ESI(neg)-QTOF nor in IC-ESI-QTOF. By the exact mass a molecular formula of $C_8H_9F_3N_4O_3$ was derived.
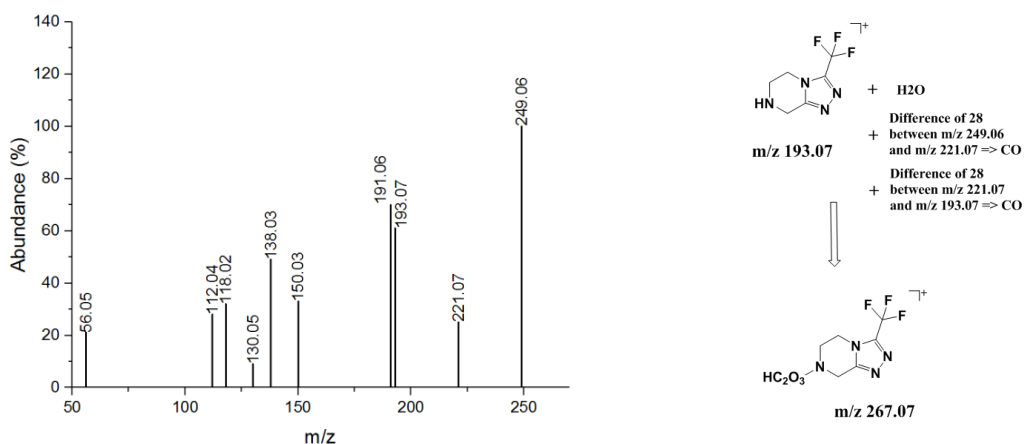
Figure A3.25. MS2 spectra of TP 266 in positive ESI (left) and structure elucidation for positive ESI (right)

TP 206a: The MS2 spectrum of positive ESI shows characteristic fragments of the triazole-piperazine unit, but fragment m/z 193.07 is missing. Therefore, alteration at this structure might have occurred.

Based on the exact mass the same molecular formula as well as the same structure as for TP 206a can be proposed. However, there are clear differences in the MS2 spectra of both and thus, the true structure of both TPs remains unclear. In negative ESI only three fragments can be observed with which no structure elucidation can be performed.
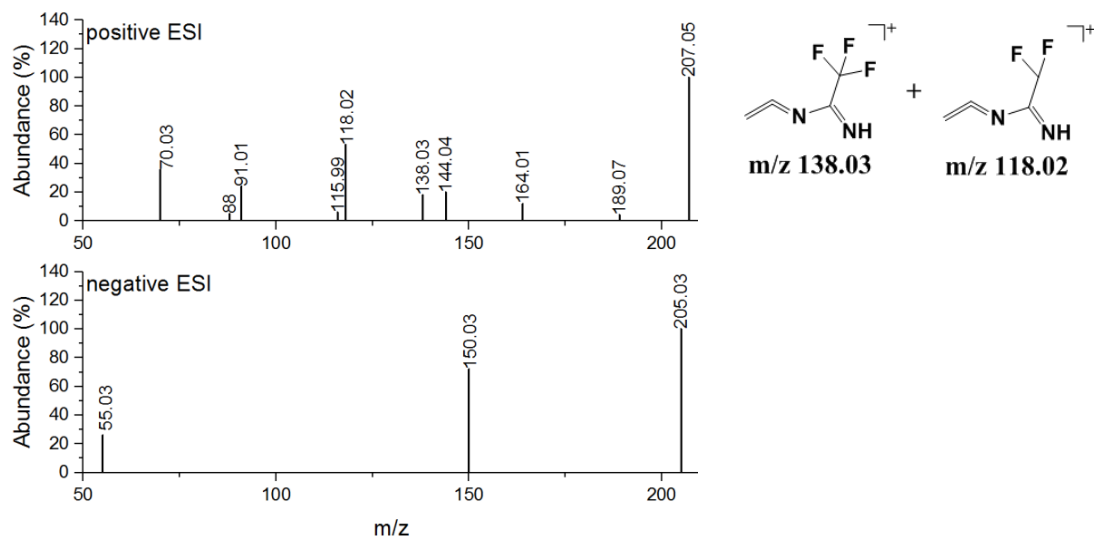
Figure A3.26. MS2 spectra of TP 206a in positive and negative ESI (left) and characteristic fragments in positive ESI (right)

TP 393: The MS2 spectrum of positive ESI for TP 393 contains the characteristic fragment for the triazole-piperazine unit (m/z 193.07) as well as fragments thereof at low intensity. Fragment m/z 235.08 appears also for STG and shows the triazole-piperazine unit with the intact amide group. The presence of the triazole-piperazine unit in TP 393 is supported by the fragment m/z 191.06 in negative ESI. However, it is not the base peak of the spectrum but the second highest after m/z 259.08. A structure for TP 393 cannot be proposed.
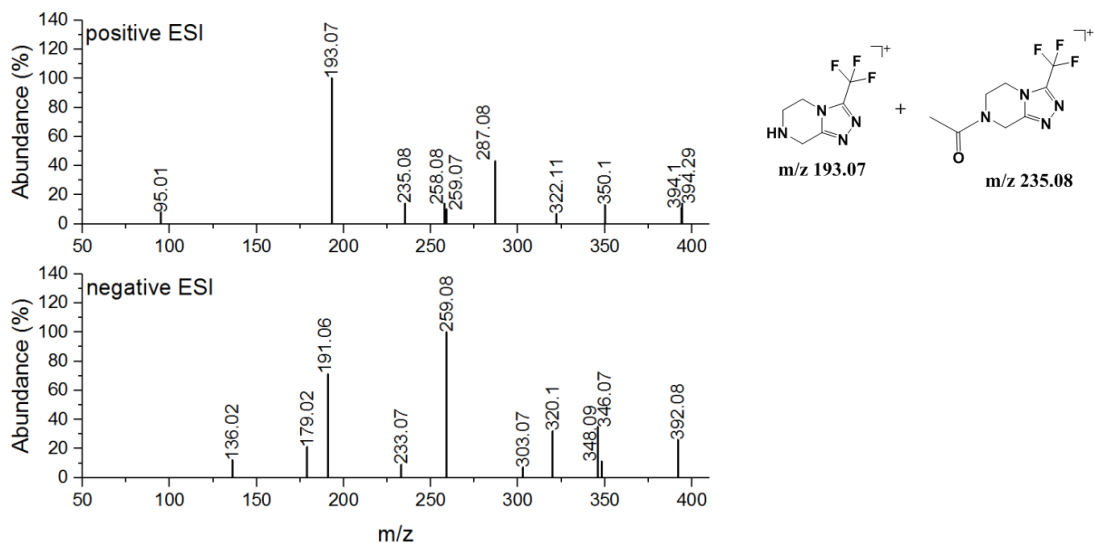
Figure A3.27. MS2 spectra of TP 393 in positive and negative ESI (left) and characteristic fragments in positive ESI (right)

TP 288: The MS2 spectrum of TP 228 in positive ESI does not contain any characteristic fragments. Base peak is the quasi-molecular ion, thus, there is no functional group which would be easy to cleave off. The mass difference of the [M+H]+ to the highest mass fragment m/z 169.91 is 60 which usually can be found in ester compounds[3]. It could not be detected in negative ESI. A structure for TP 288 could not be proposed.
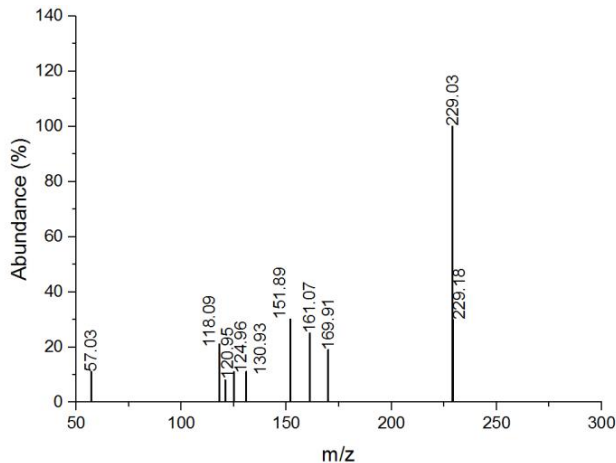
Figure A3.28. MS2 spectrum of TP 288 in positive ESI

TP 244: For TP 244 no characteristic fragments could be observed in the MS2 spectrum of positive ESI and it could not be detected in negative ESI.
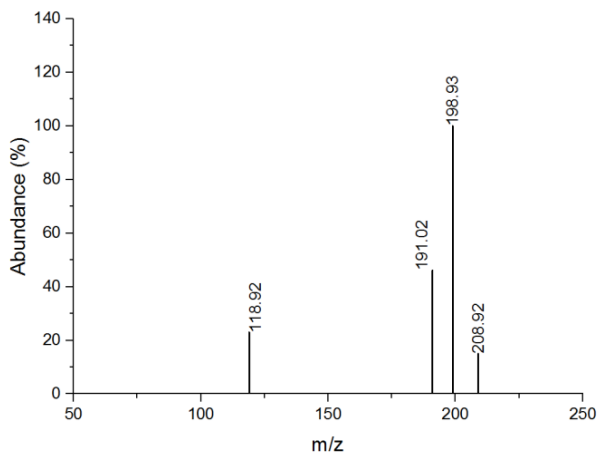
Figure A3.29. MS2 spectrum of TP 244 in positive ESI

TP 335: Characteristic fragments do not occur in the MS2 spectrum of positive ESI. However, base peak is 207.06 which might be the structure of TP 206 a and/or b. Furthermore there is an unspecific loss of -18 (H_2O) from the [M+H]+ to a low intensity fragment (m/z 318.08). Further losses of -18 occur as well as a -42. Base peak in negative ESI is m/z 205.03 which, as in positive ESI, might correspond with the structure of TP 206 a and/or b.
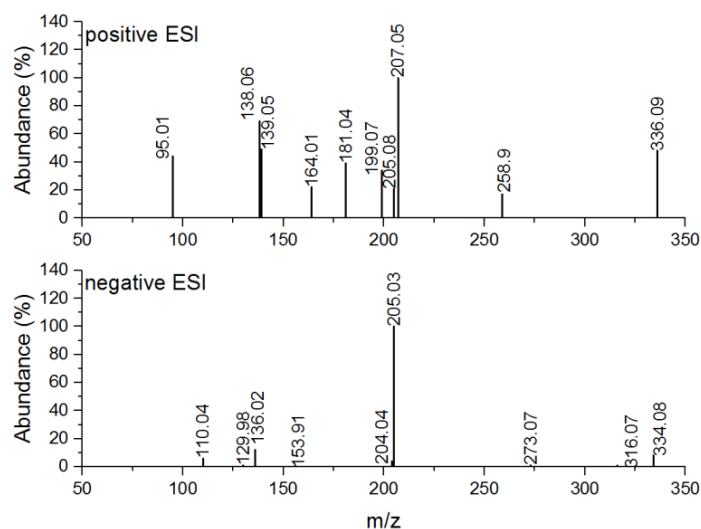
Figure A3.30. MS2 spectra of TP 335 in positive and negative ESI

TP 278: For TP 278 the characteristic fragments for the triazole-piperazine unit are observable as well as the fragment for the intact amide group (m/z 235.08). A loss of -18 can be observed from the [M+H]+ to give fragment m/z 261.06, followed by a -26 loss to fragment m/z 235.08.
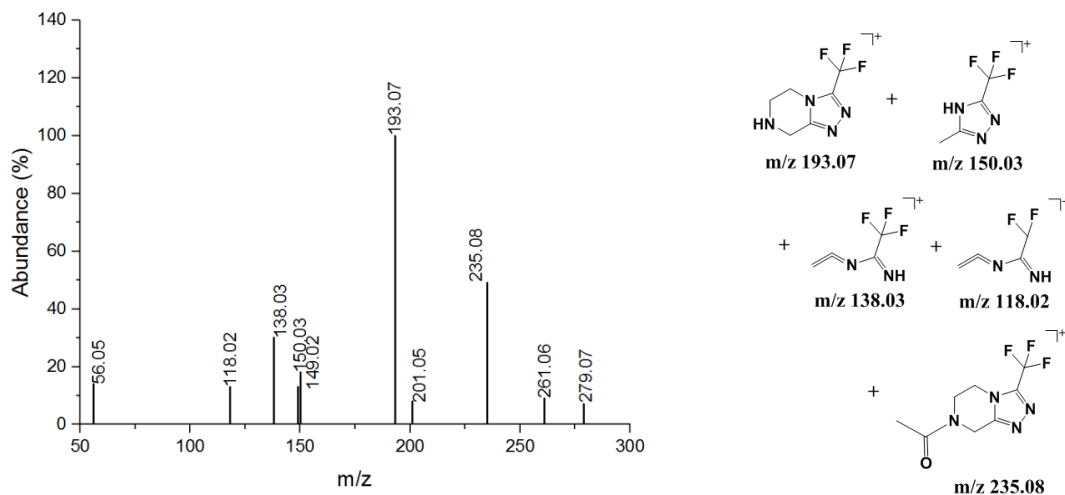
Figure A3.31. MS2 spectrum of TP 278 in positive ESI (left) and characteristic fragments ESI (right)

TP 339: TP 339 does not show any characteristic fragments in its positive ESI MS2 spectrum. Base peak is m/z 156.07 which does not appear as base peak in any other TP. The quasi-molecular ion cannot be observed, speaking for a high fragmentability but nearly no fragments can be observed in the higher mass region which is important for structure elucidation. In negative ESI base peak is m/z 136.01. This fragment already could be observed for other TPs in negative ESI (e.g. TP 363, 254, 252). Furthermore a loss of -47 appears from the [M-H]- to m/z 291.01 followed by a loss of -44 to m/z 247.08. However, also from negative ESI no precise information about a possible structure can be derived.

Figure A3.32. MS2 spectrum of TP 339 in positive and negative ESI

TP 343: TP 343 occurs only at a very low intensity in the ozonated samples. In positive ESI no MS2 was recorded. In negative ESI detected intensities were higher than in positive mode and a MS2 was recorded. As base peak it showed m/z 191.06 which is characteristic for the triazole-piperazine unit. The quasi-molecular ion could be observed, highest mass fragments show only little intensity. However, losses of -18 and -46 could be observed.
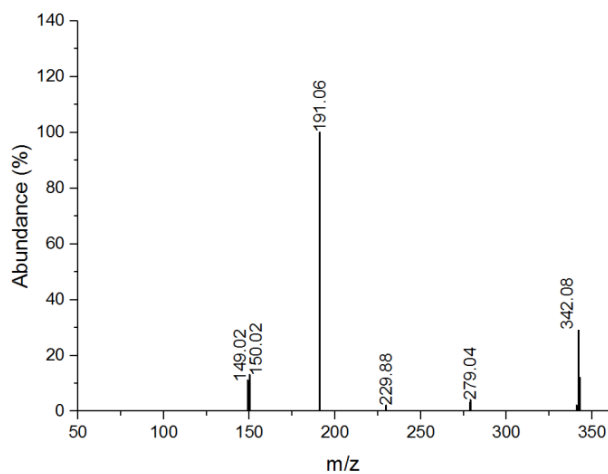
Figure A3.33. MS2 spectrum of TP 343 in negative ESI

TP 351: In positive ESI the MS2 spectrum of TP 351 is dominated by five mass peaks: the [M+H]+, m/z 305.08 (loss of -47 from [M+H]+), m/z 287.07 (loss of -18 from m/z 305.08), m/z 193.07 and m/z 191.05. The latter two fragments are characteristic for the triazole-piperazine unit. Next to the loss of -47 there is also a loss of -46 observable, giving rise to the fragment 306.09. Thus it seems as if the structure contains a nitro group and at least a further oxygen-group due to the loss of -18.
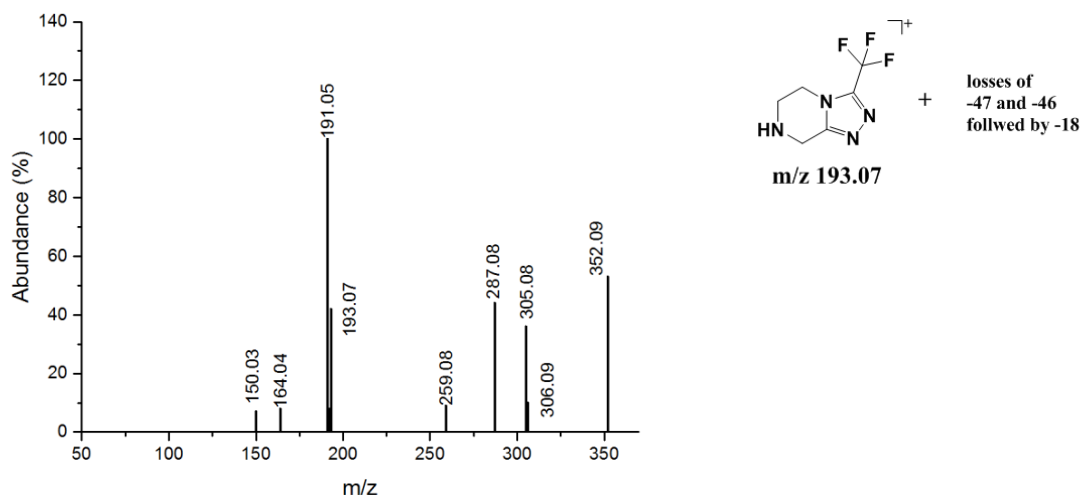
Figure A3.34. MS2 spectrum of TP 351 in positive ESI (left) and characteristic fragments ESI (right)

TP 445: The MS2 spectrum in positive ESI shows a loss of -18 from the [M+H]+ to m/z 428.08 followed by a loss of -47 to m/z 381.08 which speaks for the presence of a hydroxyl and a nitro group. The fragments m/z 193.07 and 191.05 can be assigned to the unchanged triazole-piperazine unit while characteristic fragment for the benzyol unit are not detected and thus, this part must been altered. Base peak of the MS2 spectrum in negative ESI is m/z 353.09. Second intense fragment is m/z 191.06 which, as seen in positive ESI, can be assigned to the unchanged triazole-piperazine unit.
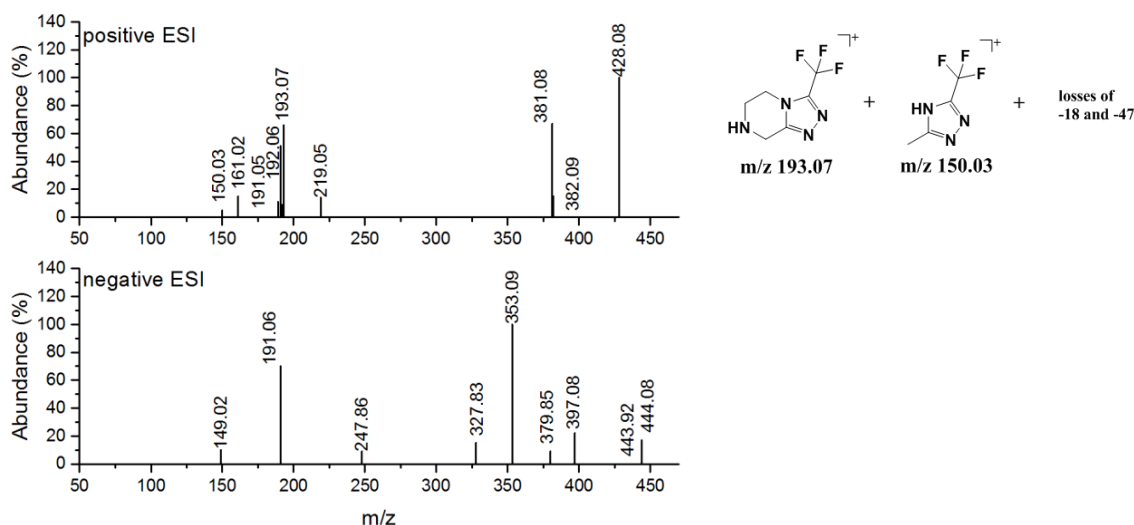
Figure A3.35. MS2 spectra of TP 445 in positive and negative ESI (left) and characteristic fragments ESI (right)

TP 438: In positive ESI TP 438 shows a loss of -44 from [M+H]+ to its base peak, m/z 395.09 follwed by a loss of -18 to fragment m/z 377.08. Assigning these losses to CO_2 and H_2O, at least three oxygen atoms are contained in the structure. Furthermore, characteristic fragments for the triazole-piperazine unit (m/z 193.07) and for the benzyol unit (m/z 145.03) can be observed. In negative ESI m/z 393.08 is the base peak, which corresponds with the MS2 of positive ESI. And also in negative ESI the characteristic fragment for the triazole-piperazine unit can be observed. Calculating the molecular formula from the exact mass gives C16H12F6N4O4 with a double bond equivalent of 10 as

possible result. Thus, the basic structure of STG might be conserved with additional three oxygen atoms and without the primary amine.
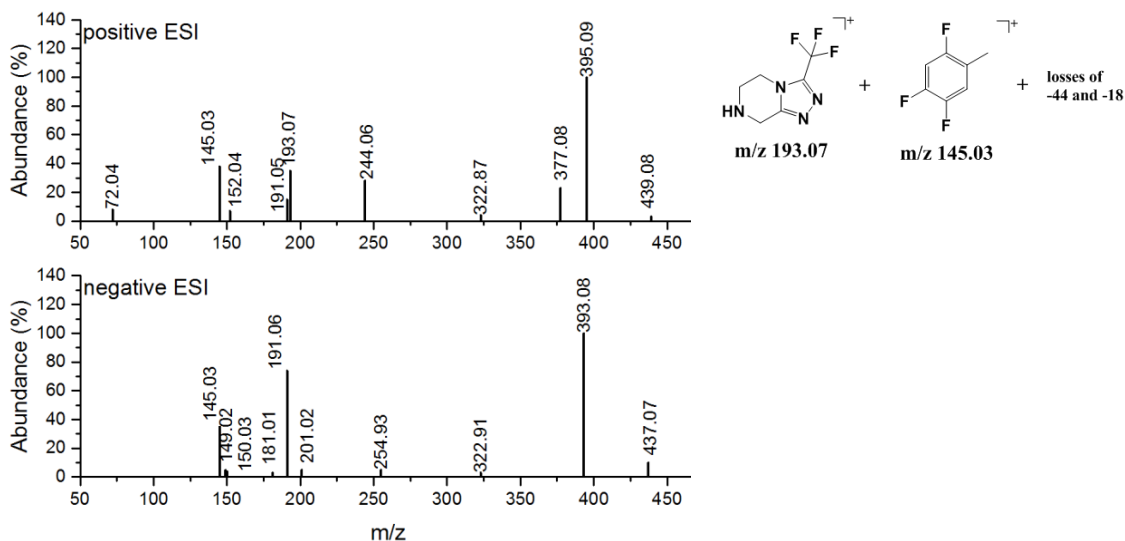
Figure A3.36. MS2 spectra of TP 438 in positive and negative ESI (left) and characteristic fragments in positive ESI (right)

TP 426: TP 426 shows a characteristic fragment for the benzyol unit (m/z 145.03) but none for the triazole-piperazine unit. The fragments of the high mass region have only low intensity and thus, neutral losses cannot be assigned.
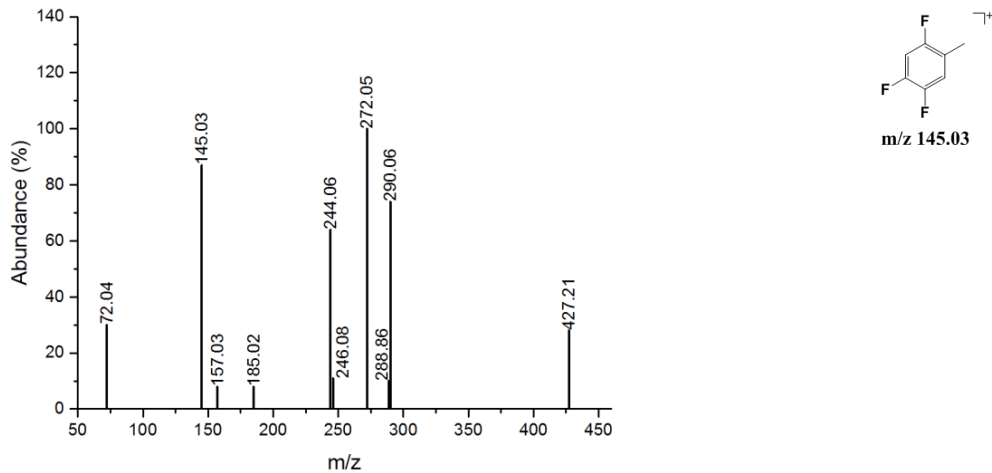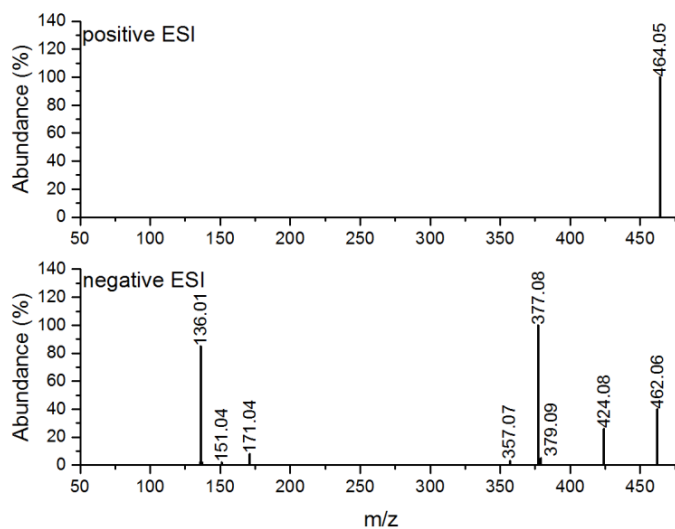

Figure A3.37. MS2 spectrum of TP 426 in positive ESI (left) and characteristic fragments ESI (right)

TP 425: TP 425 shows the characteristic fragments for the benzoyl unit (m/z 171.04, 145.03, 199.04) but at a very low intensity. Base peak is m/z 242.08. The quasi-molecular ion is observable at a very low intensity and there are no fragments in the high mass region which could be used for structure elucidation.
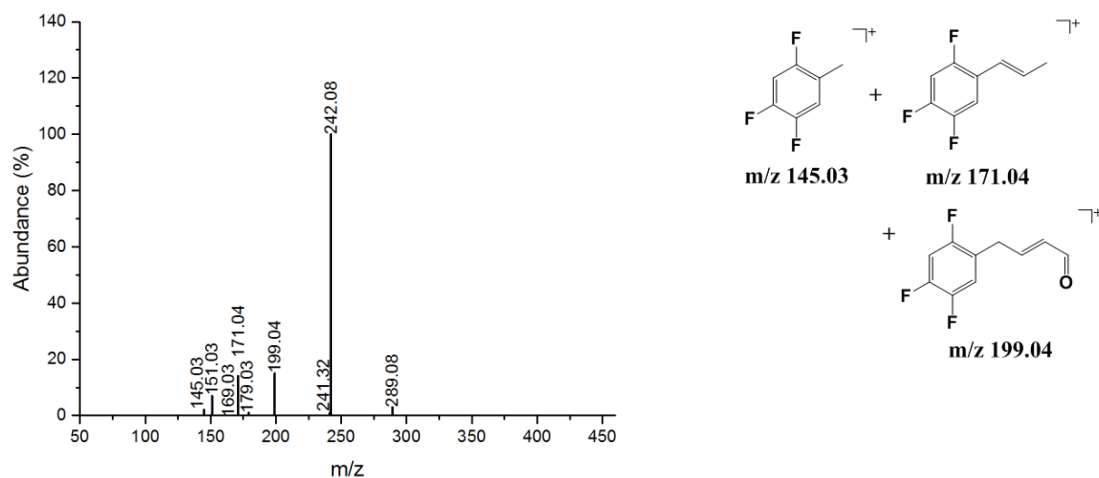
Figure A3.38. MS2 spectrum of TP 425 in positive ESI (left) and characteristic fragments ESI (right)

TP 463: In positive ESI no fragmentation occurred. In negative ESI no characteristic fragments could be observed, neither for the benzoyl nor for the triazole-piperazine unit. Fragment 424.08 is formed by a loss of -38 from the quasi-molecular ion, followed by a loss of -47 to give the base peak, m/z 377.08. Second highest fragment is m/z 136.01 which is already known as intense fragment for other TPs but could not be assigned to any structure yet.

Figure A3.39. MS2 spectra of TP 425 in positive and negative ESI

Text A3.2: TFA is a known TP of STG[4]. Its formation is reported under radical reactions. The time series experiments under different pH values therefore were analysed for TFA formation under both reaction types, with t-BuOH and without.

With increasing pH formation of TFA increases when radicals were involved in the reaction. With the radical scavenger an initial TFA formation can be observed, maybe originating from a contamination.

TFA formation only accounts for a minor amount in the transformation of STG, with only 2% of the initial STG concentration. This result is in accordance with the study of Scheurer, et al. [4].
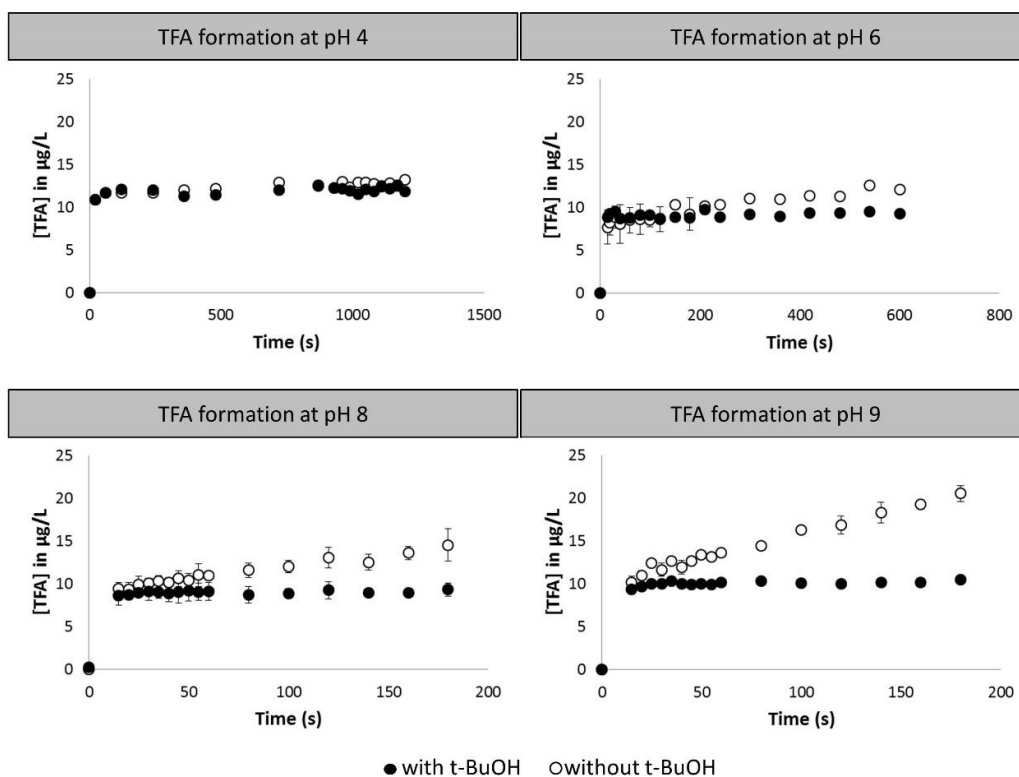
Figure A3.40: Formation of TFA in batch experiments (50 mM phosphate buffer) at different pH values, with and without addition of t-BuOH

Text A3.3: The kinetic experiments indicated a comparably low removal of STG in the ozonation. Lab-scale experiments in WWTP effluent (a) and ozonation in a pilot plant (b) at different ozone concentrations confirm this. In comparison to fexofenadine and candesartan STG showed slow and incomplete removal in both experimental set-ups while it showed faster attenuation than gabapentin and similar attenuation as denatonium.

Formation of TFA from STG was studied in lab-scale experiments in WWTP effluent at different ozone concentrations at non-spiked and spiked samples. Spike concentration of STG was 1 mg/L. TFA concentrations increased with increasing ozone dosage; for spiked samples a maximum concentration of 75 µg/L was achieved, for non-spiked samples it was 70 µg/L. The low difference between these values showed that the presence of STG has only minor influence on overall TFA formation. This is in accordance with findings of Scheurer, et al. [4].
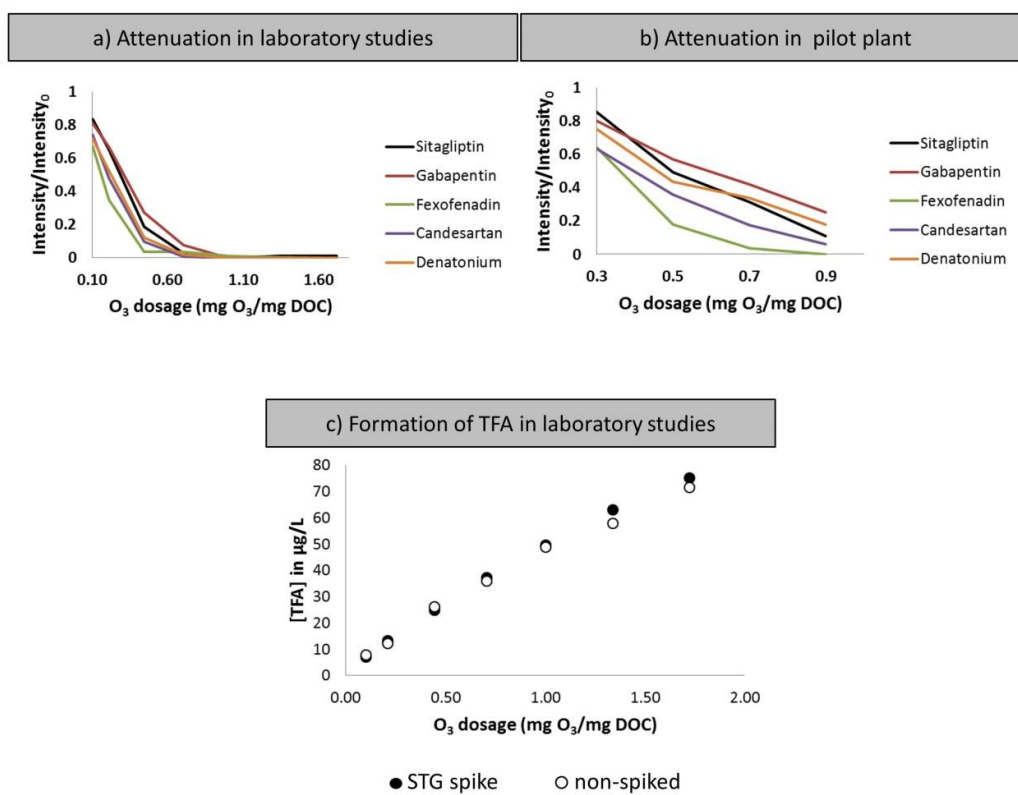
Figure A3.41: Comparison of STG attenuation with the attenuation of gabapentin, fexofenadine, candesartan and denatonium at different ozone dosages in (a) laboratory batch experiments in effluent from a German WWTP (DOC = 12 mg/L, pH = 8, T = room temperature) and in (b) ozonation at a pilot plant in Sweden (DOC = 10 mg/L, pH = 7, T = 10 – 12 °C). Formation of TFA (c) in laboratory batch experiments with spiked (spike concentration STG = 1 mg/L) and non-spiked effluent from a German WWTP at different ozone dosages.

Text A3.4: Biological degradability of TP 437 in MBBR treatment.

Ozonation as treatment step in WWTPs usually is not applied as stand-alone technique but combined with subsequent treatment techniques. Oftentimes biological treatment is used for polishing.

Lab-scale batch experiments in an MBBR system were performed on an ozonated sample of STG. Ozonation was done in phosphate buffer including t-BuOH at pH 8 with an initial STG-concentration of 5 mg/L. Ozone was added in an STG:O_3-ration of 1:15 and the reaction was allowed to proceed for 2 h. LC-ESI-QTOF analysis revealed the complete removal of STG, the main TP, TP 437, was formed to an high extend and traces of TP 406 also could be detected.

For lab-scale MBBR experiments, effluent from a pilot reactor at a German WWTP containing carriers were taken. Sample volume was set to 100 mL, each sample bottle was equipped with 25 carriers (biomass per bottle: 1 g/L). Experiments were performed in triplicates for two different spike volumes (100 µL and 10 µL from the ozonated sample). Sampling was performed at different time points over three days. In addition, samples from an ozonation pilot plant with subsequent MBBR treatment (HRT = 6h) were taken from a WWTP in Sweden and analysed for STG attenuation and TP 437 formation.

The lab-scale experiments showed only minor removal for both TPs over three days. STG, as background concentration, was evaluated as comparison and showed moderate removal. The lab-scale results for TP 437 were confirmed by the samples of the pilot plant, where TP 437 was formed during ozonation and could not be removed in the subsequent MBBR treatment. Here, STG showed a removal of about 50% during ozonation, however, during subsequent MBBR treatment no further attenuation could be achieved, possibly due to the very low HRT of only 6 h. Further studies and lab-scale experiments would be needed to verify these results.
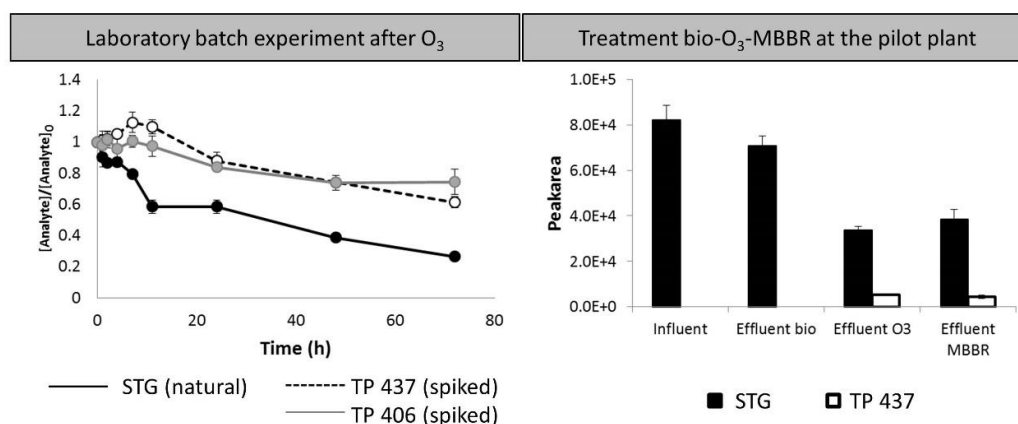
Figure A3.42: Attenuation of TP 437 and TP 406 in laboratory batch experiments spiked to effluent and carriers from a pilot reactor at a WWTP in Germany (DOC = 12 mg/L, pH = 8, T = room temperature, STG was not spiked and is used as reference) and attenuation of STG and TP 437 during the whole treatment train of the pilot plant at a WWTP in Sweden (Influent and effluent bio taken from the municipal WWTP, effluent O3 and effluent MBBR from the pilot plant)

References

1.   Yinon, J., Mass spectrometry of explosives: nitro compounds, nitrate esters, and nitramines. *Mass Spectrom Rev* **1982,** *1*, 257-307.

2.   Chizov, O. S.; Kadentsev, V. I.; G., P. G.; Burstein, K. I.; Shevelev, S. A.; Feinsilberg, A. A., Chemical ionization of aliphatic nitro compounds. *Organic Mass Spectrometry* **1978,** *13*, (11), 611-617.

3.   McLafferty, F. W.; Turecek, F., *Interpretation of mass spectra*. University Science Books: Sausalito, California, 1993.

4.   Scheurer, M.; Nodler, K.; Freeling, F.; Janda, J.; Happel, O.; Riegel, M.; Muller, U.; Storck, F. R.; Fleig, M.; Lange, F. T.; Brunsch, A.; Brauch, H. J., Small, mobile, persistent: Trifluoroacetate in the water cycle - Overlooked sources, pathways, and consequences for drinking water supply. *Water Res* **2017,** *126*, 460-471.

5.   Lim, S.; McArdell, C. S.; von Gunten, U., Reactions of aliphatic amines with ozone: Kinetics and mechanisms. *Water Research* **2019,** *157*, 514-528.